Archives of Mechanics

Archiwum Mechaniki Stosowanej

Porous media at finite strains
The new model with the balance equation for porosity

K. WILMAŃSKI (ESSEN)

THE PURPOSE of this work is the presentation of the governing equations describing the two-component porous material as the mixture with the additional field of the porosity. The additional field equation for this field is proposed. The governing equations are formulated in the new Lagrangian description. The constitutive relations under arbitrary elastic deformations of the skeleton are proposed. Various simplified models and their basic properties such as the propagation of sound waves are discussed. The work should be of interest for scientists working on continuum mechanics (problems with the free boundary), on numerical methods in continuum mechanics and on the wave propagation as the method of diagnosis of media with microstructure.

1. Introduction

THE THEORIES of porous materials have been developed primarily within the frame of soil mechanics. For granular soils (e.g. sand), clays and rocks, various engineering models were proposed to describe the flow of water or other fluids through the pores. The extensive literature concerning this subject as well as the introduction into the nomenclature of porous media can be found, for instance, in the excellent classical book of J. BEAR [1]. The connection of continuous models of porous materials with the modern theory of mixtures is explained in the review article of R.M. BOWEN [2].

R. DE BOER [3] presents in his major historical paper not only many details concerning the pioneering works of Terzaghi, Fillunger and some other engineers, who have contributed to the practical soil mechanics but he discusses also some new tendencies in the theories of porous media. Another practical aspect of these theories stems from combustion problems of granular materials which describe the behaviour of solid fuels. The review article on this subject has been written by S.L. PASSMAN, J.W. NUNZIATO, E.K. WALSH [4]. Much less has been done on the subject of multicomponent continua with large deformations of solids. Large elastic deformations which appear, for instance, in foams damping the sound waves or some filters in the chemical industry, were investigated experimentally but very little has been done from the continuum-mechanical point of view. Large plastic deformations, which accompany almost any loading of sands, are still described by means of the one-component models and, for instance, the influence of the changes of porosity is usually entirely neglected. Even the problems of large static deformations with the small dynamical disturbance (e.g. diagnosis of soils by propagating sound waves) are understood much better from the experimental standpoint than through some theoretical description. As an example, let us

mention a very competent book of T. Bourbie, O. Coussy, B. Zinszner, [5] who give the account on the wave experiments on porous materials but describe them theoretically by means of the old model of Biot in which the multicomponent character of the medium is accounted in a very poor and deficient manner.

The purpose of the present work is the presentation of the mechanical two-component model of the porous materials in which the skeleton may undergo arbitrary large elastic deformations, the fluid is inviscid but it may interact with the skeleton in an almost arbitrary way, and the porosity can change according to its own field equation. The irreversibility of processes in such a model follows from the diffusion and from the pore relaxation.

In the next section we present the necessity of the formulation of additional equations in the theory of porous materials when compared with the usual theory of mixtures of the same number of components. The third section is devoted to the brief presentation of the new consistent way of description of porous materials when the reference configuration of the skeleton is chosen as the reference for all other components as well. Apart from the advantages of this Lagrangian description in cases of large deformations, it is also a very convenient starting point for the numerical investigations of the model of porous media. In the fourth section we present the family of fields and field equations for this Lagrangian description of the two-component porous medium with the elastic skeleton and an ideal fluid component. The fifth section is devoted to the thermodynamic restrictions imposed on the constitutive relations assumed in the section four. The sixth section limits further the constitutive relations by the assumption of isotropy. One of the most important and rather surprising, very restrictive results follows in this section for the flux in the balance equation of porosity. In the seventh section we discuss some possibilities of further restrictions of constitutive relations by simplifying the way in which the components interact with each other. These simplifications are motivated by experimental results for rocks and granular materials.

The presentation of the model is supplemented in the eighth section with the discussion of the dynamic compatibility conditions and their connection with the boundary conditions for the porous medium. The most important part of this section concerns the conditions for the case of the free outstreaming fluid which yields the necessity of the additional scalar boundary condition describing the free boundary.

As an example of applications of the model we present in the ninth section the analysis of the propagation conditions for the sound waves. It is shown that the model indeed describes all these waves which are observed in reality. We present as well some possibilities of the application of this model to the diagnosis of porous media. The tenth section contains one of the possible linear models following from the general formulation. It is shown that quasi-static solutions of some boundary value problems for such a linear model are identical with the corresponding solutions of soil mechanics.

2. Closure problem: constitutive relations vs. differential equations for volume fractions

The main difference between the classical theory of mixtures of fluid-like components (miscible components) and the theory of porous materials (immiscible components) is connected with the existence of additional fields – a sort of internal variables – for the porous material, which describe the volume fraction of each component in the total microscopic control volume. For the A different components these volume fractions must satisfy the obvious normalisation condition

$$(2.1) \qquad \sum_{\alpha=1}^{A} n^{\alpha} = 1\,,$$

where n^{α} denotes the volume fraction of the α-component, $1 \leq \alpha \leq A$.

This relation is sometimes called the saturation condition. This name stems from the soil mechanics in which the porous materials with pores partially filled with water are frequently considered. In such cases the air is not accounted for as the third component and the medium is considered to be not fully saturated. The sum of volume fractions of the solid and of the water is smaller than one. It is quite obvious that it is not necessery to do so in the construction of the model. Particularly in processes of phase transitions such as the evaporation (drying processes, cavitation) the role of the gaseous phase is important. This gaseous component cannot be left out of the model even if its kinematics is identical with this of the fluid component.

It is easy to see that, in contrast to the classical theory of mixtures of miscible components, a theory of porous materials requires additional field equations. The continuum models of miscible components have been constructed by means of the partial balance equations of mass, momentum and energy for each component. In the Eulerian description these laws together with apppropriate constitutive relations were sufficient to yield the field equations for the partial mass densities ϱ^{α}, the partial velocities $\mathbf{v}^{\alpha}$ and the partial temperatures Θ^{α}. These balance laws are also used in models of the immiscible components but we have to supplement the theory with relations for the volume fractions.

A few solutions of this problem have been proposed. They can be divided into two classes:

1) additional constitutive relations are introduced,

2) additional differential equations in the form of either evolution equations or balance equations are proposed.

The simplest example of the model of the first class is the model proposed by R.M. Bowen [6]. Its prototype can be found in the papers of J.J. van Deemter and E.R. van der Laan [7] as well as of J.O. Hinze [8]. Also the work of R.S. Sampaio and W.O. Williams [9] is based on the similar notions. In this model

it is assumed that the volume fractions are proportional to the corresponding partial mass densities

(2.2)
$$n^\alpha = \frac{\varrho^\alpha}{\varrho^{\alpha R}}, \qquad 1 \le \alpha \le A,$$

where $\varrho^{\alpha R}$ are constants. These constants are called *true mass densities* and the corresponding components are called *incompressible*. In the Bowen's model this notion of incompressibility has nothing to do with the usual incompressibility of one-component continua. The classical incompressibility is the constraint requiring the sustaining reaction forces (e.g. reaction pressure). Such reaction forces do not appear in the Bowen's model. There is however a reaction force due to the saturation condition. Namely the relations (2.2) specify all volume fractions in terms of partial mass densities but they cannot be arbitrary due to the constraint of the saturation condition (2.1). This model has been extensively applied. However the recent results concerning in particular the boundary value problems for dynamic processes and the relaxation properties seem to indicate that the model has many very serious physical flaws.

Another model of the same class has been introduced by J.L.W. MORLAND [10]. He has assumed the constitutive relations describing the volume fractions. The model presented in the paper [11], concerning the two-component porous material belongs as well to this class. In the latter paper the saturation condition reduces the number of independent volume fractions to one. The additional constitutive relation has been proposed in a quite general form

(2.3)
$$\pi(\mathcal{C}) = 0,$$

where π denotes the arbitrary scalar function and $\mathcal{C}$ denotes the collection of all constitutive variables of the model. The thermodynamic considerations as well as the construction of the boundary value problems for such a model have been presented in the above mentioned paper. No practical applications have been made as yet.

Recently the much more sophisticated version of such a model is being investigated by J. BLUHM and R. DE BOER (see: [3, 12]). It is based on the semi-microscopic considerations referring to the "true" components. The local configuration of each component is assumed to be described by the so-called *realistic deformation gradient* $\mathbf{F}^{\alpha R}$ which is mapping the material vectors of the α-component from the reference configuration to the current configuration. These gradients are *not* assumed to be integrable. However one assumes that there exists the supplementary gradient $\mathbf{F}^{\alpha N}$ which combines with the realistic deformation gradient into the integrable partial deformation gradient $\mathbf{F}^\alpha$ of the α-component

(2.4)
$$\mathbf{F}^\alpha = \mathbf{F}^{\alpha N} \mathbf{F}^{\alpha R}.$$

The constitutive relations are assumed to hold for the objective combination of the realistic deformation gradients

(2.5) $$\mathbf{C}^{\alpha R} = \mathbf{C}^{\alpha R}(\mathcal{C}), \qquad \mathbf{C}^{\alpha R} \equiv \mathbf{F}^{\alpha RT}\mathbf{F}^{\alpha R}.$$

In particular these relations define the constitutive relations for volume fractions and the saturation condition becomes again the constraint. It has been shown that in some particular cases this model describes the phenomena which have been observed in the experimental soil mechanics. Moreover the model seems to be an appropriate starting point for the description of anisotropic structure of pores. Nothing has been done yet in this direction.

It should be mentioned that the models of this class do not describe the pore relaxation processes because the volume fractions are controlled by other macroscopic deformation variables.

Within the second class of the models, the most commonly used one seems to be that started by the M.A. Goodman and S.C. Cowin [13] who have proposed an additional balance equation for a scalar quantity with a rather obscure physical interpretation. This equation is called the *balance of equilibrated forces* and in various versions it has been extensively used to describe the two-component granular materials (e.g. see: J.W. Nunziato, E.K. Walsh [14], D.S. Drumheller, A. Bedford [15], A. Bedford, D.S. Drumheller [16], S.L. Passman [17], S.L. Passman, J.W. Nunziato, E.K. Walsh [4]). In particular the results for the combustion problems (solid fuels) indicate that such a model is quite reasonable in spite of its rather unclear microscopic foundations.

The same sort of the model has been investigated by J. Bluhm, R. de Boer and K. Wilmański [18]. They have considered the model with balance equations for true mass densities $\varrho^{\alpha R}$. These were not assumed to be constant any more as it was the case for the "incompressible" model of Bowen. The purpose of this work was however solely to show that the incompressibilities in the Bowen's model, if considered in the same way as in the classical continuum mechanics, yield the structure of the partial stress tensors which eliminates some flaws of the original Bowen's model. The local properties of this model have been investigated in order to check the appearance of sound waves. It has been proved [19] that the so-called P1- and P2- longitudinal waves may appear as required by experimental observations if very specific constitutive restrictions on fluxes are satisfied.

Another type of the model in this class has been introduced by R.M. Bowen [20] who postulates the *evolution equation* for each volume fraction. This procedure is quite common in thermodynamic theories with internal variables (e.g. macroscopic theories of mixtures with chemical reactions). It yields the spontaneous pore relaxation.

It should be mentioned that most of the above models admit large deformations of the skeleton. Although these have not been investigated in the above quoted papers, the problem has been recognized rather early. Some of its aspects

were mentioned, for instance, in the early papers of J.E. Adkins [21] and A.E. Green and J.E. Adkins [22]. These works do not contain however any propositions concerning the changes of volume fractions. An extension of these works under the Bowen's "incompressibility" assumption has been proposed by J. Kubik [23]. His work contains also many references connected with the problem of large deformations.

In the present work we shall discuss in some details a new version of the two-component model with the balance equation for porosity. It will be shown that the model easily admits large deformations of the skeleton (the solid component of the porous medium). Simultaneously it complies in the limit cases with the early engineering models of soils and rocks. The semi-microscopic motivation and thermodynamic details can be found in the paper [24]. A brief presentation of these arguments is contained in the Appendix to this paper.

3. Lagrangian description

The continuous theory of mixture with fluid components relies usually on the Eulerian description of the motion of components, similarly to the classical fluid mechanics of the single component. In the case of one solid component such as the skeleton of the porous medium this method is also possible but not very convenient. Namely, to describe the large deformations of the skeleton in the Eulerian way we have to introduce the deformation gradient F^S of the skeleton as the field in the space of actual configurations and then use the integrability condition for this gradient as the additional tensorial field equation (e.g. see: [25]). The attempts to use the mixed description – the Eulerian one for the fluid components and the Lagrangian one for the solid components (see: R.M. Bowen [2]) – does not seem to be appropriate either. It yields certain basic technical difficulties in the evaluation of the second law of thermodynamics and, most important of all, it is not suitable for the analysis of the boundary value problems. In the latter case, the field equations must be first transformed to the same independent variables – either Eulerian or Lagrangian and this transformation leads again to the technical difficulties apart from the fact that the problem can be formulated in the uniform description from the very beginning. In addition, the numerical analysis based on the finite element methods is simplified considerably when we use the same reference configuration for all components to define the spatial (Lagrangian) independent variables.

The most natural choice of such a reference configuration is the configuration of the skeleton for which its deformation gradient is the identity. Then the description of the deformation and of the kinematics is Lagrangian as in the nonlinear mechanics of solids. It remains to clear the question how to describe the fluid components in such a reference. This question has been answered in [11] (see also [26] for many details) where the two-component porous material

has been considered. We present here briefly these results limiting the further considerations of this work to the two-component porous materials as well. The extension to the cases of larger number of components is straightforward.

Let us begin with the motion of the skeleton. In the Lagrangian description it is given by the *function of motion*

$$(3.1) \qquad \mathbf{x} = \boldsymbol{\chi}^S(\mathbf{X}, t), \qquad \mathbf{x} \in E^3, \qquad \mathbf{X} \in \mathcal{B},$$

where $\mathbf{x}$ denotes the current position of the material point $\mathbf{X}$ of the skeleton, E^3 is the three-dimensional Euclidean space of motion and $\mathcal{B}$ denotes the reference configuration of the skeleton which, for the purpose of this work, can be identified for instance with the real configuration of the skeleton at the instant of time $t = t_0$. Then the deformation gradient and the velocity of the skeleton are defined as follows

$$(3.2) \qquad \mathbf{F}^S(\mathbf{X}, t) = \operatorname{Grad}\boldsymbol{\chi}^S(\mathbf{X}, t), \qquad \mathbf{x}'^S(\mathbf{X}, t) = \frac{\partial \boldsymbol{\chi}^S}{\partial t}(\mathbf{X}, t).$$

In the case of the fluid component described in the Eulerian way, the kinematics is given by the velocity field defined on the current configuration

$$(3.3) \qquad \mathbf{v}^F = \mathbf{v}^F(\mathbf{x}, t), \qquad \mathbf{x} \in \boldsymbol{\chi}^S(\mathcal{B}, t).$$

It is rather obvious that the kinematics of the fluid is defined solely within the domain of the current configuration of the solid $\boldsymbol{\chi}^S(\mathcal{B}, t)$. We are not interested in the motion beyond this domain except for the phenomena appearing on the boundary of the skeleton. This problem shall be discussed in the sequel. We proceed to transform the relation (3.3) into the Lagrangian description of the skeleton. Let us concentrate the attention on the material point of the fluid which occupies the position $\mathbf{x}$ at the instant of time t. For the small time increment Δt the position of this material point is given by the relation

$$(3.4) \qquad \mathbf{x}(t + \Delta t) = \mathbf{x}(t) + \mathbf{v}^F(\mathbf{x}(t), t)\Delta t \equiv \mathbf{x}(t) + \mathbf{F}^S(\mathbf{X}, t)\Delta \mathbf{X} + \mathbf{x}'^S(\mathbf{X}, t)\Delta t,$$

where

$$(3.5) \qquad \begin{aligned} \mathbf{X} &\equiv \mathbf{X}(t) = \boldsymbol{\chi}^{S-1}(\mathbf{x}(t), t), \\ \Delta \mathbf{X} &= \boldsymbol{\chi}^{S-1}(\mathbf{x}(t + \Delta t), t + \Delta t) - \boldsymbol{\chi}^{S-1}(\mathbf{x}(t), t). \end{aligned}$$

The second part of the relation (3.4) follows certainly from the fact that the material point of the fluid has changed the material point of the skeleton $\mathbf{X}$ with which it had shared the position at the instant of time t into the material point of the skeleton $\mathbf{X} + \Delta \mathbf{X}$, as indicated in the relation (3.5) (diffusion!). Consequently, after easy manipulations in (3.4) we see that the *image* of the material point of the

fluid in the reference configuration of the skeleton $\mathcal{B}$ moves with the following velocity

(3.6)
$$X'^F(X,t) = \lim_{\Delta t \to 0} \frac{\Delta X}{\Delta t} = F^{S-1}(x'^F - x'^S),$$
$$x'^F \equiv v^F(\chi^S(X,t),t).$$

We call this velocity the *Lagrangian velocity of the fluid component*. It is obvious that this velocity together with the velocity of the skeleton and with the deformation gradient of the skeleton, determines uniquely the usual Eulerian velocity of the fluid component v^F. Hence both ways of the description of kinematics of the fluid component are equivalent. However the Lagrangian way has the advantage that all fields are defined in the same domain $\mathcal{B}$.

4. Field equations

We proceed to specify the basic fields of the two-component model and the appropriate field equations. We limit our attention solely to *isothermal processes*. Then the processes in the skeleton are described by the initial mass density ϱ^S which is assumed to be constant (independent of the position in $\mathcal{B}$ – homogeneous material) and by the function of motion $\chi^S(\cdot,\cdot)$. In addition to this vector field for the skeleton, the process in the porous medium is described by the vector field of the Lagrangian velocity $X'^F(.,.)$ as well as the mass density of the fluid component and the volume fraction of the fluid. We have to find the Lagrangian representation for the last two fields.

The usual current mass density of the fluid component $\varrho_t^F(x,t)$ satisfies the following mass conservation law

(4.1)
$$\forall \, \mathcal{P}_t \subset \chi^S(\mathcal{B},t): \frac{d}{dt}\int_{\mathcal{P}_t} \varrho_t^F \, dv = 0,$$

where $\mathcal{P}_t$ is *material* with respect to the motion of the fluid. It has been assumed that there are no mass sources which could appear in the case of the exchange of mass between components. The above relation can be easily written in the image on the reference configuration $\mathcal{B}$ of the skeleton. Namely

(4.2)
$$\forall \, \mathcal{P} \subset \mathcal{B}: \frac{d}{dt}\int_{\mathcal{P}} \varrho^F \, dv \equiv \int_{\mathcal{P}} \frac{\partial \varrho^F}{\partial t} dv + \oint_{\partial \mathcal{P}} \varrho^F X'^F \cdot N ds = 0,$$
$$dv = J^{S-1} \, dv,$$

where

(4.3)
$$\varrho^F = J^S \varrho_t^F, \qquad J^S \equiv \det F^S, \qquad \mathcal{P} = \chi^{S-1}(\mathcal{P}_t,t),$$

and $\partial \mathcal{P}$ denotes the boundary of the set $\mathcal{P}$, *material* with respect to the fluid component. The presence of the surface integral is certainly connected with the fact that the image of fluid on $\mathcal{B}$ changes in time according to the field of the Lagrangian velocity of the fluid component.

It remains to introduce the representation for the volume fractions. It can be done, for instance, by the consideration of the true mass densities defined by the relations (2.2). If these are going to have the meaning of the mass densities then they have to transform in the same way as ϱ^F in the relation (4.3), i.e.

$$(4.4) \qquad \varrho^{FR} = J^S \varrho_t^{FR} \;\Rightarrow\; n^F = n_t^F \,,$$

where ϱ^{FR} and ϱ_t^{FR} denote the reference value and the current value of the true mass density of the fluid component, respectively. The implication in the relation (4.4) follows, certainly, from (4.3). Consequently, we have the following relation for the volume fraction of the skeleton

$$(4.5) \qquad n^S = 1 - n = n_t^S \,, \qquad n \equiv n^F \,.$$

In the above relation the saturation condition for the two-component porous medium has been used. The volume fraction of the fluid component n^F is frequently called the *porosity* of such a medium and it is denoted by n, as indicated in (4.5). According to the above choice of the transformation rules preserving the geometrical meaning of the volume fractions, the porosity in the Lagrangian description is identical with that in the Eulerian description.

The above considerations yield the following set of fields which must be determined by the mechanical model of the two-component porous medium

$$(4.6) \qquad (\mathbf{X}, t) \mapsto \left\{ \varrho^F, n, \boldsymbol{\chi}^S, \mathbf{X}'^F \right\} \in V^8 \,, \qquad \mathbf{X} \in \mathcal{B},$$

where V^8 is the eight-dimensional vector space of values of the fields.

For these fields we have to formulate the field equations. As usual we shall make use of the conservation laws. Obviously, the conservation of mass of the solid component is identically satisfied in the Lagrangian description. The local conservation of mass of the fluid component follows easily from the equation (4.2). We obtain

$$(4.7) \qquad \frac{\partial \varrho^F}{\partial t} + \mathrm{Div}\, \varrho^F \mathbf{X}'^F = 0.$$

The balance laws of momentum for both components are not conservation laws due to the interaction of components in the relative motion (*diffusive force*). We write first the integral form of these laws. Namely

$$\frac{d}{dt} \int_{\mathcal{P}} \varrho^S \mathbf{x}'^S \, dv = \oint_{\partial \mathcal{P}} \mathbf{P}^S \mathbf{N} \, ds + \int_{\mathcal{P}} (\mathbf{p}^* + \varrho^S \mathbf{b}^S) \, dv$$

for $\forall \mathcal{P} \subset \mathcal{B}$ – material with respect to skeleton,

$$(4.8) \qquad \frac{d}{dt} \int_{\mathcal{P}} \varrho^F \mathbf{x}'^F \, dv = \oint_{\partial \mathcal{P}} \mathbf{P}^F \mathbf{N} \, ds + \int_{\mathcal{P}} (-\mathbf{p}^* + \varrho^F \mathbf{b}^F) \, dv$$

for $\forall \mathcal{P} \subset \mathcal{B}$ – material with respect to fluid,
where $\mathbf{P}^S$ and $\mathbf{P}^F$ denote the *partial Piola-Kirchhoff stress tensors* related to the reference configuration of the skeleton. They are related to the Cauchy stress tensors of the current configuration by the relations

$$(4.9) \qquad \mathbf{P}^S = J^S \mathbf{T}^S \mathbf{F}^{S-T}, \qquad \mathbf{P}^F = J^S \mathbf{T}^F \mathbf{F}^{S-T},$$

$\mathbf{T}^S$ and $\mathbf{T}^F$ being the partial Cauchy stresses in the skeleton and in the fluid component, respectively.

The vector $\mathbf{p}^*$ denotes the *momentum source (diffusive force)* resulting from different velocity fields of the components. These, in reality, two sources for two momentum balance equations differ solely in sign as required by the continuum theory of mixtures.

The vector $\mathbf{N}$ is the unit vector orthogonal to the boundary $\partial \mathcal{P}$ and oriented outwards.

In any regular point of the domain $\mathcal{B}$, the above balance laws yield the following local equations

$$(4.10) \qquad \varrho^S \frac{\partial \mathbf{x}'^S}{\partial t} - \mathrm{Div} \mathbf{P}^S = \mathbf{p}^* + \varrho^S \mathbf{b}^S,$$

$$\frac{\partial}{\partial t}(\varrho^F \mathbf{x}'^F) + \mathrm{Div}(\varrho^F \mathbf{x}'^F \otimes \mathbf{X}'^F - \mathbf{P}^F) = -\mathbf{p}^* + \varrho^F \mathbf{b}^F.$$

These equations and the mass balance for the fluid component (4.7) form the basis for the formulation of field equations if supplemented with constitutive laws. However we are still missing one equation for the eight fields (4.6). This is the closure problem which we have presented in Sec. 2. As indicated already we solve it by adding the *balance equation* for the porosity n. The semi-microscopic motivation of this equation can be found in the paper [24] and in the Appendix. In the present work this equation can be considered on the purely phenomenological footing (see as well: [27]). Namely we assume

$$(4.11) \qquad \frac{\partial n}{\partial t} + \mathrm{Div} \mathbf{J} = \nu,$$

and call $\mathbf{J}$ the *flux of porosity* and ν the *source of porosity*. Their physical meaning shall be presented in the sequel (see, also: [27, 28]).

In order to formulate the field equations we have to introduce the constitutive relations for the following *constitutive quantities*

$$(4.12) \qquad \mathcal{Z} = \left\{ \mathbf{J}, \nu, \mathbf{F}^{S-1}\mathbf{P}^S, \mathbf{F}^{S-1}\mathbf{P}^F, \mathbf{F}^{ST}\mathbf{p}^* \right\},$$

where the Piola–Kirchhoff stress tensors were multiplied by the deformation gradient for the *objectivity* reasons. We do not need to discuss this problem in the present work because it does not differ from the same problem of the nonlinear continuum mechanics of single-component media. However it is worth noticing that the vector **J** is also assumed to be independent of the observer which can be easily done in the Lagrangian description as we see further in this work. It is connected with the fact that the Lagrangian velocity is independent of the observer being defined by means of the relative velocity (see: (3.6)).

Further in this work we consider the simplest possible two-component porous medium for which it is assumed that the skeleton is *elastic* and the fluid is *ideal*. This certainly does not mean the reversibility of processes which are influenced by the diffusion and the sources of porosity, both these factors yielding dissipation. In terms of our fields the collection of *constitutive variables* in such a case is as follows

$$(4.13) \qquad C = \left\{ \varrho^F, n, \mathbf{C}^S, \mathbf{X}'^F \right\}, \qquad \mathbf{C}^S \equiv \mathbf{F}^{ST} \mathbf{F}^S,$$

where $\mathbf{C}^S$ denotes the right Cauchy–Green deformation tensor of the skeleton.

Finally we have the following *constitutive relations*

$$(4.14) \qquad \mathcal{Z} = \mathcal{Z}(C),$$

all these functions being assumed to be twice continuously differentiable with respect to all arguments.

Equations (4.7), (4.10) and (4.11) together with the constitutive relations (4.14) form the closed set of eight field equations for the eight fields (4.6). It remains to formulate the boundary and initial conditions to obtain the initial-boundary value problem for the set of differential equations. We shall discuss the boundary conditions after the presentation of some thermodynamic admissibility conditions for the constitutive relations (4.14) which are as yet almost arbitrary except for the above mentioned mathematical regularity conditions.

5. Thermodynamic restrictions

We proceed to present the restrictions of the above described constitutive relations following from the assumption that the processes must satisfy the second law of thermodynamics.

Any solution of the field equations is called the *thermodynamic process*. According to the *second law of thermodynamics*, the thermodynamic process is *thermodynamically admissible* if the following inequality

$$(5.1) \qquad \varrho^S \frac{\partial \Psi^S}{\partial t} + \varrho^F \left(\frac{\partial \Psi^F}{\partial t} + \mathbf{X}'^F \cdot \operatorname{Grad} \Psi^F \right) - \mathbf{P}^S \cdot \frac{\partial \mathbf{F}^S}{\partial t}$$
$$- \mathbf{P}^F \cdot \operatorname{Grad} \mathbf{x}'^F - \mathbf{F}^{ST} \mathbf{p}^* \cdot \mathbf{X}'^F \leq 0$$

is identically satisfied. In the above inequality Ψ^S, Ψ^F denote the partial Helmholtz free energies of components. These are assumed to be the constitutive quantities, i.e.

$$(5.2) \qquad \Psi^S = \Psi^S(\mathcal{C}), \qquad \Psi^F = \Psi^F(\mathcal{C}).$$

The simple derivation of the inequality (5.1) from the entropy balance equations and the entropy inequality for isothermal conditions can be found, for instance, in the work [11].

In the standard way we eliminate now the constraint on solutions of the inequality (5.1) that it should hold solely for the thermodynamic processes. Namely we introduce the Lagrange multipliers for the field equations and require that the inequality

$$
(5.3) \qquad \varrho^S \frac{\partial \Psi^S}{\partial t} + \varrho^F \left(\frac{\partial \Psi^F}{\partial t} + \mathbf{X}'^F \cdot \operatorname{Grad} \Psi^F \right) - \mathbf{P}^S \cdot \frac{\partial \mathbf{F}^S}{\partial t}
$$
$$
- \mathbf{P}^F \cdot \operatorname{Grad} \mathbf{x}'^F - \mathbf{F}^{ST} \mathbf{p}^* \cdot \mathbf{X}'^F
$$
$$
- \Lambda^\varrho \left(\frac{\partial \varrho^F}{\partial t} + \operatorname{Div} \varrho^F \mathbf{X}'^F \right) - \Lambda^n \left(\frac{\partial n}{\partial t} + \operatorname{Div} \mathbf{J} - \nu \right)
$$
$$
- \mathbf{L}^S \cdot \left(\varrho^S \frac{\partial \mathbf{x}'^S}{\partial t} - \operatorname{Div} \mathbf{P}^S - \mathbf{p}^* - \varrho^S \mathbf{b}^S \right)
$$
$$
- \mathbf{L}^F \cdot \left(\frac{\partial}{\partial t} (\varrho^F \mathbf{x}'^F) + \operatorname{Div} (\varrho^F \mathbf{x}'^F \otimes \mathbf{X}'^F - \mathbf{P}^F) + \mathbf{p}^* - \varrho^F \mathbf{b}^F \right) \leq 0
$$

should hold for *arbitrary fields*. The multipliers are functions of the same constitutive variables as all other constitutive functions, i.e.

$$
(5.4) \qquad \begin{aligned}
\Lambda^\varrho &= \Lambda^\varrho(\mathcal{C}), & \Lambda^n &= \Lambda^n(\mathcal{C}), \\
\mathbf{L}^S &= \mathbf{F}^S \mathbf{L}_0^S(\mathcal{C}), & \mathbf{L}^F &= \mathbf{F}^S \mathbf{L}_0^F(\mathcal{C}).
\end{aligned}
$$

The solutions of the above inequality are constructed in two different ways. In early 60-ies B.D. COLEMAN has proposed the method in which it was assumed that the class of volume forces was large enough to accomodate arbitrary changes of the other terms in the momentum balance equations. This means that these equations do not constrain the class of solutions of the entropy inequality. In such a case

$$(5.5) \qquad \mathbf{L}^S \equiv 0, \qquad \mathbf{L}^F \equiv 0.$$

However, if the class of volume forces is not large enough (e.g. if $\mathbf{b}^S = \mathbf{b}^F$ as it is the case for the gravitational forces), the inequality must be exploited by the absence of these forces. This has been investigated for the first time by

I. MÜLLER in 70-ies. It can be easily shown that the second way is less restrictive for the multicomponent media and both methods yield the same results for the single-component continua.

For the purpose of this work we rely on the COLEMAN'S method. Consequently the results remain on the safe side as far as the thermodynamic restrictions are concerned.

Bearing in mind the constitutive relations (4.14) and (5.2) and making use of the chain rule of differentiation in (5.3) we obtain the inequality which is linear with respect to the following derivatives

$$
(5.6) \qquad \left\{ \frac{\partial \varrho^F}{\partial t}, \frac{\partial n}{\partial t}, \operatorname{Grad} \varrho^F, \operatorname{Grad} n, \frac{\partial \mathbf{X}'^F}{\partial t}, \operatorname{Grad} \mathbf{F}^S, \operatorname{Grad} \mathbf{X}'^F \right\}.
$$

Consequently the inequality can hold for arbitrary fields solely in the case when the coefficients of these derivatives vanish. We arrive at the set of the following identities

$$
\begin{aligned}
\Lambda^\varrho &= \varrho^S \frac{\partial \Psi^S}{\partial \varrho^F} + \varrho^F \frac{\partial \Psi^F}{\partial \varrho^F}, \qquad & \Lambda^n &= \varrho^S \frac{\partial \Psi^S}{\partial n} + \varrho^F \frac{\partial \Psi^F}{\partial n}, \\
(5.7) \qquad \varrho^S \frac{\partial \Psi^S}{\partial \varrho^F} \mathbf{X}'^F + \Lambda^n \frac{\partial \mathbf{J}}{\partial \varrho^F} &= 0, \qquad & \varrho^F \frac{\partial \Psi^F}{\partial n} \mathbf{X}'^F + \Lambda^n \frac{\partial \mathbf{J}}{\partial n} &= 0, \\
\varrho^S \frac{\partial \Psi^S}{\partial \mathbf{X}'^F} + \varrho^F \frac{\partial \Psi^F}{\partial \mathbf{X}'^F} &= 0, & &
\end{aligned}
$$

$$
\begin{aligned}
\mathbf{P}^S + \mathbf{P}^F &= 2\mathbf{F}^S \left(\varrho^S \frac{\partial \Psi^S}{\partial \mathbf{C}^S} + \varrho^F \frac{\partial \Psi^F}{\partial \mathbf{C}^S} \right), \\
(5.8) \qquad \mathbf{F}^{ST} \mathbf{P}^F &= -\varrho^F \Lambda^\varrho \mathbf{1} + \varrho^F \frac{\partial \Psi^F}{\partial \mathbf{X}'^F} \otimes \mathbf{X}'^F - \Lambda^n \left(\frac{\partial \mathbf{J}}{\partial \mathbf{X}'^F} \right)^T, \\
\operatorname{sym}^{23} \mathbf{P}^F \otimes \mathbf{X}'^F &= \operatorname{sym}^{23} \left[2\mathbf{F}^S \left(\varrho^F \frac{\partial \Psi^F}{\partial \mathbf{C}^S} \otimes \mathbf{X}'^F - \Lambda^n \left(\frac{\partial \mathbf{J}}{\partial \mathbf{C}^S} \right)^{T13} \right) \right].
\end{aligned}
$$

There remains the *residual inequality* which defines the *dissipation* $\mathcal{D}$ of the process

$$
(5.9) \qquad \mathcal{D} \equiv \mathbf{F}^{ST} \mathbf{p}^\ast \cdot \mathbf{X}'^F - \Lambda^n \nu \geq 0.
$$

The above relations determine the Lagrange multipliers, relate partial stress tensors to the partial Helmholtz free energies and to the flux $\mathbf{J}$ and introduce certain additional restrictions on the constitutive relations. We do not try to exploit these results in their full generality and restrict our attention to the particular case of the *isotropic porous media*. This is the subject of the next section.

6. Isotropy

The assumption of the isotropy does not seem to limit the applicability of the present model very considerably because we have already assumed the porosity to be described by the volume fraction. Such an assumption eliminates any influence of the geometrical anisotropy of the pore structure from the model. In this respect the full isotropy assumption concerns solely the mechanical responses of the skeleton and reactions to the relative motion.

The constitutive relations for scalar functions of the isotropic medium must be invariant with respect to an arbitrary orthogonal transformation of the reference configuration. In our model there are three scalar functions (see: (4.12) and (5.2))

$$(6.1) \qquad \left\{ \nu, \Psi^S, \Psi^F \right\},$$

and these functions of constitutive variables (4.13) satisfy the above requirement if they depend on these variables solely through their invariants

$$(6.2) \qquad \mathcal{C}_{\text{iso}} = \left\{ \varrho^F, n^F, \mathrm{I}, \mathrm{II}, \mathrm{III}, \mathrm{IV}, \mathrm{V}, \mathrm{VI} \right\},$$

where

$$(6.3) \qquad
\begin{aligned}
\mathrm{I} &= \mathbf{1} \cdot \mathbf{C}^S, & \mathrm{II} &= \frac{1}{2}(\mathrm{I}^2 - \mathbf{1} \cdot \mathbf{C}^{S2}), \\
\mathrm{III} &= \det \mathbf{C}^S \equiv J^{S2}, & \mathrm{IV} &= \mathbf{X}'^F \cdot \mathbf{X}'^F, \\
\mathrm{V} &= \mathbf{C}^S \cdot (\mathbf{X}'^F \otimes \mathbf{X}'^F), & \mathrm{VI} &= \mathbf{C}^{S2} \cdot (\mathbf{X}'^F \otimes \mathbf{X}'^F).
\end{aligned}$$

Simultaneously the model contains two vector constitutive functions for which the general isotropic representation is of the following form

$$(6.4) \qquad
\begin{aligned}
\mathbf{J} &= (\Phi_0 \mathbf{1} + \Phi_1 \mathbf{C}^S + \Phi_2 \mathbf{C}^{S2})\mathbf{X}'^F, \\
\mathbf{F}^{ST}\mathbf{p}^* &= (\pi_0 \mathbf{1} + \pi_1 \mathbf{C}^S + \pi_2 \mathbf{C}^{S2})\mathbf{X}'^F.
\end{aligned}$$

In the above relations the coefficients are arbitrary isotropic scalar functions, i.e.

$$(6.5) \qquad \Phi_a = \Phi_a(\mathcal{C}_{\text{iso}}), \qquad \pi_a = \pi_a(\mathcal{C}_{\text{iso}}), \qquad a = 0, 1, 2.$$

Further we do not need the isotropic constitutive relations for the partial stress tensors because these follow from the identities (5.8) whose right-hand sides are determined by the isotropic scalar and vector functions.

Bearing in mind the thermodynamic relations (5.6) and (5.7) as well as the symmetries of the partial Cauchy stress tensors $\mathbf{T}^S$, $\mathbf{T}^F$ we obtain the following results.

The flux in the balance equation for the porosity must be parallel to the Lagrangian velocity $\mathbf{X}'^F$

$$(6.6) \qquad \mathbf{J} = \Phi_0 \mathbf{X}'^F, \qquad \Phi_1 = \Phi_2 \equiv 0.$$

The dependence of the Helmholtz free energies and of the coefficient Φ_0 on the invariants is restricted by the relations

$$(6.7) \quad
\begin{aligned}
& \varrho^S \frac{\partial \Psi^S}{\partial \varrho^F} + \Lambda^n \frac{\partial \Phi_0}{\partial \varrho^F} = 0, \\[2mm]
& \varrho^F \frac{\partial \Psi^F}{\partial \mathcal{A}_1} - \Lambda^n \frac{\partial \Phi_0}{\partial \mathcal{A}_1} = 0, \qquad \mathcal{A}_1 = n, \mathrm{I}, \mathrm{II}, \mathrm{IV}, \mathrm{VI}, \\[2mm]
& \varrho^F \left(\varrho^F \frac{\partial \Psi^F}{\partial \varrho^F} + 2\mathrm{III} \frac{\partial \Psi^F}{\partial \mathrm{III}} \right) \\[2mm]
& \qquad\qquad - \Lambda^n \sqrt{\mathrm{III}} \left[\varrho^F \frac{\partial}{\partial \varrho^F} \left(\frac{\Phi_0}{\sqrt{\mathrm{III}}} \right) + 2\mathrm{III} \frac{\partial}{\partial \mathrm{III}} \left(\frac{\Phi_0}{\sqrt{\mathrm{III}}} \right) \right] = 0,
\end{aligned}$$

where the multiplier Λ^n is given by the relation $(5.7)_2$. Simultaneously

$$(6.8) \qquad \varrho^S \frac{\partial \Psi^S}{\partial \mathcal{A}_2} + \varrho^F \frac{\partial \Psi^F}{\partial \mathcal{A}_2} = 0, \qquad \mathcal{A}_2 = \mathrm{IV}, \mathrm{V}, \mathrm{VI}.$$

The Piola–Kirchhoff partial stress tensors have the following form

$$(6.9)_1 \quad \mathbf{P}^F = -\left[\varrho^F \left(\varrho^F \frac{\partial \Psi^F}{\partial \varrho^F} + \varrho^S \frac{\partial \Psi^S}{\partial \varrho^F} \right) + \Lambda^n \Phi_0 \right] \mathbf{F}^{S-T}$$

$$+ 2 \left[\varrho^F \frac{\partial \Psi^F}{\partial \mathbf{V}} + \Lambda^n \frac{\partial \Phi_0}{\partial \mathbf{V}} \right] \mathbf{F}^S (\mathbf{X}'^F \otimes \mathbf{X}'^F),$$

$$(6.9)_2 \quad \mathbf{P}^S = 2\mathbf{F}^{S-T} \left\{ \varrho^S \left[\frac{\partial \Psi^S}{\partial \mathrm{I}} \mathbf{C}^S + \left(\mathrm{II} \frac{\partial \Psi^S}{\partial \mathrm{II}} + \mathrm{III} \frac{\partial \Psi^S}{\partial \mathrm{III}} \right) \mathbf{1} \right. \right.$$

$$\left. - \mathrm{III} \frac{\partial \Psi^S}{\partial \mathrm{II}} \mathbf{C}^{S-1} + 2 \frac{\partial \Psi^S}{\partial \mathbf{V}} \mathbf{C}^S \mathbf{X}'^F \otimes \mathbf{X}'^F \right]$$

$$+ \Lambda^n \left[\frac{\partial \Phi_0}{\partial \mathrm{I}} \mathbf{C}^S + \left(\mathrm{II} \frac{\partial \Phi_0}{\partial \mathrm{II}} + \mathrm{III} \frac{\partial \Phi_0}{\partial \mathrm{III}} \right) \mathbf{1} - \mathrm{III} \frac{\partial \Phi_0}{\partial \mathrm{II}} \mathbf{C}^{S-1} \right.$$

$$\left. \left. + 2 \frac{\partial \Psi_0}{\partial \mathbf{V}} \mathbf{C}^S \mathbf{X}'^F \otimes \mathbf{C}^S \mathbf{X}'^F \right] \right\}.$$

The proofs of these relations are rather technical; they are based on the spectral representation of the deformation tensor and of the Lagrangian velocity. They shall not be quoted in the present paper. The details can be found in the work [25].

In spite of the complexity of the above relations, some important properties of the isotropic model are immediately seen.

First of all the relations (6.6) yield the considerable simplification of the additional field equation (4.11) of the model. The collinearity of the flux of porosity and of the relative Lagrangian velocity of components couples the diffusion processes with this surface mechanism of changes of the porosity which is absent in the models based on the evolution equations for porosity. This property simplifies as well the problem of an additional boundary condition which is necessary for this field equation in the fully nonlinear case of the present model. The latter problem shall not be discussed in this work.

Simultaneously the scalar coefficient Φ_0 in the relation for the flux $\mathbf{J}$ plays the crucial role in the "static" coupling between the components. This "static" coupling is understood as the description of the interactions between components reflected by the dependence of the free energy of the fluid Ψ^F on the deformation of the skeleton through the invariants I, II, III of the Cauchy–Green deformation tensor, as well as the dependence of the free energy of the skeleton Ψ^S on the mass density of the fluid ϱ^F. The former is easily seen in the relations $(6.7)_{2,3}$ and the latter in the relations $(6.7)_1$. The additional most important "static" coupling is reflected by the dependence of both partial free energies on the current values of the porosity n. The dependence on n of at least one of these energies is necessary for the non-triviality of the relation $(5.7)_2$ for the multiplier Λ^n. This multiplier is solely responsible for the additional static interaction terms in all relations quoted above. For instance in the case of lack of diffusion, the vanishing multiplier Λ^n would yield the classical relation for the stress tensor in the one-component ideal fluid and the classical relation for the stress tensor in the one-component nonlinear elastic solid. In addition, all these interactions of components are described by the model independently of the fact whether the particular process is connected with the relative motion of components or not.

The above relations for stresses show also a rather complicated influence of the relative velocity on the mechanical responses of the two-component medium. Quite clearly this influence is at least quadratic. This means that the small diffusion velocity yields primarily the explicit linear dependence of the diffusion forces (momentum source) p^* and of the porosity flux $\mathbf{J}$ on this velocity, and the partial stresses contain solely the influence of the static interactions of components. In such a case the partial Cauchy stress tensor for the fluid component is reduced to the spherical form (pressure!).

Let us finally mention that the residual inequality (5.9) is in the isotropic case of the following form

$$(6.10) \qquad (\pi_0 \mathbf{1} + \pi_1 \mathbf{C}^S + \pi_2 \mathbf{C}^S) \cdot (\mathbf{X}'^F \otimes \mathbf{X}'^F) - \left(\varrho^S \frac{\partial \Psi^S}{\partial n} + \varrho^F \frac{\partial \Psi^F}{\partial n} \right) \nu \geq 0.$$

Obviously the first term of this dissipation inequality describes the dissipation

due to the diffusion, and the second one – due the changes of porosity caused by the source ν in the field equation of porosity. In the thermodynamical equilibrium the relative velocity as well as the porosity source must vanish. These are the two mechanisms of the thermodynamical relaxation in the present model.

Let us briefly review the above results for the general case. The thermodynamic admissibility and the isotropy reduce the constitutive problem of the model to the following scalar constitutive functions

$$(6.11) \qquad \left\{ \Psi^S, \Psi^F, \Phi_0, \pi_0, \pi_1, \pi_2, \mathcal{N} \right\},$$

which, in general, may depend on the constitutive variables (6.2) and are subject to the conditions (6.7), (6.8) as well as (6.10). The vector fluxes and the stress tensors are then determined by these functions through the appropriate differentiation. Further in this paper we discuss some possibilities of the effective construction of these functions for certain real porous materials.

7. Simplified nonlinear models

The purpose of this section is the construction of some simplified models based on the general considerations of the sixth section. We shall not discuss all important particular cases because the research on this subject is still in progress. We want solely to illustrate the connection of the general mechanical model of large deformations of the porous two-component medium with some other models whose range of applicability is more restricted and with observations of some real materials.

We begin with the assumption that processes deviate not too far from the *thermodynamical equilibrium*. The latter is defined as the state with the vanishing dissipation. According to the inequality (6.10) we have in such a state

$$(7.1) \qquad \mathbf{X}'^F|_E = 0, \qquad \nu|_E = 0, \qquad \to n|_E = n_0 = \text{const.}$$

The above assumption means then that the relative velocity of components is small and the deviation of the porosity from the homogeneous initial state n_0 is small as well. In this approximation

$$\nu = -\frac{\mathcal{N}}{\varrho^F} \left(\varrho^S \frac{\partial \Psi^S}{\partial n} + \varrho^F \frac{\partial \Psi^F}{\partial n} \right),$$

$$(7.2)$$

$$\mathcal{N} = \mathcal{N}(n_0, \mathrm{I}, \mathrm{II}, \mathrm{III}, \varrho^F) \geq 0,$$

and the functions π_0, π_1, π_2 must be dependent on the same variables as $\mathcal{N}$.

Simultaneously the state of the thermodynamical equilibrium is the state in which the dissipation reaches its minimum. Consequently

$$(7.3) \qquad \frac{\partial}{\partial n}(\varrho^S \Psi^S + \varrho^F \Psi^F)|_{n=n_0} = 0, \qquad \frac{\partial^2}{\partial n^2}(\varrho^S \Psi^S + \varrho^F \Psi^F)|_{n=n_0} > 0.$$

Bearing in mind the identities (6.7) in the first approximation of the deviation from the state of equilibrium, we obtain after easy calculations

(7.4)
$$\Psi^S = \Psi_0^S + \frac{1}{2}\Psi_2^S(n - n_0)^2,$$
$$\Psi^F = \Psi_0^F + \frac{1}{2}\Psi_2^F(n - n_0)^2,$$
$$\Phi_0 = \left[\gamma(n_0) + \Phi_0^1(n - n_0)\right]\sqrt{\mathrm{III}},$$

where

(7.5)
$$\Psi_0^S = \Psi_0^S(n_0, \mathrm{I}, \mathrm{II}, \mathrm{III}), \qquad \Psi_0^F = \Psi_0^F(n_0, \varrho_t^F),$$
$$\varrho_t^F \equiv \varrho^F \mathrm{III}^{-1/2},$$

and

(7.6) $\nu = -\dfrac{n - n_0}{\tau}, \qquad \tau \equiv \dfrac{\varrho^F}{\mathcal{N}}(\varrho^S\Psi_2^S + \varrho^F\Psi_2^F)^{-1}, \qquad \Lambda^n = \dfrac{\varrho^F}{\tau\mathcal{N}}(n - n_0).$

The material parameter τ has the interpretation of the *relaxation time* of the porosity and, according to the condition (7.3)$_2$ of the *stability of the thermodynamic equilibrium*, it must be positive. It creates the damping of the acoustic waves in addition to the damping connected with the diffusion.

Simultaneously

(7.7)
$$\frac{1}{2}\varrho^S\frac{\partial\Psi_2^S}{\partial\varrho_t^F} + \frac{\varrho^F}{\tau\mathcal{N}}\sqrt{\mathrm{III}}\frac{\partial\Phi_0^1}{\partial\varrho_t^F} = 0,$$
$$\frac{1}{2}\frac{\partial\Psi_2^F}{\partial\mathcal{A}_3} - \frac{1}{\tau\mathcal{N}}\sqrt{\mathrm{III}}\frac{\partial\Phi_0^1}{\partial\mathcal{A}_3} = 0, \qquad \mathcal{A}_3 = \mathrm{I}, \mathrm{II}, \mathrm{III}.$$

It is convenient to use further the spatial representation of the constitutive variables and functions. In order to do so we introduce the current mass density ϱ_t^S, the left Cauchy–Green deformation tensor $\mathbf{B}^S$ and the real relative velocity $\mathbf{w}$

(7.7)′ $\varrho_t^S = \varrho^S J^{S-1}, \qquad \varrho_t^F = \varrho^F J^{S-1}, \qquad \mathbf{B}^S = \mathbf{F}^S\mathbf{F}^{ST}, \qquad \mathbf{w} = (\mathbf{x}'^F - \mathbf{x}'^S).$

The invariants I, II, III are certainly identical for the tensor $\mathbf{B}^S$ with those of the tensor $\mathbf{C}^S$, and the invariants IV, V, VI are immaterial under the present simplifying assumption of the small deviation from the thermodynamical equilibrium.

The partial Cauchy stress tensors, related to the Piola–Kirchhoff stress tensors by the relations (4.9), are in this case given by the following relations

(7.8)
$$\mathbf{T}^S = \mathcal{I}_1\mathbf{B}^S + \mathcal{I}_0\mathbf{1} + \mathcal{I}_{-1}\mathbf{B}^{-1},$$
$$\mathbf{T}^F = -p^F\mathbf{1},$$

where

$$
\mathcal{I}_1 = 2\varrho_t^S \frac{\partial \Psi_0^S}{\partial \mathrm{I}},
$$

(7.9)

$$
\mathcal{I}_{-1} = -2\mathrm{III}\varrho_t^S \frac{\partial \Psi_0^S}{\partial \mathrm{II}},
$$

$$
\mathcal{I}_0 = 2\varrho_t^S \left(\mathrm{II} \frac{\partial \Psi_0^S}{\partial \mathrm{II}} + \mathrm{III} \frac{\partial \Psi_0^S}{\partial \mathrm{III}} \right) + \gamma \varrho^F \frac{n - n_0}{\tau \mathcal{N}},
$$

and

(7.10)

$$
p^F = (\varrho_t^F)^2 \frac{\partial \Psi_t^F}{\partial \varrho_t^F} + \gamma \varrho^F \frac{n - n_0}{\tau \mathcal{N}}.
$$

We have used the relations (7.5) and neglected terms quadratic in the deviation of the porosity n from its equilibrium value n_0. The latter causes the symmetry of interactions in the partial stress tensors.

The similarity of the relations (7.8) to the classical relations for nonlinear elastic materials and for the ideal fluids is, certainly, only apparent. The *response coefficient* $\mathcal{I}_0$ depends in the present case not only on the deformation invariants I, II, III, as it is the case in the classical one-component model but also on the mass density ϱ_t^F and on the porosity n. Simultaneously the *partial pressure* in the fluid p^F depends not only on the current mass density ϱ_t^F but also on the invariants I, II, III and on the porosity n. Crucial for this coupling of components is the presence of the constant γ which is the part of the flux of porosity as well as the presence of the two additional material parameters τ and $\mathcal{N}$, both of them connected with the changes of porosity.

Let us finally mention two other simplified models which may have the practical bearing on the soil mechanics. In both models we assume the linearity with respect to the diffusion velocity.

The first one follows from the assumption that the balance equation for the porosity (4.11) reduces to the evolution equation which describes the changes of the porosity along trajectories of the fluid. Then

(7.11) $\quad \Phi_0 \approx n, \quad$ i.e. $\quad \gamma(n_0) = n_0, \quad \Phi_0^1 = 1, \quad \mathrm{III} \approx 1.$

In such a case the identities (6.7) yield

$$
\Psi^S = \Psi^S(n_0, \mathrm{I}, \mathrm{II}, \mathrm{III}),
$$

(7.12)

$$
\Psi^F = \Psi^F(n_0, \varrho_t^F, \kappa), \quad \kappa \equiv nJ^{S-1},
$$

$$
\Lambda^n = \varrho_t^F \frac{\partial \Psi^F}{\partial \kappa},
$$

and the partial Cauchy stress tensors have the form

(7.13)
$$\mathbf{T}^S = 2\varrho_t^S \frac{\partial \Psi^S}{\partial \mathrm{I}} \mathbf{B}^S + 2\varrho_t^S \left(\mathrm{II} \frac{\partial \Psi^S}{\partial \mathrm{II}} + \mathrm{III} \frac{\partial \Psi^S}{\partial \mathrm{III}} \right) \mathbf{1} - 2\mathrm{III}\varrho_t^S \frac{\partial \Psi^S}{\partial \mathrm{II}} \mathbf{B}^{S-1},$$

$$\mathbf{T}^F = -\left[(\varrho_t^F)^2 \frac{\partial \Psi^F}{\partial \varrho_t^F} + \varrho_t^F \frac{\partial \Psi^F}{\partial \kappa} n \right] \mathbf{1}.$$

Hence the interaction of components is not symmetric in this case. The changes of porosity influence the stresses in the fluid but not in the skeleton.

The second simplified model follows from the assumption that the evolution equation of porosity is carried by the skeleton, i.e.

(7.14)
$$\Phi_0 \approx 0.$$

According to the identities (6.7) we obtain then

(7.15)
$$\Psi^S = \Psi^S(n, \mathrm{I}, \mathrm{II}, \mathrm{III}),$$
$$\Psi^F = \Psi^F(n_0, \varrho_t^F),$$
$$\Lambda^n = \varrho^S \frac{\partial \Psi^S}{\partial n},$$

and the partial Cauchy stresses are

(7.16)
$$\mathbf{T}^S = 2\varrho_t^S \frac{\partial \Psi^S}{\partial \mathrm{I}} \mathbf{B}^S + 2\varrho_t^S \left(\mathrm{II} \frac{\partial \Psi^S}{\partial \mathrm{II}} + \mathrm{III} \frac{\partial \Psi^S}{\partial \mathrm{III}} \right) \mathbf{1} - 2\mathrm{III}\varrho_t^S \frac{\partial \Psi^S}{\partial \mathrm{II}} \mathbf{B}^{S-1},$$

$$\mathbf{T}^F = -\left[(\varrho_t^F)^2 \frac{\partial \Psi^F}{\partial \varrho_t^F} \right] \mathbf{1}.$$

Consequently the interaction of components is again non-symmetric. The changes of porosity influence solely stresses in the skeleton through the dependence of the free energy Ψ^S on the porosity.

We rest here as far as the discussion of the construction of nonlinear models is concerned. In the next section we present briefly the boundary conditions which are necessary to pose the mathematical problem for the field equations. Some physical properties of various models will be discussed in connection with the wave propagation.

8. Boundary value problems, permeable boundary of the skeleton

The set of field equations for the fields (4.6) requires – similarly to the mixture theory – *two vector conditions* on the boundary, connected with the vector

equations following from the momentum balance laws and, in general, *one scalar condition* for the scalar balance equation of porosity. The latter may not appear in particular cases when the coefficient of the flux of porosity Φ_0 is identical with n itself. It is easy to show that it may appear at least in two cases. The first one concerns the skeleton whose interactions with the fluid vanish entirely from the Helmholtz free energy Ψ^S as discussed in the previous section. This seems to appear for some rocks in the range of moderate porosities. The second one follows from the relation (7.4)$_3$ as the approximation of the small volume changes of the skeleton: III $\cong 1$, $\gamma(n_0) = n_0$ and $\Phi_0^1 = 1$. In both cases the stress tensor in the skeleton does not contain contributions from the fluid – it is indeed purely elastic. We skip here the details justifying these assumptions in some practical applications whose main purpose is to estimate the order of magnitude of the new material parameters. We shall accept them however in examples to be considered further in this paper. The general case has not been considered as yet.

In addition to the above boundary conditions one has to describe the motion of the *free surface* if the fluid flows out of the porous skeleton and the boundary is identified with the boundary of the skeleton. We proceed to present some elements of these problems.

Let us begin with the so-called *dynamical compatibility conditions*. These are the jump conditions for fields and their functions which follow from the general balance equations in the limit on singular surface. The derivation is standard and we shall not present here any details.

In order to simplify the considerations let us assume that the surface is *material with respect to the skeleton*. This means that its velocity is identically zero in the Lagrangian image used in the work. The general case has been considered in the paper [11]. Then the mass balance for the skeleton does not yield any non-trivial conditions. The mass balance of the fluid (4.2) leads to the following relation

$$(8.1) \quad m^F \equiv (\varrho^F \mathbf{X}'^F)^- \cdot \mathbf{N} = (\varrho^F \mathbf{X}'^F)^+ \cdot \mathbf{N}, \qquad \text{i.e.}$$

$$\left[[\varrho^F \mathbf{X}'^F] \right] \cdot \mathbf{N} = 0, \qquad [[...]] \equiv (...)^+ - (...)^-,$$

where $(...)^-$ is the limit of the expression in parenthesis from the negative side of the surface (this is the internal side of the surface if the surface is the boundary), and $(...)^+$ is the limit from the positive side (the exterior for the boundary) for the other quantity. The quantity m^F describes the amount of the mass of the fluid which flows through the unit surface in the unit time. According to the above condition, the mass is neither produced nor does it sink on the surface. Such surfaces are called *ideal*.

The momentum balance equations (4.8) yield the following conditions

$$(8.2) \quad \left[[\mathbf{P}^S] \right] \cdot \mathbf{N} = 0,$$

$$\left[[\mathbf{P}^F] \right] \mathbf{N} = m^F \left[[\mathbf{x}'^F] \right],$$

where the first condition does not differ from the classical *Poisson's condition* of continuity of the stress vector in the skeleton. The presence of the right-hand side in the relation for the fluid means that due to the non-material character of the surface, it is not the ideal surface for the fluid with respect to the convective transport of momentum.

The surface balance for porosity is determined by the equation (4.11) which holds for an arbitrary regular point but can be easily written in the integral form and then extended to hold also in the limit on the singular surface. The corresponding jump condition is then of the form

$$(8.3) \qquad \left[\left[\Phi_0 \mathbf{X}'^F\right]\right] \cdot \mathbf{N} = 0.$$

We shall not discuss this problem any further in this work.

We proceed now to formulate the boundary conditions for the boundary of the skeleton on which the external load is given and the boundary is permeable for the fluid. Many details concerning this problem as well as its applications in the weak formulation and numerical codes for the two-component porous media can be found in the work of W. KEMPA [30].

The first vector boundary condition follows from the assumption that the external load, say $\mathbf{t}_{\text{ext}}$, is given on the boundary of the skeleton ∂B. We assume that this load is taken over by the resultant stress vector of both components on the positive side of the boundary, i.e.

$$(8.4) \qquad \left\{ (\mathbf{P}^S \mathbf{N})^- + (\mathbf{P}^F \mathbf{N})^- + m^F \left[\left[\mathbf{x}'^F\right]\right] \right\} \big|_{\partial B} = \mathbf{t}_{\text{ext}},$$

where the sum of the dynamic compatibility conditions (8.2) has been used. Apart from the limits of fields from the interior, this relation contains as well the unspecified quantity $(\mathbf{x}'^F)^+$. We relate this vector to a scalar quantity in the sequel (Eq. $(8.6)_1$).

In order to expose the most essential feature we consider the second vector condition under the additional assumption that the Cauchy stress tensor in the fluid is spherical, i.e. we neglect the higher order contributions of the relative velocity. In such a case we can assume that the tangential component of the relative velocity is continuous on the boundary of the skeleton and the fluid does not flow tangentially to the skeleton in the exterior. In the Lagrangian description we have then

$$(8.5) \qquad (\mathbf{X}'^F - (\mathbf{X}'^F \cdot \mathbf{N})\mathbf{N})^- \big|_{\partial B} = 0.$$

Solely two components of this vector are independent. For this reason we need in addition one scalar condition. We formulate this condition assuming that the flow of the fluid m^F on the boundary of the skeleton is controlled by the pressure

difference between the fluid inside of the porous material $(p^F)^-$ and the pressure of the surrounding p_{ext}. Consequently

$$\left[\left[x'^F\right]\right] = (C^{S-1} \cdot (N \otimes N))^{1/2} m^F \left[\left[\frac{1}{\varrho^F}\right]\right] n,$$

(8.6)
$$m^{F2} \left[\left[\frac{1}{\varrho^F}\right]\right] = -J^S C^{S-1} \cdot (N \otimes N) \left[\left[p^F\right]\right],$$

$$m^F = -\alpha(p_{ext} - p^{F-}),$$

where the relation (8.4) has been accounted for, as well as the following relations for the unit vector n normal to the boundary in the current configuration [11] and for the pressure in the fluid have been used

(8.7)
$$n = (C^{S-1} \cdot (N \otimes N))^{-1/2} F^{S-T} N, \qquad p^F = -\frac{1}{3} J^S (P^F F^{ST}) \cdot 1,$$

and the parameter α is constitutive. If this parameter as well as the mass density $(\varrho^F)^+$ and the pressure p_{ext} were known, the relations (8.6) would complete the formulation of the boundary value problem. We shall not go into any further details referring an interested reader to the work [30]. Let us solely notice that the *constitutive relation* for the boundary $(8.6)_3$ does not contain any influence of the pressure gradient projected on the normal to the boundary. Sometimes it seems to be necessery to have this type of condition. The linear combination of the jump of pressure and such a normal derivative would yield the boundary condition similar to that appearing in the heat conduction problems with the boundary characterised by its own thermal conductivity.

9. Acceleration waves in two-component media

The model constructed above in this paper contains a number of constitutive quantities which must be measured in experiments. In the case of porous materials such experiments are usually of the two different types. Either the measurements are done by means of devices which are in contact with real components or they are delivering the mean quantities in which the contribution of separate real components is not clearly specified. To the first type belong, for instance, the measurements of true mass densities of components separated from each other or the measurements of the real pore water pressure. The most important class of measurements of the second class are the measurements of speeds of propagation and the attenuation of acoustic waves in porous materials. The waves propagate in the multicomponent porous media and they deliver an information on the whole system rather than on separate real components. Many examples of such measurements can be found in the book of T. Bourbie, O. Coussy, B. Zinszner [5].

In this section we present the most fundamental properties of acoustic waves described by the present two-component model. We follow here the papers [19, 27, 28]) where also the extensive discussion and the comparison with the experimental data can be found.

Within the continuum mechanics the *acoustic wave* is defined as the so-called *weak discontinuity wave* in which the motion and the velocities are continuous and the accelerations suffer the jump on a singular surface. This surface is assumed to be orientable and it is called the *wave front*. It moves through the material with the *speed of propagation of the wave*.

According to the above definition we assume in the case of the two-component medium the following relations to hold on the wave front of the acoustic wave

$$(9.1) \qquad \left[[\chi^S]\right] = 0, \qquad \left[[x'^S]\right] = 0, \qquad \left[[x'^F]\right] = 0, \qquad [[n]] = 0.$$

Under these conditions the so-called *iterated geometrical* and *kinematical compatibility conditions* yield

$$
\begin{aligned}
&\left[[F^S]\right] = 0, \qquad \left[[X'^S]\right] = 0, \qquad \left[[\varrho^F]\right] = 0, \\
&\left[[P^S]\right] N = 0, \qquad \left[[P^F]\right] N = 0, \\
&\left[\left[\frac{\partial x'^S}{\partial t}\right]\right] = a^S U^2, \qquad \left[[\operatorname{Grad} F^S]\right] = a^S \otimes N \otimes N, \\
&\left[\left[\frac{\partial F^S}{\partial t}\right]\right] = -U a^S \otimes N, \\
&\left[\left[\frac{\partial x'^F}{\partial t}\right]\right] = a^F U^2, \qquad \left[[\operatorname{Grad} x'^F]\right] = -U a^F \otimes N, \\
&\left[[\operatorname{Grad} X'^F]\right] = (U - X'^F \cdot N) F^{S-1} a^S \otimes N - U F^{S-1} a^F \otimes N, \\
&\left[\left[\frac{\partial \varrho^F}{\partial t}\right]\right] = -U r, \qquad \left[[\operatorname{Grad} \varrho^F]\right] = r N, \qquad \left[\left[\frac{\partial n}{\partial t}\right]\right] = -U n, \\
&[[\operatorname{Grad} n]] = n N,
\end{aligned}
$$

(9.2)

where N denotes the unit normal vector to the wave front and a^S, a^F, r and n denote the so-called *amplitudes* of discontinuity of the acceleration in the skeleton, the acceleration in the fluid, the fluid mass density gradient and the porosity gradient, respectively. The *speed of propagation* of the wave front is denoted by U.

In order to find the speed of propagation U and the relation between the direction of the amplitude and the direction of propagation, it is now sufficient to evaluate the limits of field equations on both sides of the wave front. This evaluation for the mass balance in the fluid (4.7) and for the balance equation of

porosity (4.11) yield

$$rU\left(1 - \frac{X_N'^F}{U}\right) - \varrho^F U\left(1 - \frac{X_N'^F}{U}\right)\mathbf{F}^{S-T}\cdot(\mathbf{a}^S \otimes \mathbf{N})$$

$$+\varrho^F U\mathbf{F}^{S-T}\cdot(\mathbf{a}^F \otimes \mathbf{N}) = 0,$$

$$(9.3) \qquad nU\left(1 - \frac{\partial\Phi_0}{\partial n}\frac{X_N'^F}{U}\right) - \frac{\partial\Phi_0}{\partial\varrho^F}rX_N'^F - 2X_N'^F\frac{\partial\Phi_0}{\partial\mathbf{C}^S}\cdot(\mathbf{F}^{ST}\mathbf{a}^S \otimes \mathbf{N})$$

$$-\Phi_0 U\left(1 - \frac{X_N'^F}{U}\right)\mathbf{F}^{S-T}\cdot(\mathbf{a}^S \otimes \mathbf{N}) + \Phi_0 U\mathbf{F}^{S-T}\cdot(\mathbf{a}^F \otimes \mathbf{N}) = 0,$$

$$X_N'^F = \mathbf{X}'^F\cdot\mathbf{N}.$$

In most cases of the practical bearing the relative velocity of components is much smaller than the smallest speed of propagation of the acoustic wave. For this reason we can make the simplifying assumption

$$(9.4) \qquad\qquad \left|\frac{X_N'^F}{U}\right| \ll 1;$$

the usual order of magnitude of the left-hand side is 10^{-4}. If all other terms in the relations (9.3) are of the same order of magnitude then we have approximately

$$(9.5) \qquad r = \varrho^F\mathbf{F}^{S-T}\cdot(\mathbf{a}^S - \mathbf{a}^F)\otimes\mathbf{N}, \qquad n = \Phi_0\mathbf{F}^{S-T}\cdot(\mathbf{a}^S - \mathbf{a}^F)\otimes\mathbf{N}.$$

Hence the amplitudes of the mass density gradient in the fluid and the amplitude of the porosity gradient are determined by the amplitudes of the acceleration. They do not yield their own waves and are carried by the other sorts of waves. This would not be the case if we did not make the simplifying assumption (9.4). A rather unusual type of waves appears if we make a better approximation (see: [28]) but there is no experimental evidence that such waves do indeed exist.

We proceed now to investigate the momentum balance equations (4.10) from both sides of the wave front. We limit the attention to the case of small relative velocities for which the Cauchy stress tensor in the fluid is spherical (see: (7.2)). Then bearing in mind the simplification (9.4) and the remaining constitutive assumptions we obtain easily

$$\varrho^S\mathbf{a}^S U^2 = J^S(\mathbf{F}^{S-T}\cdot(\mathbf{a}^S-\mathbf{a}^F)\otimes\mathbf{N})\left\{\varrho^F\frac{\partial\mathbf{T}^S}{\partial\varrho^F} + \Phi_0\frac{\partial\mathbf{T}^S}{\partial n}\right\}\cdot(\mathbf{F}^{S-T}\mathbf{N}) + \mathbf{Q}^S\mathbf{a}^S,$$

$$(9.6) \quad \varrho^F\mathbf{a}^F U^2 = -J^S\left\{(\mathbf{F}^{S-T}\cdot(\mathbf{a}^S - \mathbf{a}^F)\otimes\mathbf{N})\left(\varrho^F\frac{\partial p^F}{\partial\varrho^F} + \Phi_0\frac{\partial p^F}{\partial n}\right)\right.$$

$$\left.+2\frac{\partial p^F}{\partial\mathbf{B}^S}\cdot(\mathbf{a}^S \otimes \mathbf{F}^S\mathbf{N})\right\}\mathbf{F}^{S-T}\mathbf{N},$$

where

$$(9.7) \qquad \mathbf{Q}^S \equiv 2J^S \left(\frac{\partial \mathbf{T}^S}{\partial \mathbf{B}^S} \right)^{T^{23}} \cdot (\mathbf{F}^{S-T}\mathbf{N} \otimes \mathbf{F}^S\mathbf{N}).$$

This tensor of the second order is called the *acoustic tensor* in the classical theory of acoustic waves in single-component nonlinear elastic materials. Its eigenvalues determine the wave speeds, and its eigenvectors – the relation of the directions of amplitude to the directions of propagation in this classical case. It is not so in the case under considerations.

Let us notice that the second relation (9.6) implies that the amplitude $\mathbf{a}^F$ must be parallel to the vector $\mathbf{n}$ which is given in the current configuration by the relation (8.7) and which is perpendicular to the wave front. Consequently the waves carrying the discontinuity of the acceleration in the fluid must be *longitudinal*.

It is also easy to check that the amplitude $\mathbf{a}^S$ can have an arbitrary direction. As pointed out in the work [27], these solutions of the set of algebraic equations (9.6) determine three types of acoustic waves: *two longitudinal* so-called P1- and P2-*waves* and *one transversal* S-*wave*.

We shall discuss some properties of these waves for the linear model in the next section. However it is important to stress that all three waves are observed in porous materials. The fastest one is the P1-wave. It propagates, for instance, in soils with the speed $3 - 5$ km/s. The second fastest is the transversal wave carried primarily by the skeleton. The slow P2-wave (Biot's wave) has, for instance, in soils the speed $0.5 - 1.5$ km/s. These speeds as well as other properties of the waves (for instance – attenuation) are dependent on the deformation of both components and on the current porosity. This delivers the *in situ* methods of diagnosis of porous materials by propagating acoustic waves and measuring the arrival time and amplitudes of various sorts of waves. To a certain extent such methods are already used, for instance, in geology. The difficulties are connected with the analysis of the available data for which the old models of porous materials were not adequate.

10. Linear models, some simple analytical considerations

For the purpose of illustration we close this work with a few remarks concerning the linear version of the model. It is obvious that the construction of any analytical solution of the fully nonlinear boundary value problem shall be almost impossible. We can expect, however, that the numerical codes shall be developed. The work on this subject is already in progress. For this reason it is convenient to have some simple hints from the linear and simplified problems in which we do not have to eliminate the artefacts connected with the numerical approximations. We consider now a few examples of such problems.

Let us consider the case in which the following assumptions are satisfied

$$\mathbf{E}^S \equiv \frac{1}{2}(\mathbf{C}^S - \mathbf{1}), \qquad \|\mathbf{E}^S\| = \sup_{\mathbf{n}, |\mathbf{n}|=1} |\mathbf{E}^S \cdot (\mathbf{n} \otimes \mathbf{n})|,$$

$$\sup_{x,t} \|\mathbf{E}^S\| \ll 1,$$

(10.1)

$$\sup_{x,t} \left| \frac{\varrho^F - \varrho_0^F}{\varrho_0^F} \right| \ll 1,$$

$$\sup_{x,t} \left| \frac{\Delta}{n_0} \right| \ll 1, \qquad \Delta \equiv n - n_0,$$

where ϱ_0^F and n_0 denote the constant initial values of the mass density of the fluid and of the porosity, respectively.

Under these assumptions the constitutive relations for the source of porosity (7.11) and for the partial stresses (7.2) become

$$\nu = -\frac{\Delta}{\tau}, \qquad \tau = \tau(n_0),$$

$$\mathbf{T}^S = \lambda^S(\mathbf{E}^S \cdot \mathbf{1})\mathbf{1} + 2\mu^S \mathbf{E}^S, \qquad \lambda^S = \lambda^S(n_0), \qquad \mu^S = \mu^S(n_0),$$

(10.2)

$$\mathbf{T}^F = -p^F \mathbf{1}, \qquad p^F = K^F \varrho^F + \frac{n_0 \varrho_0^F}{\tau \mathcal{N}} \Delta,$$

$$K^F = K^F(n_0), \qquad \mathcal{N} = \mathcal{N}(n_0).$$

In the above relations we have used the assumption mentioned in the section on the boundary conditions and concerning the form of the flux Φ_0. Namely it has been assumed to be equal to the porosity n itself. In the linear model this assumption yields the constant flux of the value n_0. The coupling of stresses is then one-sided: the stress in the skeleton is independent of the presence and properties of the fluid in pores.

The fields in this case

(10.3) $$\left\{ \varrho^F, \Delta, \mathbf{u}^S, \mathbf{v}^F \right\}, \qquad \mathbf{u}^S \equiv \boldsymbol{\chi}^S(\mathbf{X}, t) - \mathbf{X},$$

where $\mathbf{u}^S$ is the *displacement* of the skeleton, are described by the following fully linearized set of field equations

$$\frac{\partial \varrho^F}{\partial t} + \varrho_0^F \mathrm{Div}(\mathbf{v}^F) = 0,$$

(10.4) $$\frac{\partial \Delta}{\partial t} + n_0 \mathrm{Div}(\mathbf{v}^F) = -\frac{\Delta}{\tau},$$

$$\varrho^S \frac{\partial^2 \mathbf{u}^S}{\partial t^2} = (\lambda^S + \mu^S)\mathrm{Grad}\,\mathrm{Div}(\mathbf{u}^S) + \mu^S \mathrm{Div}\,\mathrm{Grad}(\mathbf{u}^S) + \pi_3 \mathbf{w} + \varrho^S \mathbf{b}^S,$$

(10.4)
[cont.]
$$\varrho_0^F \frac{\partial \mathbf{v}^F}{\partial t} = -\mathrm{Grad}\left(K^F \varrho^F + \frac{n_0 \varrho_0^F}{\tau \mathcal{N}} \Delta\right) - \pi_3 \mathbf{w} + \varrho^F \mathbf{b}^F,$$

$$\mathbf{w} \equiv \mathbf{v}^F - \frac{\partial \mathbf{u}^S}{\partial t},$$

where

(10.5)
$$\pi_3 = \pi_0 + \pi_1 + \pi_2 = \pi_3(n_0).$$

We can now make the analysis of the propagation condition of acoustic waves completely explicit. We obtain the following equations for the amplitudes

(10.6)
$$r + \varrho_0^F \mathbf{a}^F \cdot \mathbf{n} = 0,$$
$$\mathbf{n} + n_0 \mathbf{a}^F \cdot \mathbf{n} = 0,$$
$$\varrho^S U^2 \mathbf{a}^S = (\lambda^S + \mu^S)(\mathbf{a}^S \cdot \mathbf{n})\mathbf{n} + \mu^S \mathbf{a}^S,$$
$$\varrho_0^F U^2 \mathbf{a}^F = \left\{-K^F r - \frac{n_0 \varrho_0^F}{\tau \mathcal{N}} \mathbf{n}\right\} \mathbf{n}.$$

Consequently the amplitudes of the mass density gradient r and the amplitude of the porosity gradient n are not connected with their own waves – as it was already the case in the nonlinear problem. The amplitude of the acceleration wave in the fluid possesses solely the normal component and the speeds of propagations are given by the following relations

(10.7)
$$U_L^S = \sqrt{\frac{\lambda^S + 2\mu^S}{\varrho^S}} \qquad \text{longitudinal P1-wave,}$$

$$U_T^S = \sqrt{\frac{\mu^S}{\varrho^S}} \qquad \text{transversal S-wave,}$$

$$U_L^F = \sqrt{K^F + \frac{n_0^2}{\tau \mathcal{N}}} \qquad \text{longitudinal P2-wave.}$$

Hence the measurements of these three speeds of propagation deliver immediately three relations for the material parameters in function of the porosity n_0. These data are easily available and we show further a numerical example.

In order to analyze the attenuation of waves it is easier to consider a one-dimensional example of the monochromatic wave. Let us denote by v^F the x-component of the velocity of the fluid, by v^S – the x-component of the velocity of the skeleton and by ε^S – the extension of the skeleton in the x-direction. These three quantities together with ϱ^F and Δ fully describe the one-dimensional process. We look for the solution of the set of field equations in the following

form

$$\begin{aligned}
\varrho^F &= \varrho_0^F + \varepsilon R^F \exp(i(\omega t - k^* x)), \\
v^F &= \varepsilon V^F \exp(i(\omega t - k^* x)), \\
v^S &= \varepsilon V^S \exp(i(\omega t - k^* x)), \\
\Delta &= \varepsilon D \exp(i(\omega t - k^* x)), \\
\varepsilon^S &= \varepsilon E^S \exp(i(\omega t - k^* x)),
\end{aligned}$$

(10.8)

where $\varrho_0^F, R^F, V^F, V^S, D, E^S$ are constants and

(10.9) $$0 < \varepsilon \ll 1.$$

In the above relations the frequency ω denotes the real frequency of the monochromatic wave which is considered to be given. The wave number k^* is assumed to be complex. Namely

(10.10) $$k^* = k + i\alpha,$$

where k is the inverse of the *wavelength* and α denotes the *attenuation* of the wave.

Substitution of the relations (10.8) in the field equations yields the following *dispersion relation for the monochromatic waves*

(10.11) $$\left\{ \omega^2 - U_L^{F2} k^{*2} + \frac{n_0^2}{\tau \mathcal{N}} \frac{i 1/\tau}{\omega + i 1/\tau} k^{*2} - i \frac{\pi_3}{\varrho_0^F} \omega \right\}$$
$$\cdot \left\{ \omega^2 - U_L^{S2} k^{*2} - i \frac{\pi_3}{\varrho^S} \omega \right\} + \left(\frac{\pi_3}{\varrho^S} \right) \left(\frac{\pi_3}{\varrho_0^F} \right) \omega^2 = 0,$$

which is the equation for k^* as a function of ω. It is easy to check that the limit case of almost empty pores for which we can neglect the influence of diffusion yields the frequency-dependent speeds of propagation of two different types of waves corresponding to the two longitudinal waves discussed above. Moreover the limit $\omega \to \infty$ yields the same speeds of propagation as before.

As far as the attenuation coefficient α is concerned we obtain the following relation

(10.12) $$\frac{1}{\tau} = \frac{\omega}{2Q} \left\{ \left(Q^2 - \frac{1}{4} \right) \frac{n_0^2}{\tau \mathcal{N} K^F} \right.$$
$$\left. + \sqrt{ \left(Q^2 - \frac{1}{4} \right)^2 \left(\frac{n_0^2}{\tau \mathcal{N} K^F} \right)^2 - 4Q^2 \left(1 + \left(\frac{n_0^2}{\tau \mathcal{N} K^F} \right) \right) } \right\},$$

where

(10.13)
$$Q = \frac{k}{2\alpha},$$

is the so-called the *quality factor* of the monochromatic wave (see: Sec. 3.3.3. of [5]). Hence the relaxation time τ for the porosity is indeed one of the two parameters describing the attenuation of waves. The second one is the classical diffusion coefficient π_3. The quality factor is also easily attainable to the measurements. This yields the possibility of measuring the additional parameter τ of the model discussed in this section.

In order to illustrate the above considerations we present the numerical results for the *Massillon sandstone*. For the porosity $n_o = 23\%$ and the water saturation $S_w = 0.1\%$ we have the following experimental data [5] and the results of the wave analysis

Measurements:	$U_L^S \cong 3.1 \times 10^3$ m/s	$U_L^F \cong 0.9 \times 10^3$ m/s	$\dfrac{1000}{Q} = 40$ for $\omega = 2 \times 10^3$ Hz		
	$U_T^S \cong 1.6 \times 10^3$ m/s	$U_{\text{air}} \cong 0.3 \times 10^3$ m/s	$\varrho^S \cong 2.4 \times 10^3$ kg/m^3		

Results (the wave analysis):	$\lambda^S = 10.776$ $\times 10^3$ MPa	$\mu^S = 6.144$ $\times 10^3$ MPa	$K^F = 0.9$ $\times 10^5$ m^2/s^2	$\tau\mathcal{N} = 7.347$ $\times 10^{-8}$ s^2/m^2	$\tau = 3.699$ $\times 10^{-6}$ s

These values check well with the available experimental results obtained by the standard methods of measuring the material parameters.

In addition, the above simple examples justify to a certain extent the assumptions made in the nonlinear model. For instance the measurements of the speeds of the P1-wave in many rocks show that they are almost independent of the water saturation in pores. It means that these speeds do not react to the art of the substance in the pores – they are independent of ϱ^F and Δ. This justifies for such materials the assumption of independence of the free energy of the skeleton of the mass density of the fluid and of the changes of the porosity which we have mentioned in the section on the boundary conditions.

We complete this section with another standard example stemming from the soil mechanics (see: [29] for further details). First of all let us notice that the equations $(10.4)_{1,2}$ can be combined in the following way

(10.14)
$$\frac{\partial \Delta}{\partial t} + \frac{\Delta}{\tau} = \frac{n_0}{\varrho_0^F} \frac{\partial \varrho^F}{\partial t}.$$

If the mass density ϱ^F were known, we could find the changes of porosity from this equation. Consequently the *formal solution* can be written in the form

(10.15)
$$\Delta = \frac{n_0}{\varrho_0^F} \left\{ \varrho^F - \varrho_0^F e^{-t/\tau} - \frac{1}{\tau} \int_0^t \varrho^F(\mathbf{x}, \eta) e^{-(t-\eta)\tau} \, d\eta \right\}.$$

As expected, the equation for porosity yields a sort of *memory effect* which in the linear theory is described by the Boltzmann integral. It means that the present value of the porosity depends not only on the present value of the mass density but also on its past history. The influence of the past history is, however, modified by the exponential function. Hence, in the first approximation, we can neglect these effects entirely. We obtain

(10.16)
$$\Delta \approx \frac{n_0}{\varrho_0^F}(\varrho^F - \varrho_0^F).$$

Substitution of this relation in Eq. (10.14) shows immediately that this equation is satisfied solely in the case of the infinite relaxation time. In such a case there is no dissipation due to the changes of porosity. The porosity changes according to the change of the mass density of the fluid. The similar property appears under the assumption of the incompressibility of real materials of components which has been discussed by R. BOWEN [6]. However in contrast to the work of Bowen, in our case it is only the approximation which does not lead to any reaction forces on constraints.

Bearing in mind the above approximation we solve now the one-dimensional quasi-static consolidation problem which has been solved for the first time by Fröhlich in 1938 within the frame of the Terzaghi model of consolidation. Namely we consider the compression of the semi-infinite prism of the porous material filled with water with the free flow of the water through the boundary $x = 0$. The external pressure p_a is atmospheric and the loading is given as the body force on the skeleton

(10.17)
$$\varrho^S b^S = qH(t)\delta(x),$$
$$\varrho^F b^F = 0,$$

where $H(\cdot)$ is the Heaviside distribution and $\delta(\cdot)$ is the Dirac distribution. The constant q is the load in the direction of the x-axis.

Simple manipulations of the field equations yield the following set of equations for the pressure p^F and the normal component of the stress σ^S in the direction of the x-axis

(10.18)
$$\frac{\partial}{\partial t}\left(\frac{\partial p^F}{\partial x}\right) - D\frac{\partial^2}{\partial x^2}\left(\frac{\partial p^F}{\partial x}\right) = Mq\delta(t)\delta(x),$$
$$\frac{\partial \sigma^S}{\partial x} - \frac{\partial p^F}{\partial x} = -qH(t)\delta(x),$$

where

$$M \equiv \frac{\varrho_0^F \left(K^F + \dfrac{n_0^2}{\tau \mathcal{N}} \right)}{E^S + \varrho_0^F \left(K^F + \dfrac{n_0^2}{\tau \mathcal{N}} \right)}, \qquad E^S \equiv \lambda^S + 2\mu^S,$$

(10.19)

$$D \equiv \frac{\varrho_0^F}{\pi_3} \frac{\varrho_0^F \left(K^F + \dfrac{n_0^2}{\tau \mathcal{N}} \right) E^S}{E^S + \varrho_0^F \left(K^F + \dfrac{n_0^2}{\tau \mathcal{N}} \right)}.$$

The equations (10.18) can be easily solved. For instance, we obtain the following result for the so-called *hydraulic gradient* i

(10.20)

$$\left(\frac{2\sqrt{\pi} H}{Mq} \right) i = \frac{1}{\sqrt{t'}} \exp\left(-\frac{x'^2}{4t'} \right),$$

$$i \equiv \frac{\partial p^F}{\partial x}, \qquad t' \equiv t\frac{D}{H^2}, \qquad x' \equiv \frac{x}{H},$$

and H is a constant with the dimension of length.
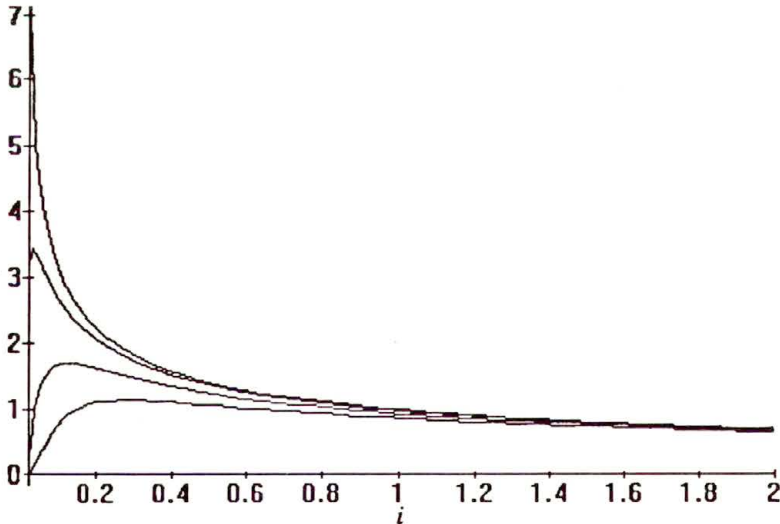
FIG. 1. Time changes of the hydraulic gradient i for $x/H = 0$, 0.25 and 0.75.

This solution is shown in the Fig. 1 for various values of the depth. The result complies quantitatively with the results obtained for the model of Terzaghi for times shorter than app. 1.5.

For large times the decay in the present model is much slower even though both solutions approach zero for the infinite time. This is most likely the result of approximations applied by Fröhlich.

The above results allow also to find the last material constant of the linear model – the coefficient of diffusion π_3. Consequently the model can be used in the practical applications to describe processes of small deformations and small changes of porosity. Little is known about the constitutive functions for nonlinear cases. This is however also the deficiency of the experiments which are available at the present time.

11. Final remarks

The simple examples of the last section have demonstrated how strong must be the simplifying assumptions to lead to the classical results of the theory of porous materials. Almost nothing has been done yet as far as the solutions for large deformations are concerned. At the present stage of research there seems to be a good chance for obtaining the first numerical results in the case of purely mechanical processes in materials with the elastic skeleton and the ideal fluid. However even in this case there are no mathematical results available and the free boundary may yield difficulties connected with the existence of classical solutions.

Even less developed are the models combining the large deformations with non-mechanical variables. Particularly important are here the non-isothermal problems. There exist already the first attempts to incorporate these effects, particularly in connection with the phase transformations (e.g. drying processes in ceramics). The situation is, however, not very satisfactory. The thermal variables connected with the problem of free boundaries yield difficulties with the construction of the model which would contain physically measurable quantities (e.g. see [11]).

On the other hand there seems to be no doubt that the modern continuum theory of mixtures of immiscible components is the only possibility to obtain the mathematical models of porous materials. The purely structural theories may deliver some important hints concerning, for instance, transport coefficients but they are hardly in the position to be applicable in numerous engineering problems of geology, chemistry, acoustics etc. independently of the capacity of future computers. The new chance for the continuum theories is certainly connected with the unified Lagrangian description of all components. Its application in this work has shown that the relatively complex model can be handled without many technical difficulties and the first experience with this description in numerical methods also indicates considerable simplifications.

Appendix: Motivation of the equation for porosity (4.11)

In this Appendix we present the brief semimicroscopical motivation of the balance equation for the porosity (4.11). Mathematical details of the derivation of this equation are rather involved due to the lack of smoothness. We discuss them elsewhere [24].

It is assumed that the skeleton, the solid component of the porous medium, is a continuum on the semimicroscopical level of observation. This means that each point X of the macroscopical manifold $\mathcal{B}$ is connected with a certain time-dependent microstructure $\mathcal{M}_X$ which is schematically shown in Fig. 2.
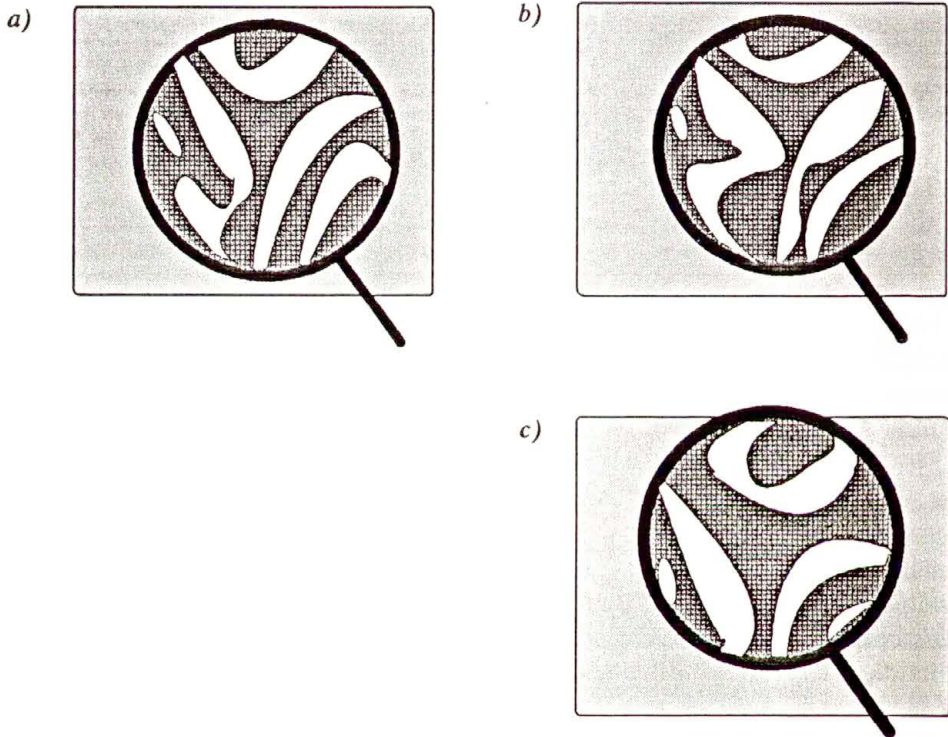
FIG. 2. The semimicroscopical mechanisms yielding the changes of porosity. The centre of the magnifying glass is located in all three cases at the same point X; a) initial microstructure, b) changes of microstructure due to the pore relaxation (micromotion and microsources), c) changes of microstructure due to the macroscopical flux (motion of microstructure relative to the macroscopical skeleton).

The instantaneous geometry of this microstructure is established by the real solid body $\mathcal{B}_{\text{real}}$ embedded for each instant of time in the three-dimensional Euclidean configuration space $\mathcal{R}^3$. The hull which is identical with the closed boundary surface of the geometrical three-dimensional figure $\mathcal{M}_X$ (the frame of the magnifying glass in Fig. 2) is now shifted over the configuration space and the

average properties of the part of the real body contained in the interior of the hull are prescribed to the point of the space $\mathcal{R}^3$ coinciding with a chosen internal point of $\mathcal{M}_X$ (the centre of the magnifying glass in the simple example of Fig. 2) and occupied at the same instant of time by the material point $\mathbf{X}$ of the skeleton. For simplicity one assumes that the shape of the hull does not change in time.

This type of the volume averages are used quite commonly in the theories of bodies with microstructure. For instance the volume averages of material properties of composites are calculated in this way. In the theory of porous materials with diffusion processes there are also numerous attempts in this direction (e.g. F. DOBRAN [31], W.A. GRAY, S.M. HASSANIZADEH [32], J. BEAR, Y. BACHMAT [33]). None of them seems to be yet effective and reliable enough to yield the macroscopical model without any need for additional macroscopical constitutive relations. For this reason we use the above described construction solely to motivate the equation for the porosity.

Instead of constructing averages in the configuration space $\mathcal{R}^3$ we use the procedure on the reference configuration $\mathcal{B}$ of the macroscopical skeleton. This corresponds with our Lagrangian approach.

We seek the equation describing the volume changes of the part of the real skeleton which at a given point $\mathbf{X} \in \mathcal{B}$ and at a given instant of time t lies inside the hull of the figure $\mathcal{M}_X$. The arbitrary point $\mathbf{Y}$ from $\mathcal{M}_X$ can be described by the location vector

$$(A.1) \qquad \mathbf{Y} = \mathbf{X} + \varepsilon\mathbf{Z}, \qquad \mathbf{X} \in \mathcal{B}, \qquad \mathbf{Y} \in \mathcal{M}_X,$$

where ε is the small parameter of the order of the cubic root of the ratio of the volume of microstructure to the characteristic macroscopic volume. If we denote by $\mathcal{H}(., t)$ the characteristic function of the real skeleton contained in $\mathcal{M}_X$

$$(A.2) \qquad \mathcal{H}(\mathbf{Y}, t) = \begin{cases} 1 & \text{for } \mathbf{Y} \text{ belonging to the domain of the real skeleton,} \\ 0 & \text{otherwise,} \end{cases}$$

then the porosity is defined by the relation

$$(A.3) \qquad 1 - n(\mathbf{X}, t) \equiv \frac{1}{V_C} \int\limits_{\mathcal{M}_X} \mathcal{H}(\mathbf{Y}, t)\, dV, \qquad V_C \equiv \int\limits_{\mathcal{M}_X} dV = \text{const},$$

where V_c is sometimes called the control volume of the averaging.

We want to find the time changes of the porosity. The changes of the microscopic geometry of the real skeleton are due to the two factors:

• The redistribution of the real solid material in the domain $\mathcal{M}_X$ due to its microscopic deformation. This may follow from the compressibility of the real material and/or from the microscopic motion of the skeleton inside of this domain which shifts the solid material to the parts of the pore space. Such processes are

not controllable on the macroscopical level and yield the *pore relaxation processes*. They are schematically shown in Fig. 2b. The material of the real skeleton in the microscopic configurations of Fig. 2a and 2b (the interior of the magnifying glass) is the same but its distribution within $\mathcal{M}_X$ has changed due to the above described mechanisms;

• The flux of the real material through the hull of the microstructure into the neighbouring regions of the real body. This is demonstrated in Fig. 2c by the shift of the real material relative to the magnifying glass whose centre still lies in **X**.

The balance equation for the whole microstructure describing these changes of the geometry has the form

$$(A.4) \qquad \frac{\partial}{\partial t} \int_{\mathcal{M}_X} \mathcal{H}(\mathbf{Y}, t)\, dV = \oint_{\mathcal{M}_X} \mathcal{H}(\mathbf{Y}, t)\mathbf{v}_{\mathrm{real}}^S \cdot \mathbf{n}\, dA + \int_{\mathcal{M}_X} \widehat{\mathcal{H}}(\mathbf{Y}, t)\, dV,$$

where $\mathbf{v}_{\mathrm{real}}^S$ denotes the velocity field for the points occupied in the microstructure by the real skeleton. This field is highly singular and usually cannot be integrated to describe any smooth trajectories (see: [24]). The operations performed on the above equation, which must be understood in the distributional sense, require certain additional smoothing procedures which we do not present in this Appendix. The vector **n** is the outward normal vector of the boundary of the microstructure $\partial\mathcal{M}_X$ and $\widehat{\mathcal{H}}(\mathbf{Y}, t)$ is the intensity of the source of the domain occupied by the real skeleton. The latter is due to the changes of the volume of the real skeleton in the microstructure caused by the changes of the real mass density of the skeleton (see: Fig. 2b).

The surface integral in (A.4) can be transformed into the volume integral under the above mentioned smoothing procedures. Subsequently we apply the *multiscaling* indicated by the relation (A.1) and obtain

$$(A.5) \qquad \oint_{\mathcal{M}_X} \mathcal{H}(\mathbf{Y}, t)\mathbf{v}_{\mathrm{real}}^S \cdot \mathbf{n}\, dA = \mathrm{Div}_X \int_{\mathcal{M}_X} \mathcal{H}(\mathbf{X}, \mathbf{Z}, t)\mathbf{v}_{\mathrm{real}}^S(\mathbf{X}, \mathbf{Z}, t)\, dV_Z$$

$$+ \varepsilon \int_{\mathcal{M}_X} \mathrm{Div}_Z(\mathcal{H}(\mathbf{X}, \mathbf{Z}, t)\mathbf{v}_{\mathrm{real}}^S(\mathbf{X}, \mathbf{Z}, t))\, dV_Z,$$

where the differentiation and integration with respect to the microvariable **Z** has been separated from the differentiation with respect to the macroscopical Lagrange variable **X**.

The first term on the right-hand side of this relation describes the macroscopical flux of the porosity defined by the relation (A.3). Simultaneously the second term follows from the microscopical motions of the real skeleton within the microstructure and contributes to the pore relaxation processes – independently of the fact whether the real components are assumed to be compressible or incompressible.

Consequently, if we introduce the notation

$$- \mathbf{J}(\mathbf{X}, t) = \frac{1}{V_C} \left\{ \int_{\mathcal{M}_X} \mathcal{H}(\mathbf{X}, \mathbf{Z}, t) \mathbf{v}_{\text{real}}^S(\mathbf{X}, \mathbf{Z}, t) \, dV_Z \right\},$$

$$(\text{A.6}) \qquad - \hat{n}(\mathbf{X}, t) = \frac{1}{V_C} \left\{ \varepsilon \int_{\mathcal{M}_X} \text{Div}_Z \mathcal{H}(\mathbf{X}, \mathbf{Z}, t) \mathbf{v}_{\text{real}}^S(\mathbf{X}, \mathbf{Z}, t) \, dV_Z \right\}$$

$$+ \frac{1}{V_C} \left\{ \int_{\mathcal{M}_X} \hat{\mathcal{H}}(\mathbf{X}, \mathbf{Z}, t) \, dV_Z \right\},$$

we obtain from the equation (A.4) the balance equation of the porosity (4.11).

The above considerations must be considered solely as the clarification of certain microscopical mechanisms yielding the "internal" variables and the motivation of this balance equation and not as its derivation because, apart from the above mentioned smoothness problems, the relations of this Appendix are not effective if we do not have the full set of microscopical field equations. The problem must be still closed by constitutive relations and this is obviously simpler on the macroscopical level as we have done in the paper.

Acknowledgement

References

1. J. BEAR, *Dynamics of fluids in porous media*, Dover Publications, Inc., N.Y. 1988.

2. R.M. BOWEN, *Diffusion models implied by the theory of mixtures*, [in:] Rational Thermodynamics, C. TRUESDELL [Ed.], Second Edition, 237–263, Springer-Verlag, N.Y. 1984.

3. R. DE BOER, *Highlights in the historical development of the porous media theory – towards a consistent theory*, Appl. Mech. Rev., 1995 [to appear].

4. S.L. PASSMAN, J.W. NUNZIATO and E.K. WALSH, *A theory of multiphase mixtures*, [in:] Rational Thermodynamics, C. TRUESDELL [Ed.], Second Edition, 286–325, Springer-Verlag, N.Y. 1984.

5. T. BOURBIE, O. COUSSY and B. ZINSZNER, *Acoustics of porous media*, Editions Technip, Paris 1987.

6. R.M. BOWEN, *Incompressible porous media models by use of the theory of mixtures*, Int. J.Engng. Sci., **18**, 1129–1148, 1980.

7. J.J. VAN DEEMTER and E.R. VAN DER LAAN, *Momentum and energy balances for dispersed two-phase flow*, Appl. Sci. Res., **A10**, 102–108, 1961.

8. J.O. HINZE, *Momentum and mechanical-energy balance equations for a flowing homogeneous suspension with slip between the two phases*, Appl. Sci. Res., **A11**, 33–46, 1962.

9. R.S. SAMPAIO and W.O. WILLIAMS, *Thermodynamics of diffusing mixtures*, J.de Mechanique, **18**, 19–45, 1979.

10. J.L.W. MORLAND, *A simple constitutive theory for a fluid-saturated porous solid*, J. Geophys. Res., **77**, 890–900, 1972.

11. K. WILMAŃSKI, *Lagrangean model of two-phase porous material*, J. Non-Equilibrium Thermodyn., **20**, 50–77, 1995.

12. J. BLUHM, Habilitation Thesis, University of Essen, Germany, 1996 [in preparation].

13. M.A. GOODMAN, S.C. COWIN, *A continuum theory for granular materials*, Arch. Rat. Mech. Anal., **44**, 249–266, 1972.

14. J.W. NUNZIATO and E.K. WALSH, *On ideal multiphase mixtures with chemical reactions and diffusion*, Arch. Rat. Mech. Anal., **73**, 285–311, 1980.

15. D.S. DRUMHELLER and A. BEDFORD, *A thermomechanical theory for reacting immiscible mixtures*, Arch. Rat. Mech. Anal., **73**, 257–284, 1980.

16. A. BEDFORD and D.S. DRUMHELLER, *Recent advances: theories of immiscible and structured mixtures*, Int. J. Engng. Sci., **21**, 8, 863–960, 1983.

17. S.L. PASSMAN, *Mixtures of granular materials*, Int. J. Engng. Sci., **15**, 117–129, 1977.

18. J. BLUHM, R. DE BOER and K. WILMAŃSKI, *The thermodynamic structure of the two-component model of porous incompressible materials with true mass densities*, Mechanics Research Comm., **22**, 2, 171–180, 1995.

19. K. WILMAŃSKI, *Acceleration waves in two-component porous media. Part I. The model and speeds of propagation*, MECH-Bericht 94/1, 1-23, Universität-GH Essen, Essen 1994.

20. R.M. BOWEN, *Compressible porous media models by use of the theory of mixtures*, Int. J. Engng. Sci., **20**, 697–763, 1982.

21. J.E. ADKINS, *Diffusion of fluids through aeolotropic highly elastic solids*, Arch. Rat. Mech. Anal., **15**, 222–234, 1964.

22. A.E. GREEN and J.E. ADKINS, *A contribution to the theory of non-linear diffusion*, Arch. Rat. Mech. Anal., **15**, 235–246, 1964.

23. J. KUBIK, *Large elastic deformations of fluid-saturated porous solid*, J. de Mechanique theorique et appliquee, Numero spécial, 203–218, 1982.

24. K. WILMAŃSKI, *The thermodynamical model of the compressible porous material with the balance equation for porosity*, J. Non-Equilibrium Thermodyn. [to appear, 1996].

25. K. WILMAŃSKI, *Two-component compressible porous materials – the construction of the thermodynamical model*, MECH-Bericht 95/1, 1–24. Universität-GH Essen, Essen 1995.

26. K. WILMAŃSKI, *Skeleton as reference for two-phase porous materials*, Mech-Bericht 93/5, 1–23, Universität-GH Essen, Essen 1993.

27. K. WILMAŃSKI, *On weak discontinuity waves in porous materials*, [in:] Trends in Applications of Mathematics to Mechanics, J. RODRIGUES [Ed.], Longman Scientific & Technical, Essex 1995.

28. K. WILMAŃSKI, *Acceleration waves in two-component porous media. Part II. Supplementary remarks on the model and the evolution equation of amplitudes*, MECH-Bericht 95/2, 1-20 Universität-GH Essen, Essen 1995.

29. K. WILMAŃSKI, *Quasi-static plane-strain problems of the linear porous material*, MECH-Bericht 95/7, 1-19, Universität-GH Essen, Essen 1995.

30. W. KEMPA, *Das Grenzwertproblem bei Konsolidation – eine konsistente Konstruktion der schwachen Formulierung*, MECH-Bericht 95/13, Universität-GH Essen, Essen 1995.

31. F. DOBRAN, *Theory of structured multiphase mixtures*, Springer-Verlag, Berlin 1991.

32. W.A. GRAY and S.M. HASSANIZADEH, *Averaging theorems and averaged equations for transport of interface properties in multiphase systems*, Int. J. Multiphase Flow, 15, 81–95, 1989.

33. J. BEAR and Y. BACHMAN, *Transport phenomena in porous media – basic equations*, [in:] Fundamentals of Transport Phenomena in Porous Media, NATO ASI Series, Series E: Applied Sciences, 82, 5–61, 1984.

INSTITUT FÜR MECHANIK, FB 10
UNIVERSITÄT-GH ESSEN, GERMANY.

Double-diffusive convection in compressible fluids with suspended particles in porous medium

R. C. SHARMA (SHIMLA), TRILOK CHAND (NALAGARH)
and V. K. BHARDWAJ (SHIMLA)

THE DOUBLE-DIFFUSIVE convection in compressible fluids with suspended particles in porous medium is considered. The suspended particles are found to have destabilizing effect whereas stable solute gradient, rotation and compressibility have stabilizing effect on the system. The medium permeability has a destabilizing effect in the absence of rotation but has both stabilizing and destabilizing effects in the presence of rotation. The stable solute gradient and rotation are found to introduce oscillatory modes in the system which are non-existent in their absence.

1. Introduction

THE PROBLEM of thermosolutal convection in fluids in a porous medium is of importance in geophysics, soil sciences, ground-water hydrology and astrophysics. The development of geothermal power resources holds increased general interest in the study of the properties of convection in porous media. The scientific importance of the field has also increased because hydrothermal circulation is the dominant heat transfer mechanism in the development of young oceanic crust (LISTER [3]). Generally it is accepted that comets consist of a dusty "snowball" of a mixture of frozen gases which, in the process of their journey, changes from solid to gas and *vice-versa*. The physical properties of comets, meteorites and interplanetary dust strongly suggest the importance of porosity in the astrophysical context. A mounting evidence, both theoretical and experimental, suggests that Darcy's equation provides an unsatisfactory description of the hydrodynamic conditions, particularly near the boundaries of a porous medium. BEAVERS *et al.* [10] have experimentally demonstrated the existence of shear within the porous medium near surface, where the porous medium is exposed to a freely flowing fluid, thus forming a zone of shear-induced flow field. The Darcy's equation however, cannot predict the existence of such a boundary zone, since no macroscopic shear term is included in this equation (JOSEPH and TAO [11]). To be mathematically compatible with the Navier–Stokes equations and physically consistent with the experimentally observed boundary shear zone mentioned above, Brinkman proposed the introduction of the term $\dfrac{\mu}{\varepsilon}\nabla^2 \mathbf{V}$ in addition to $-\left(\dfrac{\mu}{k_1}\right)\mathbf{V}$ in the equations of fluid motion. The elaborate statistical justification of the Brinkman equations has been presented by SAFFMAN [12] and LUNDGREN [13]. STOMMEL and FEDOROV [14] and LINDEN [2] have remarked that the length scales characteristic of double-diffusive convecting layers in the ocean could be sufficiently large for Earth's rotation to

become important in their formation. Moreover, the rotation of the Earth distorts the boundaries of a hexagonal convection cell in a fluid flowing through a porous medium, and the distortion plays an important role in the extraction of energy in the geothermal regions. Brakke [1] explained a double-diffusive instability that occurs when a solution of a slowly diffusing protein is laid over a denser solution of more rapidly diffusing sucrose. Nason *et al.* [5] found that this instability, which is deleterious to certain biochemical separations, can be suppressed by rotation in the ultracentrifuge. Scanlon and Segel [6] have studied the effect of suspended particles on the onset of thermal convection.

The conditions under which convective motions in double-diffusive convection are important (e.g. in lower parts of the Earth's atmosphere, astrophysics and several geophysical situations) are usually far removed from the consideration of a single component fluid and rigid boundaries and therefore, it is desirable to consider a fluid acted on by solute gradient and free boundaries. The compressibility and suspended particles are important in such situations. Sharma and Sharma [7] and Sharma and Veena Kumari [8] have considered the thermosolutal convection in porous medium under varying assumptions of hydrodynamics and hydromagnetics.

Keeping in mind the importance in geophysics, astrophysics and various applications mentioned above, the thermosolutal convection in compressible fluids with suspended particles in a porous medium, in the absence and presence of a uniform rotation, separately, has been considered in the present paper.

2. Formulation of the problem and perturbation equations

Consider an infinite horizontal, compressible fluid-particle layer of thickness d bounded by the planes $z = 0$ and $z = d$ in a porous medium of porosity ε and permeability k_1. This layer is heated from below and subjected to a stable solute gradient such that steady adverse temperature gradient $\beta(= |dT/dz|)$ and a solute concentration gradient $\beta'(= |dC/dz|)$ are maintained.

Let ϱ, μ, p and $\mathbf{V}(u, v, w)$ denote respectively the density, viscosity, pressure and filter velocity of the pure fluid; $\mathbf{V}_d(\overline{x}, t)$ and $N(\overline{x}, t)$ denote filter velocity and number density of the particles, respectively. If g is acceleration due to gravity, $K = 6\pi\varrho\nu\varepsilon'$ where ε' is the particle radius, $\mathbf{V}_d = (l, r, s)$, $\overline{x} = (x, y, z)$ and $\lambda_1 = (0, 0, 1)$, then the equation of motion and continuity for the fluid are

$$(2.1) \qquad \frac{\varrho}{\varepsilon}\left[\frac{\partial \mathbf{V}}{\partial t} + \frac{1}{\varepsilon}(\mathbf{V}\cdot\nabla)\mathbf{V}\right] = -\nabla p - \varrho g\lambda_1 + \left(\frac{\mu}{\varepsilon}\nabla^2 - \frac{\mu}{k_1}\right)\mathbf{V} + \frac{KN}{\varepsilon}(\mathbf{V}_d - \mathbf{V}),$$

$$(2.2) \qquad \left(\varepsilon\frac{\partial}{\partial t} + \mathbf{V}\cdot\nabla\right)\varrho + \varrho\nabla\cdot\mathbf{V} = 0.$$

Since the distances between particles are assumed to be quite large compared with their diameter, the interparticle relations, buoyancy force, Darcian force and

pressure force on the particles are ignored. Therefore the equations of motion and continuity for the particles are

$$(2.3) \qquad mN \left[\frac{\partial \mathbf{V}_d}{\partial t} + \frac{1}{\varepsilon} (\mathbf{V}_d \cdot \nabla) \mathbf{V}_d \right] = KN(\mathbf{V} - \mathbf{V}_d),$$

$$(2.4) \qquad \varepsilon \frac{\partial N}{\partial t} + \nabla \cdot (N \mathbf{V}_d) = 0.$$

Let c_v, c_p, c_{pt}, T, C and q denote respectively the heat capacity of fluid at constant volume, heat capacity of fluid at constant pressure, heat capacity of particles, temperature, solute concentration and "effective thermal conductivity" of the clean fluid. Let c'_v, c'_{pt} and q' denote the analogous solute coefficients. When particles and the fluid are in thermal and solute equilibrium, the equations of heat and solute conduction give

$$(2.5) \qquad [\varrho c_v \varepsilon + \varrho_s c_s (1 - \varepsilon)] \frac{\partial T}{\partial t} + \varrho c_v (\mathbf{V} \cdot \nabla) T$$

$$+ mN c_{pt} \left(\varepsilon \frac{\partial}{\partial t} + \mathbf{V}_d \cdot \nabla \right) T = q \nabla^2 T,$$

$$(2.6) \qquad [\varrho c'_v \varepsilon + \varrho_s c'_s (1 - \varepsilon)] \frac{\partial C}{\partial t} + \varrho c'_v (\mathbf{V} \cdot \nabla) C$$

$$+ mN c'_{pt} \left(\varepsilon \frac{\partial}{\partial t} + \mathbf{V}_d \cdot \nabla \right) C = q' \nabla^2 C,$$

where ϱ_s, c_s are the density and heat capacity of the solid matrix, respectively.

SPIEGEL and VERONIS [9] have expressed any state variable (pressure, density or temperature), say X, in the form

$$X = X_m + X_0(z) + X'(x, y, z, t),$$

where X_m stands for the constant space distribution of X, X_0 is the variation in X in the absence of motion, and $X'(x, y, z, t)$ stands for the fluctuations in X due to the motion of the fluid. Following SPIEGEL and VERONIS [9], we have

$$T(z) = -\beta z + T_0,$$

$$p(z) = p_m - g \int_0^z (\varrho_m + \varrho_0) \, dz,$$

$$\varrho(x) = \varrho_m \left[1 - \alpha(T - T_m) + \alpha'(C - C_m) + \alpha''(p - p_m) \right],$$

$$\alpha = -\left(\frac{1}{\varrho} \frac{\partial \varrho}{\partial T} \right), \qquad \alpha' = \left(\frac{1}{\varrho} \frac{\partial \varrho}{\partial C} \right), \qquad \alpha'' = \left(\frac{1}{\varrho} \frac{\partial \varrho}{\partial p} \right).$$

Thus p_m, ϱ_m stand for the constant space distribution of p and ϱ and T_0, ϱ_0 stand for the temperature and density of the fluid at the lower boundary (and in the absence of motion).

Since density variations are mainly due to variations in temperature and solute concentration, Eqs. (2.1) – (2.6) must be supplemented by the equation of state

$$(2.6') \qquad \varrho(z) = \varrho_m \left[1 - \alpha(T - T_m) + \alpha'(C - C_m) \right].$$

Let $\delta\varrho$, δp, θ, γ, $\mathbf{V}$, $\mathbf{V}_d$ and N denote the perturbations in fluid density ϱ, pressure p, temperature T, solute concentration C, fluid velocity $(0,0,0)$, particles velocity $(0,0,0)$ and particle number density N_0, respectively. Then the linearized perturbation equations, under the Spiegel and Veronis assumptions, are

$$(2.7)$$

$$\frac{1}{\varepsilon}\frac{\partial \mathbf{V}}{\partial t} = -\frac{1}{\varrho_m}\nabla\delta p - g\left(\frac{\delta\varrho}{\varrho_m}\right)\boldsymbol{\lambda}_1 + \left(\frac{\nu}{\varepsilon}\nabla^2 - \frac{\nu}{k_1}\right)\mathbf{V} + \frac{KN_0}{\varrho_m\varepsilon}(\mathbf{V}_d - \mathbf{V}),$$

$$\nabla\cdot\mathbf{V} = 0,$$

$$mN_0\frac{\partial \mathbf{V}_d}{\partial t} = KN_0(\mathbf{V} - \mathbf{V}_d),$$

$$\varepsilon\frac{\partial N}{\partial t} + \nabla\cdot(N_0\mathbf{V}_d) = 0,$$

$$(E + h\varepsilon)\frac{\partial \theta}{\partial t} = \left(\beta - \frac{g}{c_p}\right)(w + hs) + \kappa\nabla^2\theta,$$

$$(E' + h'\varepsilon)\frac{\partial \gamma}{\partial t} = \beta'(w + h's) + \kappa\nabla^2\gamma.$$

Here

$$E = \varepsilon + (1 - \varepsilon)\frac{\varrho_s c_s}{\varrho_m c_v}, \qquad E' = \varepsilon + (1 - \varepsilon)\frac{\varrho_s c'_s}{\varrho_m c'_v},$$

$$h = f\frac{c_{pt}}{c_v}, \qquad h' = f\frac{c'_{pt}}{c'_v}, \qquad f = \frac{mN_0}{\varrho_m}, \qquad \kappa = \frac{q}{\varrho_m c_v}, \qquad \kappa' = \frac{q'}{\varrho_m c'_v}$$

and

$$\delta\varrho = -\varrho_m(\alpha\theta - \alpha'\gamma).$$

Using d, d^2/κ, κ/d, $\varrho\nu\kappa/d^2$, βd and $\beta' d$ to denote the length, time, velocity, pressure, temperature and solute concentration scale factors, respectively, the linearized dimensionless perturbation equations become

$$(2.8) \qquad p_1^{-1}\frac{\partial \mathbf{V}^*}{\partial t^*} = -\nabla^*\delta p^* + R\theta^*\boldsymbol{\lambda}_1 - S\gamma^*\boldsymbol{\lambda}_1 + \left(\frac{1}{\varepsilon}\nabla^{*2} - \frac{1}{P}\right)\mathbf{V}^* + \omega(\mathbf{V}_d^* - \mathbf{V}^*),$$

$$(2.9) \qquad \nabla^*\cdot\mathbf{V}^* = 0,$$

$$(2.10) \qquad \left(\tau\frac{\partial}{\partial t^*} + 1\right)\mathbf{V}_d^* = \mathbf{V}^*,$$

$$(2.11) \qquad \left(\frac{\partial M}{\partial t^*} + \nabla^*\cdot\mathbf{V}_d^*\right) = 0,$$

(2.12)
$$(E + h\varepsilon)\frac{\partial\theta^*}{\partial t^*} = \frac{G-1}{G}(w^* + hs^*) + \nabla^{*2}\theta^*,$$

$$(E' + h'\varepsilon)\frac{\partial\gamma^*}{\partial t^*} = (w^* + h's^*) + \frac{1}{\lambda}\nabla^{*2}\gamma^*,$$

where

$$P = \frac{k_1}{d^2}, \qquad G = \frac{c_p\beta}{g}, \qquad p_1 = \frac{\varepsilon\nu}{\kappa}, \qquad R = \frac{g\alpha\beta d^4}{\nu\kappa}, \qquad S = \frac{g\alpha'\beta' d^4}{\nu\kappa'},$$

$$M = \frac{\varepsilon N}{N_0}, \qquad \omega = \frac{K N_0 d^2}{\varrho_m\nu\varepsilon}, \qquad \tau = \frac{m\kappa}{K d^2}, \qquad f = \frac{m N_0}{\varrho_m} = \tau\omega p \quad \text{and} \quad \lambda = \frac{\kappa}{\kappa'},$$

and starred (*) quantities are expressed in dimensionless form. Hereafter, we suppress the stars for convenience.

Eliminating $\mathbf{V}_d$ from Eq. (2.8) with the help of (2.10) and then eliminating u, v, δp from the three scalar equations of (2.8), and using (2.9), we obtain

(2.13)
$$\left[L_1 - L_2\left(\frac{1}{\varepsilon}\nabla^2 - \frac{1}{p}\right)\right]\nabla^2 w = L_2(R\nabla_1^2\theta - S\nabla_1^2\gamma),$$

$$L_2\left[(E + h\varepsilon)\frac{\partial}{\partial t} - \nabla^2\right]\theta = \left(\frac{G-1}{G}\right)\left(\tau\frac{\partial}{\partial t} + H\right)w,$$

$$L_2\left[(E' + h'\varepsilon)\frac{\partial}{\partial t} - \frac{1}{\lambda}\nabla^2\right]\gamma = \left(\tau\frac{\partial}{\partial t} + H'\right)w,$$

where

$$L_1 = p_1^{-1}\left(\tau\frac{\partial^2}{\partial t^2} + F\frac{\partial}{\partial t}\right), \qquad L_2 = \left(\tau\frac{\partial}{\partial t} + 1\right), \qquad \nabla_1^2 = \frac{\partial^2}{\partial x^2} + \frac{\partial^2}{\partial y^2},$$

$$\nabla^2 = \frac{\partial^2}{\partial x^2} + \frac{\partial^2}{\partial y^2} + \frac{\partial^2}{\partial z^2}, \qquad F = f + 1, \qquad H = h + 1, \qquad H' = h' + 1.$$

Decomposing the perturbations into normal modes by seeking solutions in the form of functions of x, y and t

(2.14) $[w, \theta, \gamma] = [W(z), \Theta(z), \Gamma(z)]\exp(ik_x x + ik_y y + nt),$

where n is, in general, complex, and $k = (k_x^2 + k_y^2)^{1/2}$ is the wave number of disturbance.

Eliminating θ, γ between Eqs. (2.13) and using expression (2.14), we obtain

(2.15)
$$\left[L_1 + \frac{L_2}{P} - \frac{L_2}{\varepsilon}(D^2 - k^2)\right]\left[D^2 - k^2 - n(E + h\varepsilon)\right]$$

$$\cdot\left[D^2 - k^2 - \lambda n(E' + h'\varepsilon)\right](D^2 - k^2)W$$

$$= \left(\frac{G-1}{G}\right)(\tau n + H)Rk^2\left[D^2 - k^2 - \lambda n(E' + h'\varepsilon)\right]W$$

$$-\lambda(\tau n + H')Sk^2\left[D^2 - k^2 - n(E + h\varepsilon)\right]W,$$

where

$$L_1 = p_1^{-1}(\tau n^2 + Fn),$$

$$L_2 = \tau n + 1 \quad \text{and} \quad D = \frac{d}{dz}.$$

3. Principle of exchange of stabilities and oscillatory modes

Let

(3.1) $U = (D^2 - k^2)W \quad \text{and} \quad X = \left[L_1 + \frac{L_2}{P} - \frac{L_2}{\varepsilon}(D^2 - k^2)\right] U.$

In terms of X, the equation satisfied by W is

(3.2) $\left[D^2 - k^2 - n(E + h\varepsilon)\right]\left[D^2 - k^2 - \lambda n(E' + h'\varepsilon)\right] X$

$$= k^2 \left(\frac{G-1}{G}\right) R(\tau n + H)\left[D^2 - k^2 - \lambda n(E' + h'\varepsilon)\right] W$$

$$-\lambda k^2 S(\tau n + H')\left[D^2 - k^2 - n(E + h\varepsilon)\right] W.$$

Consider the case of two free surfaces having uniform temperature and solute concentration. The boundary conditions appropriate for the problem are

(3.3) $W = D^2 W = 0, \quad \Theta = \Gamma = 0 \quad \text{at} \quad z = 0 \text{ and } 1.$

Multiplying Eq. (3.2) by X^*, the complex conjugate of X, integrating over the range of z and using the boundary conditions (3.3), we obtain

(3.4) $I_1 + n\left[(E + h\varepsilon) + \lambda(E' + h'\varepsilon)\right] I_2 + \lambda n^2(E + h\varepsilon)(E' + h'\varepsilon)I_3$

$$= k^2 \left(\frac{G-1}{G}\right) R(\tau n + H)\left(L_1^* + \frac{L_2^*}{P}\right)[I_4 + \lambda n(E' + h'\varepsilon)I_5]$$

$$-\lambda k^2 S(\tau n + H')\left(L_1^* + \frac{L_2^*}{P}\right)[I_4 + \lambda n(E + h'\varepsilon)I_5]$$

$$+k^2 \frac{L_2^*}{\varepsilon}\left[\left(\frac{G-1}{G}\right)R(\tau n + H) - \lambda S(\tau n + H')\right]I_6$$

$$+k^2\lambda n\frac{L_2^*}{\varepsilon}\left[\left(\frac{G-1}{G}\right)R(\tau n + H)(E' + h'\varepsilon) - S(\tau n + H')(E + h\varepsilon)\right]I_7,$$

where

$$I_1 = \int_0^1 (|D^2 X|^2 + 2k^2|DX|^2 + k^4|X|^2)dz,$$

$$I_2 = \int_0^1 (|DX|^2 + k^2|X|^2)dz,$$

$$I_3 = \int_0^1 (|X|^2)dz,$$

(3.5)

$$I_4 = \int_0^1 (|U|^2)dz,$$

$$I_5 = \int_0^1 (|DW|^2 + k^2|W|^2)dz,$$

$$I_6 = \int_0^1 (|DU|^2 + k^2|U|^2)dz,$$

$$I_7 = \int_0^1 (|D^2 W|^2 + 2k^2|DW|^2 + k^4|W|^2)dz.$$

The integrals $I_1 - I_7$ are all positive definite.

Putting $n = in_0$, where n_0 is real, into Eq. (3.4) and equating imaginary parts, we obtain

(3.6) $$n_0^2 = \left\{ [(E + h\varepsilon) + \lambda(E' + h'\varepsilon)] I_2 + k^2 \left[\left(\frac{G-1}{G} \right) R \left(\frac{HF}{p_1} + \frac{\tau h}{P} \right) \right. \right.$$
$$\left. - \lambda S \left(\frac{H'F}{p_1} + \frac{\tau h'}{P} \right) \right] I_4 + \lambda k^2 \left[S(E + h\varepsilon)H' - \left(\frac{G-1}{G} \right) R(E' + h'\varepsilon)H \right]$$
$$\cdot \left(\frac{I_5}{P} + \frac{I_7}{\varepsilon} \right) + \frac{\tau k^2}{\varepsilon} \left[\left(\frac{G-1}{G} \right) Rh - \lambda Sh' \right] I_6 \right\}$$
$$\left/ \left\{ \lambda k^2 \left[- \left(\frac{G-1}{G} \right) R(E' + h'\varepsilon) \left\{ \frac{\tau(f-h)}{p_1} + \frac{\tau^2}{P} \right\} \right. \right. \right.$$
$$+ S(E + h\varepsilon) \left\{ \frac{\tau(f-h)}{.\ \ p_1} + \frac{\tau^2}{P} \right\} \right] I_5 + \frac{k^2 \tau^2}{p_1} \left\{ \left(\frac{G-1}{G} \right) R - \lambda S \right\} I_4$$
$$+ \frac{k^2 \tau^2 \lambda}{\varepsilon} \left[- \left(\frac{G-1}{G} \right) R(E' + h'\varepsilon) + S(E + h\varepsilon) \right] I_7 \right\},$$

or

(3.7) $n_0 = 0.$

In the absence of stable solute gradient, Eqs. (3.6) and (3.7) become

(3.8) $n_0^2 = - \dfrac{\left(\dfrac{G}{G-1}\right)(E + h\varepsilon)I_2 + k^2 R\left\{p_1^{-1} H F + \dfrac{\tau h}{P}\right\} I_4 + \dfrac{k^2 \tau}{\varepsilon} R h I_6}{k^2 \tau^2 R p_1^{-1} I_4},$

or

(3.9) $n_0 = 0.$

Since the integrals are positive definite and n_0 is real, it follows that $n_0 = 0$ and the principle of exchange of stabilities is satisfied, in the absence of stable solute gradient. In the presence of stable solute gradient, the principle of exchange of stabilities is not satisfied and oscillatory modes come into play. The stable solute gradient, thus, introduces oscillatory modes which were non-existent in its absence.

4. Dispersion relation and discussion

When instability sets in as stationary convection, the marginal state will be characterized by $n = 0$ and Eq. (2.15) reduces to

(4.1) $\left[\dfrac{1}{P} - \dfrac{1}{\varepsilon}(D^2 - k^2)\right](D^2 - k^2)^2 W = \left(\dfrac{G-1}{G}\right) k^2 R H W - \lambda k^2 S H' W.$

Considering the case of two free boundaries, it can be shown that all the even order derivatives of W vanish on the boundaries and hence the proper solution of Eq. (4.1) characterizing the lowest mode is

(4.2) $W = W_0 \sin \pi z,$

where W_0 is a constant. Substituting the solution (4.2) in Eq. (4.1), we obtain

(4.3) $R = \dfrac{\left(\dfrac{G}{G-1}\right)\left[\left(\dfrac{1}{P} + \dfrac{\pi^2 + k^2}{\varepsilon}\right)(\pi^2 + k^2)^2 + \lambda k^2 H' S\right]}{k^2 H}.$

If R_c denotes the critical Rayleigh number in the absence of compressibility and $\overline{R}_c$ stands for the critical Rayleigh number in the presence of compressibility, then we find that

$$\overline{R}_c = \left(\dfrac{G}{G-1}\right) R_c.$$

Since critical Rayleigh number is positive and finite, so $G > 1$ and we obtain a stabilizing effect of compressibility as its result is to postpone the onset of double-diffusive convection in a fluid-particle layer of porous medium.

It is evident from Eq. (4.3) that

(4.4)

$$\frac{dR}{dP} = -\left(\frac{G}{G-1}\right)\frac{(\pi^2 + k^2)^2}{k^2 H P^2},$$

$$\frac{dR}{dH} = -\left(\frac{G}{G-1}\right)\frac{\left(\frac{1}{P} + \frac{\pi^2 + k^2}{\varepsilon}\right)(\pi^2 + k^2)^2 + \lambda k^2 H' S}{k^2 H^2},$$

and

(4.5)

$$\frac{dR}{dS} = \lambda\left(\frac{G}{G-1}\right)\frac{H'}{H}.$$

The medium permeability and suspended particles have thus destabilizing effects, whereas the stable solute gradient has a stabilizing effect on the thermosolutal convection in compressible fluids with suspended particles in a porous medium.

5. Effect of rotation

In this section, we consider the same problem as that studied above except that the system is in a state of uniform rotation $\Omega(0, 0, \Omega)$. The Coriolis force acting on the particles is also neglected under the assumptions made in the problem. The linearized nondimensional perturbation equations of motion for the fluid are

(5.1)

$$p_1^{-1}\frac{\partial u}{\partial t} = -\frac{\partial}{\partial x}\delta p + \omega(l - u) + T_A^{1/2}v + \left(\frac{1}{\varepsilon}\nabla^2 - \frac{1}{P}\right)u,$$

$$p_1^{-1}\frac{\partial v}{\partial t} = -\frac{\partial}{\partial y}\delta p + \omega(r - v) - T_A^{1/2}u + \left(\frac{1}{\varepsilon}\nabla^2 - \frac{1}{P}\right)v,$$

$$p_1^{-1}\frac{\partial w}{\partial t} = -\frac{\partial}{\partial z}\delta p + \omega(s - w) + R\theta - S\gamma + \left(\frac{1}{\varepsilon}\nabla^2 - \frac{1}{P}\right)w,$$

where $T_A = \dfrac{4\Omega^2 d^4}{\varepsilon^2 \nu^2}$ is the nondimensional number accounting for rotation, and Eqs. (2.8)–(2.12) remain unaltered.

Eliminating $\mathbf{V}_d(l, r, s)$ with the help of (2.10) and then eliminating u, v, δp between Eqs. (5.1), using (2.9) we obtain

(5.2)

$$\left(L_1 + \frac{L_2}{P} - \frac{L_2}{\varepsilon}\nabla^2\right)^2 \nabla^2 w + L_2^2 T_A\frac{\partial^2 w}{\partial z^2}$$

$$= L_2\left(L_1 + \frac{L_2}{P} - \frac{L_2}{\varepsilon}\nabla^2\right)\nabla_1^2(R\theta - \lambda S\gamma).$$

Eliminating θ and γ between Eqs. $(2.13)_{2,3}$ and (5.2) and using expression (2.14), we get

$$(5.3) \quad \left[D^2 - k^2 - n(E + h\varepsilon)\right]\left[D^2 - k^2 - \lambda n(E' + h'\varepsilon)\right]$$

$$\cdot \left[\left\{L_1 + \frac{L_2}{P} - \frac{L_2}{\varepsilon}(D^2 - k^2)\right\}^2 (D^2 - k^2) + L_2^2 T_A D^2\right] W$$

$$= \left\{L_1 + \frac{L_2}{P} - \frac{L_2}{\varepsilon}(D^2 - k^2)\right\} k^2 \left[\left(\frac{G-1}{G}\right)\left\{D^2 - k^2 - \lambda n(E' + h'\varepsilon)\right\}\right.$$

$$\left. \cdot(\tau n + H)R - \lambda\left\{D^2 - k^2 - n(E + h\varepsilon)\right\}(\tau n + H')S\right] W.$$

For the stationary convection, $n = 0$ and Eq. (5.3) reduces to

$$(5.4) \quad (D^2 - k^2)\left[\left\{\frac{1}{P} - \frac{D^2 - k^2}{\varepsilon}\right\}^2 (D^2 - k^2) + T_A D^2\right] W$$

$$= k^2 \left\{\frac{1}{P} - \frac{D^2 - k^2}{\varepsilon}\right\}\left[\left(\frac{G-1}{G}\right) RH - \lambda SH'\right] W.$$

Considering again the case of two free boundaries with constant temperature and solute concentration and using the proper solution (4.2), we obtain from Eq. (5.4)

$$(5.5) \quad R = \left(\frac{G}{G-1}\right)\left[\frac{\pi^2 + k^2}{k^2 H}\left\{\frac{(\pi^2 + k^2)\left(\frac{1}{P} + \frac{\pi^2 + k^2}{\varepsilon}\right)^2 + \pi^2 T_A}{\left(\frac{1}{P} + \frac{\pi^2 + k^2}{\varepsilon}\right)}\right\} + \lambda S \frac{H'}{H}\right].$$

It is evident from Eq. (5.5) that

$$\frac{dR}{dT_A} = \left(\frac{G}{G-1}\right)\frac{\pi^2(\pi^2 + k^2)}{\left(\frac{1}{P} + \frac{\pi^2 + k^2}{\varepsilon}\right)k^2 H},$$

$$(5.6) \quad \frac{dR}{dH} = -\left(\frac{G}{G-1}\right)(\pi^2 + k^2)\left[\frac{\left(\frac{1}{P} + \frac{\pi^2 + k^2}{\varepsilon}\right)^2 (\pi^2 + k^2) + \pi^2 T_A}{\left(\frac{1}{P} + \frac{\pi^2 + k^2}{\varepsilon}\right)k^2 H^2} + \lambda S \frac{H'}{H^2}\right],$$

$$\frac{dR}{dS} = \lambda\left(\frac{G}{G-1}\right)\frac{H'}{H}.$$

Therefore the suspended particles have a destabilizing effect, whereas the rotation and stable solute gradient have stabilizing effects on the system under consideration.

Equation (5.5) also yields

$$(5.7) \quad \frac{dR}{dP} = \left(\frac{G}{G-1}\right) \frac{(\pi^2 + k^2)}{k^2 H} \left[-\frac{\pi^2 + k^2}{P^2} + \frac{\pi^2 T_A}{P^2 \left(\frac{1}{P} + \frac{\pi^2 + k^2}{\varepsilon}\right)^2} \right].$$

If

$$T_A > \left(1 + \frac{k^2}{\pi^2}\right)\left(\frac{1}{P} + \frac{\pi^2 + k^2}{\varepsilon}\right)^2,$$

then dR/dP is possitive.

If

$$T_A < \left(1 + \frac{k^2}{\pi^2}\right)\left(\frac{1}{P} + \frac{\pi^2 + k^2}{\varepsilon}\right)^2,$$

then dR/dP is negative.

Thus the medium permeability has both stabilizing and destabilizing effects, depending on the rotation parameter, on the thermosolutal convection in a compressible fluid with suspended particles rotating in a porous medium.

References

1. M.K. Brakke, Arch. Biochem. Biophysics, 55, 175, 1955.
2. P.F. Linden, Geophys. Fluid Dynamics, 6, 1, 1974.
3. C.R.B. Lister, Geophys. J. Roy. Astr. Soc., 26, 515, 1972.
4. J.A.M. McDonnel, Cosmic dust, John Wiley and Sons, Toronto, p. 330, 1978.
5. P. Nason, V. Schumaker, B. Halsall and J. Schwedes, Biopolymers, 7, 241, 1969.
6. J.W. Scanlon and L.A. Segel, Phys. Fluids, 16, 1573, 1973.
7. R.C. Sharma and K.N. Sharma, J. Math. Phys. Sci., 16, 167, 1982.
8. R.C. Sharma and V. Kumari, Japan J. Industrial Appl. Math., 9, 79, 1992.
9. E.A. Spiegel and G. Veronis, Astrophys. J., 131, 442, 1960.
10. G.S. Beavers, E.M. Sparrow and R.A. Magnuson, J. Basic Engng. Trans. ASME, D92, 843, 1970.
11. D.D. Joseph and L.N. Tao, Zeit. Angew. Math. Mech., 44, 361, 1964.
12. P.G. Saffman, Stud. Appl. Math., 50, 93, 1971.
13. T.S. Lundgren, J. Fluid Mech., 51, 273, 1972.
14. H. Stommel and K.N. Fedorov, Tellus, 19, 306, 1967.

DEPARTMENT OF MATHEMATICS, GOVT. COLLEGE, NALAGARH,
DEPARTMENT OF MATHEMATICS, ST. BEDES COLLEGE, SHIMLA
and
DEPARTMENT OF MATHEMATICS
HIMACHAL PRADESH UNIVERSITY, SHIMLA, INDIA.

Stability of the wall jet formed by the impingement of a single-phase jet

İ. B. ÖZDEMİR (İSTANBUL)

THIS PAPER DESCRIBES a theoretical investigation of the possibility that the large structures of the wall jet flow formed after oblique impingement of an axisymmetric jet were generated by the flow instabilities, so that the experimentally reported discrete frequencies were synonymous with instability modes. The wall jet flow was triple-decomposed into a time-independent, pseudolaminar motion defined by the time-averaged velocity field, upon which incoherent and coherent turbulent fluctuations were superimposed. Solution of the inviscid, one-dimensional flow equations with large coherent structures, which were modelled by spatially evolving waves, was given in detail and revealed that the distribution of the radial fluctuation intensity and the frequency of large structures compare well with the experiments justifying the deterministic nature of the coherent motion.

Notations

Symbols

A_p, A_r, A_z, A_ϕ	amplitude modulation functions,
f	real-valued frequency,
$\mathcal{F}(f)$	complex amplitude of the rotating vector defined in Eq. (4.2),
H	nozzle-to-plate distance,
i	$\sqrt{-1}$,
m	real-valued azimuthal wavenumber,
p	parameter defined in Eq. (3.2),
$\tilde{p}$	coherent pressure fluctuation,
p'	incoherent pressure fluctuation,
P	instantaneous value of pressure,
$\overline{P}$	time-averaged value of pressure,
$\mathbb{P}(f)$	total power associated with frequency f,
r	radial coordinate defined from geometrical impingement point,
r_w	wetted radius defined in Eq. (2.3),
Re	Reynolds number,
s	parameter defined in Eq. (3.1),
t	time,
$\tilde{u}_r, \tilde{u}_z, \tilde{u}_\phi$	components of coherent velocity fluctuations in three directions,
u'_r, u'_z, u'_ϕ	components of incoherent velocity fluctuations in three directions,
U_r, U_z, U_ϕ	components of instantaneous velocity field in three directions,
$\overline{U}_r, \overline{U}_z, \overline{U}_\phi$	components of time-averaged velocity field in three directions,
$\overline{U}_{r,M}$	maximum of the time-averaged radial velocity component,
z	coordinate normal to the plate,
$z_{0.5}$	wall distance at which time-averaged radial velocity attains half of the maximum value,
$(\ )^*$	superscript refers to nondimensional form of variables.

Greek Symbols

α complex-valued wavenumber,
α_i imaginary part of α,
α_r real part of α,
β real-valued circular frequency $(2\pi f)$,
η parameter defined in Eq. (3.1),
γ half-cone angle of the inflowing jet,
λ wavelength of the educed coherent structures,
ν kinematic viscosity of the air,
ϕ azimuthal coordinate,
ϱ density of the air,
σ parameter defined in Eq. (3.2),
θ angle of impingement,
ζ parameter defined in Eq. (3.2),
τ parameter defined in Eq. (3.2).

1. Introduction

THE RADIAL WALL JET formed after impingement of an axisymmetric jet on a flat surface has been of interest in many engineering applications, including heat or mass transfer to or from the flow, and the interaction between the pressure waves radiating from the plate and coherent structures of the inflowing jet. In response to these enquiries, time-averaged flow fields have been explored for normal impingement usually in the vicinity of the stagnation region, but knowledge of the downstream evolution of the flow has remained elusive. Recently, the radial wall jet has attracted particular attention in terms of instantaneous patterns of large structures (Ho and Nosseir [1, 2], Landreth and Adrian [3]) whose characteristic dimensions are commensurate with the width of the wall jet and lead to the time-averaged flow field with higher turbulence intensities (Poreh, Tsuei and Cermak [4]) than in aerodynamic boundary layers. Özdemir and Whitelaw [5] investigated the downstream evolution of the time-averaged and instantaneous flow fields of a radial wall jet formed after oblique impingement of an axisymmetric jet, and showed that the symmetry of the toroidal vortices (Didden and Ho [6]) was distorted as impingement deviated from normal, resulting in a complex cluster of concentric yet asymmetric toroidal vortices.

It is known (Ho and Huerre [7]) that the evolution of vortical structures in laminar and turbulent shear layers is governed by essentially the same dynamical processes, so that the concepts of hydrodynamic stability can be applied to turbulent shear layers. Inflectional instability of the shear layers has taken a great deal of attention, as for example Gregory, Stuart and Walker [8] and Stuart [9], because disturbances generated near the point of inflection could dominate the fluctuations and propagate at a speed smaller than the corresponding velocity at the inflection point. Howard [10] and Tsuji et al. [11] argued that the number of

distinct unstable disturbances associated with the inflection points could not exceed the number of neutral modes. The roll-up of travelling instability waves into the periodic array of vortices in a plane mixing layer was studied by MICHALKE [12] and MICHALKE and HERMANN [13] in that the evolution of disturbances in the basic flow direction seemed to be better modelled by spatially growing disturbances and, when the width of the flow region varied considerably, quantities controlled by the history of the flow development required an additional scaling parameter to account for the coordinate stretching (BOUTHIER [14], GASTER [15], CRIGHTON and GASTER [16]).

The purpose of the present study was to examine the possibility that the large vortical structures observed by ÖZDEMIR and WHITELAW [5] in their radial wall jet were generated by the flow instabilities, so that the discrete frequencies measured were synonymous with instability modes. The conjecture that the wall jet flow was not so obviously nonlinear gave impetus to the present linear analysis and should not be far from reality, since the array of vortices observed was discrete and no nonlinear vortex interaction processes, such as vortex pairing or tearing as described by HUSSAIN [17], were observed.

2. Equations for coherent structures

It can be envisaged that large scale motion of the wall jet was caused by deterministic instability waves which were, together with stochastic background fluctuations, superimposed on the pseudolaminar flow defined by the time-averaged velocity field. Therefore, since the wall flow was temporarily stationary, an instantaneous quantity can be decomposed into a time-independent mean, a coherent and an incoherent turbulence quantities (HUSSAIN [17], HUSSAIN and REYNOLDS [18]) and, in cylindrical coordinates, the instantaneous velocity vector can be given as (see Fig. 1, for the coordinate system and the flow domain)
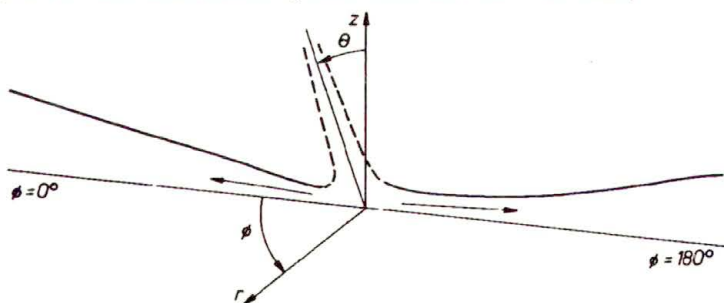
FIG. 1. Schematic of the flow configuration.

$$
\begin{aligned}
U_r(r,\phi,z,t) &= \overline{U}_r(r,\phi,z) + \tilde{u}_r(r,\phi,z,t) + u'_r(r,\phi,z,t), \\
U_\phi(r,\phi,z,t) &= \tilde{u}_\phi(r,\phi,z,t) + u'_\phi(r,\phi,z,t), \\
U_z(r,\phi,z,t) &= \overline{U}_z(r,\phi,z) + \tilde{u}_z(r,\phi,z,t) + u'_z(r,\phi,z,t),
\end{aligned}
$$

(2.1)

with the pressure field

$$P(r,\phi,z,t) = \overline{P}(r,\phi,z) + \tilde{p}(r,\phi,z,t) + p'(r,\phi,z,t),$$

where the over-bar, tilda and prime refer the quantities for the mean flow, the coherent (wave motion) and incoherent (random) turbulent fluctuations, respectively. Note that, based on the surface flow visualisation experiments [5], the mean azimuthal velocity, $\overline{U}_\phi$, was assumed to be zero. Provided there is a large difference between the length scales of the coherent and incoherent motions (STRANGE and CRIGHTON [19]), the incompressible Navier–Stokes equation can be used with the triple-decomposition to yield nonlinear equations for the wave motion (ÖZDEMİR [20]). Linearisation of such equations implies that the space-time evolution of one wavenumber associated with a given eddy size will not affect that of the others so that the coherent structures develop independently. Although the question often arises as to the extent of validity of linearised theory, MICHALKE [12] points out that the error due to the linearisation of the disturbance equations is larger for higher disturbance frequencies than for lower ones. This justifies the present linear analysis since the frequencies measured in the wall jet were fairly low.

Provided that the deterministic motion is associated with the discrete part of the spectrum accessible by the modal equations, the coherent components of fluid motion can be represented by instability modes even though the set is not complete (BETCHOV and CRIMINALE [21], DRAZIN and REID [22]). For the present analysis, disturbances travelling and evolving in the basic flow direction were of interest and, since the growth rates obtained from a stability calculation for temporally growing disturbances cannot be transformed linearly with the phase velocity into spatial growth rates (MICHALKE [12]), solutions to the linearised equations can be assumed of the form

(2.2)
$$\tilde{u}_r = A_r(z)\exp\left\{i(\alpha r - \beta t + m\phi)\right\} + (*),$$

$$\tilde{u}_\phi = A_\phi(z)\exp\left\{i(\alpha r - \beta t + m\phi)\right\} + (*),$$

$$\tilde{u}_z = A_z(z)\exp\left\{i(\alpha r - \beta t + m\phi)\right\} + (*),$$

$$\tilde{p} = A_p(z)\exp\left\{i(\alpha r - \beta t + m\phi)\right\} + (*),$$

where $(*)$ refers the complex-conjugate term, A_r, A_z, A_ϕ, and A_p are the (complex) amplitude modulation functions of $\tilde{u}_r$, $\tilde{u}_z$, $\tilde{u}_\phi$, and $\tilde{p}$, respectively. β is the real-valued circular-frequency $(2\pi f)$ and α is the complex wavenumber defined as

$$\alpha = \alpha_r + i\alpha_i,$$

where α_r is the spatial wavenumber $(2\pi/\lambda)$, and α_i is the rate of spatial evolution of a given component. It should also be pointed out that the curvilinear coordinate, ϕ, introduces a direction which can permit the evolution of the discrete

azimuthal modes of instability similar to the helical modes of the axisymmetric shear layer (STRANGE and CRIGHTON [19], PLASCHKO [23], COHEN and WYGNANSKI [24]). Indeed, the azimuthal instability modes of the wall jet flow could be a continuation of the helical shear layer structures of the inflowing jet which were, in some cases, known to survive after impingement (WIDNALL and TSAI [25], LUGT [26]) leading to large correlation between the wall jet and inflowing jet turbulence. The above formulation, therefore, accounts for the presence of the spinning modes (with azimuthal wavenumber, m) which, in some cases, have been as unstable as the axisymmetric modes (COHEN and WYGNANSKI [24]).

Since the stability of the flow is a local characteristic, the radial velocity maximum, $\overline{U}_{r,M}(r, \phi)$, has to be selected as the velocity scale, and the wall distance, z, is assumed to scale with the half-velocity thickness, $z_{0.5}$. It was shown by ÖZDEMİR [27] that the azimuthal symmetry of the wall flow was distorted due to the angled impingement of the inflowing jet and, therefore, it was necessary to take into account the azimuthal variation of the radial spreading. However, transforming the distorted coordinates of the wall jet flow of the angled impingement to those of the normal impingement, which can be treated analytically by the cylindrical coordinate system centered at the geometrical impingement point, required knowledge of the function relating the azimuthal and radial coordinates, which is difficult to deduce from the contour plots of surface pressure, as for example ÖZDEMİR and WHITELAW [5] (their Fig. 2.6). Here a heuristic approach was followed in which the radial distance from the geometrical impingement point, r, is assumed to scale with a so-called wetted radius, $r_w(\theta, \phi)$, which varies azimuthally as

$$(2.3) \qquad r_w(\theta, \phi) = H\left\{\sin(\theta \cos \phi) + \cos(\theta \cos \phi)\tan(\theta \cos(180 - \phi) + \gamma)\right\},$$

where γ is half the cone angle of the spread of the inflowing jet and was taken as 15 degrees from the flow visualisation pictures. The distributions of r_w are shown for $\theta = 0$ and 20 degrees in Fig. 2 and assumes elliptical shapes with
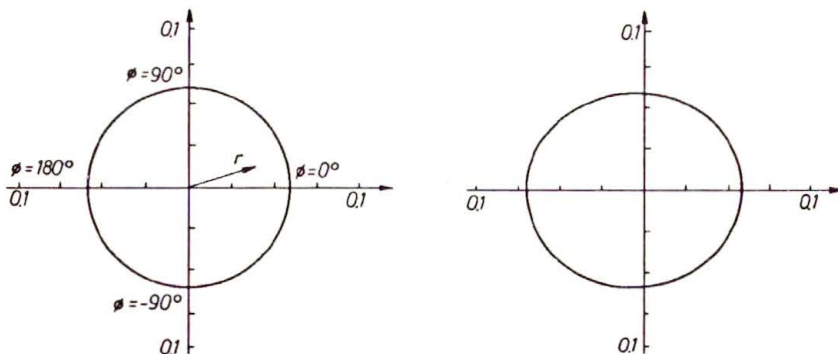

FIG. 2. Polar plot of the azimuthal distributions of the wetted radius for the impingement angles of $\theta = 0$ and 20 degrees.

increasing distance to the geometrical impingement point along the $\phi = 180-$
degree direction as impingement deviates from normal.

Further simplification of the formulation occurs when Reynolds number is
large so that the viscous effects become very small, finally leading to

continuity:

$$(2.4)_1 \qquad i\alpha^* A_r^* + \frac{z_{0.5}}{r^* r_w} A_r^* + \frac{im^* z_{0.5}}{r^* r_w} A_\phi^* + \frac{dA_z^*}{dz} = 0,$$

r-momentum:

$$(2.4)_2 \qquad -i\beta^* A_r^* + i\alpha^* \overline{U}_r^* A_r^* + \frac{z_{0.5}}{r_w} \left(\frac{\overline{U}_r^*}{\overline{U}_{r,M}} \frac{\partial \overline{U}_{r,M}}{\partial r^*} + \frac{\partial \overline{U}_r^*}{\partial r^*} \right) A_r^*$$

$$+ \frac{z_{0.5}}{r^* r_w} \left(\frac{\overline{U}_r^*}{\overline{U}_{r,M}} \frac{\partial \overline{U}_{r,M}}{\partial \phi} + \frac{\partial \overline{U}_r^*}{\partial \phi} \right) A_\phi^* + \overline{U}_z^* \frac{dA_r^*}{dz^*} + \frac{\partial \overline{U}_r^*}{\partial z^*} A_z^* + i\alpha^* A_p^* = 0,$$

ϕ-momentum:

$$(2.4)_3 \qquad -i\beta^* A_\phi^* + i\alpha^* \overline{U}_r^* A_\phi^* + \frac{\overline{U}_r^* z_{0.5}}{r^* r_w} A_\phi^* + \overline{U}_z^* \frac{dA_\phi^*}{dz^*} + \frac{im^* z_{0.5}}{r^* r_w} A_p^* = 0,$$

z-momentum:

$$(2.4)_4 \qquad -i\beta^* A_z^* + i\alpha^* \overline{U}_r^* A_z^* + \frac{z_{0.5}}{r_w} \left(\frac{\overline{U}_z^*}{\overline{U}_{r,M}} \frac{\partial \overline{U}_{r,M}}{\partial r^*} + \frac{\partial \overline{U}_z^*}{\partial r^*} \right) A_r^*$$

$$+ \frac{z_{0.5}}{r^* r_w} \left(\frac{\overline{U}_z^*}{\overline{U}_{r,M}} \frac{\partial \overline{U}_{r,M}}{\partial \phi} + \frac{\partial \overline{U}_z^*}{\partial \phi} \right) A_\phi^* + \overline{U}_z^* \frac{dA_z^*}{dz^*} + \frac{\partial \overline{U}_z^*}{\partial z^*} A_z^* + \frac{dA_p^*}{dz^*} = 0.$$

Letting $A_r^* = Y_1$, $A_\phi^* = Y_2$, $A_z^* = Y_3$, $A_p^* = Y_4$, and rearranging, the following set
of first-order ordinary differential equations can be obtained

$$\frac{dY_1}{dz^*} = \frac{1}{\overline{U}_z^*} \left\{ i\beta^* Y_1 - i\alpha^* \overline{U}_r^* Y_1 - \frac{z_{0.5}}{r_w} \left(\frac{\overline{U}_r^*}{\overline{U}_{r,M}} \frac{\partial \overline{U}_{r,M}}{\partial r^*} + \frac{\partial \overline{U}_r^*}{\partial r^*} \right) Y_1 \right.$$

$$\left. - \frac{z_{0.5}}{r^* r_w} \left(\frac{\overline{U}_r^*}{\overline{U}_{r,M}} \frac{\partial \overline{U}_{r,M}}{\partial \phi} + \frac{\partial \overline{U}_r^*}{\partial \phi} \right) Y_2 - \frac{\partial \overline{U}_r^*}{\partial z^*} Y_3 - i\alpha^* Y_4 \right\},$$

$$(2.5) \qquad \frac{dY_2}{dz^*} = \frac{1}{\overline{U}_z^*} \left\{ i\beta^* Y_2 - i\alpha^* \overline{U}_r^* Y_2 - \frac{\overline{U}_r^* z_{0.5}}{r^* r_w} Y_2 - \frac{im^* z_{0.5}}{r^* r_w} Y_4 \right\},$$

$$\frac{dY_3}{dz^*} = -i\alpha^* Y_1 - \frac{z_{0.5}}{r^* r_w} Y_1 - \frac{im^* z_{0.5}}{r^* r_w} Y_2,$$

(2.5)
[cont.]
$$\frac{dY_4}{dz^*} = i\beta^* Y_3 - i\alpha^* \overline{U}_r^* Y_3 - \frac{z_{0.5}}{r_w} \left(\frac{\overline{U}_z^*}{\overline{U}_{r,M}} \frac{\partial \overline{U}_{r,M}}{\partial r^*} + \frac{\partial \overline{U}_z^*}{\partial r^*} \right) Y_1$$

$$- \frac{z_{0.5}}{r^* r_w} \left(\frac{\overline{U}_z^*}{\overline{U}_{r,M}} \frac{\partial \overline{U}_{r,M}}{\partial \phi} + \frac{\partial \overline{U}_z^*}{\partial \phi} \right) Y_2$$

$$+ \overline{U}_z^* \left(i\alpha^* Y_1 + \frac{z_{0.5}}{r^* r_w} Y_1 + \frac{im^* z_{0.5}}{r^* r_w} Y_2 \right) - \frac{\partial \overline{U}_z^*}{\partial z^*} Y_3 .$$

Note that when $\overline{U}_z^* \to 0$, Eqs. (2.5)$_{1,2}$ have singularities which were introduced by disregarding the terms in Re^{-1}. The singularity due to diminishing value of $\overline{U}_z^*$ occurs at the wall ($z^* = 0$) and can occur at an interior point if there is a local vertical flow reversal within the flow domain. Indeed, the vertical flow reversal in radial wall jet was first observed by LANDRETH and ADRIAN [3], and there is a clear evidence that flow reversal becomes stronger in oblique impingement (ÖZDEMİR and WHITELAW [5]). The difficulties associated with the singularity are discussed in detail by ÖZDEMİR [27] and here the emphasis is given to one-dimensional mean flow for which the equations have no singularity. If the basic flow field is assumed to be locally parallel so that $\overline{U}_r^*$ is the only velocity component of the undisturbed wall jet, with $\overline{U}_z^* = 0$ everywhere, the set (2.5) further simplifies to

(2.6)
$$\frac{dY_3}{dz^*} = -i\alpha^* Y_1 - \frac{z_{0.5}}{r^* r_w} Y_1 - \frac{im^* z_{0.5}}{r^* r_w} Y_2 ,$$

$$\frac{dY_4}{dz^*} = i\beta^* Y_3 - i\alpha^* \overline{U}_r^* Y_3$$

with Y_1 and Y_2 defined as

(2.6′)
$$Y_1 = \left\{ \frac{z_{0.5}}{r^* r_w} \left(\frac{\overline{U}_r^*}{\overline{U}_{r,M}} \frac{\partial \overline{U}_{r,M}}{\partial \phi} + \frac{\partial \overline{U}_r^*}{\partial \phi} \right) Y_2 + \frac{\partial \overline{U}_r^*}{\partial z^*} Y_3 + i\alpha^* Y_4 \right\}$$
$$\cdot \frac{1}{i\beta^* - i\alpha^* \overline{U}_r^* - \frac{z_{0.5}}{r_w} \left(\frac{\overline{U}_r^*}{\overline{U}_{r,M}} \frac{\partial \overline{U}_{r,M}}{\partial r^*} + \frac{\partial \overline{U}_r^*}{\partial r^*} \right)} ,$$

$$Y_2 = \left(\frac{im^* z_{0.5}}{r^* r_w} Y_4 \right) \Big/ \left(i\beta^* - i\alpha^* \overline{U}_r^* - \frac{\overline{U}_r^* z_{0.5}}{r^* r_w} \right) .$$

3. Mean flow, boundary conditions and solution procedure

In order to obtain the full transverse eigensolution at each radial position, the coefficients of the modal equations, which are functions of the mean flow parameters, are required. The streamwise development of the mean flow, therefore, affects the evolution of the instability modes, which has been considered with

multi-scale expansions defining the divergence of the mean flow (GASTER [15], CRIGHTON and GASTER [16], PLASCHKO [23]) and, since the local mean velocity profiles are the results of the nonlinear interactions, an implicit nonlinearity is imposed on the solutions. In the present analysis, mean flow parameters and their variations were provided in the form of empirical relations (ÖZDEMİR and WHITELAW [5]) as representatives of the pseudolaminar motion upon which the perturbations were superimposed. The mean radial velocity profiles nondimensionalised by the local maximum were similar at large radial distances

$$(3.1) \quad \overline{U}_r^* = \frac{\overline{U}_r}{\overline{U}_{r,M}} = \frac{(z/z_{0.5})^{\eta-1}}{\left(\dfrac{\eta-1}{\eta}\right)^{(\eta-1)/\eta} (\sqrt{2}s)^{\eta-1}} \exp\left\{ -\left(\frac{z/z_{0.5}}{\sqrt{2}s}\right)^{\eta} + \frac{\eta-1}{\eta} \right\}$$

(see also Table 1) with the streamwise evolution represented by

Table 1. Variation of η and s.

ϕ (°):	0	90	180
η :	1.42	1.38	1.32
s :	0.54	0.52	0.54

$$(3.2) \quad \overline{U}_{r,M} = \tau(r-\zeta)^p \exp\left\{ -\left(\frac{r-\zeta}{\sqrt{2}\sigma}\right)^{\tau} \right\} \Big/ (\sqrt{2}\sigma)^{\tau}$$

which fits the experimental data (Fig. 3 and Table 2).
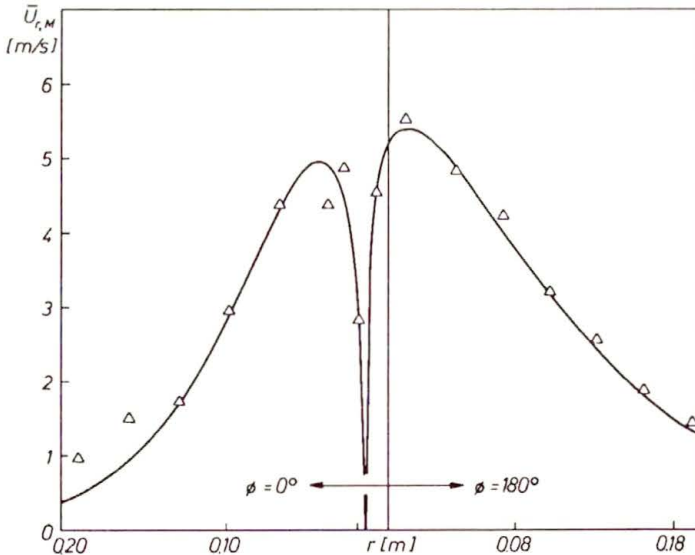
FIG. 3. Variation of the maximum of the mean radial velocity along the line of incidence.

Table 2. Parameters of Eq. (3.2).

ϕ (°) :	0	180
ζ :	0.015	−0.015
p :	0.49	0.22
τ :	1.26	1.15
σ :	0.045	0.078

The set of first-order differential equations requires a condition to be specified for each equation to obtain the transverse eigensolution. The vertical velocity component at the wall should be zero due to the impermeable plate and, thus,

$$(3.3) \qquad\qquad A_z^* = 0 \qquad \text{at} \qquad z^* = 0.$$

The eigensolution is defined over a semi-infinite interval $[z^* = 0, \ z^* = \infty]$ with the upper boundary occurring at infinity but, for numerical purposes, it was replaced by a finite interval in which the condition at $z^* = \infty$ was assumed to occur at some finite $z^* = z_\infty^*$, so that the domain of the transverse eigensolution was forced to coincide with that of the mean flow where $\overline{U}_r^* = 0$ and the pressure attained the ambient value, i.e.,

$$(3.3') \qquad\qquad A^*_p = 0 \qquad \text{at} \qquad z^* = z_\infty^* .$$

The eigenvalue problem defined in Eqs. (2.6) includes two coupled first-order linear ordinary differential equations. The solution was sought for the eigenvalues, α, and the corresponding transverse eigensolutions, $Y_k(z^*, \alpha)$, given the mean-flow parameters and the values of β and m. The solution procedure was similar to that of KELLER [28] with the reformulation of the equations, resulting in a nonlinear two-point boundary value problem. In order to avoid the growing solutions during the integration through the entire domain (BETCHOV and CRIMINALE [21]), the length of the domain of integration was divided into two in which a parallel shooting algorithm was used with the integration proceeding to an intermediate point by launching initial guesses from both ends of the interval and a matching of the solutions at the midpoint. The computations were performed on a DEC 5000 workstation in double precision and iterations for the multidimensional Newton-Raphson root finding technique concluded when the discrepancy vector was within some specified accuracy (typically 10^{-15}).

4. Numerical results and comparisons with experiments

For the first ten azimuthal modes and temporal frequency from 0 to 100 Hz, the set of inviscid equations (2.6) was solved along the line of impingement at radial positions where the experimentally observed vortices were most apparent

and the mean radial velocity achieved the similar form. The nondimensional amplification rates at $r/r_w = 2.274$ along the $\phi = 0$ degree direction, Fig. 4 a, are negative for all the waves considered, indicating decaying characteristics. Except for the axisymmetric ($m = 0$) and the first three helical modes ($m = \pm 1, \pm 2$ and ± 3), the curves show similar trends where $-\alpha_i z_{0.5}$ first increases with f and tends to a constant value which is lower for higher helical modes. For these four exceptions, there is a slight peak at around 7.5 Hz before the subsequent fall to a constant level, indicating a narrow range of frequencies at the lower end of the spectrum with the least damping relative to the other waves. It is interesting to note that the axisymmetric and the first helical modes have almost the same frequency response, which is consistent with the findings of COHEN and WYGNANSKI [24]. In order to trace the evolution of the waves, with attenuation occurring in the streamwise direction, the calculations were repeated for $r/r_w = 3.324$ and the results of Fig. 4 b show similar trends but, as would be expected, the least damped wave was shifted to a lower frequency, $f = 3.1$ Hz. This is consistent with the measured spatial evolution of the one-dimensional spectrum of radial fluctuation component of ÖZDEMİR and WHITELAW [5] in which a discrete frequency of 3.25 Hz was dominant at the same radial position. The results show that an increase of the width of the shear layer with the corresponding decrease in the mean energy along the streamwise direction, is accompanied by a negative amplification rate, i.e., attenuation with a continuous shift of the least attenuated instability waves towards lower frequencies.

The wavenumber-frequency spectra of Fig. 5 reveal that the wavenumbers are positive in the frequency range, where $-\alpha_i z_{0.5}$ has a maximum, and that a phase reversal occurs for the axisymmetric and some helical modes ($-6 \leq m \leq 6$), so that negative wavenumbers at large frequencies indicate upstream moving waves. The least attenuated waves move downstream with a positive phase velocity and indicate convection of the coherent turbulence along the mainstream with a decay quantified by the rate of attenuation of the waves. The relatively higher attenuation of the upstream moving waves is interesting in that the propagation of disturbances from the edges of the wall jet cannot interfere with the turbulence structure of the wall flow, and this is consistent with the fact that wall jet is not dependent on the conditions downstream, but affected by the initial conditions of the inflowing jet even at large radial distances. It is clear that if different frequencies were dominant at different wall distances, a transversal (vertical) eigensolution structure with a phase reversal occurring at a certain wall distance could lead to a situation which would be similar to the spatial phase reversal observed by SATO [29].

An attempt was made to compare the calculated distribution of the one-sided power spectrum of the radial fluctuation intensity for axisymmetric structures ($m = 0$) with that of measurements at $r/r_w = 2.274$ and 3.324 along the $\phi = 0$ degree direction. From the Eq. $(2.2)_1$, with $\alpha = \alpha_r + i\alpha_i$, space-time variation of the radial fluctuation that would be measured with a probe fixed at a point in the

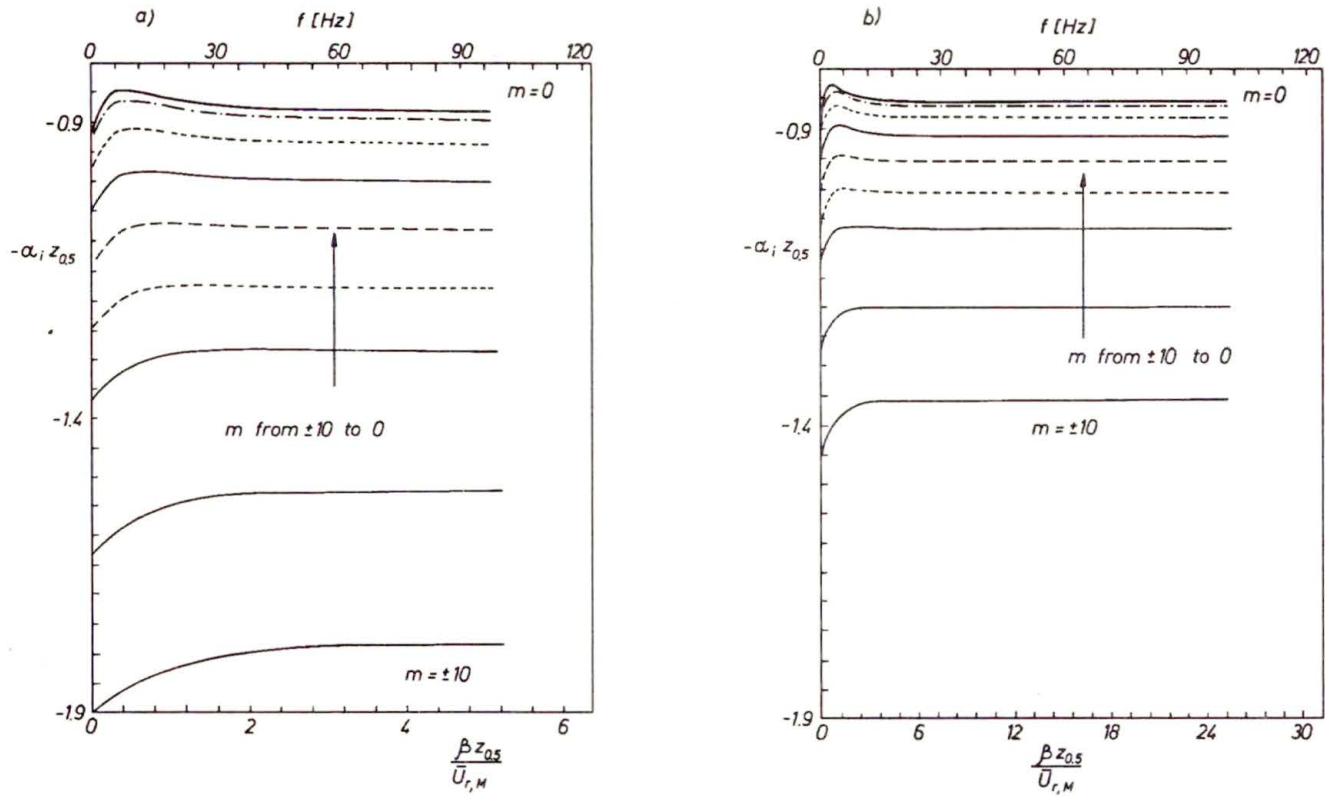FIG. 4. Nondimensional amplification rates, a) $r/r_w = 2.274$ and b) $r/r_w = 3.324$.
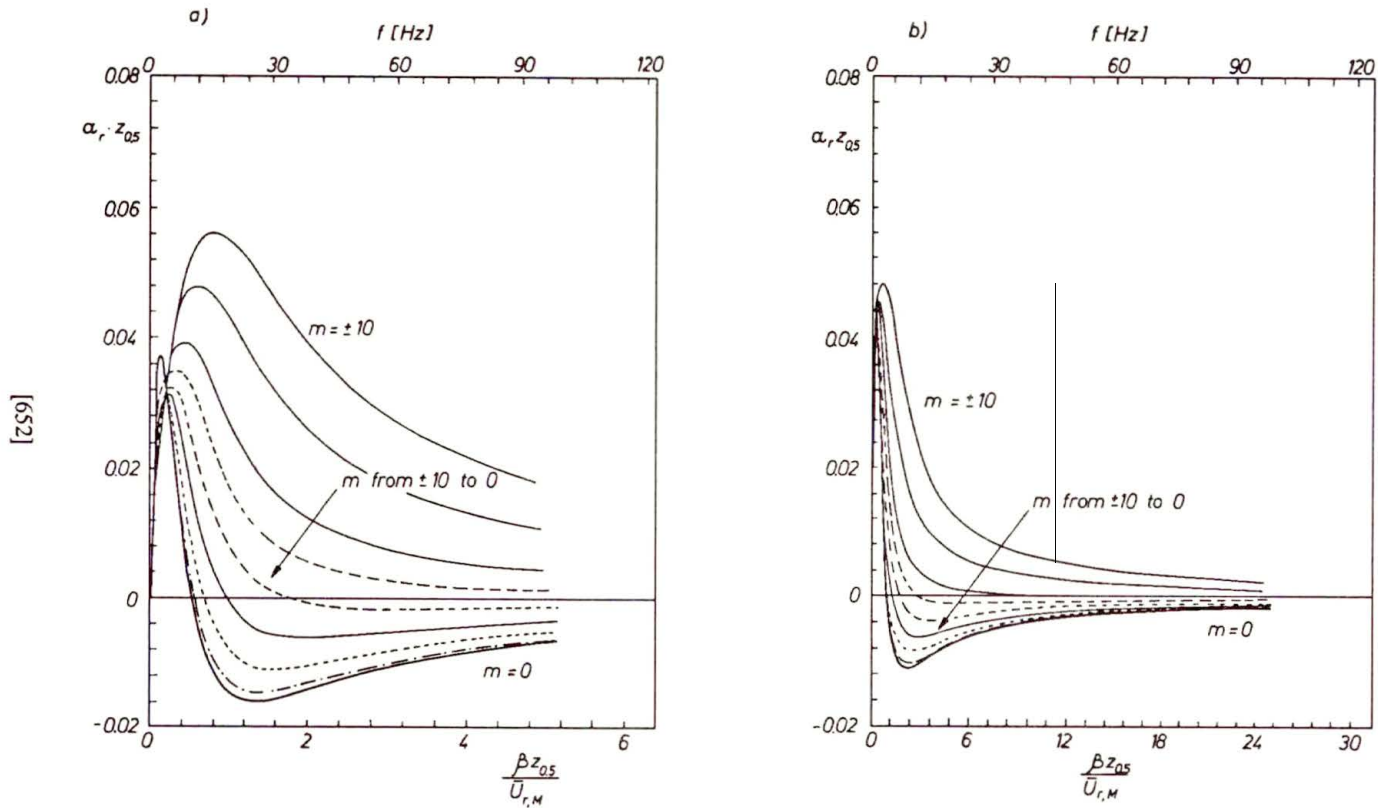
[159]

FIG. 5. Wavenumber-frequency spectrum, a) $r/r_w = 2.274$ and b) $r/r_w = 3.324$.

Eulerian coordinate, can be written as

$$(4.1) \qquad \tilde{u}_r = [A_r(z)\exp\{i\alpha_r r - \alpha_i r + im\phi)\}]\exp(-i\beta t) + (*),$$

where the term inside the bracket represents the complex amplitude of the vector rotating at a circular frequency β so that

$$(4.2) \qquad \mathcal{F}(f) = A_r(z)\exp\{i\alpha_r r - \alpha_i r + im\phi)\}.$$

As previously argued in Sec. 2, the complex conjugate term, $(*)$, in Eq. (4.1) implies that each component at a frequency f is matched by a component at $-f$ which has equal amplitude so that, except for the case of $f = 0$, the total power associated with frequency, f, is given (RANDALL [30])

$$(4.3) \qquad \mathbb{P}(f) = \frac{\mathcal{F}(f)^2}{2} = \frac{[A_r(z)\exp\{i\alpha_r r - \alpha_i r + im\phi)\}]^2}{2}.$$

Since the eigenfunctions were determined except for the arbitrary multiplicative constant, the axis for the power spectrum in Figs. 6 and 7 has an arbitrary scale. A remarkable feature is that the large peak at the outer layer diminishes as the wall is approached and shifts towards slightly higher frequencies, and this is more evident in the contour plots. This trend is consistent with the measurements of ÖZDEMIR [27], where it was attributed to the restriction imposed on the growth of the inner vortex close to the wall by the outer free shear layer vortices, and the calculated values of the peak frequency are very close to those of the measurements particularly for $r/r_w = 3.324$.

Figure 8 shows radial fluctuation intensities calculated from the one-sided power spectrum with f ranging from 0 to 100 Hz for axisymmetric and spinning modes, $m = \pm 1, \pm 2, \pm 3, \pm 4, \pm 5, \pm 6, \pm 8,$ and ± 10 at a radial position $r/r_w = 3.324$, where the radial fluctuation intensity completed its evolution towards two-peaked profile. By matching the amplitude of the radial velocity fluctuation component to the corresponding experimental value at the wall distance $z^* = 1.25$, favorable agreement was found between theory and experiment for the whole vertical eigenstructure of the radial fluctuation intensity, with large magnitudes occurring near the outer inflection point. The satisfactory agreement of the theoretical radial fluctuation intensity with the experiments was expected, since the slightly attenuated waves were known to correlate over a large distance of the order of the inverse of their damping ratio (LANDAHL [31]), and tend to dominate the non-wave-like disturbances and the whole turbulent flow field. The upper subfigure shows the relative contributions of different spinning modes with respect to the axisymmetric mode, so that the first helical mode is almost as important as the axisymmetric mode and the contribution was almost negligible for $m \geq 10$. It is also of interest to note that the calculations performed at the previous radial position, $r/r_w = 2.274$, along the $\phi = 0$ degree direction yielded
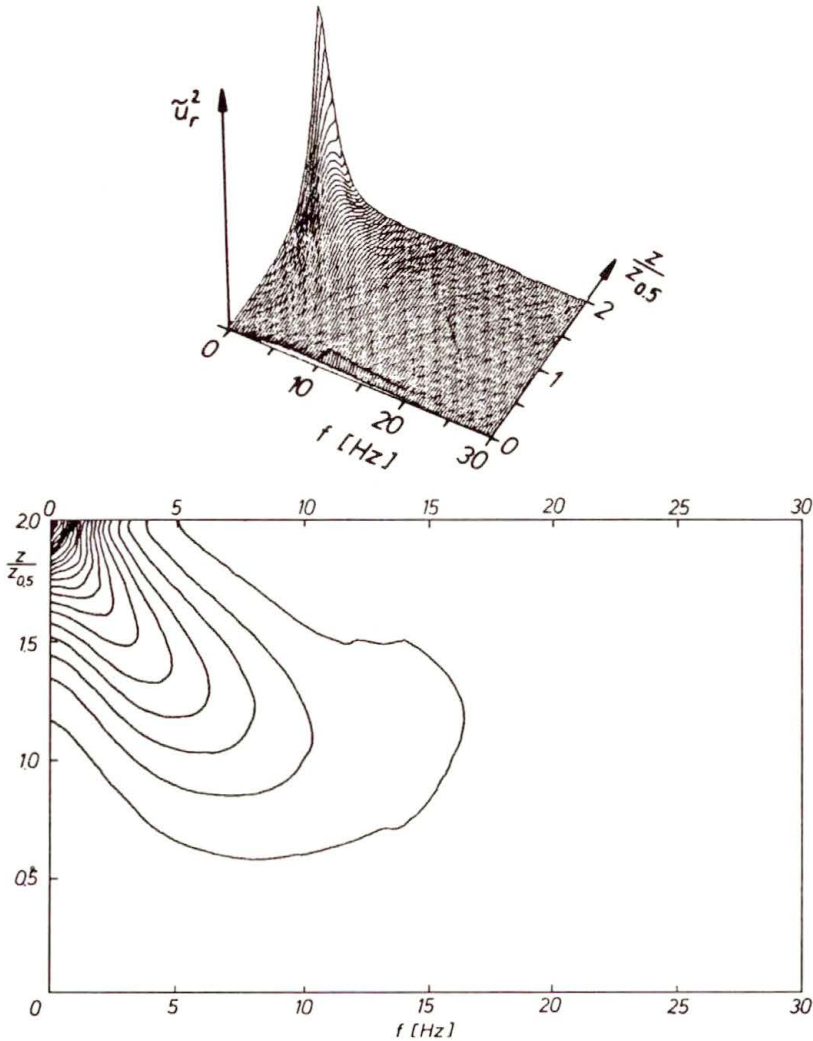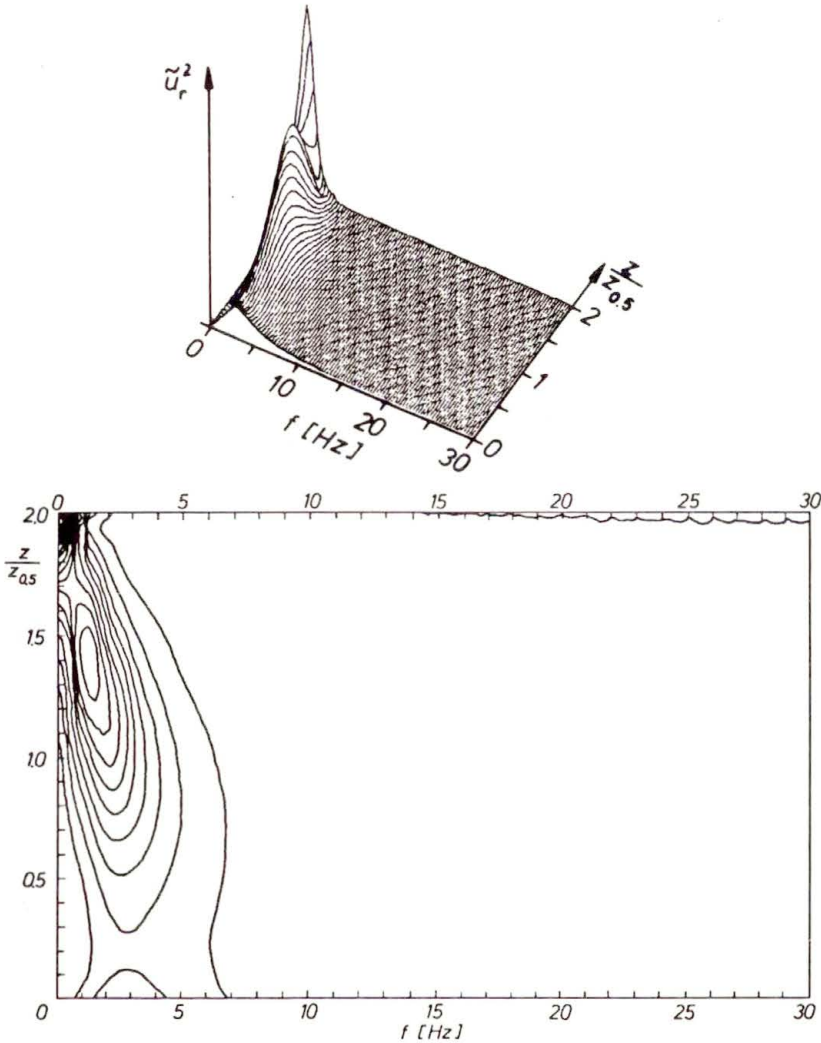
FIG. 6. One-sided power spectrum of radial fluctuation intensity for axisymmetric structures $m = 0$, $r/r_w = 2.274$ ($\widetilde{u}_r^2$ axis has arbitrary scale).

very much the same fluctuation profile, although the measured fluctuation profile was different. Since the vertical mean profiles were different at these two radial positions, the results indicate that the mean radial velocity was dominant in the perturbed mean flow field but was not sufficient to describe the whole mean vorticity field which was responsible for the generation of the fluctuations (STUART [32]). Thus, it appears that the evolution of the mean vertical velocity needs to be included in the analysis to account for local changes of the fluctuation distribution when the streamwise component of the mean flow field was similar. Also, contrary to the stability calculations of BREWSTER and GEBHART [33] for natural

FIG. 7. One-sided power spectrum of radial fluctuation intensity for axisymmetric structures, $m = 0$, $r/r_w = 3.324$ ($\tilde{u}_r^2$ axis has arbitrary scale).

convection over a vertical hot plate, the present profiles of radial fluctuation intensity do not tend to diminish very close to the wall. This is to be expected since the present results are based on simplifications of inviscid equations.

Profiles of the induced pressure fluctuations, Fig. 9, reveal that the pressure fluctuations can attain a value of 63% at the wall. Again, the relative contributions of different azimuthal modes are similar to those of the radial fluctuation intensities. It is interesting to note that the radial velocity fluctuations exhibit far more structure than is displayed by the pressure fluctuations but, since pressure was not measured across the wall jet, it is difficult to be conclusive about the
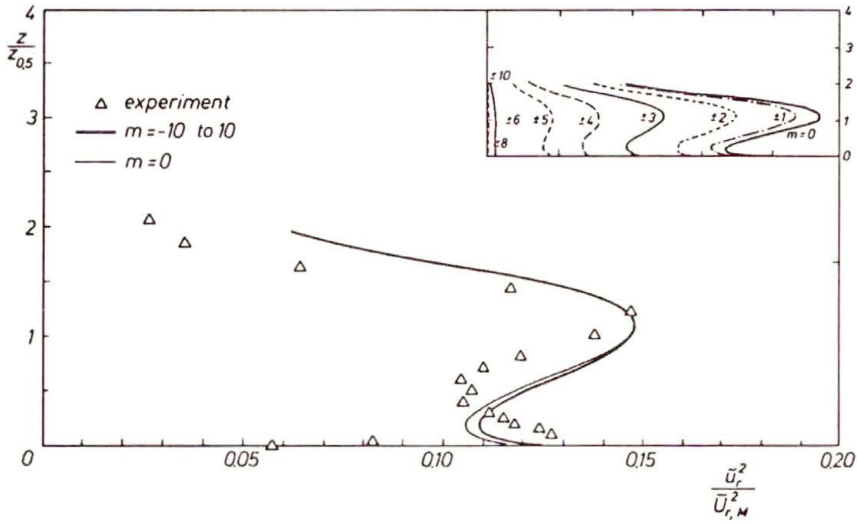
FIG. 8. Radial velocity fluctuation intensity for f from 0 to 100 Hz and m from 0 to ± 10.
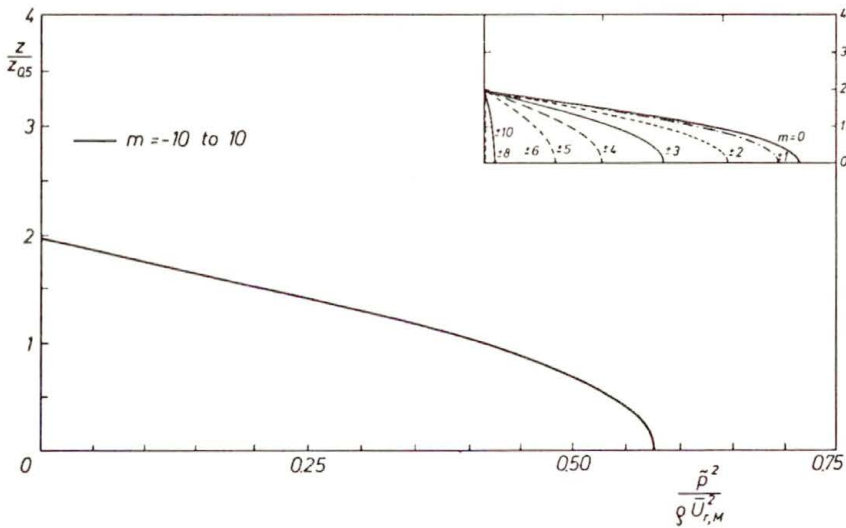
FIG. 9. Pressure fluctuation intensity for f from 0 to 100 Hz and m from 0 to ± 10.

shape of the profiles. The azimuthal fluctuation intensity, on the other hand, exhibited a finite value at the wall and this violation of the no-slip condition must be due to that the fluctuation intensity was predicted by linear, inviscid stability analysis of one-dimensional basic flow, whereas the measured intensity was generated by apparently two-dimensional viscous basic flow. For the same reasons the agreement between vertical velocity fluctuations and the measured ones was poor.

5. Conclusions

The coherent turbulence characteristics of the radial wall jet were studied using discrete instability waves and linear analysis based on the assumption of a one-dimensional inviscid flow which was represented by time-averaged radial velocity. Calculations were performed in a region where the energy of mean flow was decaying so that the instability waves were attenuated with a phase reversal in frequency, in which the least attenuated waves were convected downstream while the others moved upstream. The trend of spectrum of the radial fluctuation component was well predicted with the dominant frequency shifted towards higher values close to the wall, and a good agreement was found in the evolution of the spectrum of radial fluctuation intensity in that the spectral information was closely correlated with the decay of the mean flow energy.

The shape of the calculated radial fluctuation intensity exhibited a trend with larger magnitudes at the outer inflection point, consistent with the experimentally observed array of vortices. The success of the inviscid predictions was attributed to the fact that the large coherent structures of the wall jet were associated with small wavenumbers, far remote from the viscous subrange, so that viscous dissipation did not play any important role in their dynamics (TOWNSEND [34]). However, the shape of the radial fluctuation intensity repeated itself at different positions despite the variation observed experimentally, and this led to the conclusion that the observed variations in the shape of intensity profiles were caused by the influences of the other components of the mean flow field and particularly the mean vertical velocity, whose profiles varied with the radial coordinate, even though the radial velocity profiles were similar. In other words, the mean vorticity was the determining factor for the overall performance of the stability predictions.

Acknowledgement

References

1. C. M. HO and N.S. NOSSEIR, *Large coherent structures in an impinging jet*, [in:] Turbulent Shear Flows 2, J.S.L. BRADBURY, F. DURST, B.E. LAUNDER, F.W. SCHMIDT and J.H. WHITELAW [Eds.], Springer-Verlag, 297–304, 1980.

2. C.M. HO and N.S. NOSSEIR, *Dynamics of an impinging jet. Part 1. The feedback phenomenon*, J. Fluid Mech., 105, 119–142, 1981.

3. C.C. LANDRETH and R.J. ADRIAN, *Impingement of a low Reynolds number turbulent jet onto a flat plate at normal incidence*, Exp. Fluids, 9, 74–84, 1990.

4. M. POREH, Y.G. TSUEI and J.E. CERMAK, *Investigation of a turbulent radial wall jet*, J. Appl. Mech., **34**, 457–463, 1967.

5. İ.B. ÖZDEMİR and J.H. WHITELAW, *Impingement of an axisymmetric jet on unheated and heated flat plates*, J. Fluid Mech., **240**, 503–532, 1992.

6. N. DIDDEN and C.M. HO, *Unsteady separation in an impinging jet*, J. Fluid Mech., **160**, 235–256, 1985.

7. C.M. HO and P. HUERRE, *Perturbed free shear layers*, Ann. Rev. Fluid Mech., **16**, 365–424, 1984.

8. N. GREGORY, J.T. STUART and W.S. WALKER, *On the stability of three-dimensional boundary layers with application to the flow due to a rotating disk*, Phil. Trans. R. Soc. Lond., A **248**, 155–199, 1955.

9. J.T. STUART, *Hydrodynamic stability*, [in:] Laminar Boundary Layers, L. ROSENHEAD [Ed.], Clarendon Press, 492–579, 1963.

10. L.N. HOWARD, *The number of unstable modes in hydrodynamic stability problems*, J. Mécanique, **3**, 433–443, 1964.

11. Y. TSUJI, Y. MORIKAWA, T. NAGATANI and M. SAKOU, *The stability of a two-dimensional wall jet*, Aeronaut. Q., **28**, 235–246, 1977.

12. A. MICHALKE, *On spatially growing disturbances in an inviscid shear layer*, J. Fluid Mech., **23**, 521–544, 1965.

13. A. MICHALKE and G. HERMANN, *On the inviscid instability of a circular jet with external flow*, J. Fluid Mech., **114**, 343–359, 1982.

14. M. BOUTHIER, *Stabilité linéaire des écoulements presque parallèles*, J. Mécanique, **11**, 599–621, 1971.

15. M. GASTER, *On the effects of boundary-layer growth on flow stability*, J. Fluid Mech., **66**, 465–480, 1974.

16. D.G. CRIGHTON and M. GASTER, *Stability of slowly divergent flow*, J. Fluid Mech., **77**, 397–413, 1976.

17. A.K.M.F. HUSSAIN, *Coherent structures – reality and myth*, Phys. Fluids, **26**, 2816–2850, 1983.

18. A.K.M.F. HUSSAIN and W.C. REYNOLDS, *The mechanics of an organised wave in turbulent shear flow*, J. Fluid Mech., **41**, 241–258, 1970.

19. P.J.R. STRANGE and D.G. CRIGHTON, *Spinning modes on axisymmetric jets. Part 1*, J. Fluid Mech., **134**, 231–245, 1983.

20. İ.B. ÖZDEMİR, *Stability of the wall jet*, Section report MFMAD/95/4, Mechanics Division, School of Mech. Engng., İTU, 1995.

21. R. BETCHOV and W.O. CRIMINALE, *Stability of parallel flows*, Academic Press., 1967.

22. P.G. DRAZIN and W.H. REID, *Hydrodynamic stability*, Cambridge Univ. Press., 1981.

23. P. PLASCHKO, *Helical instabilities of slowly divergent jets*, J. Fluid Mech., **92**, 209–215, 1979.

24. J. COHEN and I. WYGNANSKI, *The evolution of instabilities in the axisymmetric jet. Part 1. The linear growth of disturbances near the nozzle*, J. Fluid Mech., **176**, 191–219, 1987.

25. S.E. WIDNALL and C.Y. TSAI, *The instability of the thin vortex ring of constant vorticity*, Phil. Trans. R. Soc. Lond., A **287**, 273–305, 1977.

26. H.J. LUGT, *Vortex flow in nature and technology*, Wiley, 1983.

27. İ.B. ÖZDEMİR, *Impingement of single and two-phase jets on unheated and heated flat plates*, Ph.D. Thesis, Imperial College, London 1992.

28. H.B. KELLER, *Numerical solution of two-point boundary value problems*, CBMS-NSF Regional Conference Series in Applied Mathematics, vol. 24, 1976.

29. H. SATO, *Further investigation on the transition of two-dimensional separated layer at subsonic speeds*, J. Phys. Soc. Japan, **14**, 1797–1810, 1959.

30. R.B. RANDALL, *Frequency analysis; Application to B&K equipment*, Brüel and Kjaer, 1977.

31. M. LANDAHL, *A wave-guide model for turbulent shear flow*, J. Fluid Mech., **29**, 441–459, 1967.

32. J.T. STUART, *Course notes on Hydrodynamic Stability*, Department of Mathematics, Imperial College, 1989.

33. R.A. BREWSTER and B. GEBHART, *Instability and disturbance amplification in a mixed-convection boundary layer*, J. Fluid Mech., **229**, 115–133, 1991.

34. A.A. TOWNSEND, *The structure of turbulent shear flow*, Cambridge Univ. Press., 1976.

İSTANBUL TECHNICAL UNIVERSITY
SCHOOL OF MECHANICAL ENGINEERING
MECHANICS DIVISION, İSTANBUL, TURKEY.

Two-dimensional tensor function representations involving third-order tensors

Q.-S. ZHENG (BEIJING)

AMONG THE PHYSICALLY possible infinitely many material symmetries of all kinds in a two-dimensional space, there exist eight kinds, i.e., the isotropy $C_{\infty\nu}$, hemitropy C_{∞}, two symmetries C_1 and C_2 in the oblique system, $C_{1\nu}$ and $C_{2\nu}$ in the rectangular system, and C_3 and $C_{3\nu}$ in the trigonal system, that can be characterized in terms of tensors of orders not higher than three. In this paper, the complete and irreducible representations relative to these eight symmetries are established for scalar-, vector-, second-order tensor- and third-order tensor-valued functions of any finite number of vectors, second-order tensors and third-order tensors. These representations allow to obtain, in the case of two-dimensional problems, general invariant forms of the physical laws; in particular, the constitutive equations involving thrid-order tensors.

1. Introduction

RECENTLY, the complete and irreducible representations in two-dimensional space were established by ZHENG [7] relative to every kind of material symmetry for scalar-,vector- and second-order tensor-valued functions of any finite number of second-order symmetric tensors $\mathbf{A}_1, \ldots, \mathbf{A}_N$ (denoted by $\mathbf{A}_\alpha$), second-order skew-symmetric tensors $\mathbf{W}_1, \ldots, \mathbf{W}_P$ (denoted by $\mathbf{W}_\xi$) and vectors $\mathbf{v}_1, \ldots, \mathbf{v}_M$ (denoted by $\mathbf{v}_\varrho$). In contrast to these general results, complete and irreducible representations for tensor functions involving tensors of order higher than two are much less well understood (PENNISI [4], ZHENG [9], ZHENG and BETTEN [10], BETTEN and HELISCH [1]). In particular, the problem of constructing of general, complete and irreducible tensor function representations which contain any finite number of third-order tensor agencies $\mathbf{T}_1, \ldots, \mathbf{T}_L$ (denoted by $\mathbf{T}_\lambda$), even for $L = 1$, is still open, although its importance can be seen in many modern physical contexts (cf., PENNISI [4]).

ZHENG and BOEHLER [11] have described and classified the physically possible infinitely many material symmetries of all kinds in two dimensions (and also in three dimensions). Among them, there are eight symmetries that can be characterized in terms of vector(s), second-order tensor(s), and/or third-order tensor, as shown below in Table 1.

In this paper, notation is based on the following conventions. We denote by $\mathbf{1}$ the second-order intensity tensor, $\boldsymbol{\varepsilon}$ the permutation tensor (a second-order skew-symmetric tensor), $\mathbf{R}(\theta)$ the rotation tensor of angle θ, $\mathbf{a}$ and $\mathbf{b}$ two unit orthogonal vectors, $\mathbf{R_b}$ the reflection transformation in $\mathbf{b}$ direction, and

$$(1.1) \qquad \mathbf{P} = \mathbf{a} \otimes \mathbf{a} \otimes \mathbf{a} - (\mathbf{a} \otimes \mathbf{b} \otimes \mathbf{b} + \mathbf{b} \otimes \mathbf{a} \otimes \mathbf{b} + \mathbf{b} \otimes \mathbf{b} \otimes \mathbf{a}).$$

Table 1. All kinds of two-dimensional material symmetry that have structural tensors as vector(s), second-order tnsor(s), and/or third-order tensor.

system	Schoenflies symbol	generators of symmetry group	structural tensors
oblique	C_1 C_2	$R(0) = 1$ $R(\pi) = -1$	$\mathbf{a}, \boldsymbol{\varepsilon}$ (or $\mathbf{a}, \mathbf{b}$) $\mathbf{M}, \boldsymbol{\varepsilon}$
rectangular	$C_{1\nu}$ $C_{2\nu}$ = orthotropy	$\mathbf{R_b} = \mathbf{a} \otimes \mathbf{a} - \mathbf{b} \otimes \mathbf{b}$ $R(\pi), \mathbf{R_b}$	$\mathbf{a}$ $\mathbf{M} = \mathbf{a} \otimes \mathbf{a} - \mathbf{b} \otimes \mathbf{b}$
trigonal	C_3 $C_{3\nu}$	$R(2\pi/3)$ $R(2\pi/3), \mathbf{R_b}$	$\mathbf{P}, \boldsymbol{\varepsilon}$ $\mathbf{P}$
circle	C_∞ = hemitropy $C_{\infty\nu}$ = isotropy	$R(\theta) \ (0 \leq \theta < 2\pi$ $R(\theta), \mathbf{R_b} \ (0 \leq \theta < 2\pi)$	$\boldsymbol{\varepsilon}$ 1

The operators $\otimes$, $\cdot$, $:$, and $\vdots$ mean tensor, scalar (or dot), double dot and triple dot products, respectively. Components of vectors and tensors are referred to an orthonormal frame, say $\{\mathbf{e}_i\}$, lower-case Latin indices $(i, j, k, \ldots)$ range from 1 to 2, repeated indices are summed from 1 to 2, and the abbreviations $\mathbf{e}_{ij} = \mathbf{e}_i \otimes \mathbf{e}_j$ and $\mathbf{e}_{ijk} = \mathbf{e}_i \otimes \mathbf{e}_j \otimes \mathbf{e}_k$ are used. The prefix tr indicates trace.

A tensor $\mathbf{H}$ is termed as *irreducible*, if it is a completely symmetric and traceless:

$$(1.2) \qquad H_{ijk\ldots l} = H_{jik\ldots l} = H_{kji\ldots l} = \ldots = H_{ljk\ldots i}, \qquad H_{mmk\ldots l} = 0_{k\ldots l},$$

where $0_{k\ldots l}$ corresponds to the zero-tensor of the relevant order. It is well known that any irreducible tensor $\mathbf{H}$ in two-dimensional space has only two independent components (e.g. $H_{111\ldots 1}$ and $H_{211\ldots 1}$). In particular, the relations among the components of an irreducible third-order tensor $\mathbf{T}$ are:

$$(1.3) \qquad T_{122} = T_{212} = T_{221} = -T_{111}, \qquad T_{112} = T_{121} = T_{211} = -T_{222}.$$

We can decompose any third-order tensor $\mathbf{D}$ into an irreducible third-order tensor $\mathbf{T}$ and three vectors $D_{ill}\mathbf{e}_i$, $D_{lil}\mathbf{e}_i$, $D_{lli}\mathbf{e}_i$ in the form:

$$(1.4) \qquad T_{ijk} = 4D_{ijk} - (3D_{llk} - D_{lkl} - D_{kll})\delta_{ij} - (3D_{ljl} - D_{jll} - D_{llj})\delta_{ik}$$
$$-(3D_{ill} - D_{lil} - D_{lli})\delta_{jk},$$

where δ_{ij} denotes the Kronecker symbol. An elementary method of reducing tensors of any order to sums of irreducible tensors is described by SPENCER [6] and HANNABUSS [3].

In view of (1.4) we further postulate that the third-order tensors $\mathbf{T}_\lambda$ (i.e., $\mathbf{T}_1, \ldots, \mathbf{T}_L$) are all irreducible. In this paper, we determine the complete and irreducible representations relative to the eight symmetries in Table 1 for scalar-, vector-, second-order tensor- and third-order tensor-valued functions of $\mathbf{A}_\alpha$, $\mathbf{W}_\xi$, $\mathbf{v}_\varrho$ and $\mathbf{T}_\lambda$.

2. Isotropic representations in different cases

In order to provide compact procedures of determining complete and irreducible tensor function representations relative to the eight symmetries given in Table 1, we derive in this section representations with respect to different cases of the variables $\mathbf{A}_\alpha$, $\mathbf{W}_\xi$, $\mathbf{v}_\varrho$, $\mathbf{T}_\lambda$. The method employed here is described by ZHENG [7, 8].

It is profitable to introduce the following abbreviations and relations:

$$
\begin{aligned}
\mathbf{t}^{\mathbf{A}} = \mathbf{T} : \mathbf{A} &= T_{ijk}A_{jk}\mathbf{e}_i \\
&= (T_{111}\mathbf{e}_1 + T_{211}\mathbf{e}_2)(A_{11} - A_{22}) + 2(T_{211}\mathbf{e}_1 - T_{111}\mathbf{e}_2)A_{12}, \\
\mathbf{t}^{\mathbf{v}} = \mathbf{T} : (\mathbf{v} \otimes \mathbf{v}) &= T_{ijk}x_jx_k\mathbf{e}_i \\
&= (T_{111}\mathbf{e}_1 + T_{211}\mathbf{e}_2)(x_1^2 - x_2^2) + 2(T_{211}\mathbf{e}_1 - T_{111}\mathbf{e}_2)x_1x_2, \\
\mathbf{T}^{\mathbf{v}} = \mathbf{T}\cdot\mathbf{v} &= T_{ijk}x_k\mathbf{e}_{ij} \\
&= (T_{111}x_1 + T_{211}x_2)(\mathbf{e}_{11} - \mathbf{e}_{22}) + (T_{211}x_1 - T_{111}x_2)(\mathbf{e}_{12} + \mathbf{e}_{21}), \\
\mathbf{T} : \mathbf{S} &= T_{ikl}S_{klj}\mathbf{e}_{ij} \\
&= 2(T_{111}S_{111} + T_{211}S_{211})\mathbf{1} + 2(T_{111}S_{211} - T_{211}S_{111})(\mathbf{e}_{12} - \mathbf{e}_{21}), \\
\mathbf{TW} &= T_{ijl}W_{lk}\mathbf{e}_{ijk} \\
&= [T_{111}(\mathbf{e}_{112} + \mathbf{e}_{121} + \mathbf{e}_{211} - \mathbf{e}_{222}) + T_{211}(\mathbf{e}_{122} + \mathbf{e}_{212} + \mathbf{e}_{221} - \mathbf{e}_{111})]W_{12},
\end{aligned}
$$

(2.1)

and

$$
\mathbf{T} \vdots \mathbf{S} = T_{ijk}S_{ijk} = 4(T_{111}S_{111} + T_{211}S_{211}),
$$

$$
(\mathbf{x}\cdot\mathbf{t_x})^2 + (\mathbf{x}\cdot\boldsymbol{\varepsilon}\mathbf{t_x})^2 = (\mathbf{T}\vdots\mathbf{T})(\mathbf{x}\cdot\mathbf{x})^3/4,
$$

(2.2)

$$
(\mathbf{t_A}\cdot\mathbf{A}\,\mathbf{t_A})^2 + (\mathbf{t_A}\cdot\boldsymbol{\varepsilon}\mathbf{A}\,\mathbf{t_A})^2 = (\mathbf{T}\vdots\mathbf{T})^2[2\operatorname{tr}\mathbf{A}^2 - (\operatorname{tr}\mathbf{A})^2]^3/64,
$$

where $\mathbf{T}$ and $\mathbf{S}$ denote any two irreducible third-order tensors, and $\mathbf{A}$, $\mathbf{W}$ and $\mathbf{v}$ any second-order symmetric tensor, second-order skew-symmetric tensor and vector, respectively. Let $\mathbf{D}$ be any third-order tensor. The symbol $\{\mathbf{D}\}$ denotes as a set of the following three tensors:

(2.3)
$$
D_{ijk}\mathbf{e}_{ijk}, \qquad D_{ijk}\mathbf{e}_{jki}, \qquad D_{ijk}\mathbf{e}_{kij},
$$

and $\langle\mathbf{D}\rangle$ is the summation of the above three tensors, that is,

(2.4)
$$
\langle\mathbf{D}\rangle = D_{ijk}(\mathbf{e}_{ijk} + \mathbf{e}_{jki} + \mathbf{e}_{kij}).
$$

2.1. Representations when there exists a non-zero vector v among $\mathbf{v}_\varrho$

We can choose an orthonormal frame $\{\mathbf{e}_i\}$ so that $\mathbf{v} = \nu_1\mathbf{e}_1$ with $\nu_1 > 0$. Thus, we can write

(2.5)
$$
\begin{aligned}
&\mathbf{v}\cdot\mathbf{v} \Rightarrow \nu_1, \qquad \mathbf{v} \Rightarrow \mathbf{e}_1, \qquad \mathbf{v}\cdot\mathbf{v}_\varrho \Rightarrow \nu_{\varrho 1} \qquad (\mathbf{v}_\varrho \neq \mathbf{v}), \\
&\mathbf{v}\otimes\mathbf{v}, \mathbf{1} \Rightarrow \mathbf{e}_{11}, \mathbf{e}_{22}, \qquad \mathbf{v}\cdot\mathbf{A}_\alpha\mathbf{v}, \operatorname{tr}\mathbf{A}_\alpha \Rightarrow A_{\alpha 11}, A_{\alpha 22}, \\
&\mathbf{v}\otimes\mathbf{v}\otimes\mathbf{v}, \{\mathbf{v}\otimes\mathbf{1}\} \Rightarrow \mathbf{e}_{111}, \{\mathbf{e}_{122}\}, \qquad \mathbf{v}\cdot\mathbf{t}_\lambda^{\mathbf{v}} \Rightarrow T_{\lambda 111}.
\end{aligned}
$$

In this paper, the notation $A \Rightarrow B$ means that B is uniquely determined by A. It is evident that the alternative of $\pm e_2$ does not affect (2.5). Thus, the undetermined quantities remain

$$\nu_{\varrho 2}, \; A_{\alpha 12}, \; W_{\xi 12}, \; T_{\lambda 211}; \qquad e_2; \qquad e_{12} \pm e_{21}; \qquad e_{222}, \{e_{112}\}.$$

If all $\nu_{\varrho 2}$, $A_{\alpha 12}$, $W_{\xi 12}$, and $T_{\lambda 211}$ equal zero, we do not need to determine e_2, $e_{12} \pm e_{21}$, $\{e_{112}\}$ and e_{222}. Otherwise, keeping (2.5) in mind, we consider the following cases 1–4.

CASE 1. $W_{12} \neq 0$ for a tensor $\mathbf{W}$ among $\mathbf{W}_\xi$. We alternate $\pm e_2$ so that $W_{12} > 0$ and then give

$$\begin{aligned}
&\operatorname{tr}\mathbf{W}^2 \Rightarrow W_{12}, \qquad \mathbf{Wv} \Rightarrow e_2, \qquad \mathbf{v}\cdot\mathbf{Wv}_\varrho \Rightarrow \nu_{\varrho 2} \qquad (\mathbf{v}_\varrho \neq \mathbf{v}), \\
&\mathbf{v}\otimes\mathbf{Wv} + \mathbf{Wv}\otimes\mathbf{v} \Rightarrow e_{12} + e_{21}, \qquad \mathbf{v}\cdot\mathbf{A}_\alpha\mathbf{Wv} \Rightarrow A_{\alpha 12}, \\
(2.6) \qquad &\mathbf{W} \Rightarrow e_{12} - e_{21}, \qquad \operatorname{tr}\mathbf{WW}_\xi \Rightarrow W_{\xi 12} \qquad (\mathbf{W}_\xi \neq \mathbf{W}), \\
&\langle \mathbf{v}\otimes\mathbf{v}\otimes\mathbf{Wv}\rangle \quad (\text{or}\;\; \mathbf{Wv}\otimes\mathbf{Wv}\otimes\mathbf{Wv}), \quad \{\mathbf{Wv}\otimes\mathbf{1}\} \Rightarrow e_{222}, \{e_{112}\}, \\
&\mathbf{v}\cdot\mathbf{Wt}_\lambda^{\mathbf{v}} \qquad (\text{or}\;\; \mathbf{v}\cdot\mathbf{Wt}_\lambda^{\mathbf{Wv}}) \Rightarrow T_{\lambda 211}.
\end{aligned}$$

CASE 2. $u_2 \neq 0$ for a vector $\mathbf{u}$ among $\mathbf{v}_\varrho$. We can select $\pm e_2$ so that $u_2 > 0$ and then have

$$\begin{aligned}
&\mathbf{u}\cdot\mathbf{u} \Rightarrow u_2, \qquad \mathbf{u} \Rightarrow e_2, \qquad \mathbf{u}\cdot\mathbf{v}_\varrho \Rightarrow \nu_{\varrho 2} \qquad (\mathbf{v}_\varrho \neq \mathbf{v}, \mathbf{u}), \\
&\mathbf{v}\otimes\mathbf{u}\pm\mathbf{u}\otimes\mathbf{v} \Rightarrow e_{12} \pm e_{21}, \qquad \mathbf{v}\cdot\mathbf{A}_\alpha\mathbf{u} \Rightarrow A_{\alpha 12}, \qquad \mathbf{v}\cdot\mathbf{W}_\xi\mathbf{u} \Rightarrow W_{\xi 12}, \\
(2.7) \qquad &\langle\mathbf{v}\otimes\mathbf{v}\otimes\mathbf{u}\rangle \quad (\text{or}\;\; \mathbf{u}\otimes\mathbf{u}\otimes\mathbf{u}, \;\; \text{if}\;\; u_2^2 \neq 3u_1^2), \quad \{\mathbf{u}\otimes\mathbf{1}\} \Rightarrow e_{222}, \{e_{112}\}, \\
&\mathbf{u}\cdot\mathbf{t}_\lambda^{\mathbf{v}} \quad (\text{or}\;\; \mathbf{u}\cdot\mathbf{t}_\lambda^{\mathbf{u}}, \;\; \text{if}\;\; u_2^2 \neq 3u_1^2) \Rightarrow T_{\lambda 211}.
\end{aligned}$$

CASE 3. $A_{12} \neq 0$ for a tensor $\mathbf{A}$ among $\mathbf{A}_\alpha$. By alternating $\pm e_2$ we can arrive at $A_{12} > 0$ and

$$\begin{aligned}
&\operatorname{tr}\mathbf{A}^2 \Rightarrow A_{12}, \qquad \mathbf{A} \Rightarrow e_{12} + e_{21}, \qquad \operatorname{tr}\mathbf{AA}_\alpha \Rightarrow A_{\alpha 12} \qquad (\mathbf{A}_\alpha \neq \mathbf{A}), \\
&\mathbf{Av} \Rightarrow e_2, \qquad \mathbf{v}\cdot\mathbf{Av}_\varrho \Rightarrow \nu_{\varrho 2} \qquad (\mathbf{v}_\varrho \neq \mathbf{v}), \\
(2.8) \qquad &\mathbf{v}\otimes\mathbf{Av} - \mathbf{Av}\otimes\mathbf{v} \Rightarrow e_{12} - e_{21}, \qquad \mathbf{v}\cdot\mathbf{AW}_\xi\mathbf{v} \Rightarrow W_{\xi 12}, \\
&\langle\mathbf{v}\otimes\mathbf{A}\rangle, \; \{\mathbf{Av}\otimes\mathbf{1}\} \Rightarrow e_{222}, \{e_{112}\}, \qquad \mathbf{v}\cdot\mathbf{t}_\lambda^{\mathbf{A}} \Rightarrow T_{\lambda 211}.
\end{aligned}$$

CASE 4. $T_{211} \neq 0$ for a tensor $\mathbf{T}$ among $\mathbf{T}_\lambda$. Choosing $\pm e_2$ so that $T_{211} > 0$ can follow

$$\begin{aligned}
&\mathbf{T}\vdots\mathbf{T} \Rightarrow T_{211}, \qquad \mathbf{t}^{\mathbf{v}} \Rightarrow e_2, \qquad \mathbf{v}_\varrho\cdot\mathbf{t}^{\mathbf{v}} \Rightarrow \nu_{\varrho 2} \qquad (\mathbf{v}_\varrho \neq \mathbf{v}), \\
&\mathbf{T}^{\mathbf{v}} \Rightarrow e_{12} + e_{21}, \qquad \mathbf{v}\cdot\mathbf{t}^{\mathbf{A}_\alpha} = \operatorname{tr}(\mathbf{A}_\alpha\mathbf{T}^{\mathbf{v}}) \Rightarrow A_{\alpha 12}, \\
(2.9) \qquad &\mathbf{v}\otimes\mathbf{t}^{\mathbf{v}} - \mathbf{t}^{\mathbf{v}}\otimes\mathbf{v} \Rightarrow e_{12} - e_{21}, \qquad \mathbf{v}\cdot\mathbf{W}_\xi\mathbf{t}^{\mathbf{v}} \Rightarrow W_{\xi 12}, \\
&\mathbf{T}, \; \{\mathbf{t}^{\mathbf{v}}\otimes\mathbf{1}\} \Rightarrow e_{222}, \{e_{112}\}, \qquad \mathbf{T}\vdots\mathbf{T}_\lambda \Rightarrow T_{\lambda 211} \qquad (\mathbf{T}_\lambda \neq \mathbf{T}).
\end{aligned}$$

2.2. Representations when all vectors v_ϱ equal zero, there exists a tensor A among A_α which has two distinct principal values, and there exists a non-zero tensor T among T_λ

By selecting $\pm e_1$ and $\pm e_2$ as orthogonal principal directions of A, we can express $A = A_{11}e_{11} + A_{22}e_{22}$ and then we have

$$(2.10) \qquad \begin{aligned} \operatorname{tr} A, \ \operatorname{tr} A^2 &\Rightarrow A_{11}, \ A_{22}, && 1, \ A \Rightarrow e_{11}, \ e_{22}, \\ \operatorname{tr} A_\alpha, \ \operatorname{tr} A A_\alpha &\Rightarrow A_{\alpha 11}, \ A_{\alpha 22} && (A_\alpha \neq A). \end{aligned}$$

Note that choices of $\pm e_1$ and of $\pm e_2$ do not influence (2.10). Since T is a non-zero irreducible third-order tensor, without loss of generality we can suppose that $T_{111} > 0$ by alternating e_1 and e_2 and choosing $\pm e_1$. It follows

$$(2.11) \qquad T \overset{.}{:} T, \ t^A \cdot A t^A \Rightarrow T_{111}, \ T_{211}^2.$$

For the remaining undetermined quantities:

$$\nu_{\varrho i}, \ A_{\alpha 12}, \ W_{\xi 12}, \ T_{\lambda i 11}; \qquad e_i; \qquad e_{12} \pm e_{21}; \qquad e_{ijk} \qquad (i, j, k = 1, 2),$$

we consider the following cases i – iv.

CASE i. $W_{12} \neq 0$ for a tensor W among W_ξ. We choose $\pm e_2$ so that $W_{12} > 0$ and then we have

$$(2.12) \qquad \begin{aligned} \operatorname{tr} W^2 &\Rightarrow W_{12}, & t^A \cdot A W t^A &\Rightarrow T_{211}, & t^A, \ W t^A &\Rightarrow e_i, \\ A W - W A &\Rightarrow e_{12} + e_{21}, & \operatorname{tr} A A_\alpha W &\Rightarrow A_{\alpha 12} & (A_\alpha \neq A), \\ W &\Rightarrow e_{12} - e_{21}, & \operatorname{tr} W W_\xi &\Rightarrow W_{\xi 12} & (W_\xi \neq W), \\ T, \ T W, & \{t^A \otimes 1\}, \ \{W t^A \otimes 1\} &\Rightarrow e_{ijk}, \\ T \overset{.}{:} T_\lambda, & \operatorname{tr}(T : T_\lambda) W &\Rightarrow T_{\lambda i 11} & (T_\lambda \neq T). \end{aligned}$$

CASE ii. $T_{111}T_{211} \neq 0$. Alternating $\pm e_2$ can yield $T_{211} > 0$ and then

$$(2.13) \qquad \begin{aligned} T \overset{.}{:} T, \ t^A \cdot A t^A &\Rightarrow T_{211}, & t^A, \ A t^A &\Rightarrow e_i, \\ t^A \otimes t^A &\Rightarrow e_{12} + e_{21}, & t^A \cdot A_\alpha t^A &\Rightarrow A_{\alpha 12} & (A_\alpha \neq A), \\ t^A \otimes A t^A - A t^A \otimes t^A &\Rightarrow e_{12} + e_{21}, & t^A \cdot A W_\xi t^A &\Rightarrow W_{\xi 12}, \\ T, \ \langle A t^A \otimes A \rangle, \ \{t^A \otimes 1\}, \ \{A t^A \otimes 1\} &\Rightarrow e_{ijk}, \\ T \overset{.}{:} T_\lambda, \ t^A \cdot A t^A_\lambda &\Rightarrow T_{\lambda i 11} & (T_\lambda \neq T). \end{aligned}$$

CASE iii. $T_{211} = 0$ and $B_{12} \neq 0$ for a tensor **B** among $\mathbf{A}_\alpha$. Selecting $\pm \mathbf{e}_2$ so that $B_{12} > 0$, we have

$$\mathrm{tr}\,\mathbf{B}^2 \Rightarrow B_{12}, \qquad \mathbf{t}^A, \ \mathbf{t}^B \Rightarrow \mathbf{e}_i,$$

$$\mathbf{B} \Rightarrow \mathbf{e}_{12} + \mathbf{e}_{21}, \qquad \mathrm{tr}\,\mathbf{B}\mathbf{A}_\alpha \Rightarrow A_{\alpha 12} \qquad (\mathbf{A}_\alpha \neq \mathbf{A}, \ \mathbf{B}),$$

(2.14) $\qquad \mathbf{A}\mathbf{B} - \mathbf{B}\mathbf{A} \Rightarrow \mathbf{e}_{12} - \mathbf{e}_{21}, \qquad \mathrm{tr}\,\mathbf{A}\mathbf{B}\mathbf{W}_\xi \Rightarrow W_{\xi 12},$

$$\mathbf{T}, \ \mathbf{T}(\mathbf{A}\mathbf{B} - \mathbf{B}\mathbf{A}), \ \{\mathbf{t}^A \otimes \mathbf{1}\}, \ \{\mathbf{t}^B \otimes \mathbf{1}\} \Rightarrow \mathbf{e}_{ijk},$$

$$\mathbf{T} \overset{:}{:} \mathbf{T}_\lambda, \ \mathrm{tr}\,(\mathbf{T} : \mathbf{T}_\lambda)\mathbf{A}\mathbf{B} \Rightarrow T_{\lambda i 11} \qquad (\mathbf{T}_\lambda \neq \mathbf{T}).$$

CASE iv. $T_{211} = 0$ and $S_{211} \neq 0$ for a tensor **S** among $\mathbf{T}_\lambda$. Selecting $\pm \mathbf{e}_2$ so that $S_{211} > 0$ can follow,

$$\mathbf{T} \overset{:}{:} \mathbf{S}, \ \mathbf{S} \overset{:}{:} \mathbf{S} \Rightarrow S_{111}, \ S_{211}, \qquad \mathbf{t}^A, \ \mathbf{s}^A \Rightarrow \mathbf{e}_i,$$

$$\mathbf{A}(\mathbf{T} : \mathbf{S}) - (\mathbf{S} : \mathbf{T})\mathbf{A} \Rightarrow \mathbf{e}_{12} + \mathbf{e}_{21},$$

$$\mathrm{tr}\,(\mathbf{T} : \mathbf{S})\mathbf{A}\mathbf{A}_\alpha \Rightarrow A_{\alpha 12} \qquad (\mathbf{A}_\alpha \neq \mathbf{A}),$$

(2.15)

$$\mathbf{T} : \mathbf{S} - \mathbf{S} : \mathbf{T} \Rightarrow \mathbf{e}_{12} - \mathbf{e}_{21}, \qquad \mathrm{tr}\,(\mathbf{T} : \mathbf{S})\mathbf{W}_\xi \Rightarrow W_{\xi 12},$$

$$\mathbf{T}, \ \mathbf{S}, \ \{\mathbf{t}^A \otimes \mathbf{1}\}, \ \{\mathbf{s}^A \otimes \mathbf{1}\} \Rightarrow \mathbf{e}_{ijk},$$

$$\mathbf{T} \overset{:}{:} \mathbf{T}_\lambda, \ \mathbf{S} \overset{:}{:} \mathbf{T}_\lambda \Rightarrow T_{\lambda i 11} \qquad (\mathbf{T}_\lambda \neq \mathbf{T}, \ \mathbf{S}).$$

2.3. Representations when all $\mathbf{v}_\varrho$ are null vectors, all $\mathbf{A}_\alpha$ have not two distinct principal values, and there is a non-zero tensor T among $\mathbf{T}_\lambda$

Since $\mathbf{A}_\alpha$ have not two distinct principal values, we can express them as $\mathbf{A}_\alpha = (\mathrm{tr}\,\mathbf{A}_\alpha)\mathbf{1}/2$. It is known from Table 2 of ZHENG and SPENCER [12] that any rotation tensor $\mathbf{R}(\varphi)$ leaves $\mathbf{1}$, $\mathbf{e}_{12} - \mathbf{e}_{21}$, $\mathbf{A}_\alpha = (\mathrm{tr}\,\mathbf{A}_\alpha/2)\mathbf{1}$ and $\mathbf{W}_\xi = W_{\xi 12}(\mathbf{e}_{12} - \mathbf{e}_{21})$ unaltered. Then, we have the following transformation relations

$$(\mathbf{e}_1 + \imath \mathbf{e}_2) \mapsto \exp(\pm \imath \varphi)(\mathbf{e}_1 + \imath \mathbf{e}_2),$$

$$\{(\mathbf{e}_1 + \imath \mathbf{e}_2) \otimes \mathbf{1}\} \mapsto \exp(\pm \imath \varphi)\{(\mathbf{e}_1 + \imath \mathbf{e}_2) \otimes \mathbf{1}\},$$

(2.16) $\quad (\mathbf{e}_{11} - \mathbf{e}_{22}) + \imath(\mathbf{e}_{12} + \mathbf{e}_{21}) \mapsto \exp(\pm \imath 2\varphi)[(\mathbf{e}_{11} - \mathbf{e}_{22}) + \imath \mathbf{e}_{12} + \mathbf{e}_{21})],$

$$(\mathbf{e}_{111} - \langle \mathbf{e}_{122}\rangle) + \imath(\langle \mathbf{e}_{112}\rangle - \mathbf{e}_{222})$$

$$\mapsto \exp(\pm \imath 3\varphi)[(\mathbf{e}_{111} - \langle \mathbf{e}_{122}\rangle) + \imath(\langle \mathbf{e}_{112}\rangle - \mathbf{e}_{222})],$$

where $\imath = \sqrt{(-1)}$ is the unit imaginary number. Thus, we can rotate $\{\mathbf{e}_i\}$ until $T_{111} > 0$ and $T_{211} = 0$, and then give

(2.17) $\qquad \mathbf{T} \overset{:}{:} \mathbf{T} \Rightarrow T_{111}, \qquad \mathbf{T} \Rightarrow \mathbf{e}_{111} - \langle \mathbf{e}_{122}\rangle, \qquad \mathbf{T} \overset{:}{:} \mathbf{T}_\lambda \Rightarrow T_{\lambda 111} \qquad (\mathbf{T}_\lambda \neq \mathbf{T}).$

From (2.16) we can see that $\mathbf{R}(2\pi/3)$ leaves $\mathbf{e}_{111} - \langle \mathbf{e}_{122}\rangle$, $\langle \mathbf{e}_{112}\rangle - \mathbf{e}_{222}$ and $\mathbf{T}_\lambda$ unaltered, but it varies $\mathbf{e}_i$, $\mathbf{e}_{11} - \mathbf{e}_{22}$, $\mathbf{e}_{12} + \mathbf{e}_{21}$ and $\{\mathbf{e}_i \otimes \mathbf{1}\}$ so that they do not

need to be determined in view of the isotropy condition. In other words, we only need to determine

$$W_{\xi 12}, \quad T_{\lambda 211}, \quad \mathbf{e}_{12} - \mathbf{e}_{21}, \quad \langle \mathbf{e}_{112} \rangle - \mathbf{e}_{222}.$$

If there exists a non-zero tensor $\mathbf{W}$ among $\mathbf{W}_\xi$ or there is a non-zero tensor $\mathbf{S}$ among $\mathbf{T}_\lambda$, we select $\pm \mathbf{e}_2$ so that $W_{12} > 0$ or $S_{211} > 0$, and then we write

$$(2.18) \quad \begin{array}{llll} \operatorname{tr} \mathbf{W}^2 \Rightarrow W_{12}, & \mathbf{W} \Rightarrow \mathbf{e}_{12} - \mathbf{e}_{21}, & \operatorname{tr} \mathbf{W} \mathbf{W}_\xi \Rightarrow W_{\xi 12} & (\mathbf{W}_\xi \neq \mathbf{W}), \\ \mathbf{T} \mathbf{W} \Rightarrow \langle \mathbf{e}_{112} \rangle - \mathbf{e}_{222}, & \operatorname{tr} (\mathbf{T} : \mathbf{S}) \mathbf{W}_\xi \Rightarrow T_{\lambda 211} & (\mathbf{T}_\lambda \neq \mathbf{T}), \end{array}$$

or

$$(2.19) \quad \begin{array}{llll} \mathbf{S} \overset{.}{:} \mathbf{S} \Rightarrow \mathbf{S}_{211}, & \mathbf{T} : \mathbf{S} - \mathbf{S} : \mathbf{T} \Rightarrow \mathbf{e}_{12} - \mathbf{e}_{21}, & \operatorname{tr} (\mathbf{T} : \mathbf{S}) \mathbf{W}_\xi \Rightarrow W_{\xi 12}, \\ \mathbf{S} \Rightarrow \langle \mathbf{e}_{112} \rangle - \mathbf{e}_{222}, & \mathbf{S} \overset{.}{:} \mathbf{T}_\lambda \Rightarrow T_{\lambda 211} & (\mathbf{T}_\lambda \neq \mathbf{T}, \ \mathbf{S}). \end{array}$$

Otherwise, if all $T_{\lambda 211}$ and $W_{\xi 12}$ equal zero, we do not need to determine $\mathbf{e}_{12} - \mathbf{e}_{21}$ and $\langle \mathbf{e}_{112} \rangle - \mathbf{e}_{222}$.

2.4. Representation when all vectors $\mathbf{v}_\varrho$ and third-order tensors $\mathbf{T}_\lambda$ are equal to zero

Since the central inversion $-\mathbf{1}$ leaves tensors of even orders unaltered but changes the sign of tensors of odd orders, the isotropy condition requires that any isotropic vector- and third-order tensor-valued functions of second-order tensor $\mathbf{A}_\alpha$ and $\mathbf{W}_\xi$ should be only a zero-vector and a third-order zero-tensor, respectively. The complete and irreducible representations for scalar- and second-order tensor-valued functions of $\mathbf{A}_\alpha$ and $\mathbf{W}_\xi$ can be seen, for example, in Tables 2, 4 and 5 of ZHENG [8].

3. The complete and irreducible tensor function representations

The complete and irreducible representations were established by ZHENG [8] for scalar-, vector-, second-order symmetric and skew-symmetric tensor-valued functions of $\mathbf{A}_\alpha$, $\mathbf{W}_\xi$, $\mathbf{v}_\varrho$ with respect to all kinds of symmetry, particularly, to the eight symmetries shown in Table 1. With these known results and the representations derived in the preceding section, we determine in the sequel the complete representations for the eight symmetries shown in Table 1. The irreducibility of the derived representations is verified in the next section.

3.1. Representation for isotropy $C_{\infty\nu}$

The complete representations for isotropic tensor functions of $\mathbf{A}_\alpha$, $\mathbf{W}_\xi$, $\mathbf{v}_\varrho$ and $\mathbf{T}_\lambda$ can be obtained by considering all the cases in Secs. 2.1–2.3 i.e., from (2.5)–(2.19), as summarized in Tables 2 and 3.

Table 2. Irreducible function bases.

$C_{\infty\nu}$	$\operatorname{tr}A,\ \operatorname{tr}A^2,\ \operatorname{tr}AB,\ \operatorname{tr}W^2,\ \operatorname{tr}ABW,\ \operatorname{tr}WV,\ v\cdot v,$ $v\cdot Av,\ v\cdot AWv,\ v\cdot u,\ v\cdot Au,\ v\cdot Wu;\ T\dot{:}T,$ $t^A\cdot At^A,\ t^A\cdot Bt^A,\ T^A\cdot AWt^A,\ v\cdot t^v,\ v\cdot t^A,\ v\cdot Wt^v,$ $u\cdot t^v,\ T\dot{:}S,\ t^A\cdot As^A,\ \operatorname{tr}(T:S)AB,\ \operatorname{tr}(T:S)W$	C_∞	$\operatorname{tr}A,\ \operatorname{tr}A^2,\ \operatorname{tr}AB,\ \operatorname{tr}AB\varepsilon,\ \operatorname{tr}\varepsilon W,$ $v\cdot v,\ v\cdot Av,\ v\cdot A\varepsilon v,\ v\cdot u,\ v\cdot\varepsilon u;$ $T\dot{:}T,\ t^A\cdot At^A,\ t^A\cdot A\varepsilon t^A,\ v\cdot t^v,$ $v\cdot\varepsilon t^v,\ T\dot{:}S,\ \operatorname{tr}(T:S)\varepsilon$
$C_{3\nu}$	$\operatorname{tr}A,\ \operatorname{tr}A^2,\ p^A\cdot Ap^A,\ \operatorname{tr}AB,\ p^A\cdot Bp^A,\ \operatorname{tr}W^2,$ $p^A\cdot AWp^A,\ \operatorname{tr}ABW,\ \operatorname{tr}WV,\ v\cdot v,\ v\cdot p^v,\ v\cdot Av,$ $v\cdot p^A,\ v\cdot Wp^v,\ v\cdot AWv,\ v\cdot u,\ u\cdot p^v,\ v\cdot Wu;$ $T\dot{:}T,\ P\dot{:}T,\ p^A\cdot At^A,\ \operatorname{tr}(P:T)W,\ v\cdot t^v,\ v\cdot t^A,$ $v\cdot(P:T)u,\ \operatorname{tr}(P:T)AB,\ T\dot{:}S$	C_3	$\operatorname{tr}A,\ p^A\cdot Ap^A,\ p^A\cdot A\varepsilon p^A,\ \operatorname{tr}AB,$ $\operatorname{tr}AB\varepsilon,\ \operatorname{tr}\varepsilon W,\ v\cdot p^v,\ v\cdot\varepsilon p^v,$ $v\cdot Av,\ v\cdot A\varepsilon v,\ v\cdot u,\ v\cdot\varepsilon u;$ $P\dot{:}T,\ \operatorname{tr}(P:T)\varepsilon$
$C_{2\nu}$	$\operatorname{tr}A,\ \operatorname{tr}A^2,\ \operatorname{tr}MA,\ \operatorname{tr}AB,\ \operatorname{tr}W^2,\ \operatorname{tr}MAW,\ \operatorname{tr}WV,$ $v\cdot v,\ v\cdot Mv,\ v\cdot Av,\ v\cdot MWv,\ v\cdot u,\ v\cdot Mu,\ v\cdot Au,$ $v\cdot Wu;\ T\dot{:}T,\ t^M\cdot Mt^M,\ t^M\cdot At^M,\ t^M\cdot MWt^M,$ $v\cdot t^v,\ v\cdot t^M,\ v\cdot t^A,\ v\cdot Wt^M,\ T\dot{:}S,\ t^M\cdot Ms^M,$ $\operatorname{tr}(T:S)MA,\ \operatorname{tr}(T:S)W$	C_2	$\operatorname{tr}A,\ \operatorname{tr}MA,\ \operatorname{tr}MA\varepsilon,\ \operatorname{tr}\varepsilon W,$ $v\cdot Mv,\ v\cdot M\varepsilon v,\ v\cdot u,\ v\cdot\varepsilon u;$ $T\dot{:}T,\ t^M\cdot Mt^M,\ t^M\cdot M\varepsilon t^M,$ $v\cdot t^M,\ v\cdot\varepsilon t^M,\ T\dot{:}S,\ \operatorname{tr}(T:S)\varepsilon$
$C_{1\nu}$	$\operatorname{tr}A,\ \operatorname{tr}A^2,\ a\cdot Aa,\ \operatorname{tr}AB,\ \operatorname{tr}W^2,\ a\cdot AWa,\ \operatorname{tr}WV,$ $v\cdot v,\ a\cdot v,\ a\cdot Av,\ a\cdot Wv,\ v\cdot u;\ T\dot{:}T,\ a\cdot t^a,\ a\cdot t^A,$ $a\cdot Wt^a,\ v\cdot t^a,\ T\dot{:}S$	C_1	$a\cdot Aa,\ b\cdot Ab,\ a\cdot Ab,\ \operatorname{tr}\varepsilon W,$ $a\cdot v,\ b\cdot v;\ a\cdot t^a,\ b\cdot t^b$

In Tables 2 and 3, the following abbreviations are employed:

$$(3.1)\qquad
\begin{aligned}
A &= A_\alpha, & B &= A_\beta, & W &= W_\xi, & V &= W_\zeta, \\
v &= v_\varrho, & u &= v_\sigma, & T &= T_\lambda, & S &= T_\mu,
\end{aligned}$$

with $\alpha,\beta = 1,\ldots,N$ and $\alpha < \beta$; $\xi,\zeta = 1,\ldots,M$ and $\xi < \zeta$; $\varrho,\sigma = 1,\ldots,P$ and $\varrho < \sigma$; and $\lambda,\mu = 1,\ldots,L$ and $\lambda < \mu$.

An explanation of the redundancy of one of $u\cdot t^v$ and $v\cdot t^u$ may be required. Without loss of generality, we set $T = e_{111} - \langle e_{122}\rangle$. Denote by (v,u) and $(\bar{v},\bar{u})$ two solutions of the equations

$$(3.2)\qquad v\cdot v,\ u\cdot u,\ v\cdot t^v,\ u\cdot t^u,\ v\cdot u,\ u\cdot t^v = \text{const.}$$

Because of $v\cdot v = \bar{v}\cdot\bar{v}$ and $u\cdot u = \bar{u}\cdot\bar{u}$, we may assume that $v = \cos\theta e_1 + \sin\theta e_2$, $u = \cos\varphi e_1 + \sin\varphi e_2$, $\bar{v} = \cos\bar{\theta}e_1 + \sin\bar{\theta}e_2$ and $\bar{u} = \cos\bar{\varphi}e_1 + \sin\bar{\varphi}e_2$. The equations $v\cdot t^v,\ u\cdot t^u,\ v\cdot u,\ u\cdot t^v = \text{constans}$ yield immediately.

$$(3.3)\qquad
\begin{aligned}
\cos 3\theta &= \cos 3\bar{\theta}, & \cos 3\varphi &= \cos 3\bar{\varphi}, \\
\cos(\theta - \varphi) &= \cos(\bar{\theta} - \bar{\varphi}), & \cos(2\theta + \varphi) &= \cos(2\bar{\theta} + \bar{\varphi}).
\end{aligned}$$

It follows that $\cos(\theta + 2\varphi) = \cos(\bar{\theta} + 2\bar{\varphi})$, i.e., $v\cdot t^u = \bar{v}\cdot t^u$. Therefore, $v\cdot t^u$ is redundant.

In a similar manner we can verify the redundancy of one of $t^A\cdot Bt^A$ and $t^B\cdot At^B$, and one of $\langle v\otimes v\otimes u\rangle$ and $\langle u\otimes u\otimes v\rangle$.

Table 3. Complete and irreducible tensor-valued function representations.

vector-valued			
$C_{\infty\nu}$	v, Av, Wv; t^A, At^A, Wt^A, t^v	C_∞	v, εv; t^A, At^A
$C_{3\nu}$	p^A, Ap^A, Wp^A, v, Wv, p^v; t^v	C_3	v, εv; p^A, εp^A
$C_{2\nu}$	v, Mv, Av, Wv; t^M, Mt^M, t^A, Wt^M	C_2	v, εv; t^M, εt^M
$C_{1\nu}$	a, Aa, Wa, v; t^a	C_1	a, b

second-order symmetric tensor-valued			
$C_{\infty\nu}$	1, A, AW − WA, v $\otimes$ v, v $\otimes$ Wv + Wv $\otimes$ v, v $\otimes$ u + u $\otimes$ v; $t^A \otimes t^A$, A(T : S) − (T : S)A	C_∞	1, A, Aε − εA, v $\otimes$ v, v $\otimes$ εv + εv $\otimes$ v
$C_{3\nu}$	1, A, $p^A \otimes p^A$, AW − WA, v $\otimes$ v, P^v, v $\otimes$ Wv + Wv $\otimes$ v; T^v, A(P : T) − (P : T)A	C_3	1, A, Aε − εA, v $\otimes$ v, v $\otimes$ εv + εv $\otimes$ v
$C_{2\nu}$	1, M, A, MW − WM, v $\otimes$ v, v $\otimes$ u + u $\otimes$ v; T^v, $t^M \otimes t^M$, M(T : S) − (T : S)M	C_2	1, M, Mε
$C_{1\nu}$	1, a $\otimes$ a, A, a $\otimes$ Wa + Wa $\otimes$ a, a $\otimes$ v + v $\otimes$ a; T^a	C_1	a $\otimes$ a, b $\otimes$ b, a $\otimes$ b + b $\otimes$ a

second-order skew-symmeric tensor-valued			
$C_{\infty\nu}$	AB − BA, W, v $\otimes$ Av − Av $\otimes$ v, v $\otimes$ u − u $\otimes$ v; $t^A \otimes At^A − At^A \otimes t^A$, v $\otimes t^v − t^v \otimes$ v, T : S − S : T	C_∞	ε
$C_{3\nu}$	$p^A \otimes Ap^A − Ap^A \otimes p^A$, AB − BA, W, v $\otimes p^v − p^v \otimes$ v, v $\otimes$ Av − Av $\otimes$ v, v $\otimes$ u − u $\otimes$ v; P : T − T : P	C_3	ε
$C_{2\nu}$	W, MA − AM, v $\otimes$ Mv − Mv $\otimes$ v, v $\otimes$ u − u $\otimes$ v; v $\otimes t^M − t^M \otimes$ v, $t^v \otimes Mt^v − Mt^v \otimes t^v$, T : S − S : T	C_2	ε
$C_{1\nu}$	a $\otimes$ Aa − Aa $\otimes$ a, W, a $\otimes$ v − v $\otimes$ a; a $\otimes t^a − t^a \otimes$ a	C_1	ε

third-order tensor-valued			
$C_{\infty\nu}$	v $\otimes$ v $\otimes$ v, {v $\otimes$ 1}, $\langle$v $\otimes$ A$\rangle$, {Av $\otimes$ 1}, $\langle$v $\otimes$ v $\otimes$ Wv$\rangle$, {Wv $\otimes$ 1}, $\langle$v $\otimes$ v $\otimes$ u$\rangle$); T, $\langle At^A \otimes$ A$\rangle$, {$t^A \otimes$ 1}, {$At^A \otimes$ 1}, T(AB − BA), TW, {$Wt^A \otimes$ 1}, {$t^v \otimes$ 1}	C_∞	v $\otimes$ v $\otimes$ v, $\langle$v $\otimes$ v $\otimes \varepsilon$v$\rangle$, {v $\otimes$ 1}, {εv $\otimes$ 1}; T, Tε, {$t^A \otimes$ 1}, {$\varepsilon t^A \otimes$ 1}
$C_{3\nu}$	P, $\langle Ap^A \otimes$ A$\rangle$, {$p^A \otimes$ 1}, {$Ap^A \otimes$ 1}, P(AB − BA), PW, {$Wp^A \otimes$ 1}, v $\otimes$ v $\otimes$ v, {v $\otimes$ 1}, {$p^v \otimes$ 1}, $\langle$v $\otimes$ A$\rangle$, {Wv $\otimes$ 1}, P(v $\otimes$ u − u $\otimes$ v), T, {$t^v \otimes$ 1}, {$t^A \otimes$ 1}	C_3	P, Pε, {$p^A \otimes$ 1}, {$\varepsilon p^A \otimes$ 1}, {v $\otimes$ 1}, {εv $\otimes$ 1}
$C_{2\nu}$	v $\otimes$ v $\otimes$ v, $\langle$v $\otimes$ M$\rangle$, {v $\otimes$ 1}, {Mv $\otimes$ 1}, $\langle$v $\otimes$ A$\rangle$, {Av $\otimes$ 1}, $\langle$Wv $\otimes$ M$\rangle$, {Wv $\otimes$ 1}; T, $\langle Mt^M \otimes$ M$\rangle$, {$t^M \otimes$ 1}, {$Mt^M \otimes$ 1}, TW, T(MA − AM), {$Wt^M \otimes$ 1}, {$t^A \otimes$ 1}	C_2	$\langle$v $\otimes$ M$\rangle$, $\langle \varepsilon$v $\otimes$ M$\rangle$, {v $\otimes$ 1}, {εv $\otimes$ 1}; T, Tε, {$t^M \otimes$ 1}, {$\varepsilon t^M \otimes$ 1}
$C_{1\nu}$	a $\otimes$ a $\otimes$ a, {a $\otimes$ 1}, $\langle$a $\otimes$ A$\rangle$, {Aa $\otimes$ 1}, $\langle$a $\otimes$ a $\otimes$ Wa$\rangle$, {Wa $\otimes$ 1}, $\langle$a $\otimes$ a $\otimes$ v$\rangle$, {v $\otimes$ 1}; T, {$t^a \otimes$ 1}	C_1	a $\otimes$ a $\otimes$ a, {a $\otimes$ 1}, b $\otimes$ b $\otimes$ b, {b $\otimes$ 1}

[667]

3.2. Representations for hemitropy $C_\infty(\varepsilon)$

From the fact that ε characterizes the group C_∞ it follows that the hemitropic functions of **A**, **W**, **v** and **T** may be considered as isotropic functions of **A**, **W**, **v**, **T** and ε. Noting that ε is a non-zero second-order skew-symmetric tensor, from (2.5), (2.6), (2.10)–(2.12), (2.17) and (2.18), by substituting ε for **W** in (2.6), (2.12) and (2.18), we obtain complete representations for hemitropic tensor functions of $\mathbf{A}_\alpha$, $\mathbf{W}_\xi$, $\mathbf{v}_\varrho$ and $\mathbf{T}_\lambda$, as shown in Tables 2 and 3.

3.3. Representations for $C_{3v}(\mathbf{P})$

To determine the complete isotropic tensor function representations of $\mathbf{A}_\alpha$, $\mathbf{W}_\xi$, $\mathbf{v}_\varrho$, $\mathbf{T}_\lambda$ and **P**, we consider the following cases instead of the cases in Sec. 2.1. First suppose that $P_{211} = 0$. We have the following invariants and form-invariants instead of those in (2.5)–(2.9), respectively.

$$
\begin{aligned}
&\mathbf{v}\cdot\mathbf{v},\ \mathbf{v}\cdot\mathbf{v}_\varrho,\ \mathbf{v}\cdot\mathbf{A}_\alpha\mathbf{v},\ \mathrm{tr}\,\mathbf{A}_\alpha,\ \mathbf{v}\cdot\mathbf{p}^\mathbf{v},\ \mathbf{P}\vdots\mathbf{T}_\lambda;\quad \mathbf{v};\quad \mathbf{v}\otimes\mathbf{v},\ \mathbf{1};\quad \mathbf{P},\ \{\mathbf{v}\otimes\mathbf{1}\},\\
&\mathrm{tr}\,\mathbf{W}^2,\ \mathbf{v}\cdot\mathbf{W}\mathbf{v}_\varrho,\ \mathrm{tr}\,\mathbf{W}\mathbf{W}_\xi,\ \mathbf{v}\cdot\mathbf{A}_\alpha\mathbf{W}\mathbf{v},\ \mathrm{tr}\,(\mathbf{P}:\mathbf{T}_\lambda)\mathbf{W};\quad \mathbf{W}\mathbf{v};\\
&\hspace{5.5cm}\mathbf{v}\otimes\mathbf{W}\mathbf{v} + \mathbf{W}\mathbf{v}\otimes\mathbf{v};\quad \mathbf{W};\quad \mathbf{P}\mathbf{W},\ \{\mathbf{W}\mathbf{v}\otimes\mathbf{1}\},\\
&\mathbf{u}\cdot\mathbf{u},\ \mathbf{u}\cdot\mathbf{v}_\varrho,\ \mathbf{u}\cdot\mathbf{p}^{\mathbf{A}_\alpha},\ \mathbf{v}\cdot\mathbf{W}_\xi\mathbf{u},\ \mathbf{v}\cdot(\mathbf{P}:\mathbf{T}_\lambda)\mathbf{u};\quad \mathbf{u};\\
&\hspace{5.5cm}\mathbf{P}^\mathbf{u},\ \mathbf{v}\otimes\mathbf{u} - \mathbf{u}\otimes\mathbf{v},\ \mathbf{P}(\mathbf{v}\otimes\mathbf{u} - \mathbf{u}\otimes\mathbf{v}),\ \{\mathbf{u}\otimes\mathbf{1}\},\\
&\mathrm{tr}\,\mathbf{A}^2,\ \mathrm{tr}\,\mathbf{A}\mathbf{A}_\alpha,\ \mathbf{v}_\varrho\cdot\mathbf{p}^\mathbf{A},\ \mathbf{v}\cdot\mathbf{A}\mathbf{W}_\xi\mathbf{v},\ \mathbf{v}\cdot\mathbf{t}^\mathbf{A}{}_\lambda;\quad \mathbf{p}^\mathbf{A};\\
&\hspace{5.5cm}\mathbf{A};\quad \mathbf{v}\otimes\mathbf{A}\mathbf{v} - \mathbf{A}\mathbf{v}\otimes\mathbf{v};\quad \langle\mathbf{v}\otimes\mathbf{A}\rangle,\ \{\mathbf{p}^\mathbf{A}\otimes\mathbf{1}\},\\
&\mathbf{T}\vdots\mathbf{T},\ \mathbf{v}_\varrho\cdot(\mathbf{P}:\mathbf{T})\mathbf{v},\ \mathbf{v}\cdot\mathbf{t}^{\mathbf{A}_\alpha},\ \mathrm{tr}\,(\mathbf{P}:\mathbf{T})\mathbf{W}_\xi,\ \mathbf{T}\vdots\mathbf{T}_\lambda;\\
&\hspace{5.5cm}\mathbf{t}^\mathbf{v};\quad \mathbf{T}^\mathbf{v};\quad \mathbf{P}:\mathbf{T} - \mathbf{T}:\mathbf{P};\quad \mathbf{T},\ \{\mathbf{t}^\mathbf{v}\otimes\mathbf{1}\}.
\end{aligned}
$$
(3.4)

Second, suppose that $P_{211} \neq 0$. Instead of (2.5) and (2.9), respectively, we have

$$
\begin{aligned}
&\mathbf{v}\cdot\mathbf{v},\ \mathbf{v}\cdot\mathbf{v}_\varrho,\ \mathbf{v}\cdot\mathbf{A}_\alpha\mathbf{v},\ \mathrm{tr}\,\mathbf{A}_\alpha,\ \mathbf{v}\cdot\mathbf{p}^\mathbf{v},\ \mathbf{v}\cdot\mathbf{t}^\mathbf{v}_\lambda;\quad \mathbf{v};\quad \mathbf{v}\otimes\mathbf{v},\ \mathbf{1};\quad \mathbf{v}\otimes\mathbf{v}\otimes\mathbf{v},\ \{\mathbf{v}\otimes\mathbf{1}\},\\
&\mathbf{v}_\varrho\cdot\mathbf{p}^\mathbf{v},\ \mathbf{v}\cdot\mathbf{p}^{\mathbf{A}_\alpha},\ \mathbf{v}\cdot\mathbf{W}_\xi\mathbf{p}^\mathbf{v},\ \mathbf{P}\vdots\mathbf{T}_\lambda;\quad \mathbf{p}^\mathbf{v};\quad \mathbf{P}^\mathbf{v};\quad \mathbf{v}\otimes\mathbf{p}^\mathbf{v} - \mathbf{p}^\mathbf{v}\otimes\mathbf{v};\quad \mathbf{P},\ \{\mathbf{p}^\mathbf{v}\otimes\mathbf{1}\}.
\end{aligned}
$$
(3.5)

Finally, from (3.4), (3.5) as well as (2.10)–(2.15), replacing **T** by **P**, we can obtain the complete representations for tensor functions of $\mathbf{A}_\alpha$, $\mathbf{W}_\xi$, $\mathbf{v}_\varrho$ and $\mathbf{T}_\lambda$ under C_{3v}, as shown in Tables 2 and 3.

3.4. Representations for $C_3(\mathbf{P}, \varepsilon)$

If there exists a non-zero vector **v** among $\mathbf{v}_\varrho$, we can write, instead of (2.5) and (2.6), the equations

$$
\begin{aligned}
&\mathbf{v}\cdot\mathbf{v}_\varrho,\ \mathbf{v}\cdot\varepsilon\,\mathbf{v}_\varrho,\ \mathbf{v}\cdot\mathbf{p}^\mathbf{v},\ \mathbf{v}\cdot\varepsilon\,\mathbf{p}^\mathbf{v},\ \mathrm{tr}\,\mathbf{A}_\alpha,\ \mathbf{v}\cdot\mathbf{A}_\alpha\mathbf{v},\ \mathbf{v}\cdot\mathbf{A}_\alpha\varepsilon\,\mathbf{v},\ \mathrm{tr}\,\varepsilon\,\mathbf{W}_\xi,\ \mathbf{P}\vdots\mathbf{T}_\lambda,\\
&\mathrm{tr}\,(\mathbf{P}:\mathbf{T}_\lambda)\varepsilon;\quad \mathbf{v},\ \varepsilon\,\mathbf{v};\quad \mathbf{1},\ \mathbf{v}\otimes\mathbf{v},\ \mathbf{v}\otimes\varepsilon\,\mathbf{v} + \varepsilon\,\mathbf{v}\otimes\mathbf{v};\quad \varepsilon;\quad \mathbf{P},\ \mathbf{P}\varepsilon,\ \{\mathbf{v}\otimes\mathbf{1}\},\ \{\varepsilon\,\mathbf{v}\otimes\mathbf{1}\},
\end{aligned}
$$
(3.6)

where the obviously redundant invariant $\mathbf{v} \cdot \mathbf{v}$ has been removed because of the identity $(\mathbf{v} \cdot \mathbf{v})^3 = (\mathbf{v} \cdot \mathbf{p}^\mathbf{v})^2 + (\mathbf{v} \cdot \mathbf{p}^\mathbf{v})^2$ according to (2.2). Setting $\mathbf{T} = \mathbf{P}$ and $\mathbf{W} = \boldsymbol{\varepsilon}$ in (2.10) – (2.12), (2.17) and (2.18) together with (3.6), we arrive at the complete representations under C_3, as shown in Tables 2 and 3.

3.5. Representations for $C_{2\nu}(\mathbf{M})$

To determine the complete isotropic tensor functions of $\mathbf{A}_\alpha$, $\mathbf{W}_\xi$, $\mathbf{v}_\varrho$, $\mathbf{T}_\lambda$ and $\mathbf{M}$, we consider the following cases instead of the cases in Sec. 2.1. First, suppose that $M_{12} = 0$. We have the following invariants and form-invariants instead of those in (2.5) – (2.9), respectively.

$$\mathbf{v} \cdot \mathbf{v}, \ \mathbf{v} \cdot \mathbf{v}_\varrho, \ \mathbf{v} \cdot \mathbf{M} \mathbf{v}, \ \mathrm{tr} \mathbf{M} \mathbf{A}_\alpha, \ \mathrm{tr} \mathbf{A}_\alpha, \ \mathbf{v} \cdot \mathbf{t}^\mathbf{M}{}_\lambda; \ \mathbf{v}; \ \mathbf{M}, \ \mathbf{1}; \ \langle \mathbf{v} \otimes \mathbf{M} \rangle, \ \{\mathbf{v} \otimes \mathbf{1}\},$$

$$\mathrm{tr} \mathbf{W}^2, \ \mathbf{v} \cdot \mathbf{W} \mathbf{v}_\varrho, \ \mathrm{tr} \mathbf{W} \mathbf{W}_\xi, \ \mathrm{tr} \mathbf{M} \mathbf{A}_\alpha \mathbf{W}, \ \mathbf{v} \cdot \mathbf{W} \mathbf{t}^\mathbf{M}{}_\lambda; \ \mathbf{W} \mathbf{v};$$

$$\mathbf{M} \mathbf{W} - \mathbf{W} \mathbf{M}; \ \mathbf{W}; \ \langle \mathbf{W} \mathbf{v} \otimes \mathbf{M} \rangle, \ \{\mathbf{W} \mathbf{v} \otimes \mathbf{1}\},$$

(3.7) $\quad \mathbf{u} \cdot \mathbf{u}, \ \mathbf{u} \cdot \mathbf{v}_\varrho, \ \mathbf{v} \cdot \mathbf{A}_\alpha \mathbf{u}, \ \mathbf{v} \cdot \mathbf{W}_\xi \mathbf{u}, \ \mathbf{u} \cdot \mathbf{t}^\mathbf{M}{}_\lambda; \ \mathbf{u}; \ \mathbf{v} \otimes \mathbf{u} \pm \mathbf{u} \otimes \mathbf{v}; \ \langle \mathbf{u} \otimes \mathbf{M} \rangle, \ \{\mathbf{u} \otimes \mathbf{1}\},$

$$\mathrm{tr} \mathbf{A}^2, \ \mathbf{v} \cdot \mathbf{A} \mathbf{v}_\varrho, \ \mathrm{tr} \mathbf{A} \mathbf{A}_\alpha, \ \mathrm{tr} \mathbf{M} \mathbf{A} \mathbf{W}_\xi, \ \mathbf{v} \cdot \mathbf{t}^\mathbf{A}{}_\lambda; \ \mathbf{A} \mathbf{v};$$

$$\mathbf{A}; \ \mathbf{M} \mathbf{A} - \mathbf{A} \mathbf{M}; \langle \mathbf{v} \otimes \mathbf{A} \rangle, \{\mathbf{A} \mathbf{v} \otimes \mathbf{1}\},$$

$$\mathbf{T} \colon \mathbf{T}, \ \mathbf{v}_\varrho \cdot \mathbf{t}^\mathbf{M}, \ \mathbf{v} \cdot \mathbf{t}_{\mathbf{A}_\alpha}, \ \mathbf{v} \cdot \mathbf{W}_\xi \mathbf{t}^\mathbf{M}, \ \mathbf{T} \colon \mathbf{T}_\lambda; \ \mathbf{t}^\mathbf{M}; \ \mathbf{T}^\mathbf{v}; \ \mathbf{M} \mathbf{T}^\mathbf{v} - \mathbf{T}^\mathbf{v} \mathbf{M}; \ \mathbf{T}, \ \{\mathbf{t}^\mathbf{M} \otimes \mathbf{1}\}.$$

Second, suppose that $M_{12} \neq 0$. Instead of (2.5) and (2.7), respectively, we have

$$\mathbf{v} \cdot \mathbf{v}, \ \mathbf{v} \cdot \mathbf{v}_\varrho, \ \mathbf{v} \cdot \mathbf{A}_\alpha \mathbf{v}, \ \mathbf{v} \cdot \mathbf{M} \mathbf{v}, \ \mathrm{tr} \mathbf{A}_\alpha, \ \mathbf{v} \cdot \mathbf{t}^\mathbf{v}{}_\lambda; \ \mathbf{v}; \ \mathbf{v} \otimes \mathbf{v}, \ \mathbf{1}; \ \mathbf{v} \otimes \mathbf{v} \otimes \mathbf{v}, \{\mathbf{v} \otimes \mathbf{1}\},$$

(3.8) $\quad \mathrm{tr} \mathbf{M} \mathbf{A}_\alpha, \ \mathbf{v} \cdot \mathbf{M} \mathbf{v}_\varrho, \ \mathbf{v} \cdot \mathbf{M} \mathbf{W}_\xi \mathbf{v}, \ \mathbf{v} \cdot \mathbf{t}^\mathbf{M}{}_\lambda; \ \mathbf{M} \mathbf{v}; \ \mathbf{M};$

$$\mathbf{v} \otimes \mathbf{M} \mathbf{v} - \mathbf{M} \mathbf{v} \otimes \mathbf{v}; \ \langle \mathbf{v} \otimes \mathbf{M} \rangle, \ \{\mathbf{M} \mathbf{v} \otimes \mathbf{1}\}.$$

Finally, from (3.7), (3.8) as well as (2.9) – (2.14), replacing $\mathbf{A}$ by $\mathbf{M}$, we can obtain complete representations for tensor functions of $\mathbf{A}_\alpha$, $\mathbf{W}_\xi$, $\mathbf{v}_\varrho$ and $\mathbf{T}_\lambda$ under $C_{2\nu}$, as shown in Tables 2 and 3.

3.6. Representations for $C_2(\mathbf{M}, \boldsymbol{\varepsilon})$

Instead of (2.5) and (2.6) we have

(3.9) $\quad \mathbf{v} \cdot \mathbf{M} \mathbf{v}, \ \mathbf{v} \cdot \mathbf{M} \boldsymbol{\varepsilon} \mathbf{v}, \ \mathbf{v} \cdot \mathbf{v}_\varrho, \ \mathbf{v} \cdot \boldsymbol{\varepsilon} \mathbf{v}_\varrho, \ \mathrm{tr} \mathbf{A}_\alpha, \ \mathrm{tr} \mathbf{M} \mathbf{A}_\alpha, \ \mathrm{tr} \mathbf{M} \mathbf{A}_\alpha \boldsymbol{\varepsilon}, \ \mathbf{v} \cdot \mathbf{t}^\mathbf{M}{}_\lambda,$

$$\mathbf{v} \cdot \boldsymbol{\varepsilon} \mathbf{t}^\mathbf{M}{}_\lambda, \ \mathrm{tr} \boldsymbol{\varepsilon} \mathbf{W}_\xi; \ \mathbf{v}, \ \boldsymbol{\varepsilon} \mathbf{v}; \ \mathbf{1}, \ \mathbf{M}, \ \mathbf{M} \boldsymbol{\varepsilon}; \ \boldsymbol{\varepsilon};$$

$$\langle \mathbf{v} \otimes \mathbf{M} \rangle, \ \langle \boldsymbol{\varepsilon} \mathbf{v} \otimes \mathbf{M} \rangle, \ \{\mathbf{v} \otimes \mathbf{1}\}, \ \{\boldsymbol{\varepsilon} \mathbf{v} \otimes \mathbf{1}\},$$

where the redundant invariant $\mathbf{v} \cdot \mathbf{v}$ is removed due to the identity $(\mathbf{v} \cdot \mathbf{v})^2 = (\mathbf{v} \cdot \mathbf{M} \mathbf{v})^2 + (\mathbf{v} \cdot \mathbf{M} \boldsymbol{\varepsilon} \mathbf{v})^2$. Setting $\mathbf{A} = \mathbf{M}$ and $\mathbf{W} = \boldsymbol{\varepsilon}$ in (2.10) – (2.12) together with (3.9), we immediately obtain the complete representations under C_2, as presented in Tables 2 and 3.

3.7. Representations for $C_{1\nu}(\mathbf{a})$

Setting $\mathbf{v} = \mathbf{a}$ in (2.5)–(2.9) yields immediately the complete isotropic tensor function representations of $\mathbf{A}_\alpha$, $\mathbf{W}_\xi$, $\mathbf{v}_\varrho$, $\mathbf{T}_\lambda$ and $\mathbf{a}$; namely, the complete tensor function representations of $\mathbf{A}_\alpha$, $\mathbf{W}_\xi$, $\mathbf{v}_\varrho$ and $\mathbf{T}_\lambda$ under $C_{1\nu}$ as given in Tables 2 and 3.

3.8. Representations for $C_1(\mathbf{a}, \varepsilon)$

Settting $\mathbf{v} = \mathbf{a}$ and $\mathbf{W} = \varepsilon$ in (2.5) and (2.6) yields immediately the complete representations with respect to C_1, as given in Tables 2 and 3, where $\varepsilon\mathbf{a}$ is replaced by $\mathbf{b}$ because of $\varepsilon\,\mathbf{a} = \pm\mathbf{b}$.

4. Proof of the irreducibility of the derived representations

To verify the irreducibility of the representations established above in Sec. 3, we employ the technique developed by PENNISI and TROVATO [5]. It is obvious that the representations in Tables 2 and 3 with respect to C_1, C_2 and C_3 are irreducible. With respect to $C_{\infty\nu}$, C_∞, $C_{3\nu}$, $C_{2\nu}$ and $C_{1\nu}$, the irreducibility of all invariants, vector form-invariants, and second-order tensor form-invariants in Tables 2 and 3 when $\mathbf{T}_\lambda = \mathbf{0}$ has ben proved by ZHENG [8]; the irreducibility of all additional invariants and form-invariants when non-zero tensors exist among $\mathbf{T}_\lambda$, is verified in Tables 4 and 5, respectively; and the irreducibility of all third-order tensor form invariants is confirmed in Table 6.

Table 4. Irreducibility of the function bases.

variables	invariant	variables	invariant
$C_{\infty\nu}$			
$T = 0$ and P	$T\!:\!T$	$T = P$, $v = u$, $W = \pm\varepsilon$	$v \cdot W t^v$
$T = P$, $A = \pm M$	$t^A \cdot A t^A$	$T = P$, $v = b$, $u = b \pm \sqrt{3}a$	$u \cdot t^v$
$T = P + P\varepsilon$, $A = M$,	$t^A \cdot B t^A$	$T = P$, $S = \pm P$	$T\!:\!S$
$\qquad B = M \pm \sqrt{3}M\varepsilon$			
$T = P + P\varepsilon$, $A = M$, $W = \pm\varepsilon$	$t^A \cdot A W t^A$	$T = P$, $S = P\varepsilon$, $A = \pm M\varepsilon$	$t^A \cdot A s^A$
$T = P$, $v = \pm a$	$v \cdot t^v$	$T = P$, $S = P\varepsilon$, $A = M$,	$\mathrm{tr}\,T : S)AB$
		$\qquad B = M \pm \sqrt{3}M\varepsilon$	
$T = P$, $A = M$, $v = \pm a$	$v \cdot t^A$	$T = P$, $S = P\varepsilon$, $W = \pm\varepsilon$	$\mathrm{tr}\,(T:S)W$
C_∞			
$T = 0$ and P	$T\!:\!T$	$T = P$, $v = \pm b$	$v \cdot \varepsilon\, t^v$
$T = P$, $A = \pm M$	$t^A \cdot A t^A$	$T = P$, $S = \pm P$	$T\!:\!S$
$T = P + P\varepsilon$, $A = M$	$t^A \cdot A\varepsilon\, t^A$	$T = P$, $S = \pm P\varepsilon$	$\mathrm{tr}\,(T:S)\varepsilon$
$T = P$, $v = \pm a$	$v \cdot t^v$		

Table 4 [cont.]

variables	invariant	variables	invariant
$C_{3\nu}$			
$T = 0$ and $P\epsilon$	$T \vdots T$	$T = P\epsilon,\ v = \pm b$	$v \cdot t^v$
$T = \pm P$	$P \vdots T$	$T = P\epsilon,\ A = M \pm \sqrt{3}M\epsilon,\ v = a$	$v \cdot t^A$
$T = P\epsilon,\ A = \pm M\epsilon,$	$p^A \cdot A t^A$	$T = P\epsilon,\ v = a,\ u = a \pm \sqrt{3}b$	$u \cdot (P:T)v$
$T = P\epsilon,\ W = \pm\epsilon$	$\mathrm{tr}\,(P:T)W$	$T = P\epsilon,\ S = \pm P\epsilon,$	$T \vdots S$
$T = P\epsilon,\ A = M,\ B = M \pm \sqrt{3}M\epsilon$	$\mathrm{tr}\,(P:T)AB$		
$C_{2\nu}$			
$T = 0$ and $P + P\epsilon$	$T \vdots T$	$T = P\epsilon,\ A = \pm M\epsilon,\ v = a$	$v \cdot t^A$
$T = P$ and $P\epsilon$	$t^M \cdot M t^M$	$T = P\epsilon,\ W = \pm\epsilon,\ v = a$	$v \cdot W t^M$
$T = P + P\epsilon,\ A = \pm M$	$t^M \cdot A t^M$	$T = P + P\epsilon,\ S = \pm(P + P\epsilon)$	$T \vdots S$
$T = P + P\epsilon,\ W = \pm\epsilon$	$t^M \cdot M W t^M$	$T = P + P\epsilon,\ S = \pm(P - P\epsilon$	$t^M \cdot M s^M$
$T = P + P\epsilon,\ v = \pm(a - b)$	$v \cdot t^v$	$T = P,\ S = P\epsilon,\ A = \pm M\epsilon$	$\mathrm{tr}\,(T:S)MA$
$T = P + P\epsilon,\ v = \pm(a + b)$	$v \cdot t^M$	$T = P,\ S = P\epsilon,\ W = \pm\epsilon$	$\mathrm{tr}\,(T:S)W$
$C_{1\nu}$			
$T = 0$ and $P\epsilon$	$T \vdots T$	$T = P\epsilon,\ W = \pm\epsilon$	$a \cdot W t^a$
$T = \pm P$	$a \cdot t^a$	$T = P\epsilon,\ v = \pm b$	$v \cdot t^a$
$T = P\epsilon,\ A = \pm M$	$a \cdot t^A$	$T = P\epsilon,\ S = \pm P\epsilon$	$T \vdots S$

Table 5. Irreducibility of vector- and second-order tensor-valued function representations.

	variables	form-invariant	variables	form-invariant
vector-valued				
$C_{\infty\nu}$	$T = P + P\epsilon,\ A = M$	t^A	$T = P,\ A = M,\ W = \epsilon$	$W t^A$
	$T = P + P\epsilon,\ A = M$	$A t^A$	$T = P,\ v = b$	t^x
C_∞	$T = P,\ A = M$	t^A	$T = P,\ A = M$	$\epsilon\, t^A$
$C_{3\nu}$	$T = P\epsilon,\ v = a$	t^v		
$C_{2\nu}$	$T = P + P\epsilon$	t^M	$T = P,\ A = M\epsilon$	t^A
	$T = P + P\epsilon$	$M t^M$	$T = P,\ W = \epsilon$	$W t^M$
$C_{1\nu}$	$T = P\epsilon$	$a,\ t^a$	$T = P\epsilon$	t^a
second-order symmetric tensor-valued				
$C_{\infty\nu}$	$T = P + P\epsilon,\ A = M$	$t^A \otimes t^A$	$T = P,\ S = P\epsilon,\ A = M$	$A(T:S) - (S:T)A$
	$T = P + P\epsilon,\ v = a$	T^v		
$C_{3\nu}$	$T = P\epsilon,\ v = a$	T^v	$T = P\epsilon,\ A = M$	$A(P:T) - (T:P)A$
$C_{2\nu}$	$T = P + P\epsilon$	$t^M \otimes t^M$	$T = P,\ S = P\epsilon$	$M(T:S) - (S:T)M$
	$T = P\epsilon,\ v = a$	T^v		
$C_{1\nu}$	$T = P\epsilon$	T^a		

Table 5 [cont.]

	variables	form-invariant	variables	form-invariant
	second-order skew-symmetric tensor-valued			
$C_{\infty v}$	$T = P + P\varepsilon,\ A = M$	$t^A \otimes A t^A - A t^A \otimes t^A$	$T = P,\ S = P\varepsilon$	$T : S - S : T$
	$T = P + P\varepsilon,\ v = a$	$v \otimes t^v - t^v \otimes v$		
C_{3v}	$T = P\varepsilon$	$P : T - T : P$		
C_{2v}	$T = P + P\varepsilon$	$t^M \otimes M t^M - M t^M \otimes t^M$	$T = P,\ S = P\varepsilon$	$T : S - S : T$
	$T = P\varepsilon,\ v = a$	$v \otimes t^M - t^M \otimes v$		
C_{1v}	$T = P\varepsilon$	$a \otimes t^a - t^a \otimes a$		

Table 6. Irreducibility of third-order tensor-valued function representations.

	variables	form-invariant	variables	form-invariant
$C_{\infty v}$	$v = a$	$v \otimes v \otimes v$	$T = P + P\varepsilon,\ A = M$	T
	$v = a$	$\{v \otimes 1\}$	$T = P + P\varepsilon,\ A = M$	$\langle A t^A \otimes A\rangle$
	$A = M\varepsilon,\ v = a$	$\langle v \otimes A\rangle$	$T = P + P\varepsilon,\ A = M$	$\{t^A \otimes 1\}$
	$A = M\varepsilon,\ v = a$	$\{Av \otimes 1\}$	$T = P + P\varepsilon,\ A = M$	$\{A t^A \otimes 1\}$
	$W = \varepsilon,\ v = a$	$\langle v \otimes v \otimes Wv\rangle$	$T = P + P\varepsilon,\ A = M,$ $B = M + \sqrt{3}M\varepsilon$	$T(AB - BA)$
	$W = \varepsilon,\ v = a$	$\{Wv \otimes 1\}$	$T = P,\ W = \varepsilon$	TW
	$v = a,\ u = a + \sqrt{3}b$	$\langle v \otimes v \otimes u\rangle$	$T = P,\ A = M,\ W = \varepsilon$	$\{W t^A \otimes 1\}$
			$T = P + P\varepsilon,\ v = a$	$\{t^v \otimes 1\}$
C_∞	$v = a$	$v \otimes v \otimes v$	$T = P,\ A = M$	T
	$v = a$	$\langle v \otimes v \otimes \varepsilon v\rangle$	$T = P,\ A = M$	$T\varepsilon$
	$v = a$	$\{v \otimes 1\}$	$T = P,\ A = M$	$\{t^A \otimes 1\}$
	$v = a$	$\{\varepsilon v \otimes 1\}$	$T = P,\ A = M$	$\{\varepsilon t^A \otimes 1\}$
C_{3v}	$A = M\varepsilon$	P	$A = M,\ B = M + \sqrt{3}M\varepsilon$	$P(AB - BA)$
	$A = M\varepsilon$	$\langle A p^A \otimes A\rangle$	$A = M,\ W = \varepsilon$	$\{W p^A \otimes 1\}$
	$A = M\varepsilon$	$\{p^A \otimes 1\}$	$A = M + \sqrt{3}M\varepsilon,\ v = a$	$\langle v \otimes A\rangle$
	$A = M\varepsilon$	$\{A p^A \otimes 1\}$	$W = \varepsilon,\ v = a$	$\{Wv \otimes 1\}$
	$W = \varepsilon$	PW	$v = a,\ u = a + \sqrt{3}b$	$P(v \otimes u - u \otimes v)$
	$v = b$	$v \otimes v \otimes v$	$T = P\varepsilon,\ A = M$	T
	$v = b$	$\{v \otimes 1\}$	$T = P\varepsilon,\ A = M$	$\{t^A \otimes 1\}$
	$v = b$	$\{p^v \otimes 1\}$	$T = P\varepsilon,\ v = a$	$\{t^v \otimes 1\}$
C_{2v}	$v = a + b$	$v \otimes v \otimes v$	$T = P + P\varepsilon$	T
	$v = a + b$	$\langle v \otimes M\rangle$	$T = P + P\varepsilon$	$\langle M t^M \otimes M\rangle$
	$v = a + b$	$\{v \otimes 1\}$	$T = P + P\varepsilon$	$\{t^M \otimes 1\}$
	$v = a + b$	$\{Mv \otimes 1\}$	$T = P + P\varepsilon$	$\{M T^M \otimes 1\}$
	$A = M\varepsilon,\ v = a$	$\langle v \otimes A\rangle$	$T = P,\ A = M\varepsilon$	$T(MA - AM)$
	$A = M\varepsilon,\ v = a$	$\{Av \otimes 1\}$	$T = P,\ A = M\varepsilon$	$\{t^A \otimes 1\}$
	$W = \varepsilon,\ v = a$	$\langle Wv \otimes M\rangle$	$T = P,\ W = \varepsilon$	TW
	$W = \varepsilon,\ v = a$	$\{Wv \otimes 1\}$	$T = P,\ W = \varepsilon$	$\{W t^M \otimes 1\}$
C_{1v}	$A = M\varepsilon$	$a \otimes a \otimes a$	$W = \varepsilon$	$\{Wa \otimes 1\}$
	$A + M\varepsilon$	$\langle a \otimes A\rangle$	$v = b$	$\langle a \otimes a \otimes v\rangle$
	$A = M\varepsilon$	$\{a \otimes 1\}$	$v = b$	$\{v \otimes 1\}$
	$A = M\varepsilon$	$\{Aa \otimes 1\}$	$T = P\varepsilon$	T
	$W = \varepsilon$	$\langle a \otimes a \otimes Wa\rangle$	$T = P\varepsilon$	$\{t^v \otimes 1\}$

[672]

Acknowledgment

References

·1. J. BETTEN and W. HELISH, *Simuleneous invariants in system of 2nd-order tensors*, ZAMM, **75**, 753–759, 1995.

2. J.P. BOEHLER, *A simple derivation of representations for non-polynominal constitutive equations in some cases of anisotropy*, ZAMM, **59**, 157–167, 1979.

3. K.C. HANNABUSS, *The irreducible components of homogeneous functions and symmetric tensors*, J. Inst. Math. Applics., **14**, 83–88, 1974.

4. S. PENNISI, *On third order tensor-valued isotropic functions*, Int. J. Engng. Sci., **30**, 679–692, 1992.

5. S. PENNISI and M. TROVATO, *On the irreducibility of Professor G.F. Smith's representations for isotropic functions*, Int. J. Engng. Sci., **25**, 1059–1065, 1987.

6. A.J.M. SPENCER, *A note on the decomposition of tensors into traceless symmetric tensors*, Int. J. Engng. Sci., **8**, 489–505, 1970.

7. Q.-S. ZHENG, *Two-dimensional tensor function representation for all kinds of material symmetry*, Proc. R. Soc. Lond., A**443**, 127–138, 1993.

8. Q.-S. ZHENG, *On the representations for isotropic vector-valued, symmetric tensor-valued and skew-symmetric tensor-valued functions*, Int. J. Engng. Sci., **31**, 1013–1024, 1993.

9. Q.-S. ZHENG, *A note on representation for isotropic functions of a 4th-order tensor in 2-dimensional space*, ZAMM, **75**, 357–359, 1994.

10. Q.-S. ZHENG and J. BETTEN, *On the tensor function representations of 2nd-order and 4th-order tensors*, I, ZAMM, **75**, 269–281, 1994.

11. Q.-S. ZHENG and J.P. BOEHLER, *The description, classification, and reality of material and physical symmetries*, Acta Mech., **102**, 73–89, 1994.

12. Q.-S. ZHENG and A.J.M. SPENCER, *On the canonical representations for Kronecker papers of orthogonal tensors with application to material symmetry problems*, Int. J. Engng. Sci., **31**, 617–635, 1993.

DEPARTMENT OF ENGINEERING MECHANICS
TSINGHUA UNIVERSITY, BEIJING, CHINA.

Travelling wave solutions to model equations of van der Waals fluids

K. PIECHÓR (WARSZAWA)

WE CONSIDER the existence and uniqueness of travelling wave solutions to the model hydrodynamics equations (without capillarity) obtained from a four-velocity kinetic model of van der Waals fluids. We analyze both the Euler and the Navier–Stokes equations. The Euler equations are shown to change their type. The Rankine–Hugoniot conditions are discussed in detail. It is shown that the Hugoniot locus can be disconnected even if the equations are hyperbolic. Using the Navier–Stokes equations we show how to modify the Oleinik–Liu conditions of admissibility of shock waves to such situations. The shock-wave structures are found numerically. In particular, the so-called impending shock splitting is obtained.

1. Introduction

THE VAN DER WAALS fluid is such a hypothetical one whose equation of state reads [1]

$$(1.1) \qquad p(w, T) = \frac{RT}{w - b} - \frac{a}{w^2},$$

where a, b are positive constants characterizing the fluid, $p(w, T)$ is the pressure, R is the gas constant, T is the temperature, and $w > b$ is the specific volume. Now much more sophisticated equations of state are known [2, 3, 4], but Eq. (1.1) is still in use since it describes qualitatively correctly the thermodynamic behaviour of real one-component fluids.

If

$$(1.2) \qquad T > \frac{81}{256} \frac{a}{bR},$$

then the isotherms in the $p-w$ plane are monotonically decreasing convex curves. This is the case of classical gases. The mathematical background is the Lax theory of hyperbolic conservation laws [5].

If

$$(1.3) \qquad \frac{8}{27} \frac{a}{bR} < T < \frac{81}{256} \frac{a}{bR},$$

then the isotherms in the $p-w$ plane are still monotonically decreasing – but they are no longer convex. This occurs in the so-called retrograde or Bethe–Zeldovich–Thompson fluids. Such materials were considered in many papers [6–17].

The third case is when T satisfies

(1.4)
$$\frac{1}{4}\frac{a}{bR} < T < \frac{8}{27}\frac{a}{bR}.$$

The left-hand inequality guarantees that the pressure is positive for all $w > b$. Now, the isotherms are nonmonotone curves in the $p - w$ plane, and the Euler equations are of mixed hyperbolic-elliptic type. In this case there is no one prevailing theory, and various approaches can be found [18–35]. Closely related problems are met in the theory of elastic rods [36–48].

The equations studied in [4–48] are those of phenomenological thermodynamics. However, at least as fluids are concerned, such a theory cannot describe correctly the structures of neither the shock waves nor the phase boundaries because, in those regions, the gradients of the flow parameters are very large. Hence, the use of kinetic theory seems to be inevitable. Usually one proceeds as follows: the Boltzmann equation is used in the gaseous domain and the fluid bulk is treated as a source (evaporation) or sink (condensation) of particles. References [49–51] represent three of many papers on the topic.

We propose a more radical approach consisting in the use of one kinetic equation both to the liquid and the gaseous phase. Thus, in a sense, we attempt to follow the lines of the van der Waals' philosophy of fluids [1], which is used in the quoted papers [2–35] on liquid-vapour phase transitions. In the papers, one system of hydrodynamic equations with one equation of state suited for liquid-vapour systems is used without any splitting into liquid and gaseous domains. The essential difference between this approach and that of ours consists in that that we want to replace the hydrodynamic description of the system with a kinetic one, and next to compare the results.

The fundamental trouble is the lack of such a universal and fully satisfactory kinetic equation. But this does not mean that there are no models that could be suitable for our purpose. We have chosen the Enskog–Vlasov equation because: i) it is relatively simple; ii) there are some results in [52, 53] suggesting its usefulness. Recently, we showed in [54] that the capillarity equations used in [18–21, 28, 32] can be deduced, at the formal level, from this equation.

Unfortunately, if we want to investigate any flow by means of the Enskog–Vlasov equation, we find it to be too complicated. That is why we elaborated its discrete velocity models (see [55, 56]). In this way we obtain a more tractable system of equations. Basing on the successes of discrete kinetic theory of ideal gases ([57–59]) we hope that this approach will not be a failure in the case of interest.

There are many problems which can be posed. First of all we have to give evidence that our discrete velocity model can be successfully applied to at least some of the phase transition problems. The next question is the relation between the results of our approach and those of [49–51], where kinetic theory was applied to the gaseous phase only.

Another group of problems concerns the connection between the fluid dynamic and kinetic descriptions of phase changes. We know from the theory of the true Boltzmann equation [60] as well as from the theory of its discrete velocity models [57, 61] that the phenomenological fluid dynamics describes correctly the shock wave structure only if the shock is sufficiently weak. In the case under consideration the situation seems to be much more complicated. Namely, in [56] we considered the stagnant phase boundary problem. It turned out that both the model kinetic and generated by it fluid dynamic equations have exactly the same solution. The description of the phase boundary obtained in [56] agrees both with the physics of equilibrium phase transitions and the theoretical analysis of [18], hence it favours our model. But, on the other hand, this result is in contrast with the results of kinetic theory of ideal gases ([57, 60, 61]), because the stagnant phase boundary by no means can be treated as a "weak" shock wave. The explanation of this apparent paradox must be sought in the structure of the local equilibrium, i.e. the Euler equations. In the case of the ideal gases both the true and the model Euler equations are strictly hyperbolic, and the characteristic speeds are either genuinely nonlinear or linearly degenerate in the sense of LAX [5]. It is worth to add that all the existing papers on the hydrodynamic limit of the true Boltzmann [62, 63, 65] or the Enskog equation [64, 65], or else the discrete Broadwell model [66 – 68], and more generally some hyperbolic systems of similar structure as the latter ones [69, 70] make an essential use of the strict hyperbolicity of the local equilibrium conservation equations. Very clearly it is pointed out in [70].

In our problem, as we show it later in this paper, the local equilibrium equations, i.e. the Euler equations, can change type from hyperbolic to elliptic. The question arises: how important is it? This will be discussed in our future papers, but for the time being let us notice that: i) the stagnant phase boundary discussed in [56] is admissible only due to the change of the type of the Euler equations; ii) if the formally deduced local equilibrium equations are elliptic, then they cannot serve as an approximation, as the Knudsen number tends to zero, to the kinetic equations if the latter are strictly hyperbolic. A brilliant example is given in [70]. Hence, the Euler, Navier – Stokes and other equations deduced from the kinetic theory should, with a great caution, be treated as "approximation" to the corresponding kinetic equations.

With the present paper we open systematic studies of various "approximations" to the model kinetic equations. Now we limit ourselves to the Euler and Navier – Stokes equations only, but most of the present results will be used in the future.

In the next Section we classify the Euler equations and give sufficient and necessary criteria for their being of a definite type.

In Sec. 3 we consider shock waves and discuss the solvability of the Rankine – Hugoniot conditions. The properties of these solutions are investigated in Sec. 4.

Section 5 deals with the shock waves in the Navier–Stokes equations. The most important result is Theorem 5.8 stating the sufficient and necessary conditions for existence and uniqueness of the travelling wave solutions to our equations.

In Sec. 6 we give some numerical results concerning the structures of the shock waves discussed in Sec. 5. Our results agree qualitatively with those of [4]. In this way we obtain a consecutive confirmation of usefulness of our model for the qualitative analysis of the dynamic phase changes.

2. Classification of the Euler equations

In the lowest order of approximation to a four-velocity model of the Enskog–Vlasov equation, we obtained in [56] the following system

$$(2.1) \qquad \frac{\partial w}{\partial t} - \frac{\partial u}{\partial x} = 0,$$

$$(2.2) \qquad \frac{\partial u}{\partial t} + \frac{\partial p}{\partial x} = 0,$$

where $t \geq 0$ is the time, $x \in \mathbb{R}$ is the Lagrangian mass coordinate, u is the velocity, w is the specific volume, and p is the pressure.

The pressure formula reads

$$(2.3) \qquad p = p(w, u) = \frac{1 - u^2}{2(w - b)} - \frac{a}{w^2},$$

where a and b are positive constants; a is the ratio of the mean value of the potential of the attractive tail to the mean kinetic energy, and b can be taken to be unity.

Equations (2.1)–(2.3) form the Euler equations for our model hydrodynamics. We consider them in the following domain:

$$(2.4) \qquad w > b, \qquad \frac{a}{2b} < 1, \qquad u^2 < 1 - \frac{a}{2b}.$$

The set of (w, u) satisfying (2.4) is denoted by $\mathcal{D}$.

Condition $(2.4)_1$ is obvious: the density $1/w$ does not exceed the close-packing density $1/b$. The remaining constraints result from the physically reasonable demand that the pressure p is positive. Indeed, the immediate consequence of that and (2.3) is

$$(2.5) \qquad \frac{1 - u^2}{2} > \frac{a(w - b)}{w^2}.$$

But for every $w > b$ the following estimates hold

$$0 < \frac{a(w - b)}{w^2} \leq \frac{a}{4b}.$$

Hence, if for some u_0

$$\frac{1 - u_0^2}{2} \le \frac{a}{4b},$$

then there is $w_0 > b$ such that $p(w_0, u_0) < 0$, contrary to our assumption. Therefore we have to admit only such values of u that $(2.3)_3$ holds.

It we denote

$$(2.6) \qquad T = \frac{1 - u^2}{2},$$

then (2.3) takes the well-known form of the van der Waals equation of state (1.1) provided that T given by (2.6) is interpreted as the temperature.

We rewrite the Euler equations in the matrix form

$$(2.7) \qquad \frac{\partial}{\partial t}\begin{pmatrix} w \\ u \end{pmatrix} + \mathbb{M}(w, u) \cdot \frac{\partial}{\partial x}\begin{pmatrix} w \\ u \end{pmatrix} = 0,$$

where

$$(2.8) \qquad \mathbb{M} = \begin{bmatrix} 0 & -1 \\ -\dfrac{1 - u^2}{2(w - b)^2} + \dfrac{2a}{w^3} & -\dfrac{u}{w - b} \end{bmatrix}.$$

The eigenvalues of $\mathbb{M}$ are called the characteristic speeds. They are solutions of

$$(2.9) \qquad \lambda^2 - \frac{\partial p(w, u)}{\partial u}\lambda + \frac{\partial p(w, u)}{\partial w} = 0,$$

or explicitly

$$(2.10) \qquad \lambda^2 + \frac{u}{w - b}\lambda - \left[\frac{1 - u^2}{2(w - b)^2} - \frac{2a}{w^3}\right] = 0.$$

The system (2.1), (2.2) is called strictly hyperbolic if Eq. (2.9) has two real solutions, and elliptic if both solutions of (2.9) are complex.

We have

LEMMA 1.
i) If

$$(2.11) \qquad \frac{a}{2b} < \frac{27}{37}$$

then for every $(w, u) \in \mathcal{D}$ the Euler equations are strictly hyperbolic;

ii) if

$$(2.12) \qquad \frac{27}{37} < \frac{a}{2b} < \frac{27}{32},$$

then they are hyperbolic-elliptic. The domain $\mathcal{H}$ of hyperbolicity is simply connected and separates the two components of the domain of ellipticity $\mathcal{E}$;

iii) if

(2.13)
$$\frac{27}{32} < \frac{a}{2b} < 1,$$

then the Euler equations continue to be hyperbolic-elliptic, but the domain of ellipticity $\mathcal{E}$ is simply connected and separates the two components of the domain of hyperbolicity $\mathcal{H}$.

Cases ii) and iii) are shown in Figs. 2 and 3 where the domain of ellipticity is shaded.

P r o o f. Equation (2.10) has two real solutions if and only if

(2.14)
$$\Delta(w, u) = \frac{2 - u^2}{(w - b)^2} - \frac{8a}{w^3}$$

is positive. This is equivalent to

(2.15)
$$u^2 < \left[1 - \frac{4a(w - b)^2}{w^3} \right].$$

However, for any $w > b$

$$0 < \frac{4a(w - b)^2}{w^3} \leq \frac{16}{27} \frac{a}{b},$$

and the equality sign takes place for $w = 3b$ only. Therefore, if a/b is such that

$$u^2 < 1 - \frac{a}{2b} < 2\left(1 - \frac{16}{27}\frac{a}{b}\right),$$

then we have i). If

$$0 < 2\left(1 - \frac{16}{27}\frac{a}{b}\right) < u^2 < 1 - \frac{a}{2b},$$

we have ii), and if

$$1 - \frac{16}{27}\frac{a}{b} < 0,$$

we have iii). The proof is complete.

The change of type of the Euler equations is physically interpreted as the phase transition. Case iii) of Lemma 1 is of particular interest since it resembles the situation met in the theory of the true van der Waals fluids (see [18–48]).

PROPOSITION 1.
i) If $(w_0, u_0) \in \mathcal{E}$, and $(w, u) \in \mathcal{E}$, then

$$(2.16) \qquad \frac{p(w, u_0) - p(w_0, u_0)}{w - w_0} > \frac{u_0^2}{4(w - b)(w_0 - b)}.$$

ii) If $(w_0, u_0) \in \mathcal{H}$, $(w, u) \in \mathcal{H}$, and the interval $\langle (w_0, u_0), (w, u) \rangle \subset \mathcal{H}$, then

$$(2.17) \qquad \frac{p(w, u_0) - p(w_0, u_0)}{w - w_0} < \frac{u_0^2}{4(w - b)(w_0 - b)}.$$

P r o o f. First, let us notice that if $(w_0, u_0) \in \mathcal{E}$, $(w, u) \in \mathcal{E}$ then the interval $\langle (w_0, u_0), (w, u_0) \rangle \subset \mathcal{E}$. On the other hand, if $(w_0, u_0) \in \mathcal{H}$, $(w, u_0) \in \mathcal{H}$ then, in general, this is not true, and that is why we have to strengthen the assumptions in the hyperbolic Case ii).

Secondly, let us notice that the left-hand sides of (2.16) and (2.17) are symmetric in their arguments w and w_0. Therefore it is enough to prove these inequalities in the case of $w > w_0$ only. We have

$$\frac{p(w, u_0) - p(w_0, u_0)}{w - w_0} = \frac{1}{w - w_0} \int_{w_0}^{w} \frac{\partial}{\partial \zeta} p(\zeta, u_0) \, d\zeta.$$

CASE i)
For every $w_0 \leq \zeta \leq w$, we have $\Delta(\zeta, u_0) < 0$. Therefore

$$(2.18) \qquad \frac{\partial}{\partial \zeta} p(\zeta, u_0) > \frac{1}{4} \left(\frac{\partial p(\zeta, u_0)}{\partial u} \right)^2 - \frac{u_0^2}{4(\zeta - b)^2}.$$

Hence

$$\frac{p(w, u_0) - p(w_0, u_0)}{w - w_0} > \frac{u_0^2}{4(w - w_0)} \int_{w_0}^{w} \frac{d\zeta}{(\zeta - b)^2} - \frac{u_0^2}{4(w - b)(w_0 - b)},$$

and (2.16) is proved.

To prove (2.17) we proceed in a similar way, the only difference being that in (2.18) it is necessary to change the direction of the inequality sign. The proof is complete.

3. The shock speed problem

A discontinuous solution

$$(3.1) \qquad (w, u)(x, t) = \begin{cases} (w_l, u_l) & \text{for} \quad x < st, \\ (w_r, u_r) & \text{for} \quad x > st, \end{cases}$$

of Eq. (2.1), with shock speed s, is called a shock wave. Here, (w_l, u_l) and (w_r, u_r) are some constant values. To simplify the notation we write (w, u) for (w_l, u_l) or (w_r, u_r), and (w_0, u_0) for (w_r, u_r) or (w_l, u_l), respectively. These values have to satisfy the Rankine–Hugoniot conditions

(3.2)
$$sw + u = sw_0 + u_0,$$
$$-su + p(w, u) = -su_0 + p(w_0, u_0).$$

Eliminating u, and making use of (2.3) we obtain an equation for $s = s(w; w_0, u_0)$ which reads

(3.3) $$\frac{w^2 + w_0 - 2b}{2(w - b)}s^2 + \frac{u_0}{w - b}s - \left[\frac{1 - u_0^2}{2(w_0 - b)(w - b)} - \frac{a(w + w_0)}{w_0^2 w^2}\right] = 0.$$

This equation has two real solutions if and only if

(3.4) $$D(w; w_0, u_0) = \frac{(w + w_0 - 2b) - (u_0^2(w - b)}{(w_0 - b)(w - b)^2} - \frac{2a(w + w_0 - 2b)(w + w_0)}{w_0^2 w^2(w - b)}$$

is positive.

LEMMA 2. Let (w_0, u_0) be such that $p(w_0, u_0) > 0$. Then the set

$$\left\{w > b : \quad D(w; w_0, u_0) < 0\right\}$$

is either empty or it is a finite interval contained in $\{x \in \mathbb{R} : x > b\}$.

P r o o f. We rewrite $D(w; w_0, u_0)$ in the form

$$D(w; w_0, u_0) = \frac{1}{w^2(w - b)^2} P_3(w - b),$$

where $P(x)$ is the polynomial of grade three.

$$P_3(x) = 2p(w_0, u_0)x^3 + \left[1 + \frac{2b(1 - u_0^2)}{w_0 - b} - \frac{4a}{w_0}\right]x^2$$
$$+ \left[2b\left(1 - \frac{a}{b}\right) + \frac{b^2(1 - u_0^2)}{w_0 - b} + \frac{2ab}{w_0^2}\right]x + b^2.$$

Since $P_3(0) = b^2 > 0$, $P_3(x) > 0$ for sufficiently large positive x, and $P_3(x) < 0$ for sufficiently large negative x, then this polynomial can take negative values in the domain $x > 0$ in a finite interval only. The proof is complete.

In principle, we could make use of the theory of the cubic polynomials to get the precise answer to the question of the sign of $P_3(x)$. Unfortunately, in our

case, the coefficients in $P_3(x)$ are so complicated that we are unable to draw any conclusions. Therefore, we present only partial answers to the question of the sign of $D(w; w_0, u_0)$.

LEMMA 3.
i) If

(3.5)
$$\frac{p(w, 0) - p(w_0, 0)}{w - w_0} > 0,$$

then $D(w; w_0, u_0) < 0$;
ii) if

(3.6)
$$\frac{p(w, u_0) - p(w_0, u_0)}{w - w_0} < 0,$$

then $D(w; w_0, u_0) > 0$.

P r o o f. We have the following identity

$$D(w; w_0, u_0) = -2 \left[\frac{p(w, u_0) - p(w_0, u_0)}{w - w_0} + \frac{w_0 - b}{w - b} \frac{p(w, 0) - p(w_0, 0)}{w - w_0} \right].$$

The assertion follows immediately from the above and the estimate

(3.7)
$$\frac{p(w, u_0) - p(w_0, u_0)}{w - w_0} \geq \frac{p(w, 0) - p(w_0, 0)}{w - w_0}$$

for $w > b$, $w_0 > b$, $u_0^2 < 1$. The proof is complete.

COROLLARY 1. If $0 < u_0^2 < 1 - 16a/27b$, then for every $w > b$, $w_0 > b$, $D(w; w_0, u_0) > 0$.

P r o o f. If the assumption is satisfied, then $\partial p(w, u_0)/\partial w < 0$ for every $w > b$. Hence, (3.6) holds. The proof is complete.

LEMMA 4. If $(w_0, u_0) \in \mathcal{E}$, $(w, u_0) \in \mathcal{E}$, and $w > w_0$, then $D(w; w_0, u_0) < 0$.

P r o o f. We write

(3.8)
$$D(w; w_0, u_0) = \frac{u_0^2}{(w - b)^2} - \frac{w + w_0 - 2b}{2(w - b)} \left[4 \frac{p(w, u_0) - p(w_0, u_0)}{w - w_0} \right].$$

Making use of (2.16) we obtain

$$D(w; w_0, u_0) \leq -\frac{u_0^2(w - w_0)}{2(w_o - b)(w - b)} < 0.$$

The proof is complete.

LEMMA 5.

i) There are such pairs $(w_0, u_0) \in \mathcal{E}$, $(w, u_0) \in \mathcal{E}$ with $w < w_0$ that $D(w; w_0, u_0) > 0$;

ii) also, there are other pairs $(w_0, u_0) \in \mathcal{E}$, $(w, u_0) \in \mathcal{E}$, $w < w_0$ such that $D(w; w_0, u_0) < 0$.

P r o o f. Let $w_0 > b$ be such that

$$(3.9) \qquad 0 < 2 - \frac{8a(w_0 - b)^2}{w_0^3} < 1 - \frac{a}{2b},$$

and let $\varepsilon > 0$ be sufficiently small. We take

$$(3.10) \qquad u_0^2 = 2 + \varepsilon - \frac{8a(w_0 - b)^2}{w_0^3}.$$

Of course, then $\Delta(w_0, u_0) < 0$. Using (3.7) in (3.4) we obtain

$$(3.11) \qquad D(w; w_0, u_0) = -\frac{w - w_0}{w - b} \left[\frac{1}{(w_0 - b)(w - b)} \right.$$
$$\left. - \frac{2a\left[(3w_0 - 4b)(w - w_0) + 2w_0(2w_0 - 3b)\right]}{w_0^3 w^3} \right] - \frac{\varepsilon}{(w_0 - b)(w - b)}.$$

Owing to $D(w_0; w_0, u_0) < 0$, there is $\overline{w}$ such that $b < \overline{w} < w_0$ and

$$(3.12) \qquad D(\overline{w}; w_0, u_0) = 0,$$

and $D(w; w_0, u_0) < 0$ for $\overline{w} < w \leq w_0$. From (3.11), (3.12) we obtain

$$(3.13) \qquad \overline{w} = w_0 - \frac{\varepsilon(w_0 - b)}{1 - \dfrac{4a(w_0 - b)^2(2w_0 - 3b)}{w_0^4}} + O(\varepsilon^2).$$

We assume additionally that

$$(3.14) \qquad 1 - \frac{4a(w_0 - b)^2(2w_0 - 3b)}{w_0^4} > 0$$

for, of course, sufficiently small $\varepsilon > 0$ and $\overline{w} < w_0$.

Let us evaluate $\Delta(\overline{w}, u_0)$. Using (3.10) and (3.13) in (2.14) we obtain

$$\Delta(\overline{w}, u_0) = -\varepsilon \frac{1 - \dfrac{12ab(w_0 - b)^2}{w_0^4}}{1 - \dfrac{4a(w_0 - b)^2(2w_0 - 3b)}{w_0^4}} + O(\varepsilon^2).$$

If there is w_0 satisfying (3.9), (3.14) and

$$(3.15) \qquad 1 - \frac{12ab(w_0 - b)^2}{w_0^4} < 0,$$

then we obtain i), since it is enough to take $(w, u_0) \in \mathcal{E}$ such that $w < \overline{w}$. On the other hand, if there is w_0 such that

$$(3.16) \qquad 1 - \frac{12ab(w_0 - b)^2}{w_0^4} > 0,$$

then we obtain ii) because then there is $\overline{w} < w < w_0$ satisfying our demands.

Hence, it remains to show that there is w_0 satisfying (3.9), (3.14), (3.15), and that there is, possibly different from the previous one, another w_0 satisfying (3.9), (3.14), and (3.16).

The positive answers are readily available by noticing that (3.14) and (3.15) can be rewritten as

$$(3.14') \qquad 1 - \frac{4a(w_0 - b)^2}{w_0^3} - \frac{4a(w_0 - b)^2(w_0 - 3b)}{w_0^4} > 0,$$

$$(3.15') \qquad 1 - \frac{4a(w_0 - b)^2}{w_0^3} + \frac{4a(w_0 - b)^2(w_0 - 3b)}{w_0^4} < 0;$$

whereas (3.14), (3.16) can be rewritten in the form (3.14') and

$$(3.16') \qquad 1 - \frac{4a(w_0 - b)^2}{w_0^3} + \frac{4a(w_0 - b)^2(w_0 - 3b)}{w_0^4} > 0.$$

The proof is complete.

LEMMA 6. If $(w_0, u_0) \in \mathcal{H}$, $(w, u_0) \in \mathcal{H}$, $w \le w_0$, and the interval $\langle (w, u_0), (w_0, u_0) \rangle \subset \mathcal{H}$, then $D(w; w_0, u_0) > 0$.

P r o o f. Use (3.8) and (2.17).

LEMMA 7. If

$$\frac{27}{37} < \frac{a}{2b} < \frac{27}{32}$$

then there is u_0 such that $\Delta(w, u_0) > 0$ for every $w > b$, and there are $(w_0, u_0) \in \mathcal{H}$, $(w, u_0) \in \mathcal{H}$, $w > w_0$ such that $D(w; w_0, u_0) < 0$.

P r o o f. Let $\varepsilon > 0$ be sufficiently small. Let us take

$$(3.17) \qquad w_0 = b(3 - \varepsilon),$$

and

$$(3.18) \qquad u_0^2 = 2 - \frac{a(w_0 - b)(w_0 + b)^2}{bw_0^3}.$$

Then $0 < u_0^2 < 1 - (a/2b)$, and

$$\Delta(w, u_0) = \frac{2}{(w-b)^2}\left[1 - \frac{4a(w-b)^2}{w^3}\right] - \frac{u_0^2}{(w-b)^2}$$

$$\geq \frac{1}{(w-b)^2}\left[2 - \frac{32a}{27b} - u_0^2\right] = \frac{16a\varepsilon^2}{81bw_0^3(w-b)}\left(1 - \frac{7}{12}\varepsilon\right) > 0$$

for ε sufficiently small.

Next, we rewrite $D(w; w_0, u_0)$ in the form

$$(3.19) \qquad D(w; w, u) = \frac{1}{2(w_0 - b)(w-b)^2}\Bigg[(w + w_0 - 2b)$$

$$-u_0^2\left(2 - u_0^2 - \frac{a(w_0 - b)(w_0 + b)^2}{bw_0^3}\right) + (w_0 - w)u_0^2\Bigg]$$

$$+ \frac{a(w + w_0 - 2b)\left[(w_0 - b)w - 2bw_0\right]^2}{2bw_0^3 w^2(w-b)^2}.$$

We take also

$$(3.20) \qquad w = \frac{2bw_0}{w_0 - b}.$$

Then

$$w - w_0 = \varepsilon b \frac{3 - \varepsilon}{2 - \varepsilon} > 0.$$

Inserting (3.17), (3.18), and (3.20) into (3.19) one gets

$$D(w; w_0, u_0) = -\frac{\varepsilon b w_0 u_0^2}{2(w_0 - b)^2(w-b)^2} < 0.$$

The proof is complete. The profiles $s(w; w_0, u_0, a)$ for some values of w_0, u_0 and a are shown in Fig. 1. We can see that these profiles depend very strongly on the values of the three parameters. They can be nonmonotonic or even undefined for some values of the specific volume w. Also, the change of sign of $s(w; w_0, u_0, a)$ is noticeable. On the other hand, the profile in Fig. 1c is very much like that in the case of ideal gases, despite the fact that now the system of the Euler equations is hyperbolic-elliptic, and the domain of hyperbolicity is disconnected.
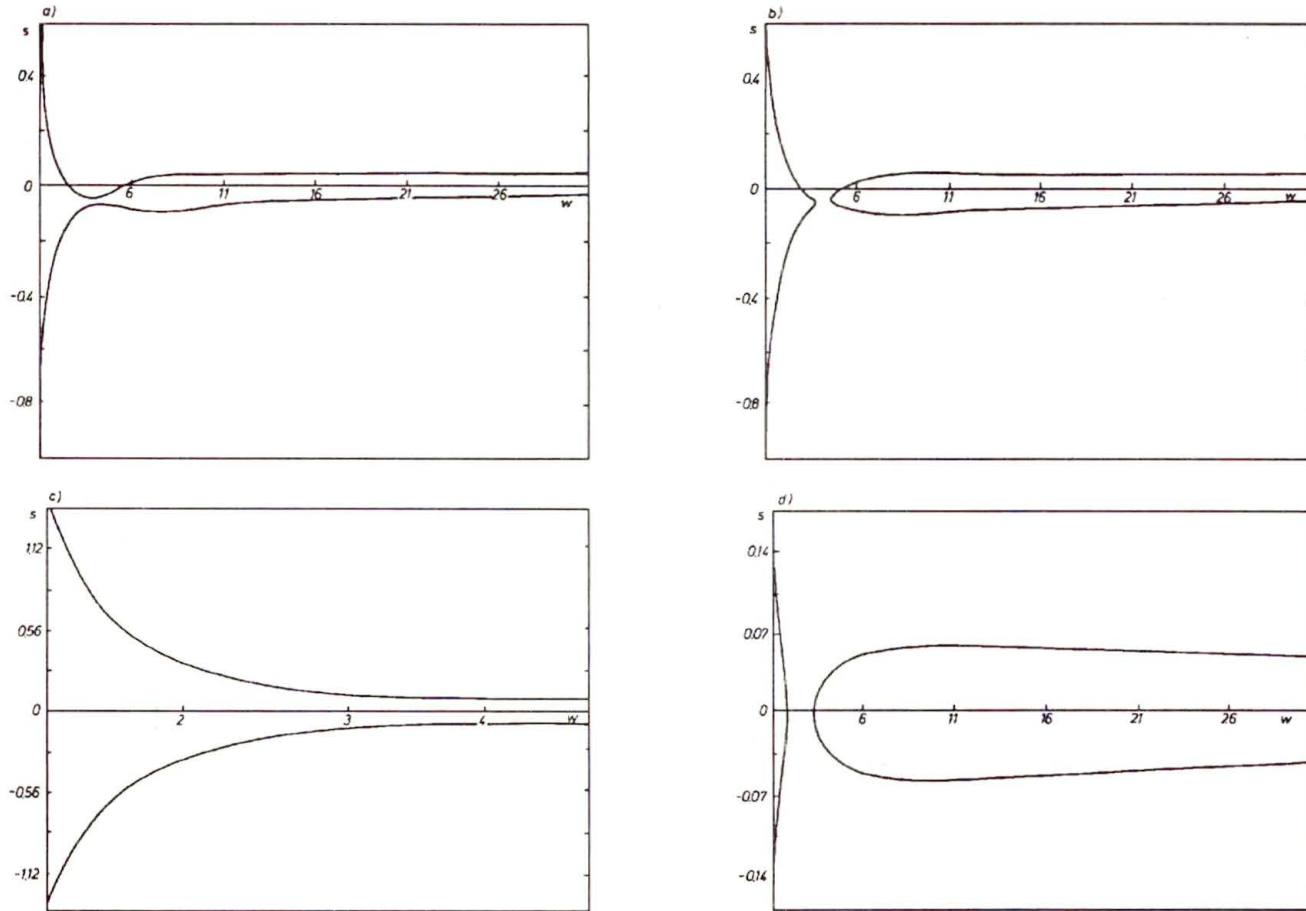
FIG. 1. The function $s(w; w_0, u_0, a)$ versus w for some values of w_0, u_0, a. a) $a = 1.65$, $w_0 = 2.25$, $u_0 = 0.25$; b) $a = 1.65$, $w_0 = 2.3$, $u_0 = 0.25$; c) $a = 1.9$, $w_0 = 1.7$, $u_0 = 0$; d) $a = 1.9$, $w_0 = 6.5$, $u_0 = 0$.

[687]

4. Properties of shock speed and the Hugoniot locus

In this Section we investigate properties of the shock speed $s(w; w_0, u_0)$ assuming, of course, its existence.

PROPOSITION 2. Let $\overline{s} = s(\overline{w}; w_0, u_0)$ be given. If

$$(4.1) \qquad \overline{w} > \frac{bw_0}{w_0 - b},$$

and

$$(4.2) \qquad 0 < s^2(\overline{w}; w_0, u_0) < \frac{a(w_0\overline{w} - b(w_0 + \overline{w}))^2}{2bw_0^3\overline{w}^3},$$

then there are exactly two $\overline{w}_1 > b$, $\overline{w}_2 > b$, $\overline{w}_1 \neq \overline{w}$, $\overline{w}_2 \neq \overline{w}$ such that

$$(4.3) \qquad s(\overline{w}_1; w_0, u_0) = s(\overline{w}_2; w_0, u_0) = s(\overline{w}; w_0, u_0).$$

In other words, any value of s can be taken at most three times.

P r o o f. Let $\overline{s} = s(\overline{w}; w_0, u_0)$ be given. Then the following identity is true

$$(4.4) \qquad \frac{\overline{w} + w_0 - 2b}{2(\overline{w} \cdot b)}\overline{s}^2 + \frac{u_0}{\overline{w} - b}\overline{s} - \left[\frac{1 - u_0^2}{2(w_0 - b)(\overline{w} - b)} - \frac{a(\overline{w} + w_0)}{w_0^2\overline{w}^2}\right] = 0.$$

Now, let us consider Eq. (3.3) with $s = \overline{s}$, but with unknown w. Using the identity (4.4) to eliminate $u_0\overline{s}$ from Eq. (3.3) we obtain

$$(4.5) \qquad (w - \overline{w})\left\{\overline{s}^2(w - b)^2 + 2\left[\overline{s}^2 b - \frac{a(\overline{w}w_0 - b(\overline{w} + w_0))}{w_0^2\overline{w}^2}\right](w - b)\right.$$
$$\left. + b^2\left[\overline{s}^2 + \frac{2a(\overline{w} + w_0)}{w_0^2\overline{w}^2}\right]\right\} = 0.$$

One solution is trivial: $w = \overline{w}$. This equation has two other solutions if and only if (4.2) holds. These two solutions are of the same sign. They are positive if additionally

$$(4.6) \qquad \overline{s}^2 < \frac{a(\overline{w}w_0 - b(\overline{w} + w_0))}{bw_0^2\overline{w}^2}.$$

This condition is not contradictory if the term on the right-hand side is positive. In turn, it happens if and only if (4.1) holds. We show now that (4.1), (4.2) imply (4.6). Indeed,

$$\frac{a(w_0\overline{w} - b(w_0 + \overline{w})^2)}{2bw_0^3\overline{w}^3} = \frac{1}{2}\left(1 - \frac{b}{w_0} - \frac{b}{w}\right)\frac{a(w_0\overline{w} - b(w_0 + \overline{w}))}{bw_0^2\overline{w}^2}$$
$$< \frac{a(w_0\overline{w} - b(w_0 + \overline{w}))}{bw_0^2\overline{w}^2}.$$

The proof is complete.

PROPOSITION 3. If $\Delta(w_0, u_0) > 0$, then the equation

(4.7) $$s(w; w_0, u_0) = \lambda(w_0, u_0)$$

has at least one solution, namely $w = w_0$. If additionally

(4.8) $$w_0 > 2b,$$

and

(4.9) $$\lambda^2(w_0, u_0) < \frac{a(w_0 - 2b)^2}{2bw_0^4},$$

then there are two other solutions w_1, w_2 satisfying $w_1 > b$, $w_2 > b$, $w_1 \neq w_0$, $w_2 \neq w_0$.

P r o o f. Since $D(w_0; w_0, u_0) = \Delta(w_0, u_0)$, then $w = w_0$ is a solution of (4.7). If (4.8) and (4.9) hold, then $\overline{w} = w_0$, and $\overline{s} = \lambda(w_0, u_0)$ satisfy (4.1), (4.2). Therefore, making use of Proposition 2 we obtain the second thesis. The proof is complete.

LEMMA 8. If

(4.10) $$\frac{d}{dw}s(w; w_0, u_0)\Big|_{w=\overline{w}} = 0,$$

then $\overline{w}$ satisfies

(4.11) $$\overline{w} > \frac{2bw_0}{w_0 - b}.$$

Moreover, there is exactly one $\widehat{w} \neq \overline{w}$ such that $s(\widehat{w}; w_0, u_0) = s(\overline{w}; w_0, u_0)$; $\widehat{w}$ is given by

(4.12) $$\widehat{w} = \frac{bw_0\overline{w}}{\overline{w}(w_0 - b) - 2bw_0} > b.$$

P r o o f. Differentiating Eq. (3.3) with respect to w we obtain

(4.13) $$\left[\frac{w + w_0 - 2b}{w - b}s + \frac{u_0}{w_0 - b}\right]\frac{ds}{dw} = \frac{w_0 - b}{2(w - b)^2}s^2 + \frac{u_0 s}{(w - b)^2}$$
$$- \left[\frac{1 - u_0^2}{2(w_0 - b)(w - b)^2} - \frac{a(w + 2w_0)}{w_0^2 w^3}\right].$$

We use Eq. (3.3) to eliminate $u_0 s$ and obtain

$$\left[\frac{w + w_0 - 2b}{w - b}s + \frac{u_0}{w_0 - b}\right]\frac{ds}{dw} = -\frac{1}{2(w - b)}\left\{s^2 - \frac{2a\left[(w_0 - b)w - 2bw_0\right]}{w_0^2 w^3}\right\}.$$

Hence, (4.10) holds if and only if

$$(4.14) \qquad s^2(\overline{w}; w_0, u_0) = \frac{2a\left[(w_0 - b)\overline{w} - 2bw_0\right]}{w_0^2 \overline{w}^3}.$$

The right-hand side is positive for

$$\overline{w} \geq \frac{2bw_0}{w_0 - b}$$

only.

Inserting (4.14) into Eq. (4.5) we find easily that it has one double solution $w = \overline{w}$, the third one is given by (4.12). The proof is complete.

Let (w_0, u_0) be given. The Hugoniot locus $H(w_0, u_0)$ is defined as the set of all states $(w, u) \in \mathcal{D}$ which satisfy (3.2) for some real s. For any (w_0, u_0) and $w > b$, if $D(w; w_0, u_0) \geq 0$, $H(w_0, u_0)$ consists of two branches $H_{\pm}(w_0, u_0)$, and each of them is defined by

$$H_{\pm}(w_0, u_0) = \left\{(w, u): \quad u = u_0 - s_{\pm}(w; w_0, u_0)(w - w_0)\right\},$$

where

$$(4.16) \qquad s_{\pm}(w; w_0, u_0) = \frac{w - b}{w + w_0 - 2b}\left[-\frac{u_0}{w - b} \pm \sqrt{D(w; w_0, u_0)}\right].$$

Of course, $(w_0, u_0) \in H_+(w_0, u_0) \cap H_-(w_0, u_0)$. However, there can be other states (w, u) belonging both to $H_+(w_0, u_0)$ and $H_-(w_0, u_0)$. As it is seen from (4.16), it occurs if $D(w; w_0, u_0) = 0$, $w \neq w_0$. Then $H(w_0, u_0)$ forms loops. Also, let us notice that the Hugoniot locus can be disconnected.

The shapes of the Hugoniot loci for a few values of w_0, u_0, and a are shown in Figs. 2 and 3. Figure 2 presents them for the case when the domain of hyperbolicity is connected. As we can see, the curves can be either connected or disconnected. In the latter case they can form loops, and enter the domain of ellipticity where the speed of sound is complex.

In Fig. 3, four examples of the Hugoniot loci are given for the case of disconnected domain of hyperbolicity. The ineresting thing is that they can traverse the domain of ellipticity. Also, loops to the right (Fig. 3b) or to the left (Fig. 3d) of the point (w_0, u_0) can be formed. In Fig. 3c the point (w_0, u_0) belongs to the domain of ellipticity. In this case, the Hugoniot locus consists of three components: the left-hand branch, the sole point (w_0, u_0), and the right-hand branch.

We have to add that these do not exhaust all possible interesting situations.

We establish two auxiliary results.

[169]
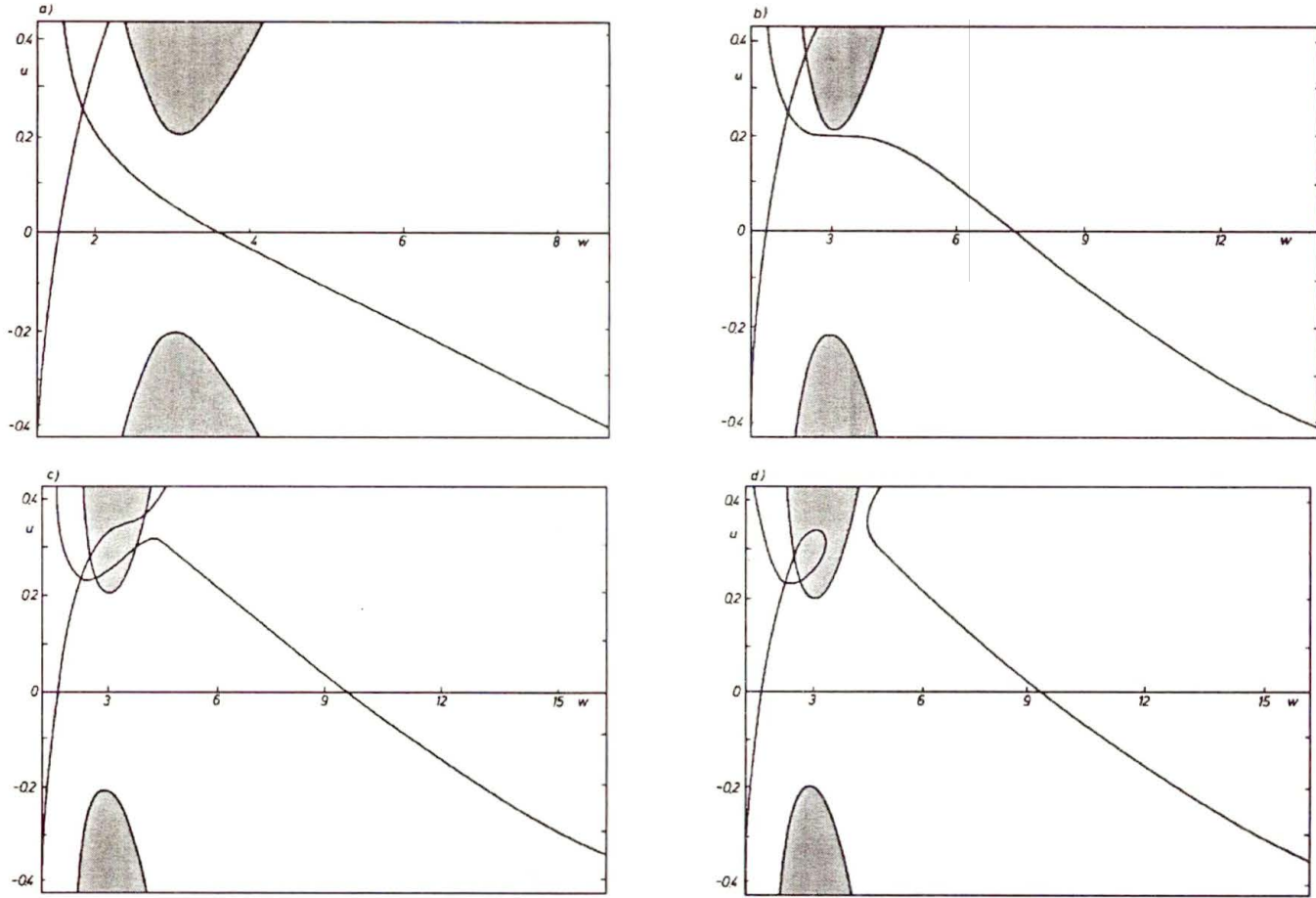
FIG. 2. The Hugoniot loci for some values of w_0, u_0. The domain of hyperbolicity is connected. a) $a = 1.65$, $w_0 = 1.7$, $u_0 = 0.25$; b) $a = 1.65$, $w_0 = 1.95$, $u_0 = 0.25$; c) $a = 1.65$, $w_0 = 2.25$, $u_0 = 0.25$; d) $a = 1.65$, $w_0 = 2.3$, $u_0 = 0.25$.
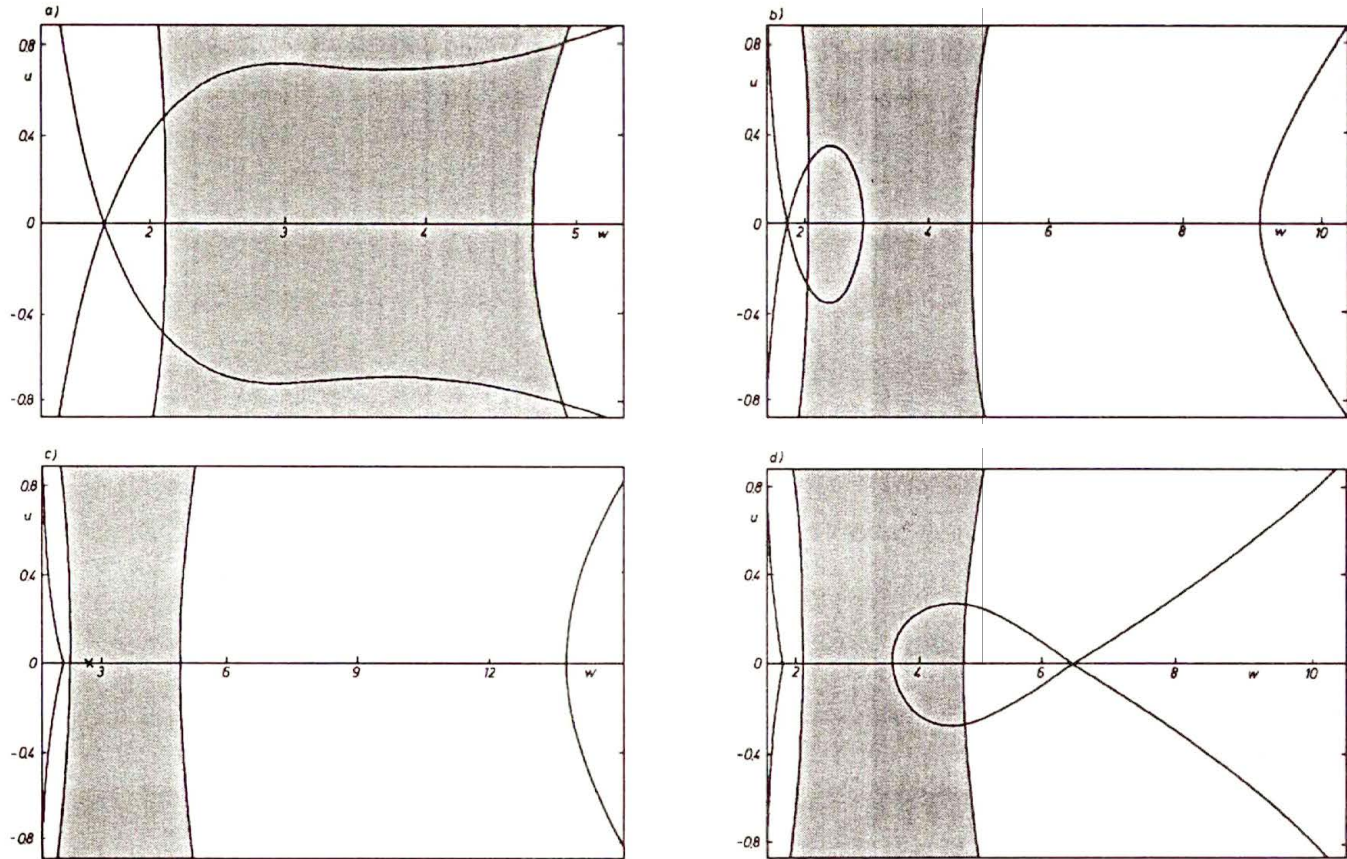
FIG. 3. The Hugoniot loci for some values of w_0, u_0. The domain of ellipticity is connected. a) $a = 1.9$, $w_0 = 1.7$, $u_0 = 0$;
b) $a = 1.9$, $w_0 = 1.8$, $u_0 = 0$; c) $a = 1.9$, $w_0 = 2.5$, $u_0 = 0$; The cross $\times$ denotes the position of (w_0, u_0) in the domain of ellipticity.
d) $a = 1.9$, $w_0 = 6.5$, $u_0 = 0$.

PROPOSITION 4. Let $s = s(w; w_0, u_0)$ be a solution of Eq. (3.3). Then

$$(4.17) \qquad (w - w_0) \left\{ \frac{w_0 - b}{2(w - b)^2} s^2 + \frac{u_0 s}{(w - b)^2} \right.$$
$$\left. - \left[\frac{1 - u_0^2}{2(w_0 - b)(w - b)^2} + \frac{a(w + 2w_0)}{w_0^2 w^3} \right] \right\}$$
$$= - \left\{ \frac{(w - b)^2 + (w_0 - b)^2}{2(w - b)^2} s^2 + \frac{u_0 s(w_0 - b)}{(w - b)^2} - \left[\frac{1 - u_0^2}{2(w - b)^2} - \frac{2a}{w^3} \right] \right\}.$$

P r o o f. Let $\mathcal{L}$ be the left-hand side of (4.17). We have trivially: $\mathcal{L} = \mathcal{L} - 0$, and substituting the left-hand side of (3.3) for zero we obtain the right-hand side of (4.17). The proof is complete.

PROPOSITION 5. If $(w, u) \in H(w_0, u_0)$, then

$$(4.18) \qquad [s(w; w_0, u_0) - \lambda_+(w, u)] [s(w; w_0, u_0) - \lambda_-(w, u)]$$
$$= \frac{(w - b)^2 + (w_0 - b)^2}{2(w - b)^2} s^2 + \frac{s u_0(w_0 - b)}{(w - b)^2} - \left[\frac{1 - u_0^2}{2(w - b)^2} - \frac{2a}{w^3} \right],$$

where $\lambda_\pm(w, u)$ are the solutions of (2.10)

$$\lambda_\pm(w, u) = \frac{1}{2} \left(-\frac{u}{w - b} \pm \sqrt{\Delta(w, u)} \right).$$

P r o o f. Setting $u = u_0 - s(w - w_0)$ in Eq. (2.10) we obtain

$$(4.19) \qquad \lambda_+(w, u) + \lambda_-(w, u) = -\frac{u_0 - s(w - w_0)}{w - b},$$

and

$$(4.20) \qquad \lambda_+(w, u)\lambda_-(w, u) = \frac{s^2(w - w_0)^2}{2(w - b)^2} - \frac{s u_0(w - w_0)}{(w - b)^2} - \left[\frac{1 - u_0^2}{2(w - b)^2} - \frac{2a}{w^3} \right].$$

Equation (4.18) is an immediate consequence of these identities. The proof is complete.

LEMMA 9. Let $D(w; w_0, u_0) > 0$.

i) If $(w, u) \in H_+(w_0, u_0)$, then

$$(w - w_0)\frac{ds_+}{dw} > 0 \qquad \left(\text{respectively}: \quad (w - w_0)\frac{ds_+}{dw} < 0 \right)$$

if and only if

$$\lambda_-(w, u) < s_+(w; w_0, u_0) < \lambda_+(w, u),$$

(respectively: $s_+(w; w_0, u_0) < \lambda_-(w, u)$ or $s_+(w; w_0, u_0) > \lambda_+(w, u)$).

ii) If $(w, u) \in H_-(w_0, u_0)$, then

$$(w - w_0)\frac{ds_-}{dw} > 0 \qquad \left(\text{respectively}: \quad (w - w_0)\frac{ds_-}{dw} < 0 \right)$$

if and only if $s_-(w; w_0, u_0) < \lambda_-(w, u)$ or $s_-(w; w_0, u_0) > \lambda_+(w, u)$
(respectively: $\lambda_-(w, u) < s_-(w; w_0, u_0) < \lambda_+(w, u)$).

P r o o f. Owing to (4.13), (4.17), and (4.18) we have

$$(4.21) \qquad \left[\frac{w + w_0 - 2b}{w - b}s + \frac{u_0}{w - b} \right]\frac{ds}{dw} = -\frac{(s - \lambda_+)(s - \lambda_-)}{w - w_0}.$$

But on $H_+(w_0, u_0)$

$$\frac{w + w_0 - 2b}{w - b}s + \frac{u_0}{w - b} = \sqrt{D(w; w_0, u_0)}.$$

Therefore on $H_+(w_0, u_0)$

$$\sqrt{D(w; w_0, u_0)}\,(w - w_0)\frac{ds_+}{dw} = -(s_+ - \lambda_-)(s_+ - \lambda_+).$$

Assertion i) is an immediate consequence of this identity. To prove ii) we use

$$\sqrt{D(w; w_0, u_0)}\,(w - w_0)\frac{ds_-}{dw} = (s_- - \lambda_-)(s_- - \lambda_+)$$

on $H_-(w_0, u_0)$. The proof is complete.

LEMMA 10. If

$$(4.22) \qquad \frac{d}{dw}s(w; w_0, u_0)\Big|_{w=\overline{w}} = 0,$$

then $s(\overline{w}; w_0, u_0) = \lambda_+(\overline{w}, \overline{u})$ or $\lambda_-(\overline{w}, \overline{u})$, where $(\overline{w}, \overline{u}) \in H(w_0, u_0)$.

Conversely, if for some $w = \overline{w} \neq w_0$ with $(\overline{w}, \overline{u}) \in H(w_0, u_0)$, $D(\overline{w}; w_0, u_0) > 0$, and $s(\overline{w}; w_0, u_0) = \lambda_+(\overline{w}, \overline{u})$ or $\lambda_-(\overline{w}, \overline{u})$, then (4.22) holds.

P r o o f. The first part of the Assertion is a consequence of (4.20) and the Assumption. Conversely, if $s = \lambda_+$ or $s = \lambda_-$ then $ds/dw = 0$, since $D > 0$. The proof is complete.

LEMMA 11. Let $(w, u) \in H(w_0, u_0)$. Then

$$(4.23) \qquad \frac{du}{dw} = -\frac{1}{2}\frac{s^2 - \lambda_-\lambda_+}{s - \dfrac{\lambda_- + \lambda_+}{2}},$$

where $s = s(w; w_0, u_0)$; $\lambda_\pm = \lambda_\pm(w, u)$.

P r o o f. Differentiating

$$u = u_0 - s(w - w_0)$$

we obtain

$$\frac{du}{dw} = -(w - w_0)\frac{ds}{dw} - s.$$

Next, making use of (4.21) we get

$$\frac{du}{dw} = -\frac{\dfrac{w_0 - b}{w - b}s^2 + s\left(\dfrac{u_0}{w - b} + \lambda_- + \lambda_+\right) - \lambda_-\lambda_+}{2s + \dfrac{u}{w - b}}.$$

Applying (4.19) we obtain (4.23). The proof is complete.

LEMMA 12. Let $D(w; w_0, u_0) > 0$, and let

$$\frac{d}{dw}s(w; w_0, u_0)\Big|_{w=\overline{w}} = 0.$$

Then

i) $s(w; w_0, u_0)$ attains a local minimum at $\overline{w}$, provided that $(w - w_0)\mathbf{r}\cdot\nabla\lambda < 0$ at $(\overline{w}, \overline{u})$;

ii) $s(w; w_0, u_0)$ attains a local maximum at $\overline{w}$, provided that $(w - w_0)\mathbf{r}\cdot\nabla\lambda > 0$ at $(\overline{w}, \overline{u})$.

Here, $\overline{u} = u_0 - s(\overline{w}; w_0, u_0)(\overline{w} - w_0)$, $\mathbf{r} = \mathbf{r}_\pm(w, u)$ is the right eigenvector of the matrix $\mathbb{M}$ corresponding to $\lambda_\pm$ respectively, and $\lambda = \lambda_+$ or λ_- according to whether $s = \lambda_+$ or $s = \lambda_-$.

P r o o f. Differentiating (4.21) and using the Assumption we get

$$(2s - \lambda_- - \lambda_+)\frac{d^2s}{dw^2} = \frac{1}{w - w_0}\left[(s - \lambda_-)\frac{d\lambda_+}{dw} + (s - \lambda_+)\frac{d\lambda_-}{dw}\right].$$

Let $s = \lambda_+$, then the above reduces to

$$\frac{d^2s}{dw^2} = \frac{1}{w - w_0}\frac{d\lambda_+}{dw}.$$

But, making use of (4.23) we obtain

$$\frac{d\lambda_+}{dw} = \frac{\partial\lambda_+}{\partial w} + \frac{\partial\lambda_+}{\partial u}\frac{du}{dw} = \frac{\partial\lambda_+}{\partial dw} - \lambda_+\frac{\partial\lambda_+}{\partial u} = \mathbf{r}_+\cdot\nabla\lambda_+.$$

Hence, at $w = \overline{w}$

$$\frac{d^2s}{dw^2} = \frac{1}{w - w_0}\mathbf{r}_+\cdot\nabla\lambda_+.$$

Similarly, if $s = \lambda$ at $w = \overline{w}$, then

$$\frac{d^2 s}{dw^2} = \frac{1}{w - w_0} \mathbf{r}_- \cdot \nabla \lambda_- .$$

The proof is complete.

PROPOSITION 6. Given w_r, w_l, u_l with $(w_l, u_l) \in \mathcal{D}$, then $(w_l, u_l) \in H(w_r, u_r)$, and

(4.24) $s(w_l; w_r, u_r) = s(w_r; w_l, u_l)$

where

(4.25) $u_r = u_l - s(w_r; w_l, u_l)(w_r - w_l),$

provided that $s(w_r; w_l, u_l)$ exists.

P r o o f. If $(w, u) \in H(w_r, u_r)$ then

$$u = u_r - s(w; w_r, u_r)(w - w_r).$$

Setting here $w = w_l$, and using (4.25) we get

$$u = u_l - \Big[s(w_r; w_l, u_l) - s(w_l; w_r, u_r) \Big](w_r - w_l).$$

It follows from the above that it is sufficient to show that (4.24) holds in order to have $(w_l, u_l) \in H(w_r, u_r)$. We introduce the shorthands $s_l = s(w_r; w_l, u_l)$ and $s_r = s(w_l; w_r, u_r)$. These quantities satisfy Eq. (3.3) with $w = w_r$, $w_0 = w_l$, $u_0 = u_l$, and $w = w_l$, $w_0 = w_r$, $u_0 = u_r$, respectively. Substituting (4.25) into the equation for s_r, and using Eq. (3.3) for s_l we obtain

$$s_r^2 + \frac{2[u_l - s_l(w_r - w_l)]}{w_r + w_l - 2b} s_r - \frac{3w_l - w_r - 2b}{w_r + w_l - 2b} s_l^2 - \frac{2u_l s_l}{w_r + w_l - 2b} = 0.$$

This equation has two real solutions, one of them is given by (4.25). The proof is complete.

PROPOSITION 7. Given w, w_0, u_0 with $(w_0, u_0) \in \mathcal{D}$. Then

(4.26) $s_\pm(w; w_0, -u_0) = -s_\mp(w; w_0, u_0).$

P r o o f. Equation (4.26) is an immediate consequence of (4.16) and the identity

(4.27) $D(w; w_0, -u_0) = D(w; w_0, u_0).$

The proof is complete.

The graphs of the shock speed as a function of the specific volume w are given in Fig. 1 for a few values of a, b, w_0, and u_0.

5. Travelling waves in the model Navier–Stokes equations

Within the Euler equations, the shock wave is a jump discontinuity propagating along the line $x - st = 0$. Let (w_l, u_l) and (w_r, u_r) be the given states to the left and to the right of the line of discontinuity. They have to satisfy the Rankine–Hugoniot relations. However, it is not enough to accept such a jump as physical. It is well known that some additional conditions have to be imposed. Various ideas were used to formulate such additional admissibility criteria [10–48].

We remind that our principal task is to investigate different approximations to the model kinetic equations of [56], and the Euler equations (2.1) are the last but crucial term in the sequence. Hence no freedom of choice of admissibility criteria is left to us, and we have to turn to the next order approximation, i.e. to the Navier–Stokes equations.

The Navier–Stokes equations read

(5.1)
$$\frac{\partial w}{\partial t} - \frac{\partial u}{\partial x} = 0,$$
$$\frac{\partial u}{\partial t} + \frac{\partial}{\partial x} p(w, u) = \varepsilon \frac{\partial}{\partial x} \left(\mu \frac{\partial u}{\partial x} \right),$$

where t, x, w, u, and $p(w, u)$ are the same as previously, but $\varepsilon \mu$ is the coefficient of viscosity, $\varepsilon > 0$ is a parameter, and $\mu = \mu(w, u)$ is given by

(5.2)
$$\mu(w, u) = \frac{1 - u^2 + 2b^2 w^2 \varrho^2(w)}{8w^2 \varrho}, \qquad \varrho(w) = \frac{w}{w - b}.$$

A travelling wave solution to (5.1) is a solution of the form

(5.3)
$$(w, u)(x, t) = (\widehat{w}, \widehat{u})(z), \qquad z = \frac{x - st}{\varepsilon} \in \mathbb{R},$$

where $s = $ const is the wave-speed, such that

(5.4)
$$\lim_{z \to -\infty} (\widehat{w}, \widehat{u})(z) = (w_l, u_l),$$

(5.5)
$$\lim_{z \to +\infty} (\widehat{w}, \widehat{u})(z) = (w_r, u_r),$$

and

(5.6)
$$\lim_{z \to \infty} \frac{d}{dz} (\widehat{w}, \widehat{u})(z) = (0, 0).$$

A discontiuous solution (3.1) to Eqs. (2.1) is said to be admissible, if Eqs. (5.1) admit a travelling wave solution (5.3)–(5.6) for sufficiently small $\varepsilon > 0$.

We substitute (5.3) into (5.1), perform one integration with respect to z, use the limit conditions (5.4)–(5.6), and obtain

(5.7)
$$\widehat{u} = u_l - s(w - w_l),$$

(5.8)
$$\mu \frac{d\widehat{u}}{dz} = -s(\widehat{u} - u_l) + p(\widehat{w}, \widehat{u}) - p(w_l, u_l),$$

as well as

(5.9)
$$sw_r + u_r = sw_l + u_l,$$
$$-su_r + p(w_r, u_r) = -su_l + p(w_l, u_l).$$

Equations (5.9) have the form of the Rankine–Hugoniot conditions (3.2), which were discussed thoroughly in the preceding sections.

Using (5.7) to eliminate $\widehat{u}$ from Eq. (5.8) we arrive at the problem:

find a solution to

(5.10)
$$s\widehat{\mu} \frac{d\widehat{w}}{dz} + f_l(\widehat{w}) = 0, \qquad \xi \in \mathbb{R},$$

such that

(5.11)
$$\lim_{z \to -\infty} \widehat{w}(z) = w_l, \qquad \lim_{z \to +\infty} \widehat{w}(z) = w_r,$$

(5.12)
$$\lim_{z \to -\infty} \widehat{w}'(\xi) = \lim_{z \to +\infty} \widehat{w}'(\xi) = 0,$$

where the prime ' denotes d/dz, and where

(5.13) $f_l(w) = s^2(w - w_l) + p(w, u_l - s(w - w_l)) - p(w_l, u_l),$

(5.14) $f_l(w_l) = f_l(w_r) = 0$

and $\widehat{\mu} = \mu(\widehat{w}, u_l - s(\widehat{w} - w_l))$. The subscript l in f_l is used to mark that $f(w)$ is related to the left state (w_l, u_l) which is treated as given. We have

LEMMA 13. Problem (5.10)–(5.14) has a unique solution if and only if
$f_l(w) < 0$ between w_l and w_r for $s(w_r - w_l) > 0$,
$f_l(w) > 0$ between w_l and w_r for $s(w_r - w_l) < 0$.

P r o o f. If $w_r > w_l$, then we must have $\widehat{w}'(z) > 0$. Hence, if $s(w_r - w_l) > 0$, then $s\widehat{w}'(z) > 0$, therefore $f(w)$ has to be negative between w_l and w_r. The second case is analyzed in a similar way. The proof is complete.

THEOREM 1. *The problem* (5.10)–(5.14) *has a unique solution if and only if:*

i) for $s(w_r - w_l) > 0$, *the chord joining* $(w_l, p(w_l, u_l))$ *to* $(w_r, p(w_r, u_r))$ *lies above the graph of* $p(w, u_l - s(w - w_l))$ *between* w_l *and* w_r;

ii) for $s(w_r - w_l) < 0$, the chord joining $(w_l, p(w_l, u_l))$ to $(w_r, p(w_r, u_r))$ lies below the graph of $p(w, u_l - s(w - w_l))$ between w_l and w_r.

P r o o f. Rewrite $f(w) < 0$ in the form $p(w, u_l - s(w - w_l)) < s^2(w - w_l) + p(w_l, u_l)$. The case of $f(w) > 0$ is analyzed similarly. The proof is complete.

This theorem reminds the similar ones of [18] or [19] for the isothermal case. The essential difference between the latter case and that of ours is that in the isothermal case p does not depend on s. Therefore changing s we change only the slope of the Rayleigh line, i.e. the chord joining $(w_l, p(w_l))$ to $(w_r, p(w_r))$, and the graph of $p(w)$ remains intact. In our case, when changing s we change not only the slope of the Rayleigh line but the graph of p itself, since $p = p(w, u_l - s(w - w_l))$. Hence, the use of this very intuitive theorem is a little bit troublesome in the case under consideration.

The assertions of Lemma 13 and Theorem 1 were essentially independent of the specific form of $p(w, u)$. If $p(w, u)$ is given by (2.3), then we can obtain analytical criteria for existence of the travelling waves. Namely, we have

LEMMA 14. Let $p(w, u)$ be given by (2.3). Then, there is a unique solution to (5.10)–(5.14) if and only if:

i) for $s > 0$:

$$(5.15) \qquad \left(s + \frac{u_l}{w + w_l - 2b}\right)^2 - \frac{(w - b)^2}{(w + w_l - 2b)^2} D(w; w_l, u_l) \leq 0$$

between w_l and w_r;

ii) for $s < 0$

$$(5.16) \qquad \left(s + \frac{u_l}{w + w_l - 2b}\right)^2 - \frac{(w - b)^2}{(w + w_l - 2b)^2} D(w; w_l, u_l) \geq 0$$

between w_l and w_r, where $D(w; w_l, u_l)$ is given by (3.4).

P r o o f. Using (2.3) we write

$$f_l(w) = \frac{(w - w_l)w + w_l - 2b}{2(w - b)} \left[\left(s + \frac{u_l}{w + w_l - 2b}\right)^2 \right.$$
$$\left. - \frac{(w - b)^2}{w + w_l - 2b} D(w; w_l, u_l)\right].$$

From this identity and with the use of Lemma 13 we obtain easily (5.15) and (5.16) by considering separately four cases of $s > 0$, $w_r - w_l > 0$, etc. The proof is complete.

Let us notice now, that the necessary condition for (5.15) to hold is $D(w; w_l, u_l) > 0$ between w_l and w_r. Hence, (w_r, u_r) has to belong to the same component

of $H(w_l, u_l)$ as (w_l, u_l) does. Next, $(5.14)_2$ means that s satisfies Eq. (3.3) with $(w_0, u_0) = (w_l, u_l)$ and $w = w_r$. Thus, $s = s(w_r; w_l, u_l)$ Therefore we can rewrite (5.15) as follows

$$(5.17) \qquad s_-(w; w_l, u_l) \leq s(w_r; w_l, u_l) \leq s_+(w; w_l, u_l)$$

between w_l and w_r.

This is a generalization of the Oleinik–Liu condition [10, 13–15] to the present problem.

Summing up we have

COROLLARY 2. If the wave speed $s = s(w_r; w_l, u_l)$ is strictly positive, then (5.10)–(5.14) has a unique solution if and only if

i) (w_r, u_r) belongs to the same component of $H(w_l, u_l)$ as (w_l, u_l) does;

ii) the Oleinik–Liu condition (5.17) is satisfied.

On the other hand, let us notice that if $s < 0$, then the case when $D(w; w_l, u_l)$ takes negative values is not excluded and (w_r, u_r) and (w_l, u_l) can belong to different components of $H(w_l, u_l)$. If so, then $s_\pm(w; w_l, u_l)$ becomes complex for some values of w between w_l and w_r. Consequently, the Oleinik–Liu condition is violated.

This asymmetry can be understood on physical grounds. Namely, if $s > 0$, then the left-hand state (w_l, u_l) is the state after the wave, and the right-hand state (w_r, u_r) is that before the wave, whereas if $s < 0$, the situation is opposite. We can see that by treating the right-hand state (w_r, u_r) is given. Then, instead of (5.7) we have $\hat{u} = u_r - s(w - w_r)$, and Eq. (5.10) is replaced by

$$(5.18) \qquad s\mu_r(\hat{w})\frac{d\hat{w}}{dz} + f_r(\hat{w}) = 0,$$

where $\mu_r(w) = \mu(w, u_r - s(w - w_r))$ and

$$(5.19) \qquad f_r(w) = s^2(w - w_r) + p(w, u_r - s(w - w_r)) - p(w_r, u_r),$$

$$(5.20) \qquad f_r(w_l) = f_r(w_r) = 0.$$

Instead of Lemma 14 we have

LEMMA 15. Let $p(w, u)$ be given by (2.2). Then, there is a unique solution to (5.11), (5.12), (5.18)–(5.20) if and only if

i) for $s > 0$

$$(5.21) \qquad \left(s + \frac{u_r}{w + w_r - 2b}\right)^2 - \frac{(w - b)^2}{(w + w_r - 2b)^2}D(w; w_r, u_r) \geq 0$$

between w_l and w_r;

ii) for $s < 0$

$$(5.22) \qquad \left(s + \frac{u_r}{w + w_r - 2b}\right)^2 - \frac{(w - b)^2}{(w + w_r - 2b)^2} D(w; w_r, u_r) \le 0$$

between w_l and w_r.

We have also

COROLLARY 3. If the speed $s = s(w_l; w_r, u_r)$ is strictly negative, then the problem (5.11), (5.12), (5.18)–(5.20) has a unique solution if and only if

i) (w_l, u_l) belongs to the same component of $H(w_r, u_r)$ as (w_r, u_r) does;

ii) the Oleinik–Liu condition in the form

$$(5.23) \qquad s_-(w; w_r, u_r) \le s(w_r; w_l, u_l) \le s_+(w; w_r, u_r)$$

holds between w_l and w_r.

LEMMA 16. Conditions (5.15) and (5.21) are equivalent, as well as (5.16) and (5.22) are.

P r o o f. Let $\mathcal{L}_l$ denote the left-hand side of (5.15) and (5.16), and let $\mathcal{L}_r$ denote the right-hand side of (5.21) and (5.22). Since $s = s(w_r; w_l, u_l)$, then using Eq. (3.3) with $w = w_r$, $(w_0, u_0) = (w_l, u_l)$ to eliminate $u_l s$ from $\mathcal{L}_l$, we obtain

$$\mathcal{L}_l = \frac{w - w_r}{w + w_l - 2b} \left\{ s^2 - \frac{2a[w(w_r w_l - bw_l - bw_r) - bw_l w_r]}{w^2 w_l^2 w_r^2} \right\}.$$

Similarly, using the fact that $s = s(w_l; w_r, u_r)$ (cf. Proposition 6) we can write

$$\mathcal{L}_r = \frac{w - w_l}{w + w_r - 2b} \left\{ s^2 - \frac{2a[w(w_r w_l - bw_l - bw_r) - bw_l w_r]}{w^2 w_l^2 w_r^2} \right\}.$$

Let $\mathcal{L} \le 0$; then either

$\alpha) \qquad w - w_r \le 0 \qquad$ and $\qquad s^2 - \dfrac{2a[w(w_r w_l - bw_l - bw_r) - bw_l w_r]}{w^2 w_l^2 w_r^2} \ge 0,$

or

$\beta) \qquad w - w_r \ge 0 \qquad$ and $\qquad s^2 - \dfrac{2a[w(w_r w_l - bw_l - bw_r) - bw_l w_r]}{w^2 w_l^2 w_r^2} \le 0.$

Let us consider $\alpha)$. The inequality $w < w_r$ implies $w_l < w < w_r$. Hence $w - w_l > 0$. Therefore (5.21) holds. In the case $\beta)$, it must be $w_l - w < 0$, and again we obtain (5.21).

If $\mathcal{L}_r \ge 0$, then we proceed similarly and obtain (5.15). The proof is complete.

To unify our considerations we introduce the following definitions:

$$(w_a, u_a) = \begin{cases} (w_l, u_l) & \text{for} \quad s > 0, \\ (w_r, u_r) & \text{for} \quad s < 0, \end{cases}$$

and

$$(w_b, u_b) = \begin{cases} (w_r, u_r) & \text{for} \quad s > 0, \\ (w_l, u_l) & \text{for} \quad s < 0, \end{cases}$$

and call (w_a, u_a) the state after the wave, whereas (w_b, u_b) the state before the wave.

We have

THEOREM 2. *Equations* (5.1) *admit the unique travelling wave solution* (5.3)– (5.6) *if and only if*

   i) (w_b, u_b) *belongs to the same component of* $H(w_a, u_a)$ *as* (w_a, u_a) *does;*

   ii) *the Oleinik–Liu condition:*

$$s_-(w; w_a, u_a) \le s(w_b; w_a, u_a) \le s_+(w; w_a, u_a)$$

is satisfied for every w between w_a and w_b.

This theorem is a compilation of Corollaries 2 and 3, and as such it needs no proof.

6. Shock-wave structure

The problem (5.10)–(5.14) with $\mu(w, u)$ given by (5.2) and $\hat{u}$ given by (5.7) admits an explicit solution. To determine it we perform some transformations and substitutions. Let w_r, w_l, u_l be given, and let s denote the shock-wave speed, i.e. $s = s(w_r; w_l, u_l)$.

First, from (5.2) and (5.7) we obtain

(6.1)
$$\hat{\mu}(w) = \frac{1}{8w^3(w - b)} \sum_{i=0}^{4} A_i w^i,$$

where

(6.2)
$$\begin{aligned} A_0 &= b^2\big(1 - (u_l + sw_l)^2\big), \\ A_1 &= -2b\big[1 - (u_l + sw_l)^2 - bs(u_l + sw_l)\big], \\ A_2 &= 1 - (u_l + sw_l)^2 - 4bs(u_l + sw_l) - b^2 s^2, \\ A_3 &= 2s\big(u_l + s(w_l + b)\big), \\ A_4 &= 2b^2 - s^2. \end{aligned}$$

Hence, $\hat{\mu}(w)$ is a rational function. Also, $f_l(w)$ is such. To show this we make use of (2.3), (5.7), (5.13), and (5.14) and obtain

$$
(6.3) \qquad f_l(w) = \frac{(w - w_l)(w - w_r)}{2w^2(w - b)}\left[s^2 w^2 - \frac{2a(w_l w_r - b w_l - b w_r)}{w_l^2 w_r^2}w + \frac{2ab}{w_l w_r}\right].
$$

Using (6.1), (6.3) we rewrite Eq. (5.10) in the explicit form

$$
(6.4) \qquad \frac{\displaystyle\sum_{i=0}^{4} A_i w_i}{w(w - w_l)(w - w_r)(w^2 - 2\alpha w + \beta)}dw = -4s\,d\xi,
$$

where

$$
(6.5) \qquad
\begin{aligned}
\alpha &= \frac{a(w_l w_r - b w_l - b w_r)}{s^2 w_l^2 w_r^2}, \\[2mm]
\beta &= \frac{2ab}{s^2 w_l w_r}
\end{aligned}
$$

are constants.

Equation (6.4) can be easily integrated. The result depends significantly on the sign of

$$
(6.6) \qquad\qquad\qquad\qquad W = \beta - \alpha^2.
$$

CASE I. $W > 0$.

Under this assumption, the equation $f_l(w) = 0$ has exactly two real solutions $w = w_l$ and $w = w_r$. Hence, the general solution of Eq. (6.4) is

$$
(6.7) \qquad A \ln w + B \ln|w - w_l| + C \ln|w - w_r| + \frac{1}{2}D \ln(w^2 - 2\alpha w + \beta)
$$

$$
+ \frac{E}{\sqrt{\beta - \alpha^2}} \arctan \frac{w + \alpha}{\sqrt{\beta - \alpha^2}} = -4sz + \text{integration constant,}
$$

where

$$
A = \frac{A_0}{\beta w_l w_r},
$$

$$
B = \frac{A_{11} - w_l A_{21}}{(w_r - w_l)(w_l^2 - 2\alpha w_l + \beta)},
$$

$$
C = \frac{A_{11} - w_r A_{21}}{(w_r - w_l)(w_r^2 - 2\alpha w_r + \beta)},
$$

$$
A_{11} = A_4 w_l w_r (w_l + w_r) + A_3 w_l w_r - A_1 - A_0\frac{w_l + w_r}{w_l w_r},
$$

$$A_{21} = -A_4(w_l^2 + w_l w_r + w_r^2) + A_3(w_l + w_r) + A_2 - \frac{A_0}{w_l w_r},$$

$$D = A_4 - A - B - C,$$

$$E = A_4(w_l + w_r) + A_3 + 2\alpha A + B(2\alpha - w_l) + C(2\alpha - w_r).$$

The explicit analytic solution (6.7) was used to obtain a series of shock profiles shown in Fig. 4. The input data were so chosen as to receive results resembling those of [4, 7]. Our Fig. 4 is qualitatively similar to Fig. 10 of [4]. In particular, we see that so-called impending shock splitting can be derived from our model equations. The notion of "impending shock splitting" was first introduced in [4] and refers to shocks having two inflexion points instead of one, what is usual.
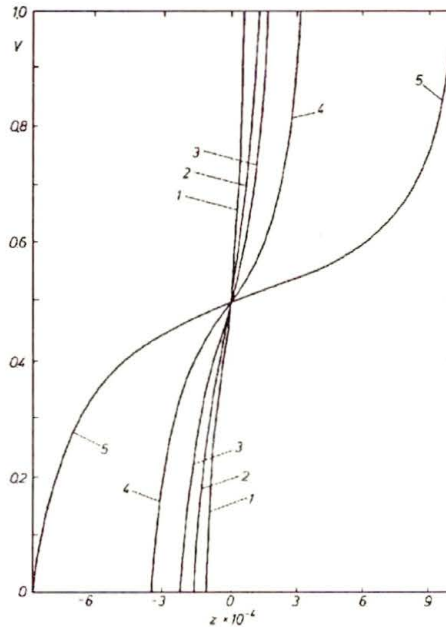
FIG. 4. Impending shock splitting. Normalized profiles $V = (w - w_l)/(w_r - w_l)$ versus $z \times 10^{-4}$, $a = 0.5$, $w_r = 10$, $u_r = 0$; $1 - w_l = 1.623$, $2 - w_l = 1.653$, $3 - w_l = 1.683$, $4 - w_l = 1.713$, $5 - w_l = 1.743$.

We omit all details of how to choose the entry data to obtain such phenomenon since it is fairly well done and explained in [4].

CASE II. $W \leq 0$.

Under this assumption the equation

$$w^2 - 2\alpha w + \beta = 0$$

has two real solutions $w_- \leq w_+$; what means that $f_l(w)$ has two additional zeros $w = w_-$ and $w = w_+$, except the "old" ones $w = w_l$ and $w = w_r$. The existence

of shock connecting (w_l, u_l) to (w_r, u_r) demands w_- and w_+ not to lie between w_l and w_r. The result of integration of Eq. (6.4) depends however on additional detailed relations between the zeros of $f_l(w)$.

i) $w_l \neq w_\pm$, $w_r \neq w_\mp$, $w_- < w_+$. In this case, the general solution of Eq. (6.4) reads

$$A \ln w + B \ln|w - w_l| + C \ln|w - w_r| + D \ln|w - w_-| + E \ln|w - w_+|$$
$$= -4sz + \text{integration constant,}$$

where now

$$A = \frac{A_0}{\beta w_l w_r},$$

$$B = -\frac{A_{11} - w_l A_{21}}{(w_l - w_r)(w_l^2 - 2\alpha w_l + \beta)},$$

$$C = -\frac{A_{11} - w_r A_{21}}{(w_l - w_r)(w_r^2 - 2\alpha w_r + \beta)},$$

$$A_{11} = -A_4 w_l w_r (w_l + w_r) - A_3 w_l w_r - A_1 + A_0 \frac{w_l + w_r}{w_l w_r},$$

$$A_{21} = A_4(w_l^2 + w_l w_r + w_r^2) + A_3(w_l + w_r) + A_2 - \frac{A_0}{w_l w_r},$$

$$D = \frac{1}{w_- - w_+}\Big[A_4(w_l + w_r + w_-) + A_3 + Aw_+ + B(w_l - w_+) + C(w_r - w_+)\Big],$$

$$E = A_4 - A - B - C - D.$$

This case we illustrate with a series of expansion shock profiles presented in Fig. 5. A shock wave is called expansion shock if the graph of $p(w, u_l - s(w - w_l))$ lies entirely above the Rayleigh line joining (w_l, u_l) with (w_r, u_r). Our Fig. 5 can be treated as a counterpart of Figs. 3 and 7 of [4]. We can notice easily that the shock thickness increases rather than decreases, with strength. Also this phenomenon was discovered first in [4] and it is thoroughly discussed in the cited paper.

ii) Either $w_l = w_\pm$ or $w_r = w_\mp$, or both. In this case we have one-sided or two-sided sonic shocks, i.e. shocks moving at the speed equal to the characteristic speed before or after the shock, or else all three of them are equal. In a situation like that, the asymptotic states of the shock are achieved algebraically rather than exponentially and shock thickness is much greater than in the previous cases. This is very similar to what is discussed in detail in [6]. Therefore we omit a discussion of the case.

Summing up, we can say that our model equations produce results qualitatively similar to those obtained within the framework of the true Navier–Stokes equations.
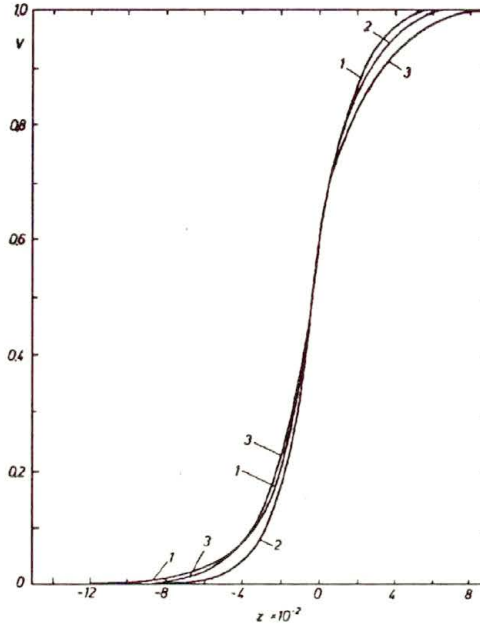
Fig. 5. Rarefaction shocks. Normalized profiles $V = (w - w_l)/(w_r - w_l)$ versus $z \times 10^{-2}$;
$a = 0.5$, $w_r = 10$, $u_r = 0.5$; $1 - w_l = 6.5$, $2 - w_l = 7.25$, $3 - w_l = 8.0$.

References

1. J.D. van der Waals, *On the continuity of the gaseous and liquid states*, Edited with an introductory essay by J.S. Rowlinson, Studies in Statistical Mechanics, vol. XIV, North-Holland, Amsterdam 1988.

2. P.A. Thompson and K. Lambrakis, *Negative shock waves*, J. Fluid Mech., **60**, part 1, 187–208, 1973.

3. M.S. Cramer, *Negative nonlinearity in selected fluorocarbons*, Physics Fluids, A1, 11, 1894–1897, 1989.

4. M.S. Cramer and A.B. Crickenberger, *The dissipative structure of shock waves in dense gases*, J. Fluid Mech., **223**, 325–355, 1991.

5. P.D. Lax, *Hyperbolic systems of conservation laws II*, Comm. Pure Appl. Math., **2**, 537–566, 1957.

6. A. Kluwick, *Small-amplitude finite-rate waves in fluids having both positive and negative nonlinearity*, [in:] Nonlinear Waves in Real Fluids, A. Kluwick [Ed.], CISM Courses and Lectures 315, 1–43, Springer-Verlag, Wien 1991.

7. M.S. Cramer, *Nonclassical dynamics of classical gases*, [in:] Nonlinear Waves in Real Fluids, A. Kluwick [Ed.], CISM Courses and Lectures 315, 93–145, Springer-Verlag, Wien 1991.

8. M.S. Cramer, *A general scheme for the derivation of evolution equations describing mixed nonlinearity*, Wave Motion, **15**, 333–355, 1992.

9. M. Brio and J.K. Hunter, *Asymptotic equations for conservation laws of mixed type*, Wave Motion, **16**, 57–64, 1992.

10. O.A. Oleinik, *Uniqueness and stability of generalized solution of the Cauchy problem for a quasilinear equation*, Amer. Math. Soc. Transl., **42**, 285–290, 1964.

11. B. Wendroff, *The Riemann problem for materials with nonconvex equation of state. I. Isentropic flow*, J. Math. Anal. and Appl., **38**, 454–464, 1972.

12. L. Leibovich, *Solutions of the Riemann problem for hyperbolic systems of quasilinear equations without convexity conditions*, **45**, 81–90, 1974.

13. T.-P. Liu, *The Riemann problem for general* 2×2 *conservation laws*, Trans. Amer. Math. Soc., **199**, 89–112, 1974.

14. T.-P. Liu, *The Riemann problem for general systems of conservation laws*, J. Differential Equations, **18**, 218–234, 1975.

15. T.-P. Liu, *Admissible solutions of hyperbolic conservation laws*, Memoirs of AMS, 240, Providence 1981.

16. R.L. Pego, *Nonexistence of a shock layer in gasdynamics with nonconvex equation of state*, Arch. Rational Mech. and Anal., **94**, 2, 165–178, 1986.

17. M. Sever, *A class of hyperbolic systems of conservation laws satisfying weaker conditions than genuine nonlinearity*, J. Differential Equations, **73**, 1–29, 1988.

18. M. Slemrod, *Admissibility criteria for propagating boundaries in a van der Waals fluid*, Arch. Rational Mech. and Anal., **81**, 301–315, 1983.

19. R. Hagan and M. Slemrod, *The viscosity-capillarity admissibility criterion for shocks and phase transitions*, Arch. Rational Mech. and Anal., **83**, 333–361, 1983.

20. R. Hagan and J. Serrin, *One-dimensional shock layers in Korteweg fluids*, [in:] Phase Transformations and Material Instabilities in Solids, M.E. Gurtin [Ed.], 113–127, Academic Press, Orlando 1984.

21. M. Slemrod, *Dynamics of first order phase transitions*, [in:] Phase Transformations and Material Instabilities in Solids, M. Gurtin [Ed.], 163–203, Academic Press, Orlando 1984.

22. M. Slemrod, *Dynamic phase transitions in a van der Waals fluid*, J. Differential Equations, **52**, 1–23, 1984.

23. H. Hattori, *The Riemann problem for a van der Waals fluid with entropy rate admissibility criterion. Isothermal case*, Arch. Rational Mech. and Anal., **92**, 3, 247–263, 1986.

24. H. Hattori, *The Riemann problem for a van der Waals fluid with entropy rate admissibility criterion – nonisotermal case*, J. Differential Equations, **65**, 2, 158–174, 1986.

25. V. Roytburd and M. Slemrod, *Positively invariant regions for a problem in phase transitions*, Arch. Rational Mech. and Anal., **93**, 1, 61–79, 1986.

26. H. Hattori, *The entropy rate admissibility criterion and the double phase boundary problem*, Contemp. Math., **60**, 51–65, 1987.

27. M. Shearer, *Dynamic phase transitions in a van der Waals gas*, Quarterly of Appl. Math., **46**, 4, 631–636, 1987.

28. M. Grinfeld, *Nonisothermal dynamic phase transitions*, Quarterly of Appl. Math., **47**, 1, 71–84, 1989.

29. M. Slemrod, *A limiting "viscosity" approach to the Riemann problem for materials exhibiting change of phase*, Arch. Rational Mech. and Anal., **105**, 4, 327–365, 1989.

30. L. Hsiao, *Admissible weak solution for nonlinear system of conservation laws of mixed type*, J. Partial Differential Equations, **2**, 1, 1989.

31. L. Hsiao, *Uniqueness of admissible solutions of the Riemann problem for a system of conservation laws of mixed type*, J. Differential Equations, **86**, 2, 197–233, 1990.

32. K. Mischaikov, *Dynamic phase transitions: a connection matrix approach*, [in:] Nonlinear Evolution Equations that Change Type, B.L. Keyfitz, M. Shearer [Eds.], 164–180, Springer-Verlag, Berlin 1990.

33. H.-T. Fan, *A vanishing viscosity approach to the dynamics of phase transition in van der Waals fluids*, J. Differential Equations, **103**, 179–204, 1993.

34. D. Hoff and M. Khodja, *Stability of coexisting phases for compressible van der Waals fluids*, SIAM J. Appl. Math., **53**, 1, 1–14, 1993.

35. H.-T. Fan, *One-phase Riemann problem and wave interactions in systems of conservation laws of mixed type*, SIAM J. Math. Anal., **24**, 4, 840–865, 1993.

36. R.D. James, *The propagation of phase boundaries in elastic bars*, Arch. Rational Mech. and Anal., **73**, 125–158, 1980.

37. M. Shearer, *The Riemann problem for a class of conservation laws of mixed type*, J. Differential Equations, **46**, 426–443, 1982.

38. M. Shearer, *Nonuniqueness of admissible solutions of Riemann initial value problem for a system of conservation laws of mixed type*, Arch. Rational Mech. and Anal., **93**, 45–59, 1986.

39. R.L. PEGO, *Phase transitions in one-dimensional nonlinear viscoelasticity: admissibility and stability*, Arch. Rational Mech. and Anal., **97**, 4, 354–394, 1987.

40. L. TRUSKINOVSKY, *Dynamics of nonequilibrium phase boundaries in a heat conducting nonlinear elastic medium*, J. Appl. Math. Mech. (PMM), **51**, 777–784, 1987.

41. M. AFFOUF and R.E. CAFLISCH, *A numerical study of Riemann problem solutions and stability for a system of viscous conservation laws of mixed type*, SIAM J. Appl. Math., **51**, 3, 605–634, 1991.

42. H. HATTORI and K. MISCHAIKOV, *A dynamical system approach to a phase transition problem*, J. Differential Equations, **94**, 340–378, 1991.

43. R. ABEYARATNE and J.K. KNOWLES, *Kinetic relations and the propagation of phase boundaries in solids*, Arch. Rational Mech. Anal., **114**, 119–154, 1991.

44. R. ABEYARATNE and J.K. KNOWLES, *Implications of viscosity and strain-gradient effects for the kinetics of propagating phase boundaries in solids*, SIAM J. Appl. Math., **51**, 5, 1205–1211, 1991.

45. T.J. PENCE, *On the mechanical dissipation of solutions to the Riemann problem for impact involving a two-phase elastic material*, Arch. Rational Mech. Anal., **117**, 1–52, 1992.

46. P. LE FLOCH, *Propagating phase boundaries: formulation of the problem and existence via the Glimm method*, Arch. Rational Mech. and Anal., **123**, 2, 153–197, 1993.

47. L. TRUSKINOVSKY, *Transition to detonation in dynamic phase changes*, Arch. Rational Mech. and Anal., **125**, 4, 375–397, 1994.

48. R. ABEYARATNE and J.K. KNOWLES, *Dynamics of propagating phase boundaries: thermoelastic solids with heat conduction*, Arch. Rational Mech. and Anal., **126**, 203–230, 1994.

49. T. YTREHUS, *A nonlinear half-space problem in the kinetic theory of gases*, [in:] Lecture Notes in Mathematics, 1048, C. CERCIGNANI [Ed.], 221–242, Springer-Verlag, 1984.

50. Y. SONE and H. SUGIMOTO, *Strong evaporation from a plane condensed phase*, [in:] Adiabatic Waves in Liquid-Vapor Systems, G.E.A. MEIER, P.A. THOMPSON [Eds.], 293–304, Springer-Verlag, Berlin 1990.

51. Y. ONISHI, *On the macroscopic boundary conditions at the interface for a vapour-gas mixture*, [in:] Adiabatic Waves in Liquid-Vapor Systems, G.E.A. MEIER, P.A. THOMPSON [Eds.], 315–324, Springer-Verlag, Berlin 1990.

52. J. KARKHECK and G. STELL, *Kinetic mean-field theories*, J. Chem. Phys., **75**, 1475–1486, 1981.

53. J. KARKHECK and G. STELL, *Maximization of entropy, kinetic equations, and irreversible thermodynamics*, Physical Review A, **25**, 6, 3302–3326, 1982.

54. K. PIECHÓR, *Kinetic theory and thermocapillarity equations*, Arch. Mech., **46**, 6, 937–951, 1994.

55. K. PIECHÓR, *Discrete velocity models of the Enskog-Vlasov equation*, Transport Theory and Stat. Phys., **23**, 1–3, 39–74, 1994.

56. K. PIECHÓR, *A four-velocity model for van der Waals fluids*, Arch. Mech., **47**, 6, 1995.

57. R. GATIGNOL, *Theorie cinetique des gaz a repartition discrete de vitesses*, Lecture Notes in Physics, 36, Springer-Verlag, Berlin 1974.

58. T. PŁATKOWSKI and R. ILLNER, *Discrete velocity models of the Boltzmann equation: A survey on the mathematical aspects of the theory*, SIAM Review, **30**, 213–255, 1988.

59. R. MONACO and L. PREZIOSI, *Fluid dynamic applications of the discrete Boltzmann equation*, World Scientific, Singapore 1991.

60. W. FISZDON, *The structure of a plane shock wave*, [in:] Rarefied Gas Flows, Theory and Experiment, W. FISZDON [Ed.], CISM Courses and Lectures, 224, 447–524, Springer-Verlag, Berlin 1981.

61. R.E. CAFLISCH, *Navier-Stokes and Boltzmann shock profiles for model gasdynamics*, Comm. Pure and Appl. Math., **32**, 521–554, 1979.

62. N. BELLOMO, A. PALCZEWSKI and G. TOSCANI, *Mathematical topics in nonlinear kinetic theory*, World Scientific, Singapore 1988.

63. C. CERCIGNANI, R. ILLNER and M. PULVIRENTI, *The mathematical theory of dilute gases*, Springer-Verlag, New York 1994.

64. N. Bellomo, M. Lachowicz, J. Polewczak and G. Toscani, *Mathematical topics in nonlinear kinetic theory II. The Enskog equation*, World Scientific, Singapore 1991.

65. M. Lachowicz, *Asymptotic analysis of nonlinear kinetic equations: the hydrodynamic limit*, Uniwersytet Warszawski, Wydział Matematyki, Informatyki i Mechaniki, Preprint 1/94, Warsaw 1994.

66. R.E. Caflisch and G.C. Papanicolau, *The fluid-dynamical limit of a nonlinear model Boltzmann equation*, Comm. Pure and Appl. Math., **32**, 589–616, 1979.

67. Z. Xin, *The fluid-dynamic limit of the Broadwell model of the nonlinear Boltzmann equation in the presence of shocks*, Comm. Pure and Appl. Math., **44**, 679–713, 1991.

68. M. Slemrod and A.E. Tzavaras, *Self-similar fluid-dynamic limits for the Broadwell system*, Arch. Rational Math. and Anal., **122**, 353–392, 1993.

69. G.-Q. Chen and T.-P. Liu, *Zero relaxation and dissipation limits for hyperbolic conservation laws*, Comm. Pure and Appl. Math., **46**, 755–781, 1993.

70. G.-Q. Chen, C.D. Levermore and T.-P. Liu, *Hyperbolic conservation laws with stiff relaxation terms and entropy*, Comm. Pure and Appl. Math., **47**, 787–830, 1994.

POLISH ACADEMY OF SCIENCES
INSTITUTE OF FUNDAMENTAL TECHNOLOGICAL RESEARCH.

Boundary value problems for Poisson's equation in a multi-wedge – multi-layered region
Part II. General type of interfacial conditions

G. S. MISHURIS (RZESZÓW)

THE BOUNDARY VALUE problems for Poisson's equation in the plane domains represented by wedges and layers are considered. Conditions of a general form along all the interior and exterior boundaries are prescribed. The analysis is significantly simplified by incorporating the geometrical features of the layers and wedges: they present chain-like systems. The essence of the method applied consists in using the Fourier and Mellin transforms for the corresponding regions, and in combining the transformations of respective functions along the common boundaries. The problems are reduced to systems of functional or functional-difference equations, and later to systems of singular integral equations with fixed point singularities. The results, concerning the solvability of the obtained systems of the integral equations are presented. In the Appendix the formulae are also given making it possible to use directly the results obtained from this and the previous paper to solve the boundary value problems for linear partial-differential equations of divergence form in a similar domain, corresponding to physical problems for anisotropic nonhomogeneous bodies.

1. Introduction

IN THE PREVIOUS PAPER [12] we have considered the boundary value problems for Poisson's equation in the plane domains represented by wedges and layers. Linear conditions of general form have been prescribed on the exterior boundaries and all the interfaces except the one between the regions of different geometry (layers and wedges). Along these interior boundaries $\Gamma_\pm$ we assume now general interfacial conditions in the form: $\left[\mu \dfrac{\partial u}{\partial n}\right]\Big|_{\Gamma_\pm} = f_\pm$, $\left([u] - (\tau_\pm r + \tau)\mu \dfrac{\partial u}{\partial n}\right)\Big|_{\Gamma_\pm} = g_\pm$ $(\tau_\pm, \tau \geq 0)$. These relations generalize the usual "ideal" contact conditions $(\tau, \tau_\pm = 0)$ considered in the previous paper [12]. They appear, for example, if we presuppose that there are special thin intermediate regions between the layered part and the wedge parts of the domain, and which are represented in turn by a thin layer and two thin wedges. Thus in the case of Mode III problem it can be proved that $\tau = h_a/\mu_a$, $\tau_\pm = \theta_a^\pm/\mu_a^\pm$. Here μ_a, $\mu_a^\pm$ are the shear moduli and h_a, $\theta_a^\pm$ are the respective geometric parameters of these thin elastic adhesive regions (μ is a piecewise constant function prescribed for the shear modulus of the materials). Moreover, from the assumptions (the intermediate regions are thin) it follows that $\tau, \tau_\pm \ll 1$.

These general conditions can be independently considered on the particular model of a thin interconnecting adhesive surface. Then the parameters τ, $\tau_\pm$ can be interpreted as a measure of flexibility of the adhesive. The mentioned models have been discussed and investigated in details in [13]. Particularly, it is shown that when a crack terminates at the bimaterial interface prescribed

by the "nonideal" contact, the asymptotic behaviour of the stresses is different in comparison with the case of the "ideal" contact and essentially depends on the parameters $\tau_\pm$, τ. Consequently, *a priori* estimations of the solutions in the general case $(\tau_+^2 + \tau_-^2 + \tau^2 > 0)$ should be corrected. Moreover, in spite of the fact that the method of investigation is similar to that proposed in [12], all the problems can be reduced (using a common scheme) to systems of functional $(\tau = 0)$ or functional-difference $(\tau > 0)$ equations, contrary to [12], where only the systems of the functional equations appear. However, even if we deal only with the systems of functional equations $(\tau = 0)$ and reduce them (following [12]) to the systems of integral equations, then some of the systems obtained lead to ill-posed (incorrect) problems. If this takes place (for certain values of the remaining nonzero parameters $\tau_\pm$ and the exterior boundary conditions), there are two possibilities: the symbols of the corresponding singular integral operators with fixed point singularities are degenerate at infinity, or the systems of integral equations degenerate from the second kind to the first one at zero point. Hence, the respective systems are incorrect problems, in general.

Returning to the systems of the functional-difference equations $(\tau > 0)$, they cannot be uniquelly transformed, in the general case, to the systems of integral equations. The process depends essentially on the external boundary conditions, and the parameters $\tau_\pm$, τ. Nevertheless, all the systems of functional-difference equations for all values of the parameters are reduced to a similar class of systems of singular integral equations with fixed point singularities investigated in [10, 11]. In the majority of cases the systems obtained are degenerate. Taking this fact into account, other procedures to reduce the systems of the functional-difference equations to the systems of integral equations for certain cases are also proposed. For all cases of the boundary conditions under consideration and all values of the parameters $\tau_\pm$, τ characterizing the "nonideal" interfacial contact, the systems of the integral equations are investigated. So the indices of the nondegenerate operators in Banach spaces of summable functions with a weight are calculated for different parameters of the spaces. In the cases when the operators are degenerate, the theories developed in [18, 19] are used to investigate the corresponding systems, and the indices of normalized operators are calculated.

In the first section we formulate the problems. In the next one, all the problems are reduced to certain systems of functional-difference equations. In the third section, the systems obtained are transformed to systems of singular integral equations for such values of parameters for which the initial systems are of functional type only $(\tau = 0)$. The symbols of the corresponding integral operators are investigated and theorems concerning the solvability of the systems of equations are presented. Separately we consider those systems for which the corresponding integral operators are not normally solvable. In the fourth section, the general functional-difference systems $(\tau > 0)$ are reduced to systems of integral equations and the symbols of the corresponding operators are investigated for nondegenerate operators as well as in opposite cases.

So, all problems of Poisson's equations under different exterior and interior boundary conditions have been solved. In the Appendix the formulae are given which make it possible to use the results of this paper and [12] in solving the boundary value problems for linear partial-differential equations of divergence form. Such equations prescribe Mode III problems or similar physical problems (e.g. heat conduction and mass diffusion in solids, theory of consolidation and the like [16]) in anisotropic nonhomogeneous bodies.

2. Problem formulation

Let us consider the infinite domain presented in Fig. 1 consisting of a layered part $\Omega_L = \bigcup_{i=1}^{n} \Omega_i$ and two wedge parts $\Omega^+ = \bigcup_{j=1}^{l} \Omega_j^+$, $\Omega^- = \bigcup_{k=1}^{m} \Omega_k^-$.
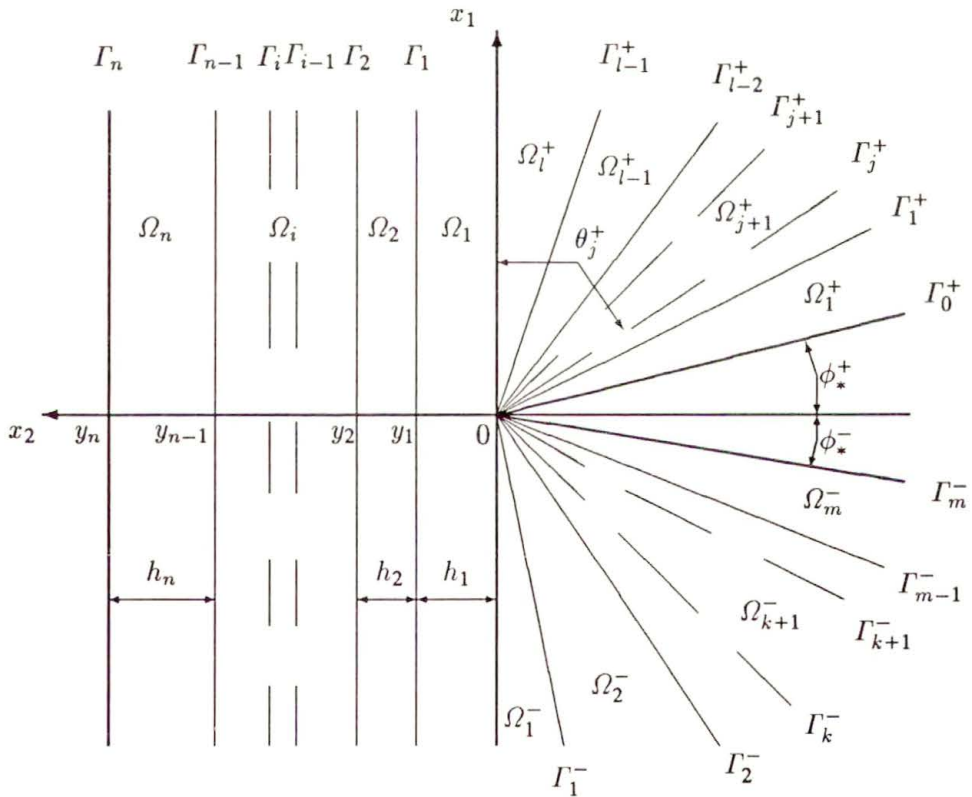

FIG. 1. Domain Ω under consideration.

By Γ_i $(i = 1, 2, ..., n-1)$ we denote interior boundaries between the regions Ω_i and Ω_{i+1}. Similarly, Γ_j^+ $(j = 1, 2, ..., l-1)$ and Γ_k^- $(k = 1, 2, ..., m-1)$ are the interior boundaries between the corresponding wedge regions. Thus, by Γ_n,

Γ_0^+ and Γ_m^- we denote the exterior boundaries of the layered region (Ω_L), or the wedges $(\Omega^\pm)$, respectively. Besides, let $\Gamma_0 = \Gamma_l^+ \cup \Gamma_0^-$ denote the interior boundary between the different parts of the domain Ω.

We shall seek the function $u(x_1, x_2)$ which satisfies Poisson's equation (2.1) inside the corresponding regions Ω_i, Ω_j^+, Ω_k^-:

$$(2.1) \qquad \begin{aligned} -\mu_i\,\Delta u_i &= W_i\,, & (x_1, x_2) &\in \Omega_i\,, \\ -\mu_j^+\,\Delta u_j^+ &= W_j^+\,, & (r, \theta) &\in \Omega_j^+\,, \\ -\mu_k^-\,\Delta u_k^- &= W_k^-\,, & (r, \theta) &\in \Omega_k^-\,, \end{aligned}$$

with certain positive constants μ_i, μ_j^+, μ_k^-.

Along the interior boundaries of the layered domain Ω_L the conditions hold:

$$(2.2) \qquad \begin{aligned} \left(u_{i+1} - u_i - \mu_i\tau_i\frac{\partial}{\partial x_2}u_i\right)\bigg|_{\Gamma_i} &= \delta u_i(x_1), & x_1 &\in \mathbb{R}, \\ \frac{\partial}{\partial x_2}\left(\mu_{i+1}u_{i+1} - \mu_i u_i\right)\bigg|_{\Gamma_i} &= \delta q_i(x_1), & x_1 &\in \mathbb{R}, & i = 1, 2, ..., n-1. \end{aligned}$$

Analogous relations for the interior boundaries of wedged domains $\Omega^\pm$ are given in the form:

$$(2.3) \qquad \begin{aligned} \left(u_{j+1}^+ - u_j^+ - \mu_j^+\tau_j^+\frac{\partial}{\partial\theta}u_j^+\right)\bigg|_{\Gamma_j^+} &= \delta u_j^+(r), & r &\in \mathbb{R}_+, \\ \frac{1}{r}\frac{\partial}{\partial\theta}\left(\mu_{j+1}^+u_{j+1}^+ - \mu_j^+u_j^+\right)\bigg|_{\Gamma_j^+} &= \delta q_j^+(r), & r &\in \mathbb{R}_+, & j = 1, 2, ..., l-1; \end{aligned}$$

$$(2.4) \qquad \begin{aligned} \left(u_{k+1}^- - u_k^- - \mu_k^-\tau_k^-\frac{\partial}{\partial\theta}u_k^-\right)\bigg|_{\Gamma_k^-} &= \delta u_k^-(r), & r &\in \mathbb{R}_+, \\ \frac{1}{r}\frac{\partial}{\partial\theta}\left(\mu_{k+1}^-u_{k+1}^- - \mu_k^-u_k^-\right)\bigg|_{\Gamma_k^-} &= \delta q_k^-(r), & r &\in \mathbb{R}_+, & k = 1, 2, ..., m-1, \end{aligned}$$

where τ_i, τ_j^+, $\tau_k^- \geq 0$ are certain constants.

Finally, the last of the interior conditions between the regions of different geometry (along the boundaries Γ_l^+, Γ_0^-) are of the general form:

$$(2.5) \qquad \begin{aligned} \left(u_1 - u_l^+ - \mu_1\tau\frac{\partial}{\partial x_2}u_1 - \mu_l^+\tau_+\frac{\partial}{\partial\theta}u_l^+\right)\bigg|_{\Gamma_l^+} &= \delta u^+(x_1), \\ \frac{\partial}{\partial x_2}\left(\mu_1 u_1 - \mu_l^+ u_l^+\right)\bigg|_{\Gamma_l^+} &= \delta q^+(x_1), & x_1 &> 0; \end{aligned}$$

$$(2.6) \qquad \begin{aligned} \left(u_1 - u_1^- - \mu_1\tau\frac{\partial}{\partial x_2}u_1 + \mu_1^-\tau_-\frac{\partial}{\partial\theta}u_1^-\right)\bigg|_{\Gamma_0^-} &= \delta u^-(x_1), \\ \frac{\partial}{\partial x_2}\left(\mu_1 u_1 - \mu_1^- u_1^-\right)\bigg|_{\Gamma_0^-} &= \delta q^-(x_1), & x_1 &< 0, \end{aligned}$$

with the constants τ, $\tau_\pm \geq 0$.

Now we define the exterior boundary conditions for the domain Ω. So, on the wedge boundaries Γ_0^+, Γ_m^-, one of the following relations holds:

(2.7)

(a) $\qquad u_1^+|_{\Gamma_0^+} = \delta u_0^+(r), \qquad r \in \mathbb{R}_+,$

(b) $\qquad \mu_1^+ \dfrac{1}{r} \dfrac{\partial}{\partial \theta} u_1^+|_{\Gamma_0^+} = \delta q_0^+(r), \qquad r \in \mathbb{R}_+,$

(2.8)

(a) $\qquad u_m^-|_{\Gamma_m^-} = -\delta u_m^-(r), \qquad r \in \mathbb{R}_+,$

(b) $\qquad \mu_m^- \dfrac{1}{r} \dfrac{\partial}{\partial \theta} u_m^-|_{\Gamma_m^-} = -\delta q_m^-(r), \qquad r \in \mathbb{R}_+.$

On the exterior boundary Γ_n we shall consider conditions (a), (b) analogous to (2.7), (2.8) and the relation (c):

(2.9)

(a) $\qquad u_n|_{\Gamma_n} = -\delta u_n(x_1), \qquad x_1 \in \mathbb{R},$

(b) $\qquad \mu_n \dfrac{\partial}{\partial x_2} u_n|_{\Gamma_n} = -\delta q_n(x_1), \qquad x_1 \in \mathbb{R},$

(c) $\qquad \lim\limits_{x_2 \to \infty} u_{n+1} = 0.$

In the case (c) we assume that the last region Ω_{n+1} is a half-plane. Then the condition $(2.9)_a$ means that the solution of the problem tends to zero both at $x_2 \to \infty$ and $x_1 \to \infty$. Consequently, we have here nine different combinations of exterior conditions. The corresponding problems $(2.1) - (2.6)$ with the boundary conditions $(2.7) - (2.9)$ are denoted by $(\mathcal{J}^+, \mathcal{J}^-, \mathcal{J})$, where $(\mathcal{J}^+ = 1, 2; \mathcal{J}^- = 1, 2; \mathcal{J} = 1, 2, 3)$. Here the value of $\mathcal{J}^+$ is 1 (or 2) if the condition $(2.7)_a$ (or $(2.7)_b$) holds. In an analogous way, one can define the values of $\mathcal{J}^-$, $\mathcal{J}$ from the conditions (2.8) and (2.9), respectively.

We assume that all known functions which appear in the equations and the boundary conditions are sufficiently smooth and their behaviour near zero and infinity points is specifically defined (for details see (1.10) in [12]). In the opposite case (when the defined functions are not smooth and have some singularities), it is easy to find special solutions of the problems accounting for these singularities. Then due to the linearity of the problems, the solution of the initial problem can be represented as a sum of the solutions.

We shall seek the regular solutions of the problems $(\mathcal{J}^+, \mathcal{J}^-, \mathcal{J})$ in the class of functions $\mathbf{LW}(\Omega)$ such that $u \in \mathbf{LW}(\Omega)$ if the following relations are true:

$(2.10)_1 \qquad u|_G \in \mathbf{C}^2(G);$

$(2.10)_2 \qquad \begin{cases} u(x_1, x_2) = O(r^{-\gamma_1}), \\ r\mathbf{grad}\, u(r) = O(r^{-\gamma_2}), \qquad (x_1, x_2) \in G, \quad r = \sqrt{x_1^2 + x_2^2} \to \infty; \end{cases}$

$$(2.10)_3 \qquad \begin{cases} u(x_1, x_2) = u_* + O(r^{\gamma_0} \ln^k r), & (x_1, x_2) \in \Omega_L, \\ u(x_1, x_2) = v_\pm + O(r^{\gamma_0}), & (x_1, x_2) \in \Omega^\pm, \quad r \to 0. \end{cases}$$

Here G denotes all regions of Ω, and $\gamma_0, \gamma_1, \gamma_2$ $(0 < \gamma_0 \le 1; \gamma_1, \gamma_2 > 0)$, $k + 1 \in \mathbb{N}$ are certain constants which will be found by solving the problem. Besides, in the cases of the first type boundary condition, at least on one exterior boundary of the wedge $(\mathcal{J}^+ \mathcal{J}^- < 4)$, additional relation corresponding to the respective notch surface holds:

$$(2.11) \qquad v_\pm(\mathcal{J}^+, \mathcal{J}^-, \mathcal{J}) = 0 \qquad (\mathcal{J}^\pm = 1).$$

It has been shown in [12] for the case of the "ideal" contact conditions along the interfacial boundary Γ_0 $(\tau, \tau_\pm = 0)$ that $v_\pm = u_*$, $k = 0$. In spite of the fact that the values of parameters $\gamma_0, \gamma_1, \gamma_2$ are different for the "ideal" contact and the "nonideal" one, they are positive. Therefore, all problems $(2.1)-(2.9)$ in the class $\mathbf{LW}(\Omega)$ have unique solutions, because functions of that class belong to "energetic spaces" ([14]) of the respective boundary value problems. The fact that $v_\pm = 0$ in the same problems follows from the corresponding boundary conditions and from the properties of the functions belonging to $\mathbf{LW}(\Omega)$.

3. Reduction of the problems to systems of functional-difference equations

Applying the Fourier and Mellin transforms to the Poisson's equation (2.1) and to the exterior and interior boundary conditions $(2.2)-(2.9)$ in each respective composite domains Ω_L, $\Omega^\pm$, and using the sweep method [7], we obtain the following relations between the transformations of unknown functions and their derivatives along the boundary Γ_0 (see Eqs. (A.22), (A.45), (A.46) in Appendix A [12]):

$$(3.1) \qquad \mathbf{u}_b^1(\lambda) = M_p(\lambda)\mathbf{p}_b^1(\lambda) + m_p^+(\lambda) + m_p^-(\lambda),$$

$$(3.2) \qquad \mathbf{v}_t^l(s) = M_q(s)\mathbf{q}_t^l(s) + m_q(s),$$

$$(3.3) \qquad \mathbf{w}_b^1(s) = M_r(s)\mathbf{r}_b^1(s) + m_r(s),$$

where

$$\mathbf{u}_b^1(\lambda) = \overline{u}_1|_{\Gamma_0}, \qquad \mathbf{v}_t^l(s) = \widetilde{u}_l^+|_{\Gamma_l^+}, \qquad \mathbf{w}_b^1(s) = \widetilde{u}_1^-|_{\Gamma_0^-},$$

$$\mathbf{p}_b^1(\lambda) = \mu_1 \frac{\partial}{\partial x_2}\overline{u}_1|_{\Gamma_0}, \qquad \mathbf{q}_t^l(s) = \mu_l^+ \frac{\partial}{\partial \theta}\widetilde{u}_l^+|_{\Gamma_l^+}, \qquad \mathbf{r}_b^1(s) = \mu_1^- \frac{\partial}{\partial \theta}\widetilde{u}_1^-|_{\Gamma_0^-}.$$

Here, the Fourier transformation $\overline{f}(\lambda)$ and Mellin transformation $\widetilde{f}(s)$ of a function f are defined in the usual way (see (A.2), (A.28) [12]). Functions M_p, $m_p^\pm$, M_q, m_q, M_r, m_r are obtained in [12] (Appendix A (A.23), (A.47)). Their behaviour depends essentially on the exterior boundary conditions $(2.7)-(2.9)$ (see Lemma A1, Lemma A2 of the mentioned paper).

Define the unknown odd and even functions z_-, z_+ by the relation:

$$(3.4) \qquad z_+(x_1) + z_-(x_1) = \mu_1 \frac{\partial}{\partial x_2} u_1|_{r_0};$$

then, applying the line of reasoning used in Sec. 2 [12], the remaining contact conditions (2.5), (2.6) can be reduced to the following systems of functional-difference equations:

$$(3.5) \qquad \hat{\mathbf{Y}}(s) - \mu_1 \tau \hat{\mathbf{Z}}(s-1) = \Phi(s)\hat{\mathbf{Z}}(s) + F(s), \qquad \max\{0, 1-\gamma_0\} < \Re s < \gamma_\infty,$$

where we introduce the symbols: $\hat{u}(s) = \tilde{u}(-s)$, $d_*(s) = z_*^+ \pi \Gamma(s)$, $\gamma_\infty = \min\{1, \gamma_1, \gamma_2\}$,

$$\mathbf{Y}(\lambda) = \mu_1 \lambda M_p \mathbf{Z}(\lambda) + H_Z(\lambda), \qquad \mathbf{Z}(\lambda) = \begin{bmatrix} \bar{z}_+^*(\lambda) \\ i\bar{z}_-(\lambda) \end{bmatrix},$$

$$H_Z(\lambda) = \mu_1 \lambda \begin{pmatrix} \dfrac{M_p z_*^+}{1+\lambda^2} + m_p^+ \\ i m_p^- \end{pmatrix},$$

$$F(s) = F(s, t_+, t_-, \tau) = \frac{\mu_1}{\Gamma(s)\sin \pi s} \begin{pmatrix} (d_+(s) + [sM_+ + st_- + \tau]d_*(s))\sin\dfrac{\pi s}{2} \\ (d_-(s) - s[M_- + t_+]d_*(s))\cos\dfrac{\pi s}{2} \end{pmatrix},$$

$$\Phi(s) = \Phi(s, t_+, t_-) = \mu_1 \begin{pmatrix} -s[M_-(s) + t_+]\mathrm{tg}\dfrac{\pi s}{2} & -s[M_+(s) + t_-] \\ s[M_+(s) + t_-] & s[M_-(s) + t_+]\mathrm{ctg}\dfrac{\pi s}{2} \end{pmatrix},$$

$$\bar{z}_+^*(\lambda) = \bar{z}_+(\lambda) - z_*^+(1 + \lambda^2)^{-1}, \qquad z_+^*(x_1) = z_+(x_1) - z_*^+ \pi \exp(-|x_1|),$$

$$2M_\pm(s) = M_q(s) \pm M_r(s), \qquad 2t_\pm = \tau^+ \pm \tau^-,$$

$$2d_\pm(s) = [M_r - \tau^-]\widetilde{\delta q}^-(s+1) \mp [M_q + \tau^+]\widetilde{\delta q}^+(s+1)$$
$$+ m_r \pm m_q + \widetilde{\delta u}^-(s) \pm \widetilde{\delta u}^+(s).$$

The unknown constant $z_*^+ = \bar{z}_+(0)$ for some types of the boundary conditions can be defined from *a priori* estimates (see (A.24), (A.49) [12]):

$$(3.6) \qquad z_*^+ = \begin{cases} \dfrac{1}{2\pi}\Xi_W, & \mathcal{J}^+ = \mathcal{J}^- = 2, \quad \mathcal{J} = 1,2,3, \\ -\Xi_L, & \mathcal{J} = 2,3, \quad \mathcal{J}^\pm = 1,2, \\ \text{unknown}, & \text{for remaining problems.} \end{cases}$$

Here $2\pi\Xi_L$, $\Xi_W = \Xi_W^+ + \Xi_W^-$ are the resultant vectors of all the exterior forces in the respective regions Ω_L, $\Omega^\pm$, and are defined in Lemma A1, Lemma A2 [12]. Besides, an additional condition should be satisfied

$$(3.7) \qquad 2\pi\Xi_L + \Xi_W = 0$$

for the solvability of the problems $(\mathcal{J}, \mathcal{J}^+, \mathcal{J}^-)$, $\mathcal{J}^\pm = 2$; $\mathcal{J} = 2, 3$ (see Remark A1 [12]). But, for the remaining problems $(1,1,1)$ and $(1,2,1)$ the value of z_*^+ can not be calculated from *a priori* estimates and will be obtained by solving the problems.

A priori estimates (A24) [12] following from the properties of the functions from the class $\mathbf{LW}(\Omega)$ lead to the result that the vector-functions $\hat{\mathbf{Y}}(s)$, $\hat{\mathbf{Z}}(s)$ are analytic in the strips $-\gamma_0 < \Re s < \gamma_1$ and $-\gamma_0 < \Re s < \gamma_2$, respectively. Using Lemma A1 and Eq. (2.17) from [12] it can be seen that

$$(3.8) \qquad \mathbf{Y}(\lambda) + \mathbf{Z}(\lambda) = O(\lambda^{-2}), \qquad \lambda \to \infty.$$

Taking this fact into account, we rewrite the systems of functional-difference equations (3.5) inside the strip $\max\{0, 1 - \gamma_0\} < \Re s < \gamma_\infty$, in the form:

$$(3.9) \qquad [\hat{\mathbf{Y}} + \hat{\mathbf{Z}}](s) = \mu_1 \tau \hat{\mathbf{Z}}(s - 1) + \mathbf{\Phi}_*(s)\hat{\mathbf{Z}}(s) + F(s), \qquad \mathbf{\Phi}_*(s) = \mathbf{I} + \mathbf{\Phi}(s);$$

then the left-hand side of (3.9) is an analytic vector-function in the strip $-2 < \Re s < \gamma_\infty$, which is wider than the analyticity strips of $\hat{\mathbf{Y}}(s)$, $\hat{\mathbf{Z}}(s)$.

These systems for the case $\tau, \tau_\pm = 0$ have been investigated in [12]. Note that in the general case $\tau, \tau_\pm > 0$ not only there exists the term with the shifted argument, but the behaviour of the matrix-functions $\mathbf{\Phi}_*(s)$ (depending on the values of $\tau_\pm$) is different from that in [12].

4. Analysis of the system of equations (3.9) in the case $\tau = 0$, $t_+ > 0$

First of all let us note, that the system of Eqs. (3.9) in this case is not a difference system, but a functional system only:

$$(4.1) \qquad [\hat{\mathbf{Y}} + \hat{\mathbf{Z}}](s) = \mathbf{\Phi}_*(s)\hat{\mathbf{Z}}(s) + F(s), \qquad 0 < \Re s < \gamma_\infty.$$

We need the following Lemma generalizing the corresponding one from [12]:

LEMMA. For each problem $(\mathcal{J}^+, \mathcal{J}^-, \mathcal{J})$ there exists $\nu_\infty = \nu_\infty(\mathcal{J}^+, \mathcal{J}^-)$ $(0 < \nu_\infty < 1)$ such that a matrix-function $\mathbf{\Phi}_*^{-1}(s)$ inverse to $\mathbf{\Phi}_*$ is analytic in region $|\Re s| < \nu_\infty(\mathcal{J}^+, \mathcal{J}^-)$, and satisfies the estimates:

1.

$$\mathbf{\Phi}_*^{-1}(s) = \begin{cases} \chi_+\mathbf{I} + \chi_-\mathbf{E}\,\mathrm{tg}(\pi s/2), & t_- = t_+ = 0, \\ (2\varpi_\pm)^{-1}[\mathbf{I} \mp \mathbf{E}\,\mathrm{tg}(\pi s/2)], & t_- = \mp t_+, \quad t_+ > 0, \\ \mathbf{T}(s), & t_+^2 \neq t_-^2, \quad t_+ > 0, \end{cases} \Bigg\} + \mathbf{\Phi}_{**}(s);$$

$$\mathbf{\Phi}_{**}(s) = \begin{cases} O(e^{-\varepsilon|\Im s|}), & t_- = t_+ = 0, \\ O(|\Im s|^{-1}), & t_- = \mp t_+, \quad t_+ > 0, \\ O(|\Im s|^{-2}), & t_+^2 \neq t_-^2, \quad t_+ > 0, \end{cases} \Bigg\}, \qquad |\Im s| \to \infty;$$

$$\det \Phi_*^{-1}(s) = \begin{cases} O(1), & t_- = t_+ = 0, \\ O(|\Im s|^{-1}), & t_- = \mp t_+, \quad t_+ > 0, \\ O(|\Im s|^{-2}), & t_+^2 \neq t_-^2, \quad t_+ > 0, \end{cases} \qquad |\Im s| \to \infty;$$

for all problems $(\mathcal{J}^+, \mathcal{J}^-, \mathcal{J})$, $\mathcal{J}^\pm = 1, 2$; $\mathcal{J} = 1, 2, 3$;

2.

$$\Phi_*^{-1}(s) = \begin{cases} \mathbf{A}_1 + a_1 s \mathbf{E}, & \mathcal{J}^\pm = 1, \quad \mathcal{J} = 1, 2, 3, \\ \mathbf{A}_2 + a_2 s \mathbf{E}, & \mathcal{J}^+ \mathcal{J}^- > 1, \quad \mathcal{J} = 1, 2, 3, \end{cases} + O(s^2), \qquad s \to 0;$$

$$\det \Phi_*^{-1}(s) = \begin{cases} b_1, & \mathcal{J}^\pm = 1, \quad \mathcal{J} = 1, 2, 3, \\ 0, & \mathcal{J}^+ \mathcal{J}^- > 1, \quad \mathcal{J} = 1, 2, 3, \end{cases} + O(s^2), \qquad s \to 0.$$

Here the constants and the matrices are calculated by the relations:

$$\chi_\pm = \frac{\varpi_- \pm \varpi_+}{\varpi_-^2 + \varpi_+^2}, \qquad b_1 = \frac{\pi}{\pi + \mu_1(\eta_+ + \eta_- + 2t_+)},$$

$$a_1 = \frac{\mu_1 b_1}{2}(\eta_+ - \eta_- + 2t_-), \qquad b_2 = \frac{c_+ + c_-}{c_+ + c_- + \pi \mu_1 c_- c_+},$$

$$a_2 = \frac{\pi}{2} \frac{c_+ - c_-}{c_+ + c_-} b_2, \qquad \varpi_- = 1 + \frac{\mu_1}{\mu_1^-}, \qquad \varpi_+ = 1 + \frac{\mu_1}{\mu_1^+},$$

$$c_+ = (\mathcal{J}^+ - 1)\zeta_l^+, \qquad c_- = (\mathcal{J}^- - 1)\zeta_1^-, \qquad \varepsilon = \min\{\phi_l^+, \phi_1^-\},$$

$$\mathbf{T}(s) = \frac{1}{s \mu_1 (t_-^2 - t_+^2)} \begin{pmatrix} -t_+ \mathrm{tg}(\pi s/2) & t_- \\ -t_- & -t_+ \mathrm{tg}(\pi s/2) \end{pmatrix},$$

$$\mathbf{E} = \begin{pmatrix} 0 & 1 \\ -1 & 0 \end{pmatrix}, \qquad \mathbf{A}_1 = \begin{pmatrix} 1 & 0 \\ 0 & b_1 \end{pmatrix}, \qquad \mathbf{A}_2 = \begin{pmatrix} b_2 & 0 \\ 0 & 0 \end{pmatrix},$$

but the values of constants ζ_l^+, ζ_1^-, η_+, η_- are defined in Lemma A2 from [12].

As one can see, the behaviour of the matrix-function $\Phi_*^{-1}(s)$ at infinity depends on the type of the interfacial contact conditions (on the values of the parameters t_+, t_-). The corresponding three cases (see 1) we shall denote by the upper index $j = 1, 2, 3$. However, the behaviour near the zero point depends on the conditions along the boundaries of the exterior wedges (on the values of the parameters $\mathcal{J}^\pm$). The respective two cases (see 2) we shall denote by the lower index $k = 1, 2$.

REMARK 1. Let us note that the function $\det \Phi_*(s)$ has in the strip $(0 < \Re s < 1)$ one zero in the first case of Lemma ($t_+ = t_- = 0$) only, and this zero is real (see [12]). In the remaining cases ($t_+ > 0$) the determinant has two zeros with different real parts in this strip. It means that the gradient of the solution of the corresponding boundary value problem will have two singularity terms near the wedge tip.

REMARK 2. When all geometrical and mechanical parameters of the boundary value problem are symmetrical with respect to the OX_2-axis (see Corollary A2 [12]), the systems of the equations (3.9), (4.1) split into two independent equations, because the matrix-function $\Phi_*(s)$ is diagonal in such situations. Then one can conclude that $\nu_\infty(\mathcal{J}^+, \mathcal{J}^+) = \min\{\omega_\infty(1, \mathcal{J}^+), \omega_\infty(2, \mathcal{J}^+)\}$, where $\omega_\infty(1, \mathcal{J}^+)$, $\omega_\infty(2, \mathcal{J}^+)$ are zeros of the corresponding diagonal elements of the matrix-function $\Phi_*(s)$.

Typical graphs of the function $\det \Phi_*(s)$ in the interval $(0,1)$ for the problems $(2, 2, \mathcal{J})$ ($\mathcal{J} = 1, 2, 3$) when the wedge regions $\Omega^\pm$ are represented by two symmetrical wedges with angles $\pi/2$, and the mechanical parameters are symmetrical also with respect to OX_2-axis ($\mu_1^+ = \mu_1^-$, $\tau^+ = \tau^-$), are presented in the Fig. 2 a, b.
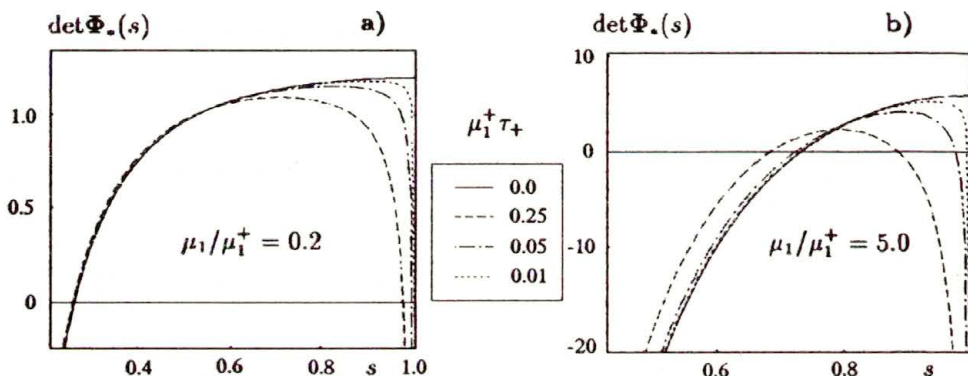
FIG. 2. Graphs of the function $\det \Phi_*(s)$ in the interval $(0,1)$ in the case $\mu_1^+ = \mu_1^-$, $\tau_+ = \tau_-$.

Here continuous lines correspond to the "ideal" ($\tau_\pm = 0$) contact, but dashed and dotted lines correspond to "non-ideal" contact with respective values of dimensionless parameter $\mu_1^+ \tau_+ = 0.01, 0.05, 0.25$.

Let us note that the values of the first zero $\nu_\infty(2, 2)$ for small magnitudes of $\mu_1^+ \tau_+ < 0.1$ differ but little from the values of the unique zero for the "ideal" contact condition ($\tau_+ = 0$). Numerical results for the values of the mentioned two zeros of the function $\Phi_*(s)$, for certain geometry and exterior boundary conditions, are presented in [13].

Taking into account the results of the Lemma, we can rewrite the systems of the functional equations (4.1) in an equivalent form:

$$(4.2) \qquad \Phi_*^{-1}(s)\left[\hat{Y} + \hat{Z}\right](s) - \Phi_*^{-1}(s)F(s) = \hat{Z}(s), \qquad 0 < \Re s < \min\{\nu_\infty, \gamma_\infty\}.$$

Note that the vector-functions $\Phi_*^{-1}(s)[\hat{Y} + \hat{Z}](s)$ and $\hat{Z}(s)$ are analytic in the strip $-\min\{\nu_\infty, \gamma_0\} < \Re s < \min\{\gamma_\infty, \nu_\infty\}$, at least. However, the vector-function $\Phi_*^{-1}(s)F(s)$ can have, in general, a pole at the point $s = 0$. By investigating the

behaviour of the vector-function $F(s)$ near the zero point in a similar way as in [12] (we do not present the respective results in this paper) it can be shown that the vector-function $\Phi_*^{-1}(s)F(s)$ is analytic in the strip $-\nu_\infty < \Re s < \nu_\infty$ for the value of the parameter z_*^+ defined in (3.6). Besides, $\Phi_*^{-1}(s)F(s)$ has also no pole in this strip in the problems for which this parameter can not be known from (3.6). Finally, this vector-function tends to zero in the strip along any line parallel to the imaginary axis for all the considered problems.

Further, it is evident that the first pole of the vector-function $\hat{Z}(s)$ which is the nearest to the imaginary axis in half-plane $\Re s < 0$ coincides with the corresponding pole of the vector-functions $\Phi_*^{-1}(s)[\hat{Y} + \hat{Z}](s)$, $\Phi_*^{-1}(s)F(s)$, hence:

$$(4.3) \qquad \gamma_0 = \nu_\infty(\mathcal{J}^+, \mathcal{J}^-).$$

The other parameters from the definition of the class $\mathbf{LW}(\Omega)$ can be also found,

$$(4.4) \qquad v_\pm = u_*,$$

$$u_* = \frac{2}{\mu_1} \int_0^\infty \mathbf{y}_1(\lambda)\frac{d\lambda}{\lambda} \equiv 2 \int_0^\infty \left[M_p(\lambda)\mathbf{z}_1(\lambda) + (\mu_1\lambda)^{-1}h_Z^{(1)}(\lambda) \right] d\lambda,$$

where $\mathbf{y}_1$, $\mathbf{z}_1$, $h_Z^{(1)}$ are the first components of the vector-functions $\mathbf{Y}$, $\mathbf{Z}$, H_Z (see (3.5)).

4.1. Reduction of the systems of functional equations to systems of integral equations

Let us recall that the system (4.1) under the first assumptions $t_+ = 0$ ($\tau^\pm = 0$) has been investigated in [12]. For the cases $t_+ > 0$ these systems can be also reduced to systems of singular integral equations, taking into account the behaviour of the matrix-functions $\Phi_*^{-1}(s)$ at the infinity point.

Thus, in the case $t_- = \mp t_+$, $t_+ > 0$ ($j = 2$ see Lemma), system (4.2) is written in the form:

$$\Phi_{**}(s)\left[\hat{Y} + \hat{Z}\right](s) + \left[\frac{1}{2\varpi_\pm}\hat{Y} + \left(\frac{1}{2\varpi_\pm} - 1\right)\hat{Z}\right](s)$$
$$\mp \frac{1}{2\varpi_\pm}\,\mathrm{tg}\,\frac{\pi s}{2}\mathbf{E}\left[\hat{Y} + \hat{Z}\right](s) = \Phi_*^{-1}(s)F(s).$$

Then, applying the inverse Mellin transform to this system, and using a line of reasoning similar to that used in Sec. 4 [12], we obtain a system of singular integral equations:

$$(4.5) \qquad \begin{aligned} B_Z^{(2)}(\mathcal{J}^+, \mathcal{J}^-, \mathcal{J})\mathbf{Z} &= \mathbf{G}_Z^{(2)}, & \mathcal{J} = 1,3, \quad \mathcal{J}^\pm = 1,2; \\ B_Y^{(2)}(\mathcal{J}^+, \mathcal{J}^-, \mathcal{J})\mathbf{Y} &= \mathbf{G}_Y^{(2)}, & \mathcal{J} = 2,3, \quad \mathcal{J}^\pm = 1,2; \end{aligned}$$

where

$$[\mathcal{B}_{Z(Y)}^{(2)}\mathbf{u}](\lambda) = \mathbf{u}(\lambda) + \int_0^\infty K_{Z(Y)}^{(2)}(\lambda,\xi)\Psi^{(2)}(\lambda,\xi)\mathbf{u}(\xi)\,d\xi$$

$$\pm \frac{1}{\pi\varpi_\pm}\mathbf{E}\int_0^\infty K_{Z(Y)}^{(2)}(\lambda,\xi)\mathbf{u}(\xi)\frac{\lambda d\xi}{\lambda^2 - \xi^2},$$

$$K_Z^{(2)}(\lambda,\xi) = \frac{2\varpi_\pm(1 + \mu_1\xi M_p(\xi))}{\lambda\mu_1 M_p(\lambda) + 1 - 2\varpi_\pm},$$

$$K_Y^{(2)}(\lambda,\xi) = \frac{2\varpi_\pm(1 + (\mu_1\xi M_p(\xi))^{-1})}{1 + (1 - 2\varpi_\pm)(\lambda\mu_1 M_p(\lambda))^{-1}},$$

$$\mathbf{G}_Z^{(2)}(\lambda) = \frac{2\varpi_\pm}{\lambda\mu_1 M_p(\lambda) + 1 - 2\varpi_\pm}$$

$$\times \left(\frac{1}{2\pi i}\int_{-i\infty}^{i\infty}\lambda^s\mathbf{\Phi}_*^{-1}(s)F(s)\,ds - \left[\mathcal{B}_0^{(2)}H_Z\right](\lambda)\right),$$

$$\mathbf{G}_Y^{(2)}(\lambda) = \frac{2\varpi_\pm}{(1 - 2\varpi_\pm)(\lambda\mu_1 M_p(\lambda))^{-1} + 1}$$

$$\times \left(\frac{1}{2\pi i}\int_{-i\infty}^{i\infty}\lambda^s\mathbf{\Phi}_*^{-1}(s)F(s)\,ds - \left[\mathcal{B}_0^{(2)}H_Y\right](\lambda) + H_Y(\lambda)\right),$$

$$\Psi^{(2)}(\lambda,\xi) = \frac{1}{2\pi i\xi}\int_{-i\infty}^{i\infty}\mathbf{\Phi}_{**}(s)\left(\frac{\lambda}{\xi}\right)^s\,ds, \qquad H_Y(\lambda) = -\frac{1}{\mu_1\lambda M_p(\lambda)}H_Z(\lambda),$$

$$[\mathcal{B}_0^{(2)}\mathbf{u}](\lambda) = \frac{1}{2\varpi_\pm}\mathbf{u}(\lambda) + \int_0^\infty \Psi^{(2)}(\lambda,\xi)\mathbf{u}(\xi)\,d\xi \pm \frac{1}{\pi\varpi_\pm}\mathbf{E}\int_0^\infty \mathbf{u}(\xi)\frac{\lambda d\xi}{\lambda^2 - \xi^2}.$$

In the third case ($t_+^2 \neq t_-^2$, $t_+ > 0$, see Lemma) the inverse Mellin transform can be directly applied to the system (4.2). Consequently, the systems of the integral equations are found:

(4.6)
$$\mathcal{B}_Z^{(3)}(\mathcal{J}^+,\mathcal{J}^-,\mathcal{J})\mathbf{Z} = \mathbf{G}_Z^{(3)}, \qquad \mathcal{J} = 1,3, \quad \mathcal{J}^\pm = 1,2;$$
$$\mathcal{B}_Y^{(3)}(\mathcal{J}^+,\mathcal{J}^-,\mathcal{J})\mathbf{Y} = \mathbf{G}_Y^{(3)}, \qquad \mathcal{J} = 2,3, \quad \mathcal{J}^\pm = 1,2;$$

where

$$[\mathcal{B}_{Z(Y)}^{(3)}\mathbf{u}](\lambda) = f_{Z(Y)}(\lambda)\mathbf{u}(\lambda) + \int_0^\infty K_{Z(Y)}^{(3)}(\xi)\Psi^{(3)}(\lambda,\xi)\mathbf{u}(\xi)\,d\xi,$$

$$f_Z(\lambda) = 1, \qquad f_Y(\lambda) = \frac{1}{\lambda \mu_1 M_p(\lambda)},$$

$$\Psi^{(3)}(\lambda, \xi) = \frac{1}{2\pi i \xi} \int\limits_{-i\infty}^{i\infty} \Phi_*^{-1}(s) \left(\frac{\lambda}{\xi}\right)^s ds,$$

$$K_Z^{(3)}(\xi) = -(1 + \mu_1 \xi M_p(\xi)), \qquad K_Y^{(3)}(\xi) = -[1 + (\mu_1 \xi M_p(\xi))^{-1}],$$

$$\mathbf{G}_Z^{(3)}(\lambda) = -\frac{1}{2\pi i} \int\limits_{-i\infty}^{i\infty} \lambda^s \Phi_*^{-1}(s) F(s) \, ds + \int\limits_0^{i\infty} \Psi^{(3)}(\lambda, \xi) H_Z(\xi) \, d\xi,$$

$$\mathbf{G}_Y^{(3)}(\lambda) = -\frac{1}{2\pi i} \int\limits_{-i\infty}^{i\infty} \lambda^s \Phi_*^{-1}(s) F(s) \, ds + \int\limits_0^{i\infty} \Psi^{(3)}(\lambda, \xi) H_Y(\xi) \, d\xi - H_Y(\lambda).$$

Basing on the results from [2, 10, 11] it can be shown that the obtained operators $\mathcal{B}_{Z(Y)}^{(2)}(\mathcal{J}^+, \mathcal{J}^-, \mathcal{J})$, $\mathcal{B}_{Z(Y)}^{(3)}(\mathcal{J}^+, \mathcal{J}^-, \mathcal{J})$ for all of the problems $(\mathcal{J}^+, \mathcal{J}^-, \mathcal{J})$ are bounded in the spaces $\mathbf{L}_2^{p,\alpha,\beta}(\mathbb{R}_+)$ [10] with any values of the parameters $-\nu_\infty(\mathcal{J}^+, \mathcal{J}^-) < \alpha \le \beta < \nu_\infty(\mathcal{J}^+, \mathcal{J}^-)$, $1 \le p < \infty$. The right-hand sides of systems (4.5), (4.6) belong to the spaces $\mathbf{W}_{2(m)}^{p,\alpha,\beta}(\mathbb{R}_+)$ for any $m \in \mathbb{N}$. Besides, all these systems of the integral equations are of the second kind, but the operators $\mathcal{B}_Y^{(3)}(\mathcal{J}^+, \mathcal{J}^-, 2)$ are degenerate to the first kind in the point $\lambda = 0$, in view of the behaviour of the function $M_p(\lambda)$ (see Lemma A1 from [12]).

From *a priori* estimates for the solutions of class $\mathbf{LW}(\Omega)$ it follows that the inclusions should be true:

$$\mathbf{Y} \in \mathbf{W}_{2(1)}^{1,\alpha_1,\beta}(\mathbb{R}_+), \qquad \mathbf{Z} \in \mathbf{W}_{2(1)}^{1,\alpha_2,\beta}(\mathbb{R}_+), \qquad -\gamma_i < \alpha_i < 0, \quad 0 < \beta < \gamma_0.$$

Moreover, taking into account the smoothness of the kernels of the integral operators and the reasons given in Appendix B [12], it is sufficient to assume that for arbitrary $p \in [1, \infty)$:

$$(4.7) \qquad \mathbf{Y} \in \mathbf{L}_2^{p,\alpha_1,\beta}(\mathbb{R}_+), \qquad \mathbf{Z} \in \mathbf{L}_2^{p,\alpha_2,\beta}(\mathbb{R}_+), \qquad -\gamma_i < \alpha_i < 0, \quad 0 < \beta < \gamma_0.$$

Let the matrix-function $\mathbf{B}^{(j)}(\alpha - it, \mathcal{J}^+, \mathcal{J}^-, \mathcal{J})$ ($t \in \overline{\mathbb{R}}$, $j = 2, 3$, $\mathcal{J}^\pm = 1, 2$, $\mathcal{J} = 1, 2, 3$) denote the symbol of the corresponding operator $\mathcal{B}^{(j)}(\mathcal{J}^+, \mathcal{J}^-, \mathcal{J})$ in the respective space (for definition of the symbol of singular operator see, for example, [3, 18]). Then, basing on the results from [10] one can conclude that:

$$\mathbf{B}_Z^{(j)}(\alpha - it, \mathcal{J}^+, \mathcal{J}^-, 1) = \mathbf{I} - \Phi_*^{-1}(\alpha - it),$$

$$(4.8) \qquad \mathbf{B}_{Z(Y)}^{(j)}(\alpha - it, \mathcal{J}^+, \mathcal{J}^-, 3) = \mathbf{I} - \left(1 - \frac{\mu_1}{\mu_{n+1}}\right) \Phi_*^{-1}(\alpha - it),$$

$$\mathbf{B}_Y^{(2)}(\alpha - it, \mathcal{J}^+, \mathcal{J}^-, 2) = \Phi_*^{-1}(\alpha - it).$$

Taking into account the fact that formulae of symbols of the operators $B^{(2)}_{Z(Y)}$ $(\mathcal{J}^+, \mathcal{J}^-, \mathcal{J})$ and $B^{(3)}_{Z(Y)}(\mathcal{J}^+, \mathcal{J}^-, \mathcal{J})$, $(\mathcal{J} = 1, 3)$ are of similar form, we will not use the upper indices $(j = 2, 3)$ when it does not involve difficulties. Note only that the matrix-function $\Phi^{-1}_*(s)$ depends on j (on the values of $\tau_\pm$).

REMARK 3. Strictly speaking, all the operators $B(\mathcal{J}^+, \mathcal{J}^-, \mathcal{J})$ (as well as the operators from [12]) are isometrically equivalent (with the accuracy to compact operators) to some pair systems of integral equations on the axis with the kernels depending on the difference of the arguments [10]. Their symbols are represented in the forms ($t \in \overline{\mathbb{R}}$, $\theta = \pm 1$):

$$\text{Symb}\, B(\mathcal{J}^+, \mathcal{J}^-, \mathcal{J})|_{L_2^{p,\alpha,\beta}}(t, \theta) = B(\alpha - it, \mathcal{J}^+, \mathcal{J}^-, \mathcal{J})\frac{1 + \theta}{2} + I\frac{1 - \theta}{2}.$$

Hence, it is sufficient to investigate only the matrix-functions $B(\alpha - it, \mathcal{J}^+, \mathcal{J}^-, \mathcal{J})$. Thus we have denoted the symbol of the operator $B(\mathcal{J}^+, \mathcal{J}^-, \mathcal{J})$ by the corresponding matrix-function $B(\alpha - it, \mathcal{J}^+, \mathcal{J}^-, \mathcal{J})$ instead of that written above. Besides, these matrix-functions are continuous in $\mathbb{R}$, but can have a point of discontinuity at infinity. Hence, they are not the symbols, but presymbols, in general (for details see [2, 8, 18]).

Note that the operators $B^{(j)}_Z(\mathcal{J}^+, \mathcal{J}^-, 3)$ $(j = 2, 3)$ are isometrically equivalent to the operators $B^{(j)}_Y(\mathcal{J}^+, \mathcal{J}^-, 3)$ (see Remark B2 [12]). Consequently, it is sufficient to investigate only the first of them. Moreover, in the case $\mu_1 = \mu_{n+1}$ these operators are the Fredholm ones (they can be represented in the form $I + \mathcal{K}$, where $\mathcal{K}$ is a compact operator), and we will not consider such situation below.

One can see that the symbols $B^{(2)}_Y(\alpha - it, \mathcal{J}^+, \mathcal{J}^-, 2)$ of the operators $B^{(2)}_Y(\mathcal{J}^+, \mathcal{J}^-, 2)$ are degenerate at the infinity point for any values of α. Hence, these operators are not normally solvable in the considered spaces (see [18]) and the corresponding systems of integral equations are ill-posed problems [19]. The theory of such singular integral equations in classical spaces is constructed in [18].

4.2. Investigation of symbols of the nondegenerate operators

Let $\alpha = 0$, then by $\nu_0(\mathcal{J}^+, \mathcal{J}^-, \mathcal{J})$, $(\mathcal{J} = 1, 3)$ we denote the real parts of zeros of the determinants of the matrix-functions $B_Z(-it, \mathcal{J}^+, \mathcal{J}^-, \mathcal{J})$ $(\mathcal{J} = 1, 3)$, which are the nearest to the imaginary axis (inside half-plane $\Re s \geq 0$). Besides, by $\nu_*(\mathcal{J}^+, \mathcal{J}^-, \mathcal{J})$ we denote the real parts of the next zeros $(\nu_* > \nu_0)$. It can be shown that

(4.9) $0 < \nu_0(2, 2, 1)$, $\nu_0(\mathcal{J}^+, \mathcal{J}^-, 3) < 1$, $\mathcal{J}^\pm = 1, 2$,

and all zeros are real and simple. For other problems

$$\nu_0(1, 1, 1) = \nu_0(1, 2, 1) = 0,$$

and the orders of multiplicity of these real zeros are equal to two. Thus the problems with nondegenerate symbols are divided into two groups, depending on the values of the respective zeros.

First of all consider the first group (all of the problems for which $\nu_0(\mathcal{J}^+, \mathcal{J}^-, \mathcal{J})$ > 0). Denote by $\alpha_*(\mathcal{J}^+, \mathcal{J}^-, \mathcal{J}) = \min\{\nu_0(\mathcal{J}^+, \mathcal{J}^-, \mathcal{J}), \nu_\infty(\mathcal{J}^+, \mathcal{J}^-)\}$. Then it is easy to see that for all values of $|\alpha| < \alpha_*(\mathcal{J}^+, \mathcal{J}^-, \mathcal{J})$ the indices of the respective operators are equal to zero:

$$(4.10) \qquad \kappa = -\mathrm{ind}\, \mathbf{B}_{Z(Y)}(\alpha - it, \mathcal{J}^+, \mathcal{J}^-, \mathcal{J}) = 0, \qquad |\alpha| < \alpha_*(\mathcal{J}^+, \mathcal{J}^-, \mathcal{J}).$$

However, when we deal with the systems of integral equations, the partial indices κ_1, κ_2 play also an important role [4]. Using a line of reasoning similar to [12] it can be shown that the symbols of operators are definite matrix-functions [4] for these problems. Hence, we can prove the following theorem:

THEOREM 1. *Let* $1 \le p < \infty$, $m \in \mathbb{N}$, $\nu_0(\mathcal{J}^+, \mathcal{J}^-, \mathcal{J}) > 0$, $\beta < \nu_\infty(\mathcal{J}^+, \mathcal{J}^-)$, $\beta - \alpha \ge 0$, $|\alpha| < \alpha_*(\mathcal{J}^+, \mathcal{J}^-, \mathcal{J})$ *then;*

1) *the operators* $\mathcal{B}_{Z(Y)}(\mathcal{J}^+, \mathcal{J}^-, \mathcal{J})$, *in the spaces* $\mathbf{L}_2^{p,\alpha,\beta}(\mathbb{R}_+)$ *are normally solvable, and their indices and all partial (left-hand and right-hand) indices are equal to zero;*

2) *there exist the unique solutions of the corresponding systems of equations from* $\mathbf{W}_{(m),2}^{p,\alpha,\beta}(\mathbb{R}_+) \subset \mathbf{L}_2^{p,\alpha,\beta}(\mathbb{R}_+)$.

Results concerning asymptotics of the solutions near zero and infinity points, and the convergence of numerical method can be obtained analogously to those presented in [12].

Now, consider the operators for the problems (1,1,1) and (1,2,1) when $\nu_0 = 0$. In these cases the index and partial (left-hand and right-hand) indices are calculated:

$$\kappa = -\mathrm{ind}\, \mathbf{B}_{Z(Y)}(\alpha - it, 1, \mathcal{J}^-, 1) = \pm 1,$$

$$\kappa_1(1, \mathcal{J}^-, 1) = \pm 1, \qquad \kappa_2(1, \mathcal{J}^-, 1) = 0,$$

depending on the value $0 < \pm\alpha < \min\{\nu_*(\mathcal{J}^+, \mathcal{J}^-, \mathcal{J}), \nu_\infty(\mathcal{J}^+, \mathcal{J}^-)\}$. For these problems the values of z_*^+ are unknown (see (3.6)). Moreover, the right-hand sides of the systems (4.5), (4.6) can be represented in the form $\mathbf{G}_Z = \mathbf{G}_Z^1 + z_*^+\mathbf{G}_Z^2$, where the vector-functions $\mathbf{G}_Z^1$ and $\mathbf{G}_Z^2$ belong to the spaces $\mathbf{W}_{(m),2}^{p,\alpha,\beta}(\mathbb{R}_+)$. So we can prove the following theorems:

THEOREM 2. *Assume* $1 \le p < \infty$, $-\nu_* < \alpha < 0$, $\beta < \nu_\infty$, $\beta - \alpha \ge 0$, $m \in \mathbb{N}$; *then*

1) *the operators* $\mathcal{B}_Z(1,1,1)$, $\mathcal{B}_Z(1,2,1)$ *in the spaces* $\mathbf{L}_2^{p,\alpha,\beta}(\mathbb{R}_+)$ *are normally solvable with the index* $\kappa = -1$ *and the partial (left-hand and right-hand) indices* $\kappa_1 = -1$, $\kappa_2 = 0$;

2) *for these problems there exist unique values of z_*^+ for which the systems of equations* (4.5), (4.6) *have (unique) solutions* $\mathbf{Z}(\lambda)$ *in the spaces* $\mathbf{W}_{(m),2}^{p,\alpha,\beta}(\mathbb{R}_+) \subset \mathbf{L}_2^{p,\alpha,\beta}(\mathbb{R}_+)$.

Let us note that the systems of the integral equations in these cases can not be solved by applying numerical methods directly to the systems, as it has been stated in Theorem 1. To remedy this, the systems should be regularized (see [3, 9, 18]). Then the systems obtained will have unique solutions for arbitrary right-hand sides (for any values of z_*^+). Thus, solving the regularized systems for the right-hand sides corresponding to the individual vector-functions $\mathcal{G}_Z^1$ and $\mathcal{G}_Z^2$, the unique values of z_*^+ can be found from the conditions (2.11) and relations (4.4). For these values of z_*^+ the right-hand sides of the equations belong to kernels of the corresponding conjugate operators.

THEOREM 3. *Let* $1 \leq p < \infty$, $0 < \alpha < \nu_*$, $\beta < \nu_\infty$, $\beta - \alpha \geq 0$, $m \in \mathbb{N}$, *then*

1) *the operators* $\mathcal{B}_Z(1,1,1)$, $\mathcal{B}_Z(1,2,1)$ *in the spaces* $\mathbf{L}_2^{p,\alpha,\beta}(\mathbb{R}_+)$ *are normally solvable with the index* $\kappa = 1$ *and the partial (left-hand and right-hand) indices are* $\kappa_1 = 1$, $\kappa_2 = 0$;

2) *for these problems there exist unique nontrivial solutions* $\mathbf{Z}_0$ *of the homogeneous systems* (4.5), (4.6) *which belong to any spaces* $\mathbf{W}_{(m),2}^{p,\alpha,\beta}(\mathbb{R}_+)$:

$$\mathbf{Z}_0 \in \bigcap_{p,\alpha,\beta} \mathbf{W}_{(m),2}^{p,\alpha,\beta}(\mathbb{R}_+).$$

The asymptotics of the solutions from the Theorems 2–3 can be obtained analogously to [12]. Note that nontrivial solutions of homogeneous boundary value problems which can be constructed from the nontrivial solutions of the corresponding homogeneous systems of the integral equations (Theorem 3) do not belong to class $\mathbf{L}\mathbf{W}(\Omega)$. They tend to infinity (as $\ln r$) when $r \to \infty$. Such solutions play an important role in the asymptotic method theory (see [15]).

REMARK 4. For the symmetrical problem $(1,1,1)$ the operator $\mathcal{B}_Z(1,1,1)$ splits into two scalar operators (Remark 2). Then, one of them has the index which is equal to zero (see the values of partial indices) and for the corresponding singular integral equation the Theorem 1 holds also true.

4.3. Investigation of the degenerate problems

Now we consider the operators $\mathcal{B}_Y^{(2)}(\mathcal{J}^+, \mathcal{J}^-, 2)$ $(\mathcal{J}^\pm = 1, 2)$ which are not normally solvable in the spaces $\mathbf{L}_2^{p,\alpha,\beta}(\mathbb{R}_+)$ (the symbols are degenerate at infinity). They can be presented in the form:

$$\mathcal{B}_Y^{(2)}(\mathcal{J}^+, \mathcal{J}^-, 2) = \mathcal{B}_2 \mathcal{P} + \mathcal{Q} + \mathcal{K}.$$

Here $\mathcal{P}$, $\mathcal{Q}$ are complementary projectors ($\mathcal{P} + \mathcal{Q} = I$) of multiplying by the characteristic functions of the sets $(0, 1)$ and $(1, \infty)$, respectively. The operators $\mathcal{B}_2$ are isometrically equivalent to the Wiener–Hopf integral operators in the classical spaces $\mathbf{L}_2^p(\mathbb{R})$ with the symbols $\mathbf{B}_Y^{(2)}(\alpha - it, \mathcal{J}^+, \mathcal{J}^-, 2)$, but $\mathcal{K}$ are compact operators. We shall "normalize" the corresponding systems of integral equations following for the theory developed in [18]. First of all let us note, that the matrix-functions $\mathbf{B}_Y^{(2)}(\alpha - it, \mathcal{J}^+, \mathcal{J}^-, 2)$ can be represented depending on the value $t_- = \mp t_+$ (see Lemma) in the following manner:

$$\mathbf{B}_Y^{(2)}(\alpha - it, \mathcal{J}^+, \mathcal{J}^-, 2) = \mathbf{A}_2(t) \begin{pmatrix} (t+i)^{-1} & 0 \\ 0 & 1 \end{pmatrix} \begin{pmatrix} 1 & 0 \\ \pm i & 1 \end{pmatrix},$$

where the matrix-functions $\mathbf{A}_2(t)$ are not degenerate at infinity.

Let us consider the operators:

$$(4.11) \qquad \mathcal{D} = \begin{pmatrix} \mathcal{D}_1 \mathcal{P} + \mathcal{Q} & 0 \\ \pm i \mathcal{P} & I \end{pmatrix}, \qquad \mathcal{G} = \begin{pmatrix} \mathcal{P} \mathcal{G}_1 \mathcal{P} + \mathcal{Q} & 0 \\ \mp i \mathcal{P} \mathcal{G}_1 \mathcal{P} & I \end{pmatrix},$$

in the spaces $\mathbf{L}_2^{p,\alpha,\beta}(\mathbb{R}_+)$, where the scalar operators $\mathcal{D}_1$, $\mathcal{G}_1$ are of the form

$$[\mathcal{D}_1 u](\lambda) = i \int\limits_0^\lambda \frac{\varrho_{\alpha-2,\beta-2}(\xi)}{\varrho_{\alpha-1,\beta-1}(\lambda)} u(\xi)\, d\xi, \qquad [\mathcal{G}_1 u](\lambda) = i \left[[1 - \varrho_{\alpha,\beta}^*(\lambda)] u(\lambda) - \lambda u'(\lambda) \right].$$

By u' we denote the distributional derivative of a function $u \in \mathbf{L}^{p,\alpha,\beta}(\mathbb{R}_+)$, but functions connected with the weight of the spaces are defined as follows:

$$(4.12) \qquad \begin{aligned} \varrho_{\alpha,\beta}(\lambda) &= \begin{cases} \lambda^\alpha, & 0 < \lambda < 1, \\ \lambda^\beta, & 1 < \lambda < \infty; \end{cases} \\ \varrho_{\alpha,\beta}^*(\lambda) &= \frac{\lambda \varrho_{\alpha,\beta}'(\lambda)}{\varrho_{\alpha,\beta}(\lambda)} = \begin{cases} \alpha, & 0 < \lambda < 1, \\ \beta, & 1 < \lambda < \infty. \end{cases} \end{aligned}$$

Introduce spaces $\widetilde{\mathbf{L}}_2^{p,\alpha,\beta}(\mathbb{R}_+) = \mathcal{G}\left(\mathbf{L}_2^{p,\alpha,\beta}(\mathbb{R}_+)\right)$, $\mathbf{L}_2^{p,\alpha,\beta}(\mathbb{R}_+) \subset \widetilde{\mathbf{L}}_2^{p,\alpha,\beta}(\mathbb{R}_+)$. One can directly verify that the relations are true: $\mathcal{G}\mathcal{D} = I$, $\mathcal{D}\mathcal{G} = I$, and the spaces $\widetilde{\mathbf{L}}_2^{p,\alpha,\beta}(\mathbb{R}_+)$ with the norm:

$$\|u\|_{\widetilde{\mathbf{L}}_2^{p,\alpha,\beta}} = \|\mathcal{D}u\|_{\mathbf{L}_2^{p,\alpha,\beta}},$$

become the Banach spaces.

Represent the initial operators $\mathcal{B}_Y^{(2)}(\mathcal{J}^+, \mathcal{J}^-, 2)$ from $\widetilde{\mathbf{L}}_2^{p,\alpha,\beta}(\mathbb{R}_+)$ to $\mathbf{L}_2^{p,\alpha,\beta}(\mathbb{R}_+)$ in the form:

$$\mathcal{B}_Y^{(2)}(\mathcal{J}^+, \mathcal{J}^-, 2) = \overline{\mathcal{B}}_Y^{(2)}(\mathcal{J}^+, \mathcal{J}^-, 2)\mathcal{D}, \qquad \overline{\mathcal{B}}_Y^{(2)}(\mathcal{J}^+, \mathcal{J}^-, 2) = \mathcal{A}_2\mathcal{P} + \mathcal{Q} + \mathcal{K}_*.$$

Here the operators $\mathcal{A}_2 = \mathcal{A}_2(\mathcal{J}^+, \mathcal{J}^-, 2)$ are isometrically equivalent to the Wiener–Hopf operators with the symbols $\mathbf{A}_2(t)$. Besides, we can prove that the operators $\mathcal{K}_*\colon \mathbf{L}_2^{p,\alpha,\beta}(\mathbb{R}_+) \to \mathbf{L}_2^{p,\alpha,\beta}(\mathbb{R}_+)$ are also compact. By investigating the symbols of the operators $\overline{\mathcal{B}}_Y^{(2)}(\mathcal{J}^+, \mathcal{J}^-, 2)$ it is found that they are normally solvable in the spaces $\mathbf{L}_2^{p,\alpha,\beta}(\mathbb{R}_+)$ with the indices $\kappa(\mathcal{J}^+, \mathcal{J}^-, 2)$ and partial indices κ_1, κ_2:

$$\kappa(1,1,2) = 0, \qquad \kappa_1 = \kappa_2 = 0; \qquad 0 < |\alpha| < \min\{\nu_0(1,1,2), \nu_\infty(1,1)\};$$

$$\kappa(\mathcal{J}^+, \mathcal{J}^-, 2) = \pm 1, \quad \kappa_1 = 0, \ \kappa_2 = \pm 1, \qquad\qquad \mathcal{J}^+ \mathcal{J}^- > 1,$$

depending on the value $0 < \pm\alpha < \min\{\nu_*(\mathcal{J}^+, \mathcal{J}^-, 2), \nu_\infty(\mathcal{J}^+, \mathcal{J}^-)\}$.

Now we can solve the normalized systems of equations:

$$\overline{\mathcal{B}}_Y^{(2)}(\mathcal{J}^+, \mathcal{J}^-, 2)\overline{\mathbf{Y}} = \mathbf{G}_Y^{(2)},$$

instead of systems (4.5). Theorems which are similar to those proved above can be formulated for these systems. Then relation (3.7) is the usual condition of solvability of the corresponding boundary value problems. Recall that $\mathbf{G}_Y^{(2)} \in \mathbf{W}_{(m),2}^{p,\alpha,\beta}(\mathbb{R}_+)$ and consequently, the solutions $\overline{\mathbf{Y}}$ belong to spaces $\mathbf{W}_{(1),2}^{p,\alpha,\beta}(\mathbb{R}_+)$, at least. Then the solutions $\mathbf{Y} = \mathcal{G}\overline{\mathbf{Y}}$ of the initial systems (4.5) belong to the spaces $\mathbf{L}_2^{p,\alpha,\beta}(\mathbb{R}_+) \subset \widetilde{\mathbf{L}}_2^{p,\alpha,\beta}(\mathbb{R}_+)$, because the operators $\mathcal{G}\colon \mathbf{W}_{(m),2}^{p,\alpha,\beta}(\mathbb{R}_+) \to \mathbf{W}_{(m-1),2}^{p,\alpha,\beta}(\mathbb{R}_+)$ are bounded for any $m \in \mathbb{N}$. Consequently, condition (4.7) has been satisfied.

Taking into account the volume of the paper we shall not present here the integral form of the operators $\overline{\mathcal{B}}_Y^{(2)}(\mathcal{J}^+, \mathcal{J}^-, 2)\mathcal{K}_*$, and the analytic structure of the spaces $\widetilde{\mathbf{L}}_2^{p,\alpha,\beta}(\mathbb{R}_+)$.

The remaining degenerate operators $\mathcal{B}_Y^{(3)}(\mathcal{J}^+, \mathcal{J}^-, 2)$ $(\mathcal{J}^\pm = 1, 2)$ will be investigated in the Hilbert spaces $\mathbf{L}_2^{2,\alpha,\beta}(\mathbb{R}_+)$. To this end we apply the method of solution of ill-posed (incorrect) problems [19]. Consider the Tikhonov functional $(a > 0)$:

$$(4.13) \qquad \mathcal{F}_a[\mathbf{Y}, \mathbf{G}_Y^{(3)}] = \|\mathcal{B}_Y^{(3)}\mathbf{Y} - \mathbf{G}_Y^{(3)}\|_{\mathbf{L}_2^{2,\alpha,\beta}}^2 + a\|\mathbf{Y}\|_{\mathbf{L}_2^{2,\alpha,\beta}}^2.$$

Let $\mathbf{Y}_a$ be the minimal element of the functional $\mathcal{F}_a$ in the space $\mathbf{L}_2^{2,\alpha,\beta}(\mathbb{R}_+)$ with the parameters $-\nu_*(\mathcal{J}^+, \mathcal{J}^-, 2) < \alpha < 0$, $\alpha \le \beta$, $\beta < \nu_\infty(\mathcal{J}^+, \mathcal{J}^-)$. As it has been shown above, the equation $\mathcal{B}_Y^{(3)}\mathbf{Y} = \mathbf{G}_Y^{(3)}$ can have a unique solution only in the mentioned spaces. Consequently, $\mathbf{Y}_a \to \mathbf{Y}$ weakly when $a \to 0$ (see [19]). The minimal element $\mathbf{Y}_a$ of the functional $\mathcal{F}_a$ for any $a > 0$ can be calculated by any standard variational methods [8]. Moreover, we can also write Euler equation for this functional:

$$(4.14) \qquad [\mathcal{A}_3\mathbf{Y}_a](\lambda) = \frac{1}{a + f_Y^2(\lambda)}[\mathcal{B}^\star \mathbf{G}_Y^{(3)}](\lambda),$$

where $\mathcal{B}^*$ is the formal operator conjugate to the operator $\mathcal{B}_Y^{(3)}$:

$$[\mathcal{B}^*\mathbf{u}](\lambda) = f_Y(\lambda)\mathbf{u}(\lambda) + \int_0^\infty \frac{w(\xi)}{w(\lambda)} K_Y^{(3)}(\lambda)\left(\Psi^{(3)}(\xi,\lambda)\right)^\top \mathbf{u}(\xi)\,d\xi,$$

$$w(\lambda) = \varrho_{2\alpha-1,2\beta-1}(\lambda),$$

$$[A_3\mathbf{u}](\lambda) = \mathbf{u}(\lambda) + \int_0^\infty \mathbf{Q}(\lambda,\xi)\mathbf{u}(\xi)\,d\xi,$$

$$\mathbf{Q}(\lambda,\xi) = \frac{1}{a+f_Y^2(\lambda)}\left\{ f_Y(\lambda)K_Y^{(3)}(\xi)\Psi^{(3)}(\lambda,\xi) + \frac{w(\xi)}{w(\lambda)}f_Y(\xi)K_Y^{(3)}(\lambda)\left(\Psi^{(3)}(\xi,\lambda)\right)^\top \right.$$

$$\left. + \int_0^\infty \frac{w(t)}{w(\lambda)}K_Y^{(3)}(\lambda)K_Y^{(3)}(\xi)\left(\Psi^{(3)}(t,\lambda)\right)^\top \Psi^{(3)}(t,\xi)\,dt \right\}.$$

Here the functions $f_Y(\lambda)$, $K_Y^{(3)}(\lambda)$, $\varrho_{\alpha,\beta}(\lambda)$ are defined in (4.6), (4.12).

Basing on the results of [10], it can be shown that the symbol of the operator A_3 in the space $\mathbf{L}_2^{p,\alpha,\beta}(\mathbb{R}_+)$ is of the form (see Remark 3):

$$\text{Symb } A_3\big|_{\mathbf{L}_2^{p,\alpha,\beta}} = \mathbf{I} + a^{-1}\left(\Phi_*^{-1}(\alpha+it)\right)^\top \Phi_*^{-1}(\alpha-it),$$

and for $\alpha = 0$ it is the real matrix-function. Moreover, its determinant is the even real function which is not equal to zero along $\overline{\mathbb{R}}$. Consequently, the index of the operator A_3 is equal to zero for any $|\alpha| < \nu_0$. Further note that for $\alpha = 0$ the symbol of the operator is the Hermitian matrix-function (the transposed matrix-function is equal to the complex conjugate one). Then, taking into account the fact that the symbol is the definite matrix-function in the point $t = 0$ (or at infinity), we can conclude that it is definite in any point (see the corresponding theorem from [4]). Hence, for the system of equations (4.14) all partial (left-hand and right-hand) indices are equal to zero and the Theorem 1 holds true. Note only that the value of the first zero of the determinant of the operator symbol $\nu_0 = \nu_0(a)$ depends essentially on the value of $a > 0$. Besides, we should choose only negative value of α; then the convergence of the solution $\mathbf{Y}_a$ to the solution of system (4.6) has been justified.

So, the systems of integral equations (4.5), (4.6) which are obtained under the assumption $\tau = 0$ have been investigated for all problems $(\mathcal{J}^+, \mathcal{J}^-, \mathcal{J})$ $(\mathcal{J}^\pm = 1, 2, \mathcal{J} = 1, 2, 3)$ and for all values of the parameters $\tau_\pm \geq 0$. The values of the unknown parameters $\gamma_\infty(= \min\{\gamma_1, \gamma_2\})$, $k = 0$, γ_0, $u_*(= v_\pm)$ of class $\mathbf{LW}(\Omega)$ have been obtained (see the Theorems, *a priori* assumptions (4.7) and relations (4.3), (4.4)). Besides, the relation between the values of the parameters γ_1, γ_2 are given in Corollary A.1 [12].

5. Analysis of the system of functional-difference equations (3.9) in the case $\tau > 0$

It is easy to prove by contradiction that the terms of systems (3.9) can not have any pole, the real part of which lies between 0 and γ_∞ and, consequently, $\gamma_0 \geq 1$. Consider the equivalent systems

$$(5.1) \qquad \Phi_*^{-1}(s)[\hat{Y} + \hat{Z}](s) = \mu_1 \tau \Phi_*^{-1}(s)\hat{Z}(s-1) + \hat{Z}(s) + \Phi_*^{-1}(s)F(s)$$

in the strip $0 < \Re s < \min\{\nu_\infty, \gamma_\infty\}$. Taking into account the results of the Lemma and *a priori* estimates for the vector-functions $[\hat{Y} + \hat{Z}](s)$, $\hat{Z}(s)$ (see arguments before (4.2)), one can easily see that the vector-function $\hat{Z}(s-1)$ can only have a simple pole in the point $s = 0$, and for some $\delta > 0$

$$(5.2) \qquad \mathbf{Z}(\lambda) = \lambda^{-1} \begin{pmatrix} 0 \\ z_*^* \end{pmatrix} + O(\lambda^{-1-\delta}), \qquad \lambda \to \infty.$$

Here the constant z_-^* is defined for some of the problems as follows:

$$(5.3) \qquad z_-^* = \begin{cases} 0, & \mathcal{J}^\pm = 1, & \mathcal{J} = 1,2,3, \\ \text{unknown}, & \mathcal{J}^+\mathcal{J}^- > 1, & \mathcal{J} = 1,2,3. \end{cases}$$

For the remaining problems $\mathcal{J}^+\mathcal{J}^- > 1$, $\mathcal{J} = 1,2,3$, this constant will be calculated below from an additional condition.

Introduce a vector-function $\mathbf{Z}_*(\lambda)$ by the relation:

$$(5.4) \qquad \mathbf{Z}_*(\lambda) = \mathbf{Z}(\lambda) - \frac{z_-^* \lambda}{1 + \lambda^2} \begin{pmatrix} 0 \\ 1 \end{pmatrix}.$$

Note that the inverse Fourier transformation of $\mathbf{Z}_*(\lambda)$ is of the form:

$$\mathcal{F}^{-1}[\mathbf{Z}_*](x_1) = \begin{pmatrix} z_+(x_1) \\ iz_-(x_1) \end{pmatrix} + \pi e^{-|x_1|} \begin{pmatrix} -z_*^+ \\ iz_*^- \operatorname{sign}(x_1) \end{pmatrix},$$

where the functions $z_+(x_1)$, $z_-(x_1)$ and the constants z_*^+, z_*^- are defined in (3.4), (3.6), (5.3). Using *a priori* estimates of the solutions belonging to the class $\mathbf{LW}(\Omega)$, and properties of the Mellin and Fourier transforms, we can obtain the values of the parameters from the definition of $\mathbf{LW}(\Omega)$:

$$(5.5) \qquad v_\pm = u_* - 2\tau \int_0^\infty z_1(\lambda)\,d\lambda - \pi\tau(z_*^+ \mp z_*^-),$$

where the value of u_* is given by (4.4), but the integral of the first component of the vector-function $\mathbf{Z}$ (or $\mathbf{Z}_*$) is bounded in view of (5.2).

Rewrite the systems of equations (5.1) as follows:

$$(5.6) \qquad \Phi_*^{-1}(s)[\widehat{\mathbf{Y}} + \widehat{\mathbf{Z}}](s) = \mu_1 \tau \Phi_*^{-1}(s)\widehat{\mathbf{Z}}_*(s-1) + \widehat{\mathbf{Z}}_*(s) + \mathbf{F}_Z^*(s).$$

Here the vector-function

$$\mathbf{F}_Z^*(s) = \Phi_*^{-1}(s)F(s) + \frac{\mu_1 \tau \pi z_*^-}{2\sin(\pi s/2)}\Phi_*^{-1}(s)\begin{pmatrix} 0 \\ 1 \end{pmatrix} + \frac{z_*^- \pi}{2\cos(\pi s/2)}\begin{pmatrix} 0 \\ 1 \end{pmatrix}$$

tends to zero at infinity, but systems (5.6) are true in the strip $-\delta < \Re s < \min\{\nu_\infty, \gamma_\infty\}$. Note that $\mathbf{F}_Z^*(s) = \mathbf{F}_1(s) + z_*^+\mathbf{F}_2(s) + z_*^-\mathbf{F}_3(s)$, in general. Besides, the vector-functions multiplied by the unknown constants z_*^+, z_*^- are always bounded in the zero point.

Now we can reduce the systems of functional-difference equations (5.6) to systems of singular integral equations. The way to do that essentially depends on the behaviour of the matrix-function $\Phi_*^{-1}(s)$ at infinity. Using the Lemma, let us rewrite the systems for the first case ($t_+ = t_- = 0$) in the form:

$$[\chi_+\mathbf{I} + \chi_-\mathbf{E}\,\mathrm{tg}(\pi s/2) + \Phi_{**}(s)][\widehat{\mathbf{Y}}(s) + \widehat{\mathbf{Z}}(s) - \mu_1\tau\widehat{\mathbf{Z}}_*(s-1)] = \widehat{\mathbf{Z}}_*(s) + \mathbf{F}_Z^*(s).$$

Then, applying the inverse Mellin transform, we obtain

$$(5.7) \qquad [\chi_+(\mathbf{Y} + \mathbf{Z} - \mu_1\tau\lambda\mathbf{Z}_*) - \mathbf{Z}_*](\lambda)$$

$$-\frac{2\chi_-}{\pi}\mathbf{E}\int_0^\infty [\mathbf{Y} + \mathbf{Z} - \mu_1\tau\xi\mathbf{Z}_*](\xi)\frac{\lambda\,d\xi}{\lambda^2 - \xi^2} + \int_0^\infty \Psi^{(1)}(\lambda,\xi)[\mathbf{Y} + \mathbf{Z} - \mu_1\tau\xi\mathbf{Z}_*](\xi)\,d\xi$$

$$= \frac{1}{2\pi i}\int_{-i\infty}^{i\infty} \mathbf{F}_Z^*(s)\lambda^s\,ds,$$

where

$$\Psi^{(1)}(\lambda,\xi) = \frac{1}{2\pi\xi i}\int_{-i\infty}^{i\infty} \Phi_{**}(s)\left(\frac{\lambda}{\xi}\right)^s ds.$$

It remains to leave in systems (5.7) only one of the unknown vector-functions using relations (3.5), (5.4) between $\mathbf{Y}(\lambda)$, $\mathbf{Z}(\lambda)$, $\mathbf{Z}_*(\lambda)$. For the exterior boundary conditions along Γ_n of the first and the third type ($\mathcal{J} = 1,3$ see (2.9)), it is convenient to leave the vector-function $\mathbf{X}_Z(\lambda) = \mathbf{Z}_*(\lambda)(1+\lambda)$. This is because the matrix-functions belonging to the kernels of the obtained operators (which are different from the homogeneous matrix-functions of the degree -1) should be bounded at zero and infinity. The corresponding systems of integral equations are of the form:

$$(5.8) \qquad \mathcal{C}_Z^{(1)}(\mathcal{J}^+, \mathcal{J}^-, \mathcal{J})\mathbf{X}_Z = \mathbf{Q}_Z^{(1)}, \qquad \mathcal{J} = 1,3, \quad \mathcal{J}^\pm = 1,2,$$

where

$$[\mathcal{C}_Z^{(1)}\mathbf{u}](\lambda) = \mathbf{u}(\lambda) + \int\limits_0^\infty L_Z^{(1)}(\lambda,\xi)\mathbf{\Psi}^{(1)}(\lambda,\xi)\mathbf{u}(\xi)\,d\xi$$

$$-\frac{2}{\pi}\chi_- \mathbf{E}\int\limits_0^\infty L_Z^{(1)}(\lambda,\xi)\mathbf{u}(\xi)\frac{\lambda\,d\xi}{\lambda^2-\xi^2}\,,$$

$$L_Z^{(1)}(\lambda,\xi) = \frac{(1+\lambda)[1+\mu_1\xi M_p(\xi)-\mu_1\tau\xi]}{(1+\xi)[\chi_+(1+\mu_1\lambda M_p(\lambda)-\mu_1\tau\lambda)-1]}\,,$$

$$H_Z^* = H_Z + \frac{z_-^*\lambda(1+\mu_1\lambda M_p)}{1+\lambda^2}\begin{pmatrix}0\\1\end{pmatrix},$$

$$\mathbf{Q}_Z^{(1)}(\lambda) = \frac{1+\lambda}{\chi_+(1+\mu_1\lambda M_p(\lambda)-\mu_1\tau\lambda)-1}$$

$$\times\left(\frac{1}{2\pi i}\int\limits_{-i\infty}^{i\infty}\lambda^s\mathbf{\Phi}_*^{-1}(s)\mathbf{F}_Z^*(s)\,ds - [\mathcal{C}_0^{(1)}H_Z^*](\lambda)\right),$$

$$[\mathcal{C}_0^{(1)}\mathbf{u}](\lambda) = \chi_+\mathbf{u}(\lambda) + \int\limits_0^\infty \mathbf{\Psi}^{(1)}(\lambda,\xi)\mathbf{u}(\xi)\,d\xi - \frac{2}{\pi}\chi_- \mathbf{E}\int\limits_0^\infty \mathbf{u}(\xi)\frac{\lambda\,d\xi}{\lambda^2-\xi^2}\,.$$

However, when we deal with the problem $(\mathcal{J}^+,\mathcal{J}^-,2)$, systems (5.8) are not suitable, because in this case the function $M_p(\lambda) = O(\lambda^{-2})$ as $\lambda \to 0$, and consequently the corresponding integral operators are not bounded in the spaces $\mathbf{L}_2^{p,\alpha,\beta}(\mathbb{R}_+)$ under consideration. For these problems the method of reducing the systems of functional-difference equations (5.1) to systems of integral equations should be similar, but slightly different.

Namely, from (3.8) and (5.2) it follows that

$$(5.9)\qquad\qquad \mathbf{Y}(\lambda) = -\lambda^{-1}\begin{pmatrix}0\\z_-^*\end{pmatrix} + O(\lambda^{-1-\delta}), \qquad \lambda\to\infty.$$

Then denote

$$\mathbf{Y}_*(\lambda) = \mathbf{Y}(\lambda) + \frac{z_-^*\lambda}{1+\lambda^2}\begin{pmatrix}0\\1\end{pmatrix},$$

and rewrite systems (5.1) in the strip $-\delta < \Re s < \min\{\nu_\infty,\gamma_\infty\}$ in an equivalent form:

$$(5.10)\qquad \mathbf{\Phi}_*^{-1}(s)\left[\widehat{\mathbf{Y}}_* + \widehat{\mathbf{Z}}\right](s) = \mu_1\tau\mathbf{\Phi}_*^{-1}(s)\widehat{\mathbf{Z}}(s-1) + \widehat{\mathbf{Z}}(s) + \mathbf{F}_Y^*(s),$$

Here the vector-function

$$\mathbf{F}_Y^*(s) = \mathbf{\Phi}_*^{-1}(s)F(s) + \frac{z_*^-}{2\cos(\pi s/2)}\mathbf{\Phi}_*^{-1}(s)\begin{pmatrix}0\\1\end{pmatrix}$$

is analytic in the mentioned strip in view of the Lemma and tends to zero at infinity.

Repeating the former line of reasoning we are led to systems of integral equations with respect to vector-function $\mathbf{X}_Y(\lambda) = \mathbf{Y}_*(\lambda)(1 + \lambda)$:

(5.11) $\mathcal{C}_Y^{(1)}(\mathcal{J}^+, \mathcal{J}^-, \mathcal{J})\mathbf{X}_Y = \mathbf{Q}_Y^{(1)}, \qquad \mathcal{J} = 2, 3, \quad \mathcal{J}^\pm = 1, 2,$

where

$$[\mathcal{C}_Y^{(1)}\mathbf{u}](\lambda) = \mathbf{u}(\lambda) + \int_0^\infty L_Y^{(1)}(\lambda, \xi)\Psi^{(1)}(\lambda, \xi)\mathbf{u}(\xi)\,d\xi$$

$$-\frac{2}{\pi}\chi_- \mathbf{E}\int_0^\infty L_Y^{(1)}(\lambda, \xi)\mathbf{u}(\xi)\frac{\lambda\,d\xi}{\lambda^2 - \xi^2},$$

$$L_Y^{(1)}(\lambda, \xi) = \frac{(1 + \lambda)[1 + (\mu_1\xi M_p(\xi))^{-1} - \tau(M_p(\xi))^{-1}]}{(1 + \xi)(\chi_+[1 + (\mu_1\lambda M_p(\lambda))^{-1} - \tau(M_p(\lambda))^{-1}] - (\mu_1\lambda M_p(\lambda))^{-1})},$$

$$\mathbf{Q}_Y^{(1)}(\lambda) = \frac{1 + \lambda}{\chi_+[1 + (\mu_1\lambda M_p(\lambda))^{-1} - \tau(M_p(\lambda))^{-1}] - (\mu_1\lambda M_p(\lambda))^{-1}}$$

$$\times \left(\frac{1}{2\pi i}\int_{-i\infty}^{i\infty} \lambda^s\Phi_*^{-1}(s)\mathbf{F}_Y^*(s)\,ds - [\mathcal{C}_0^{(1)}H_Y^*](\lambda) + H_Y^*(\lambda)\right),$$

$$H_Y^* = H_Y - \frac{z_-^*}{\mu_1(1 + \lambda^2)M_p(\lambda)}\begin{pmatrix} 0 \\ 1 \end{pmatrix}.$$

For the second case $(t_+ > 0,\ t_- = \pm t_+)$, the systems of integral equations are analogously obtained, because the behaviour of the matrix-function at infinity is similar to that in the first case $(t_+ = 0)$. Then the corresponding operators and systems of integral equations can be obtained from (5.8), (5.11) by replacing the upper indices 1 with 2, and the constants χ_+, χ_- with the constants $(2\varpi_\pm)^{-1}$, $\mp(2\varpi_\pm)^{-1}$, respectively.

In the third case $(t_+ > 0,\ t_-^2 \neq t_+^2)$, the procedures of reducing the systems (5.1) to systems of integral equations are the same as in proving (4.6), (5.8) and (5.11). The corresponding systems are of the form:

(5.12)
$$\mathcal{C}_Z^{(3)}(\mathcal{J}^+, \mathcal{J}^-, \mathcal{J})\mathbf{X}_Z = \mathbf{Q}_Z^{(3)}, \qquad \mathcal{J} = 1, 3, \quad \mathcal{J}^\pm = 1, 2;$$
$$\mathcal{C}_Y^{(3)}(\mathcal{J}^+, \mathcal{J}^-, \mathcal{J})\mathbf{X}_Y = \mathbf{Q}_Y^{(3)}, \qquad \mathcal{J} = 2, 3, \quad \mathcal{J}^\pm = 1, 2;$$

where

$$[\mathcal{C}_{Z(Y)}^{(3)}\mathbf{u}](\lambda) = g_{Z(Y)}(\lambda)\mathbf{u}(\lambda) + \int_0^\infty L_{Z(Y)}^{(3)}(\xi)\Psi^{(3)}(\lambda, \xi)\mathbf{u}(\xi)\,d\xi,$$

$$g_Z(\lambda) = \frac{1}{1+\lambda},$$

$$g_Y(\lambda) = \frac{1}{\lambda \mu_1 M_p(\lambda)(1+\lambda)},$$

$$L_Z^{(3)}(\xi) = -\frac{1 + \mu_1 \xi M_p(\xi) - \mu_1 \tau \xi}{1+\xi},$$

$$L_Y^{(3)}(\xi) = -\frac{1 + (\mu_1 \xi M_p(\xi))^{-1} - \tau(M_p(\xi))^{-1}}{1+\xi},$$

$$Q_Z^{(3)}(\lambda) = -\frac{1}{2\pi i} \int\limits_{-i\infty}^{i\infty} \lambda^s \Phi_*^{-1}(s) F_Z^*(s) \, ds + \int\limits_0^{i\infty} \Psi^{(3)}(\lambda, \xi) H_Z^*(\xi) \, d\xi,$$

$$Q_Y^{(3)}(\lambda) = -\frac{1}{2\pi i} \int\limits_{-i\infty}^{i\infty} \lambda^s \Phi_*^{-1}(s) F_Y^*(s) \, ds + \int\limits_0^{i\infty} \Psi^{(3)}(\lambda, \xi) H_Y^*(\xi) \, d\xi - H_Y^*(\lambda).$$

Here the matrix-function $\Psi^{(3)}(\lambda, \xi)$ and the vector-functions $H_Z(\lambda)$, $H_Y(\lambda)$ have been previously defined.

Basing on the results presented in [2, 10, 11] one can show that the obtained operators $\mathcal{C}_{Z(Y)}^{(j)}(\mathcal{J}^+, \mathcal{J}^-, \mathcal{J})$ ($j = 1, 2, 3$) for all of the problems $(\mathcal{J}^+, \mathcal{J}^-, \mathcal{J})$ are bounded in the spaces $\mathbf{L}_2^{p,\alpha,\beta}(\mathbb{R}_+)$ with the parameters $-\nu_\infty(\mathcal{J}^+, \mathcal{J}^-) < \alpha \leq \beta < \nu_\infty(\mathcal{J}^+, \mathcal{J}^-)$, $1 \leq p < \infty$. As before, the right-hand sides of the corresponding systems of integral equations belong to the spaces $\mathbf{W}_{(m),2}^{p,\alpha,\beta}(\mathbb{R}_+)$ for any $m \in \mathbb{N}$. All these systems of integral equations are of the second kind, but the operators $\mathcal{C}_Z^{(3)}(\mathcal{J}^+, \mathcal{J}^-, \mathcal{J})$ ($\mathcal{J} = 1, 3$), $\mathcal{C}_Y^{(3)}(\mathcal{J}^+, \mathcal{J}^-, 3)$ are degenerate to the first kind at infinity, and the operators $\mathcal{C}_Y^{(3)}(\mathcal{J}^+, \mathcal{J}^-, 2)$ are degenerate at zero and at infinity. Note that the vector-functions $\mathbf{X}_{Z(Y)}(\lambda)$ should belong to the spaces:

(5.13)
$$\mathbf{X}_Y \in \mathbf{L}_2^{p,\alpha_1,\beta}(\mathbb{R}_+), \qquad \mathbf{X}_Z \in \mathbf{L}_2^{p,\alpha_2,\beta}(\mathbb{R}_+),$$
$$-\gamma_i < \alpha_i < 0, \qquad 0 < \beta < \delta,$$

for arbitrary $p \in [1, \infty)$ and some $\delta > 0$, in view of *a priori* estimates (5.2), (5.9) for the vector-functions $\mathbf{Z}(\lambda)$ and $\mathbf{Y}(\lambda)$ and the choice of $\mathbf{Z}_*(\lambda)$ and $\mathbf{Y}_*(\lambda)$.

REMARK 5. By assuming $z_*^- = 0$ in the systems obtained in this section, one can equivalently investigate all these systems in the spaces (5.13), however with the negative values of β ($-\delta < \beta < 0$) only.

Using the results from [10] we can write the symbols $\mathbf{C}_{Z(Y)}^{(j)}(t, \theta, \mathcal{J}^+, \mathcal{J}^-, \mathcal{J})$ ($t \in \overline{\mathbb{R}}$, $\theta = \pm 1$) of the nondegenerate operators $\mathcal{C}_{Z(Y)}^{(j)}(\mathcal{J}^+, \mathcal{J}^-, \mathcal{J})$ ($j = 1, 2$),

which are represented in the form $C = \mathcal{A}P + \mathcal{B}Q + \mathcal{K}$.

$$\mathbf{C}_Z^{(j)}(t,\theta,\mathcal{J}^+,\mathcal{J}^-,1) = \left[\mathbf{I} - \boldsymbol{\Phi}_*^{-1}(\alpha - it)\right]\frac{1+\theta}{2} + \boldsymbol{\Phi}_*^{-1}(\beta - it)\frac{1-\theta}{2},$$

(5.14) $$\mathbf{C}_{Z(Y)}^{(j)}(t,\theta,\mathcal{J}^+,\mathcal{J}^-,3) = \left[\mathbf{I} - \left(1 - \frac{\mu_1}{\mu_{n+1}}\right)\boldsymbol{\Phi}_*^{-1}(\alpha - it)\right]\frac{1+\theta}{2}$$

$$+ \boldsymbol{\Phi}_*^{-1}(\beta - it)\frac{1-\theta}{2},$$

$$\mathbf{C}_Y^{(j)}(t,\theta,\mathcal{J}^+,\mathcal{J}^-,2) = \boldsymbol{\Phi}_*^{-1}(\alpha - it)\frac{1+\theta}{2} + \boldsymbol{\Phi}_*^{-1}(\beta - it)\frac{1-\theta}{2}.$$

˙Note that the symbols of the operators $\mathcal{C}_{Z(Y)}^{(2)}(\mathcal{J}^+,\mathcal{J}^-,\mathcal{J})$ in the spaces $\mathbf{L}_2^{p,\alpha,\beta}$ $(\mathbb{R}_+)$ are degenerate for any values of β ($\det \boldsymbol{\Phi}_*^{-1}(\beta - it)$ tends to zero as $t \to \infty$). Hence we can directly investigate the operators $\mathcal{C}_{Z(Y)}^{(1)}(\mathcal{J}^+,\mathcal{J}^-,\mathcal{J})$ only. Thus the indices and the partial indices of the operators $\mathcal{C}_{Z(Y)}^{(1)}(\mathcal{J}^+,\mathcal{J}^-,\mathcal{J})$ in the spaces $\mathbf{L}_2^{p,\alpha,\beta}(\mathbb{R}_+)$ for some $|\alpha| < \alpha_*, |\beta| < \beta_*$ are calculated as follows:

$$\kappa(\alpha,\beta,\mathcal{J}^+,\mathcal{J}^-,1) = \begin{cases} \text{sign}\alpha; & (\kappa_1 = \text{sign}\alpha, \kappa_2 = 0), & \mathcal{J}^+\mathcal{J}^- = 1, \\ \text{sign}\alpha - \text{sign}\beta; & (\kappa_1 = \text{sign}\alpha, \kappa_2 = -\text{sign}\beta), & \mathcal{J}^+\mathcal{J}^- = 2, \\ -\text{sign}\beta; & (\kappa_1 = 0, \kappa_2 = -\text{sign}\beta), & \mathcal{J}^+\mathcal{J}^- = 4; \end{cases}$$

$$\kappa(\alpha,\beta,\mathcal{J}^+,\mathcal{J}^-,2) = \begin{cases} 0; & (\kappa_1,\kappa_2 = 0), & \mathcal{J}^+\mathcal{J}^- = 1, \\ \text{sign}\alpha - \text{sign}\beta; & (\kappa_1 = 0, \kappa_2 = \text{sign}\alpha - \text{sign}\beta), & \mathcal{J}^+\mathcal{J}^- > 1; \end{cases}$$

$$\kappa(\alpha,\beta,\mathcal{J}^+,\mathcal{J}^-,3) = \begin{cases} 0; & (\kappa_1,\kappa_2 = 0), & \mathcal{J}^+\mathcal{J}^- = 1, \\ -\text{sign}\beta; & (\kappa_1 = 0, \kappa_2 = -\text{sign}\beta), & \mathcal{J}^+\mathcal{J}^- > 1. \end{cases}$$

After eliminating, when the occasion requires, the index and the partial indices of the operators $\mathcal{C}_{Z(Y)}^{(1)}(\mathcal{J}^+,\mathcal{J}^-,\mathcal{J})$ (and the constituent operators $\mathcal{A}$, $\mathcal{B}$) by the methods presented in [18], we can solve the corresponding systems of equations (5.8), (5.11). The unknown constants z_+^*, z_-^* (if they are presented in the respective systems) are obtained from the conditions of solvability of the systems. For example, if the parameters α, β of the spaces $\mathbf{L}_2^{p,\alpha,\beta}(\mathbb{R}_+)$ satisfy the conditions $\alpha < 0 < \beta$ (see (5.13)), then we have $\kappa(\alpha,\beta,1,1,1) = -1$ ($\kappa_1 = -1, \kappa_2 = 0$), and the corresponding system contains the unknown constant z_+^* only. But in the problem (1,2,1) $\kappa(\alpha,\beta,1,2,1) = -2$ ($\kappa_1 = \kappa_2 = -1$) and two constants z_+^*, z_-^* are presented. However, if we choose the values of the space parameters in a different way: $\alpha < 0, \beta < 0$, then for the mentioned problem (1,2,1) $\kappa(\alpha,\beta,1,2,1) = 0$ ($\kappa_1 = -1, \kappa_2 = 1$) and there is only one constant z_+^* (see Remark 5) in the corresponding system.

5.1. Investigation of the degenerate problems

The degenerate systems with the operators $\mathcal{C}^{(2)}_{Z(Y)}(\mathcal{J}^+, \mathcal{J}^-, \mathcal{J})$ and $\mathcal{C}^{(3)}_{Z(Y)}$ $(\mathcal{J}^+, \mathcal{J}^-, \mathcal{J})$ can be analogously transformed, and investigated as it has been done in the previous section for the operators $\mathcal{B}^{(2)}_Y(\mathcal{J}^+, \mathcal{J}^-, 2)$ and $\mathcal{B}^{(3)}_Y(\mathcal{J}^+, \mathcal{J}^-, 2)$. But we shall investigate them in a different way.

Namely, return to systems of functional-difference equations (5.1) and denote by $\mathbf{Z}_0(\lambda)$ a new vector-function, using the relation similar to (5.4) with the constant z_0^*:

$$(5.15) \qquad \mathbf{Z}_0(\lambda) = \mathbf{Z}(\lambda) - \frac{z_0^* \lambda}{(1 + \lambda^2)^2} \begin{pmatrix} 0 \\ 1 \end{pmatrix}, \qquad z_0^* = \begin{cases} \text{unknown,} & \mathcal{J}^+ \mathcal{J}^- = 1, \\ -4\pi^{-1} \hat{\mathbf{f}}_2(0), & \mathcal{J}^+ \mathcal{J}^- > 1, \end{cases}$$

such that the additional condition

$$(5.16) \qquad \begin{aligned} (0, 1) \hat{\mathbf{Z}}_0(-1) &= 0, \qquad \mathcal{J}^+ \mathcal{J}^- = 1, \qquad \mathcal{J} = 1, 2, 3, \\ (0, 1) \hat{\mathbf{Z}}_0(0) &= 0, \qquad \mathcal{J}^+ \mathcal{J}^- > 1, \qquad \mathcal{J} = 1, 2, 3, \end{aligned}$$

is true for the problems $(\mathcal{J}^+, \mathcal{J}^-, \mathcal{J})$. Here $\hat{\mathbf{f}}_2(s)$ is the second component of the vector $\Phi_*^{-1}(s) F(s)$. In the case $\mathcal{J}^+, \mathcal{J}^- = 1$ the unknown constant z_0^* will be calculated below. Note that the vector-functions $\mathbf{Z}_0(\lambda)$ and $\mathbf{Z}(\lambda)$ are of a similar behaviour (see (5.2)). It means that the systems:

$$(5.17) \qquad \Phi_*^{-1}(s)[\hat{\mathbf{Y}} + \hat{\mathbf{Z}}](s) = \mu_1 \tau \Phi_*^{-1}(s) \hat{\mathbf{Z}}_0(s - 1) + \hat{\mathbf{Z}}_0(s) + \mathbf{F}_0(s)$$

are true in the strip $0 < \Re s < \min\{\nu_\infty, \gamma_\infty\}$, in general, but the vector-function

$$\mathbf{F}_0(s) = \Phi_*^{-1}(s) F(s) + \frac{\mu_1 \tau \pi z_0^- s}{4 \sin(\pi s/2)} \Phi_*^{-1}(s) \begin{pmatrix} 0 \\ 1 \end{pmatrix} + \frac{z_0^- \pi(1 + s)}{4 \cos(\pi s/2)} \begin{pmatrix} 0 \\ 1 \end{pmatrix}$$

is analytic in the strip $|\Re s| < \nu_\infty$, and its second component is equal to zero when $s = 0$ for the problems $(\mathcal{J}^+, \mathcal{J}^-, \mathcal{J})$ $(\mathcal{J}^+ \mathcal{J}^- > 1)$ in view of (5.15).

Now introduce a new vector-function $\mathbf{V}(\lambda)$ by the relation:

$$\hat{\mathbf{Z}}_0(s) = \mathbf{R}_{j,k}^{-1}(s) \hat{\mathbf{V}}(s),$$

$$\mathbf{R}_{3,k}(s) = \Gamma(s + 1) \cos \frac{\pi s}{2} \begin{pmatrix} 1 & 0 \\ 0 & x_k(s) \end{pmatrix},$$

$$(5.18) \qquad \mathbf{R}_{2,k}(s) = \frac{1}{2} \begin{pmatrix} \Gamma(s + 1) \cos \dfrac{\pi s}{2} & \pm \Gamma(s + 1) \cos \dfrac{\pi s}{2} x_k(s) \\ 1 & \mp x_k(s) \end{pmatrix},$$

$$\mathbf{R}_{1,k}(s) = \begin{pmatrix} 1 & 0 \\ 0 & x_k(s) \end{pmatrix},$$

$$x_k(s) = \begin{cases} -\mathrm{tg}(\pi s/2), & k = 1 \Leftrightarrow \mathcal{J}^+ \mathcal{J}^- = 1, \\ \\ \mathrm{ctg}(\pi s/2), & k = 2 \Leftrightarrow \mathcal{J}^+ \mathcal{J}^- > 1, \end{cases}$$

where choice of $j = 1, 2, 3$ depends on the behaviour of the matrix-function $\Phi_*^{-1}(s)$ at infinity (see Lemma). Besides, in the case $j = 2$ the sign is defined from relation $t_- = \mp t_+$. The value of k ($k = 1, 2$) depends in turn on the behaviour of $\Phi_*^{-1}(s)$ in zero point (see Lemma).

One can see that the vector-function $\widehat{V}(s)$ has no poles in points $s = 0$ and $s = -1$ in view of (5.2) and (5.16). Consequently one can assume that

$$(5.19) \qquad \mathbf{V} \in \mathbf{L}_2^{p,\alpha,\beta}(\mathbb{R}_+), \qquad -\gamma_1 < \alpha < 0, \quad 0 < \beta < 1 + \delta.$$

Besides, for the problems $(\mathcal{J}^+, \mathcal{J}^-, \mathcal{J})$ ($\mathcal{J}^+ \mathcal{J}^- = 1$ what is equivalent to $k = 1$, see (5.18)) the additional condition should be satisfied to calculate the unknown constant z_0^*:

$$(5.20) \qquad ((-1)^{j+1} - 1, 2)\,\widehat{V}(0) = 0, \qquad \mathcal{J}^+ \mathcal{J}^- = 1, \quad \mathcal{J} = 1, 2, 3, \quad j = 1, 2, 3.$$

From (5.18) one can obtain the relations between the vector-functions $\mathbf{Z}_0$ and $\mathbf{V}$:

$$(5.21) \qquad \mathbf{Z}_0(\lambda) = [\mathcal{R}_{j,k}\mathbf{V}](\lambda),$$

$$\mathcal{R}_{1,k} = \begin{pmatrix} I & 0 \\ 0 & \mathcal{S}_k \end{pmatrix}, \qquad \mathcal{R}_{2,k} = \begin{pmatrix} \mathcal{T}_3 & I \\ \pm\mathcal{T}_{2,k} & \mp\mathcal{S}_k \end{pmatrix}, \qquad \mathcal{R}_{3,k} = \begin{pmatrix} \mathcal{T}_3 & 0 \\ 0 & \mathcal{T}_{2,k} \end{pmatrix},$$

where I is the unity operator, but the other scalar integral operators are defined as follows:

$$[\mathcal{S}_1 u](\lambda) = -\frac{2}{\pi} \int_0^\infty \frac{\xi u(\xi)\, d\xi}{\xi^2 - \lambda^2}, \qquad\qquad [\mathcal{S}_2 u](\lambda) = -\frac{2}{\pi} \int_0^\infty \frac{\lambda u(\xi)\, d\xi}{\xi^2 - \lambda^2},$$

$$(5.22) \quad [\mathcal{T}_3 u](\lambda) = \frac{2}{\pi} \int_0^\infty \sin(\lambda/\xi) u(\xi) \frac{d\xi}{\xi}, \qquad [\mathcal{T}_{2,1} u](\lambda) = \frac{2}{\pi} \int_0^\infty \cos(\lambda/\xi) u(\xi) \frac{d\xi}{\xi},$$

$$[\mathcal{T}_{2,2} u](\lambda) = \frac{4}{\pi^2} \int_0^\infty [\mathrm{Si}\,(\lambda/\xi) \cos(\lambda/\xi) + \mathrm{ci}\,(\lambda/\xi) \sin(\lambda/\xi)]\, u(\xi) \frac{d\xi}{\xi}.$$

Here the singular integral operators $\mathcal{S}_2, \mathcal{T}_{2,2}, \mathcal{T}_3 : L^{p,\alpha,\beta}(\mathbb{R}_*) \to L^{p,\alpha,\beta}(\mathbb{R}_*)$ and $\mathcal{S}_1, \mathcal{T}_{2,1} : \overline{L}^{p,\alpha,\beta}(\mathbb{R}_*) \to L^{p,\alpha,\beta}(\mathbb{R}_*)$ are bounded. But $\overline{L}^{p,\alpha,\beta}(\mathbb{R}_*) \subset L^{p,\alpha,\beta}(\mathbb{R}_*)$ is the set of functions from $L^{p,\alpha,\beta}(\mathbb{R}_*)$ which satisfy the respective condition (5.20).

Rewrite the systems (5.17) in an equivalent form:

$$(5.23) \qquad \mathbf{N}_{j,k}(s)[\widehat{\mathbf{Y}} + \widehat{\mathbf{Z}}](s) = \mu_1 \tau \mathbf{M}_{j,k}(s)\widehat{\mathbf{V}}(s-1) + \widehat{\mathbf{V}}(s) + \mathbf{R}_{j,k}(s)\mathbf{F}_Z^0(s),$$

in the strip $-\delta < \Re s < \min\{\nu_\infty, \gamma_\infty\}$ for some value $\delta > 0$. Here we denote

$$(5.24) \qquad \begin{aligned} \mathbf{N}_{j,k}(s) &= \mathbf{R}_{j,k}(s)\Phi_*^{-1}(s) = \mathbf{N}_j^{(1)}(s) + \mathbf{N}_{j,k}^{(2)}(s), \\ \mathbf{M}_{j,k}(s) &= \mathbf{R}_{j,k}(s)\Phi_*^{-1}(s)\mathbf{R}_{j,k}^{-1}(s-1) = \mathbf{M}_j^{(1)} + \mathbf{M}_{j,k}^{(2)}(s). \end{aligned}$$

Note that the matrix-functions of these representations satisfy the estimates $\mathbf{N}_{j,k}^{(2)}(it) = o(t^{-1/2})$, $\mathbf{M}_{j,k}^{(2)}(it) = o(t^{-1})$ as $t \to \infty$, but

$$\mathbf{N}_1^{(1)}(s) = \begin{pmatrix} \chi_+ & \chi_- \mathrm{tg}(\pi s/2) \\ -\chi_- & -\chi_+ \mathrm{tg}(\pi s/2) \end{pmatrix}, \qquad \mathbf{M}_1^{(1)} = \begin{pmatrix} \chi_+ & -\chi_- \\ -\chi_- & \chi_+ \end{pmatrix},$$

$$\mathbf{N}_2^{(1)}(s) = \frac{1}{2\varpi_\pm} \begin{pmatrix} 0 & 0 \\ 1 & \mp\mathrm{tg}(\pi s/2) \end{pmatrix}, \qquad \mathbf{M}_2^{(1)} = \frac{1}{2\mu_1 t_+ + \varpi_\pm} \begin{pmatrix} \varpi_\pm & 0 \\ 0 & 2\mu_1 t_+ \end{pmatrix};$$

$$\mathbf{N}_3^{(1)}(s) \equiv 0, \qquad \mathbf{M}_3^{(1)} = \frac{1}{\mu_1(t_+^2 - t_-^2)} \begin{pmatrix} t_+ & -t_- \\ -t_- & t_+ \end{pmatrix}.$$

Then substituting (5.23) in systems (5.20), and applying the inverse Mellin transform, we obtain the systems of integral equations:

(5.25) $[\mathcal{N}_j^{(1)}(\mathbf{Y} + \mathbf{Z})](\lambda) + [\mathcal{N}_{j,k}^{(2)}(\mathbf{Y} + \mathbf{Z})](\lambda)$

$$= [1 + \mu_1 \tau \lambda \mathbf{M}_j]\mathbf{V}(\lambda) + \mu_1 \tau [\mathcal{M}_{j,k}^{(2)}(\xi \mathbf{V}(\xi))](\lambda) + \mathbf{G}_0(\lambda),$$

where the operators $\mathcal{N}_j^{(1)}$, $\mathcal{N}_{j,k}^{(2)}$ are defined analogously to $\mathcal{M}_{j,k}^{(2)}$:

$$[\mathcal{M}_{j,k}^{(2)} u](\lambda) = \int_0^\infty \mathbf{M}_{j,k}^{(2)}(\lambda/\xi) u(\xi) d\xi/\xi, \qquad \mathbf{M}_{j,k}^{(2)}(t) = \frac{1}{2\pi i} \int_{-i\infty}^{i\infty} \mathbf{M}_{j,k}^{(2)}(s) t^s \, ds,$$

$$\mathcal{N}_1^{(1)} = \begin{pmatrix} \chi_+ I & \chi_- \mathcal{S}_1 \\ -\chi_- I & -\chi_+ \mathcal{S}_1 \end{pmatrix}, \qquad \mathcal{N}_2^{(1)} = \frac{1}{2\varpi_\pm} \begin{pmatrix} 0 & 0 \\ I & \mp\mathcal{S}_1 \end{pmatrix}, \qquad \mathcal{N}_3^{(1)} = 0.$$

Substituting then in (5.25) the vector-functions $\mathbf{Z}$, $\mathbf{Y}$ from relations (3.5), (5.15) and (5.21), and taking into account the fact that the matrix-function $\mathbf{K}_j(\lambda) = (1 + \lambda)[1 + \mu_1 \tau \lambda \mathbf{M}_j]^{-1}$ is nondegenerate in $\overline{\mathbb{R}}$, we obtain the systems of integral equations for the new vector-function $\mathbf{V}_*(\lambda) = (1 + \lambda)\mathbf{V}(\lambda)$:

(5.26) $[\mathcal{E}^{(j)}(\mathcal{J}^+, \mathcal{J}^-, \mathcal{J})\mathbf{V}_*](\lambda) = \mathbf{H}_{j,k}(\lambda), \qquad \mathcal{J}^\pm = 1, 2, \quad \mathcal{J} = 1, 3,$

where the operators $\mathcal{E}^{(j)}(\mathcal{J}^+, \mathcal{J}^-, \mathcal{J})$ and the vector-functions $\mathbf{H}_{j,k}$ are:

$$[\mathcal{E}^{(j)}(\mathcal{J}^+, \mathcal{J}^-, \mathcal{J})\mathbf{V}_*](\lambda) = \mathbf{V}_*(\lambda) + \mathbf{K}_j(\lambda) \left[\mathcal{M}_{j,k}^{(2)}(\xi(1 + \xi)^{-1}\mathbf{V}_*(\xi)) \right](\lambda)$$

$$- \mathbf{K}_j(\lambda) \left[\left(\mathcal{N}_j^{(1)} + \mathcal{N}_{j,k}^{(2)}\right) \left([1 + \mu_1 \xi M_p(\xi)]\mathcal{R}_{j,k}((1 + t)^{-1}\mathbf{V}_*(t))(\xi)\right) \right](\lambda),$$

$$\mathbf{H}_{j,k}(\lambda) = \mathbf{K}_j(\lambda)\left([(\mathcal{N}_j^{(1)} + \mathcal{N}_{j,k}^{(2)})H_0](\lambda) - \mathbf{G}_0(\lambda)\right),$$

$$H_0(\xi) = H_Z(\xi) + \frac{[1 + \mu_1 \xi M_p(\xi)] z_0^* \xi}{(1 + \xi^2)^2} \begin{pmatrix} 0 \\ 1 \end{pmatrix},$$

$$\mathbf{G}_0(\lambda) = \frac{1}{2\pi i} \int_{-i\infty}^{i\infty} \mathbf{R}_{j,k}(s) \mathbf{F}_Z^0(s) \lambda^s \, ds.$$

These equations can not be used in the case when the gradients of the solution are prescribed along the most external boundary Γ_n ($\mathcal{J} = 2$) (with respect to the layered part of the domain).

Solutions of equations (5.26) are sought in the spaces (see (5.19)):

$$(5.27) \qquad \mathbf{V}_* \in \mathbf{L}_2^{p,\alpha,\beta}(\mathbb{R}_+), \qquad -\gamma_1 < \alpha < 0, \qquad 0 < \beta < \delta;$$

besides, for the case $k = 1$ (conditions of the first kind $\mathcal{J}^\pm = 1$ are given along the external boundaries with respect to the wedges), the additional condition (5.20) should be true. Basing on the results known from [10], the symbols of the operators $\mathcal{E}^{(j)}(\mathcal{J}^+, \mathcal{J}^-, \mathcal{J})$ from (5.26) can be calculated:

$$\operatorname{Symb} \mathcal{E}^{(j)}(\mathcal{J}^+, \mathcal{J}^-, 1)\big|_{\mathbf{L}_2^{p,\alpha,\beta}}(t, \theta) = \left(\mathbf{M}_j^{(1)}\right)^{-1} \mathbf{M}_{j,k}(\beta - it)\frac{1-\theta}{2}$$

$$+ \left[\mathbf{I} - \mathbf{N}_{j,k}(\alpha - it)\mathbf{R}_{j,k}^{-1}(\alpha - it)\right]\frac{1+\theta}{2},$$

(5.28)

$$\operatorname{Symb} \mathcal{E}^{(j)}(\mathcal{J}^+, \mathcal{J}^-, 3)\big|_{\mathbf{L}_2^{p,\alpha,\beta}}(t, \theta) = \left(\mathbf{M}_j^{(1)}\right)^{-1} \mathbf{M}_{j,k}(\beta - it)\frac{1-\theta}{2}$$

$$+ \left[\mathbf{I} - \left(1 - \frac{\mu_1}{\mu_{n+1}}\right) \mathbf{N}_{j,k}(\alpha - it)\mathbf{R}_{j,k}^{-1}(\alpha - it)\right]\frac{1+\theta}{2},$$

where the matrix-functions $\mathbf{R}_{j,k}(s)$, $\mathbf{N}_{j,k}(s)$, $\mathbf{M}_{j,k}(s)$ are defined in (5.18), (5.24). As it follows from (5.24), the symbols of operators $\mathcal{E}^{(j)}(\mathcal{J}^+, \mathcal{J}^-, \mathcal{J})$ are not degenerate for the values of $j = 2, 3$, in contrast to the symbols of operators $\mathcal{C}^{(j)}(\mathcal{J}^+, \mathcal{J}^-, \mathcal{J})$ from (5.14). Moreover, one can see that the identities: $\det\left[\mathbf{I} - y\mathbf{N}_{j,k}(s)\mathbf{R}_{j,k}^{-1}(s)\right] = \det\left[\mathbf{I} - y\Phi_*^{-1}(s)\right]$, $\det\mathbf{M}_{j,k}(s) = -(s\operatorname{ctg}(\pi s/2))^{j-1} x_k^2(s)$ $\det\Phi_*^{-1}(s)$ are true for any $y \in \mathbb{R}$. Then the indices and pair indices of the corresponding operators $\mathcal{E}^{(j)}(\mathcal{J}^+, \mathcal{J}^-, \mathcal{J})$ in the spaces $\mathbf{L}_2^{p,\alpha,\beta}(\mathbb{R}_+)$ can be calculated:

$$\kappa(\alpha, \beta, \mathcal{J}^+, \mathcal{J}^-, 1) = \begin{cases} \operatorname{sign}\alpha - \operatorname{sign}\beta; & (\kappa_1 = \operatorname{sign}\alpha, \ \kappa_2 = -\operatorname{sign}\beta), & \mathcal{J}^+\mathcal{J}^- = 1, \\ \operatorname{sign}\alpha; & (\kappa_1 = \operatorname{sign}\alpha, \ \kappa_2 = 0), & \mathcal{J}^+\mathcal{J}^- = 2, \\ 0; & (\kappa_1 = \kappa_2 = 0), & \mathcal{J}^+\mathcal{J}^- = 4; \end{cases}$$

$$\kappa(\alpha, \beta, \mathcal{J}^+, \mathcal{J}^-, 3) = \begin{cases} -\operatorname{sign}\beta; & (\kappa_1 = 0, \ \kappa_2 = -\operatorname{sign}\beta), & \mathcal{J}^+\mathcal{J}^- = 1, \\ 0; & (\kappa_1 = \kappa_2 = 0), & \mathcal{J}^+\mathcal{J}^- > 1. \end{cases}$$

So, for the values of the parameters $\alpha < 0$, $\beta > 0$ as in (5.27), the indices and the partial indices of the operators are equal to zero or negative. In the last case there exists exactly $|\kappa|$ unknown parameters (z_0^* or (and) z_+^*) which are found from the additional condition (5.20) and the corresponding condition (2.11) together with (5.5). Note here, that only one of the conditions (2.11) is independent, when both external boundary conditions along the wedge surfaces are of the first type ($\mathcal{J}^+ = \mathcal{J}^- = 1$), because $z_*^- = 0$ in (5.5) for this case.

The remaining problems $(\mathcal{J}^+, \mathcal{J}^-, 2)$ for the second and the third combinations of the parameters $\tau_\pm$ $(j = 2, 3,$ see Lemma), which have not been considered as yet, can be investigated on the basis of systems (5.11), (5.12). The corresponding degenerate operators $\mathcal{C}^{(2)}(\mathcal{J}^+, \mathcal{J}^-, 2)$, $\mathcal{C}^{(3)}(\mathcal{J}^+, \mathcal{J}^-, 2)$ could be analyzed similarly to operators $\mathcal{B}^{(2)}$ $(\mathcal{J}^+, \mathcal{J}^-, 2)$ and $\mathcal{B}^{(3)}(\mathcal{J}^+, \mathcal{J}^-, 2)$ in Sec. 4.

Finally, the systems of integral equations (5.11), (5.12), (5.26) obtained under the general assumption $\tau > 0$ have been investigated for all problems $(\mathcal{J}^+, \mathcal{J}^-, \mathcal{J})$ $(\mathcal{J}^\pm = 1, 2, \mathcal{J} = 1, 2, 3)$ and for all values of the parameters $\tau_\pm \geq 0$. The values of parameters u_*, $v_\pm$ of the class $\mathbf{LW}(\Omega)$ have been found (see (5.5)), $\gamma_0 = 1$, $k = 1$, but the value of $\gamma_\infty = \min\{\gamma_1, \gamma_2\}$ is calculated from the symbols of the corresponding operators (as in the theorems presented in the previous section).

6. Conclusions

We have considered all different combinations of the external boundary conditions, and values of the parameters τ, $\tau_\pm \geq 0$ determining the interfacial conditions near the wedge tip. As it could be expected, the singularity of $\mathbf{grad}\, u$ near the wedge tip depends essentially on the models of the interface. Thus, if the model of interface is of the form: $\left([u] - r\tau_\pm \mu \dfrac{\partial u}{\partial n} \right)\bigg|_{\Gamma_\pm} = 0$, $\left[\mu \dfrac{\partial u}{\partial n} \right]\bigg|_{\Gamma_\pm} = 0$ (corresponding to the adhesive region represented by two thin wedges only), the main exponent of the singularity is in the interval $(-1, 0)$. It has the value close to that of the case of an "ideal" bimaterial contact for small values of the normed parameters $\mu_1^- \tau_1^-$, $\mu_l^+ \tau_l^+$. Besides, there is a second exponent in the interval $(-1, 0)$, which has the value near zero. Nevertheless, the corresponding term of the asymptotic expression should be also taken into account in the process of fracture mechanics analysis.

When the geometry of the adhesive is assumed to be of the general form $\left[\mu \dfrac{\partial u}{\partial n} \right]\bigg|_{\Gamma_\pm} = 0$, $\left([u] - (r\tau_\pm + \tau)\mu \dfrac{\partial u}{\partial n} \right)\bigg|_{\Gamma_\pm} = 0$, $(\tau, \tau_\pm > 0)$ or in the case of a thin layer only (where $\tau > 0$, $\tau_\pm = 0$), $\mathbf{grad}\, u$ increases in the neighbourhood of the wedge tip as $\ln r$ inside the domains Ω only. But inside the domains $\Omega_\pm$, the value of $\mathbf{grad}\,u$ is bounded as well as the normal derivative $\partial u / \partial n$ along the interface.

Note that the cases, when at least one of the parameters τ, $\tau_\pm$ is negative, are not considered in this paper. Such situations appear on the declining segment of curve $\varepsilon - \sigma$ and are often connected with a loss of stability of bodies in contact.

Let us remark that all the used functions $M_p(\lambda)$, $m_p^\pm(\lambda)$, $M_q(s)$, $M_r(s)$ can be effectively calculated by the recurrence formulae presented in Appendix A [12], and the asymptotics of these functions have been analytically obtained. Moreover, an effective way of finding the complex zeros of determinants of the

matrix-functions $\Phi_*(s)$ (and the symbols of the singular integral operators) has been proposed in [1].

In Appendix it is shown that the method developed makes it possible to solve not only Poisson's equations but also the equations of second order of a general form. It is only necessary that the method of integral (Fourier and Mellin) transforms could be applied to these equations. Hence, the results of [12] and this paper completely solve such problems under arbitrary boundary conditions.

Appendix

Consider similar problems for the following equations:

$$v_i \frac{\partial^2 u_i}{\partial x_1^2} + \frac{\partial}{\partial x_2} \mu_i \frac{\partial}{\partial x_2} u_i = -W_i, \qquad (x_1, x_2) \in \Omega_i,$$

(A.1) $\qquad v_j^+ \frac{\partial}{r \partial r} r \frac{\partial u_j^+}{\partial r} + \frac{\partial}{r^2 \partial \theta} \mu_j^+ \frac{\partial}{\partial \theta} u_j^+ = -W_j^+, \qquad (r, \theta) \in \Omega_j^+,$

$$v_k^- \frac{\partial}{r \partial r} r \frac{\partial u_k^-}{\partial r} + \frac{\partial}{r^2 \partial \theta} \mu_k^- \frac{\partial}{\partial \theta} u_k^- = -W_k^-, \qquad (r, \theta) \in \Omega_k^-,$$

instead of the equations (2.1). Here v_i, $\mu_i = v_i$, $\mu_i(x_2)$, $v_j^\pm, \mu_j^\pm = v_j^\pm, \mu_j^\pm(\theta)$, are known bounded positive functions. Without any loss of generality we can assume that:

(A.2) $\quad v_i, \mu_i \in \mathbf{C}^2(y_{i-1}, y_i), \qquad v_j^+, \mu_j^+ \in \mathbf{C}^2(\theta_{j-1}^+, \theta_j^+), \qquad v_k^-, \mu_k^- \in \mathbf{C}^2(\theta_{k-1}^-, \theta_k^-),$

and they can be extended to closed intervals.

All external and internal boundary conditions are prescribed in (2.2)–(2.9). Such problems can be solved by using the mentioned method. We shall find in this Appendix only the necessary conditions which make it possible to use the formulae given in [12] (Appendix A) in order to obtain the equations similar to (3.1).

Applying the Fourier and Mellin transforms in the corresponding regions we obtain:

$$-\lambda^2 v_i \overline{u}_i + \frac{\partial}{\partial x_2} \mu_i \frac{\partial}{\partial x_2} \overline{u}_i = -\overline{W}_i, \quad \lambda \in \mathbb{R}, \quad x_2 \in (y_{i-1}, y_i),$$

(A.3) $\quad v_j^+ s^2 \widetilde{u}_j^+ + \frac{\partial}{\partial \theta} \mu_j^+ \frac{\partial}{\partial \theta} \widetilde{u}_j^+ = -\widetilde{W}_j^+, \quad 0 < \Re s < \gamma_1, \quad \theta \in (\theta_{j-1}^+, \theta_j^+),$

$$v_k^- s^2 \widetilde{u}_k^- + \frac{\partial}{\partial \theta} \mu_k^- \frac{\partial}{\partial \theta} \widetilde{u}_k^- = -\widetilde{W}_k^-, \quad 0 < \Re s < \gamma_1, \quad \theta \in (\theta_{k-1}^-, \theta_k^-).$$

Let $p_i^\pm(\lambda, x_2)$, $q_j^\pm(s, \theta)$, $r_k^\pm(s, \theta)$ be the linear independent solutions of the corresponding homogeneous equations (A.3). Besides, these functions can be

chosen so that they will be even functions with respect to the new variables (λ, and s). Consider in details the solutions of the first equations.

From the VKB method [5] the behaviour of the functions $p_i^{\pm}(\lambda, x_2)$ for large values of the parameter λ can be justified:

$$(A.4) \qquad p_i^{\pm}(\lambda, x_2) = \frac{1}{\sqrt[4]{v_i(x_2)\mu_i(x_2)}}$$

$$\cdot \exp\left[\pm|\lambda| \int\limits_{y_{i-1}}^{x_2} \sqrt{\frac{v_i(\xi)}{\mu_i(\xi)}} d\xi\right] \left[1 + O(|\lambda|^{-1})\right], \qquad \lambda \to \infty,$$

uniformly with respect to $x_2 \in [y_{i-1}, y_i]$. These solutions can be found, for example, from the following initial (Cauchy) conditions:

$$p_i^{\pm}(\lambda, y_{\pm}) = \frac{B_i^{\pm}(\lambda)}{\sqrt[4]{v_i\mu_i}}\Big|_{y_{\pm}}, \qquad \frac{\partial}{\partial x_2} p_i^{\pm}(\lambda, y_{\pm}) = \frac{B_i^{\pm}(\lambda)}{\sqrt[4]{v_i\mu_i}} \left[\pm|\lambda|\sqrt{\frac{v_i}{\mu_i}} - \frac{(v_i\mu_i)'}{4v_i\mu_i}\right]\Big|_{y_{\pm}},$$

where $y_+ = y_{i-1}$, $y_- = y_i$, but

$$B_i^+(\lambda) \equiv 1, \qquad B_i^-(\lambda) = \exp\left[-|\lambda| \int\limits_{y_{i-1}}^{y_i} \sqrt{\frac{v_i(\xi)}{\mu_i(\xi)}} d\xi\right].$$

We can also obtain asymptotic expansions of these functions for small values of λ:

$$(A.5) \qquad p_i^{\pm}(\lambda, x_2) = \frac{B_i^{\pm}(\lambda)}{\sqrt[4]{v_i\mu_i}}\Big|_{y_{\pm}} \left[1 - \mu_i\left[\frac{(v_i\mu_i)'}{4v_i\mu_i}\right.\right.$$

$$\left.\left.\mp|\lambda|\sqrt{\frac{v_i}{\mu_i}}\right]\Big|_{y_{\pm}} \int\limits_{y_{\pm}}^{x_2} \frac{d\xi}{\mu_i(\xi)}\right] + O(\lambda^2), \qquad \lambda \to 0.$$

Consequently, the functions $p_i^{\pm}(\lambda, x_2)$ are absolutely continuous near points $(0, x_2)$, and are sufficiently smooth in any other points (λ, x_2) from the corresponding region ($|\lambda| \in \mathbb{R}_+$, $x_2 \in [y_{i-1}, y_i]$).

Now, we can write the solutions $\overline{u}_i(\lambda, x_2)$ of the first equations (A.1):

$$(A.6) \qquad \overline{u}_i(\lambda, x_2) = A_+ p_i^+(\lambda, x_2) + A_- p_i^-(\lambda, x_2)$$

$$-p_i^+(\lambda, x_2) \int\limits_{x_2}^{y_i} \frac{p_i^-(\lambda, \xi)\overline{W}_i(\lambda, \xi)}{\mu_i(\xi)W(p_i^+, p_i^-)(\lambda, \xi)} d\xi - p_i^-(\lambda, x_2) \int\limits_{y_{i-1}}^{x_2} \frac{p_i^+(\lambda, \xi)\overline{W}_i(\lambda, \xi)}{\mu_i(\xi)W(p_i^+, p_i^-)(\lambda, \xi)} d\xi,$$

where $W(p_i^+, p_i^-)(\lambda, x_2)$ is the corresponding Wronskian.

Following [12], denote functions

(A.7)
$$\mathbf{p}_t^i(\lambda) = \mu_i \frac{\partial}{\partial x_2} \overline{u}_i|_{r_i}, \qquad \mathbf{u}_t^i(\lambda) = \overline{u}_i|_{r_i},$$

$$\mathbf{p}_b^i(\lambda) = \mu_i \frac{\partial}{\partial x_2} \overline{u}_i|_{r_{i-1}}, \qquad \mathbf{u}_b^i(\lambda) = \overline{u}_i|_{r_{i-1}}, \qquad i = 1, 2, ..., n.$$

Then, substituting (A.6) in (A.7), and eliminating the constants $A_\pm$ from these equations, we obtain the relations between functions $\mathbf{u}_{t(b)}^i$ and $\mathbf{p}_{t(b)}^i$ in the form:

(A.8)
$$\begin{pmatrix} \mathbf{u}_t^i \\ \mathbf{u}_b^i \end{pmatrix} = \mathbf{R}_i(\lambda) \begin{pmatrix} \mathbf{p}_t^i \\ \mathbf{p}_b^i \end{pmatrix} + \begin{pmatrix} u_{t0}^i \\ u_{b0}^i \end{pmatrix}, \qquad \mathbf{R}_i(\lambda) = \begin{pmatrix} R_{tt}^i & R_{tb}^i \\ R_{bt}^i & R_{bb}^i \end{pmatrix},$$

where coefficients are calculated from the equations

$$\begin{pmatrix} u_{t0}^i \\ u_{b0}^i \end{pmatrix} = \left[\mathbf{R}_i(\lambda) \begin{pmatrix} \mu_i \frac{\partial}{\partial x_2} p_i^-(\lambda, y_i) & 0 \\ 0 & \mu_i \frac{\partial}{\partial x_2} p_i^+(\lambda, y_{i-1}) \end{pmatrix} \right.$$
$$\left. - \begin{pmatrix} p_i^-(\lambda, y_i) & 0 \\ 0 & p_i^+(\lambda, y_{i-1}) \end{pmatrix} \right] \begin{pmatrix} L_i^+ \\ L_i^- \end{pmatrix},$$

$$L_i^\pm(\lambda) = \int_{y_{i-1}}^{y_1} \frac{p_i^\pm(\lambda, \xi)\overline{W}_i(\lambda, \xi)}{\mu_i(\xi)W(p_i^+, p_i^-)(\lambda, \xi)} d\xi,$$

(A.9)
$$R_{bt}^i(\lambda) = -\frac{W(p_i^+, p_i^-)(\lambda, y_{i-1})}{\mu_i(y_i)D_0^{(i)}(\lambda)},$$

$$R_{bb}^i(\lambda) = \frac{D^{(i)}(\lambda, y_{i-1}, y_i)}{\mu_i(y_{i-1})D_0^{(i)}(\lambda)},$$

$$R_{tt}^i(\lambda) = -\frac{D^{(i)}(\lambda, y_i, y_{i-1})}{\mu_i(y_i))D_0^{(i)}(\lambda)},$$

$$R_{tb}^i(\lambda) = \frac{W(p_i^+, p_i^-)(\lambda, y_i)}{\mu_i(y_{i-1}))D_0^{(i)}(\lambda)}.$$

Finally, the functions $D^{(i)}(\lambda, a, b)$, $D_0^{(i)}(\lambda)$ are expressed in terms of the solutions $p_i^\pm(\lambda, x_2)$:

$$D^{(i)}(\lambda, a, b) = p_i^+(\lambda, a)\frac{\partial}{\partial x_2}p_i^-(\lambda, b) - p_i^-(\lambda, a)\frac{\partial}{\partial x_2}p_i^+(\lambda, b),$$

$$D_0^{(i)}(\lambda) = \frac{\partial}{\partial x_2}p_i^+(\lambda, y_{i-1})\frac{\partial}{\partial x_2}p_i^-(\lambda, y_i) - \frac{\partial}{\partial x_2}p_i^-(\lambda, y_{i-1})\frac{\partial}{\partial x_2}p_i^+(\lambda, y_i).$$

Hence, we can use all the results of Appendix A [12] in order to obtain the functions $M_p(\lambda)$, $m_p^\pm(\lambda)$ in the first relation of (3.1). For some functions $v_i(x_2)$, $\mu_i(x_2)$, the mentioned solutions $p_i^\pm(\lambda, x_2)$ can be calculated exactly (see for example [17]). Anyway, the functions $p_i^\pm(\lambda, x_2)$, and consequently, all functions from (A.8) as well $M_p(\lambda)$, $m_p^\pm(\lambda)$ can be numerically calculated. Moreover, their asymptotics at the zero and infinity points with respect to the variable λ, which play an important role in the process of investigation of the systems of functional-difference equations, can be analytically determined.

$$\mathbf{R}_i(\lambda) = \frac{1}{|\lambda|} \begin{pmatrix} [v_i\mu_i(y_i)]^{-1/2} & -2B_i^-(\lambda)[v_i\mu_i(y_{i-1})]^{-1/2} \\ 2B_i^-(\lambda)[v_i\mu_i(y_i)]^{-1/2} & -[v_i\mu_i(y_{i-1})]^{-1/2} \end{pmatrix}$$

$$\times \left(1 + O\left(\frac{1}{|\lambda|}\right)\right), \qquad \lambda \to \infty,$$

$$u_{i0}^i, \; u_{b0}^i = o(|\lambda|^{-1}B_i^-(\lambda)), \qquad \lambda \to \infty;$$

$$\mathbf{R}_i(\lambda) = \frac{1}{\lambda^2} \left[\int_{y_{i-1}}^{y_i} v_i(\xi)\,d\xi\right]^{-1} \begin{pmatrix} 1 & -1 \\ 1 & -1 \end{pmatrix} + O(1), \qquad \lambda \to 0,$$

$$u_{i0}^i, \; u_{b0}^i(\lambda) = \frac{1}{\lambda^2} \left[\int_{y_{i-1}}^{y_i} v_i(\xi)\,d\xi\right]^{-1} \int_{y_{i-1}}^{y_i} \overline{W}_i(0, \xi)\,d\xi + O\left(\frac{1}{|\lambda|}\right), \qquad \lambda \to 0.$$

In conclusion let us note that we can always obtain the solutions $p_i^\pm(\lambda, x_2)$ satisfying the relations (A.5), and belonging to the class $\mathbf{C}^\infty(\mathbb{R} \times (y_{i-1}, y_i))$ by correcting the Cauchy data (A.4). But this makes no sense, because the matrix-function $\mathbf{R}_i(\lambda)$ has always the singularity in zero point, and does not depend on the choice of the solutions $p_i^\pm(\lambda, x_2)$.

In the wedge regions the relations similar to (A.8) between Mellin transformations of the solution and the tractions are constructed in a similar manner. To this end it is sufficient to replace the corresponding functions $v_i(x_2)$, $\mu_i(x_2)$ by $v_j^\pm(\theta)$, $\mu_j^\pm(\theta)$; to substitute new variable $\lambda = is$; and to consider separately the real and the imaginary parts of the solutions. The corresponding results will not be presented here.

References

1. V.G. Blinova and A.M. Linkov, *A method to derive the main asymptotic terms near the tips of elastic wedges* [in Russian], Vestn., St Petersb. Univ., Ser 1, 2, 8, 69–72, 1992.

2. R.V. Duduchava, *Integral equations with fixed singularities*, Teubner-Texte zur Mathematik, Teubner, Leipzig 1979.

3. I.C. Gohberg and N.A. Feldman, *Equations in convolutions and projectional methods of solution* [in Russian], Nauka, Moscow, 352, 1971.

4. I.C. GOHBERG and M.G. KREIN, *Systems of integral equations on semi-axis with kernels dependent on the difference of the arguments* [in Russian], Usp. Mat. Nauk, **13**, 2, 3–72, 1958.

5. M.V. FEDORYUK, *Asymptotic methods for ordinary differential equations* [in Russian], Nauka, Moscow, 352, 1983.

6. I.YA. KRUPNIK, *Banach algebras with symbols and singular integral operators* [in Russian], "Shtiica", Kishinev, 137, 1984.

7. A.M. LINKOV and N. FILIPPOV, *Difference equations approach to the analysis of layered systems*, Mecchanica, 26, 195–209, 1991.

8. S.G. MIKHLIN, *Variational methods of mathematical physics* [in Russian], "Nauka", Moscow 1970.

9. S.G. MIKHLIN, N.F. MOROZOV and M.V. PAUKSHTO, *The integral equations of the theory of elastisity*, Teubner-Texte zur Mathematik, **135**, Stuttgart–Leipzig 1995.

10. G.S. MISHURIS and Z.S. OLESIAK, *On boundary value problems in fracture of elastic composites*, Euro. J. Appl. Math., **6**, 591–610, 1995.

11. G. MISHURIS, *On a class of singular integral equations*, Demonstratio Mathematica, **28**, 4, 781–794, 1995.

12. G.S. MISHURIS, *Boundary value problems for Poisson's equations in multi-wedge – multi-layered region*, Arch. Mech., **47**, 2, 295–335, 1995.

13. G. MISHURIS, *Influence of interfacial models on stress field near a crack terminating at a bimaterial interface*, Int. J. Solids and Structures, 1996 [to appear].

14. N.F. MOROZOV, *Mathematical problems of the crack theory* [in Russian], "Nauka", Moscow, 255, 1984.

15. S.A. NAZAROV, *Introduction to asymptotic methods of the theory of elasticity* [in Russian], Edition of the Leningrad State University, Leningrad 1983.

16. W. NOWACKI and Z.S. OLESIAK, *Thermodiffusion in solid bodies* [in Polish], Polish Scientific Publishers (PWN), Warszawa 1991.

17. M. OZTURK and F. ERDOGAN, *An axisymmetrical crack in bonded materials with a nonhomogeneous interfacial zone under torsion*, ASME J. Appl. Mech., **62**, 116–125, 1995.

18. S. PRÖSSDORF, *Einige Klassen singulärer Gleichungen*, Akademie–Verlag, Berlin, 493, 1974.

19. A.N. TIKHONOV and V.YA. ARSENIN, *Methods of solution of ill-posed problems* [in Russian], "Nauka", Moscow 1979.

DEPARTMENT OF MATHEMATICS,
RZESZÓW UNIVERSITY OF TECHNOLOGY, RZESZÓW.

Non-uniform extensional motions
of materially non-uniform simple solids

S. ZAHORSKI (WARSZAWA)

NON-UNIFORM EXTENSIONAL MOTIONS of materially non-uniform simple solids are considered in greater detail. These motions may be useful as applied to quasi-elongational motions with temperature and structure variations. In particular, the constitutive equations are discussed for steady drawing processes of polymer fibres.

1. Introduction

IN OUR PREVIOUS PAPER [1] the results valid for uniform motions with constant stretch history (MCSH) have been generalized to the case of non-uniform stagnant motions (NUSM) of materially non-uniform incompressible simple fluids. The coresponding constitutive equations are very similar to those known for MCSH.

In the present paper we discuss in greater detail the non-uniform extensional motions (hereafter called NUEM) of materially non-uniform simple solids [2]. Such motions deserve more attention since in many practical situations met in the rheology of polymers (drawing of fibres, non-uniform elongations, etc.), thermal and structural effects as well as nonlinear viscoelastic properties are of major importance (cf. [3]) and can be taken into account through the assumption of the proper material non-uniformity. In solids, in contrast to fluids, the deformation energy cannot be neglected and may, through the corresponding dissipation mechanisms, lead to temperature variations and, in consequence, to variable material properties (cf. [3]).

In what follows the non-uniform extensional motions (NUEM) are defined in general and steady-state cases. Next, the corresponding constitutive equations are discussed for materially non-uniform simple locally isotropic solids.

2. Non-uniform extensional motion (NUEM)

Consider a class of isochoric motions for which the deformation gradient at the current time t, relative to a configuration at time 0, is of the following diagonal form:

$$(2.1) \qquad \mathbf{F}_0(\mathbf{X}, \tau) = \begin{bmatrix} \lambda^{-1/2} & 0 & 0 \\ 0 & \lambda^{-1/2} & 0 \\ 0 & 0 & \lambda \end{bmatrix}, \qquad \det \mathbf{F}_0 = 1,$$

where the non-uniform stretch ratio $\lambda(\mathbf{X}, t)$ depends on time t as well as on the position $\mathbf{X}$ of a particle X in an arbitrarily chosen reference configuration κ (not necessarily at time 0). Thus, a non-uniformity of the quantities considered can be expressed either by $\mathbf{X}$ or X, $\mathbf{X} = \kappa(X)$. Such a motion may be called the non-uniform extensional motion (NUEM).

In general, we obtain the velocity gradient in the form:

$$(2.2) \qquad \mathbf{L}_1(\mathbf{X}, t) = \dot{\mathbf{F}}(\mathbf{X}, t)\mathbf{F}^{-1}(\mathbf{X}, t) = \begin{bmatrix} -\dfrac{1}{2}\dfrac{\dot{\lambda}}{\lambda} & 0 & 0 \\ 0 & -\dfrac{1}{2}\dfrac{\dot{\lambda}}{\lambda} & 0 \\ 0 & 0 & \dfrac{\dot{\lambda}}{\lambda} \end{bmatrix}.$$

If, in particular, the gradient (2.1) can be presented in an exponential form:

$$(2.3) \qquad \mathbf{F}_0(\mathbf{X}, \tau) = \exp(\tau \mathbf{L}(\mathbf{X})), \qquad \mathbf{L} = \mathbf{L}^T,$$

where τ denotes any past time and the diagonal tensor $\mathbf{L}(\mathbf{X})$ depends only on the position $\mathbf{X}$, we arrive at the definition of steady NUEM.

From Eq. (2.3), the deformation gradient relative to a configuration at the current time t amounts to

$$(2.4) \qquad \mathbf{F}_t(\mathbf{X}, t) = \mathbf{F}_0(\mathbf{X}, \tau)\mathbf{F}_0^{-1}(\mathbf{X}, t) = \exp(-s\mathbf{L}(\mathbf{X})), \qquad \tau = t - s,$$

leading to the following time-independent velocity gradient:

$$(2.5) \qquad \mathbf{L}_1(\mathbf{X}) = \frac{\partial}{\partial \tau}\mathbf{F}(\mathbf{X}, \tau)\bigg|_{\tau=t} = \mathbf{L}(\mathbf{X}).$$

Therefore, for steady NUEM we can write

$$(2.6) \qquad \mathbf{L}_1(\mathbf{X}) \equiv \mathbf{L}(\mathbf{X}) = \begin{bmatrix} -\dfrac{1}{2}V' & 0 & 0 \\ 0 & -\dfrac{1}{2}V' & 0 \\ 0 & 0 & V' \end{bmatrix},$$

where $V'(\mathbf{X})$ formally denotes the z-component of the velocity gradient.

Equations (2.3) and (2.4) lead to the following expressions for the left Cauchy–Green deformation tensor $\mathbf{B}$ and the history of right relative deformation tensor $\mathbf{C}_t^t$ (cf. [4]):

$$(2.7) \qquad \mathbf{B}(\mathbf{X}, t) = \mathbf{F}_0(\mathbf{X}, t)\mathbf{F}_0^T(\mathbf{X}, t) = \exp(t\mathbf{L}(\mathbf{X})\exp(t\mathbf{L}^T(\mathbf{X})),$$

$$(2.8) \qquad \mathbf{C}_t^t(\mathbf{X}, s) \equiv \mathbf{C}_t(\mathbf{X}, t - s) = \mathbf{F}_t^T(\mathbf{X}, t - s)\mathbf{F}_t(\mathbf{X}, t - s)$$
$$= \exp(-s\mathbf{L}^T(\mathbf{X}))\exp(-s\mathbf{L}(\mathbf{X})),$$

respectively. The above expressions can be simplified a little since the tensors $L(X)$ are diagonal by assumption.

3. Constitutive equations of materially non-uniform simple isotropic solids

According to our remarks, at the beginning we assume that *a priori* unknown temperature and structure distributions lead to a material non-uniformity, i.e. to the fact that all the functionals, functions and material constants depend on the position X and vary from particle to particle or from place to place.

The general constitutive equations of materially non-uniform simple isotropic solids (cf. [2, 4]) can be expressed as

$$(3.1) \qquad T(X,t) = \underset{s=0}{\overset{\infty}{\mathcal{H}}}_{\kappa}\left(C_t^t(X,s), B(X,t), X\right),$$

where T is the non-uniform stress-tensor, $\mathcal{H}_{\kappa}$ denotes the non-uniform constitutive functional depending on the reference configuration κ and the tensors C_t^t and B have been defined by Eqs. (2.7) and (2.8). In the case of incompressible materials, the stress tensor T should be replaced by the corresponding extra-stress tensor T_E.

It can be proved that the constitutive equations (3.1) are in agreement with the principles of determinism and local action. They also satisfy the principle of objectivity (invariance with respect to the reference frame), if the group of material isotropy (symmetry) is equivalent to the full orthogonal group (cf. [2, 4]). A non-uniform material may be considered to be globally isotropic if there exists the configuration κ at which its isotropy group is the same for all the particles. In other words, in a globally isotropic non-uniform solid all possible directions of deformation are equivalent while its material properties vary from particle to particle.

For steady NUEM defined by Eq. (2.3), after introducing Eqs. (2.7), (2.8) into Eq. (3.1) and taking into account the properties of tensor exponentials, i.e.

$$(3.2) \qquad \exp A = \sum_{n=0}^{\infty} \frac{1}{n!} A^n,$$

we arrive at

$$(3.3) \qquad T(X,t) = \underset{s=0}{\overset{\infty}{\mathcal{H}}}_{\kappa}\left(\exp(-2sL(X)), \exp(2tL(X)), X\right) = h(L(X), B(X,t), X),$$

where h denotes an isotropic function of the tensor arguments. In particular, instead of $L(X)$, the first Rivlin–Ericksen kinematic tensor $A_1 = 2L$ can be used.

Various reprtesentations of Eqs. (3.3) can be constructed in the usual way. For instance, we have

$$(3.4) \quad \mathbf{T}(\mathbf{X}, t) = \alpha(\mathbf{L}(\mathbf{X}), \mathbf{X}, I_B)\mathbf{1} + \alpha_1(\mathbf{L}(\mathbf{X}), \mathbf{X}, I_B)\mathbf{B}(\mathbf{X}, t)$$
$$+ \mathbf{B}(\mathbf{X}, t)\beta_1(\mathbf{L}(\mathbf{X}), \mathbf{X}, I_B) + \mathbf{B}^2(\mathbf{X}, t)\beta_2(\mathbf{L}(\mathbf{X}), \mathbf{X}, I_B) + \alpha_2(\mathbf{L}(\mathbf{X}), \mathbf{X}, I_B)\mathbf{B}^2(\mathbf{X}, t),$$

where the material (tensor) coefficients depend on the velocity gradient $\mathbf{L}(\mathbf{X})$, the invariants of tensor $\mathbf{B}$, and explicitly on the position $\mathbf{X}$.

4. Application to steady non-uniform drawing of materially non-uniform polymer fibres

In the case of drawing of solid polymer fibres (cf. [3]), we may assume that, under a quasi-elongational approximation, the deformation gradient as well as the velocity gradient are of the form (2.1) and (2.6), respectively, with

$$(4.1) \qquad \lambda = \frac{V}{V_0}, \qquad \dot{\varepsilon} = \ln \lambda, \qquad \dot{\varepsilon} = \frac{\dot{\lambda}}{\lambda} = \frac{\lambda'}{\lambda}V = V',$$

where $V(z)$ denotes the axial velocity depending on the spatial position z, and the primes denote differentiation with respect to z. The possibility of replacement of the particle position $\mathbf{X}$ by its place in space $\mathbf{x}$ (or rather z) results from the assumption that the motion considered is steady; then the reference configuration can be chosen at the current time t.

Under the above assumption, Eqs. (3.3) lead to the following stress difference:

$$(4.2) \qquad T^{33} - T^{11} = \sigma(V, V'; z) = \sigma_1(\lambda, \lambda'; z) = \sigma_2(\varepsilon, \dot{\varepsilon}; z).$$

Thus, in the case of non-uniform drawing of solid polymer fibres, the corresponding elongational stress may depend at most on the velocity and its axial gradient or on the strain and its time-derivative, respectively.

It is worth noting that the constitutive equations desribing drawing processes of polymer fibres were also considered by Coleman [5]. He proposed the particular approximate form

$$(4.3) \qquad T = \tau(\lambda) + \beta(\lambda)\lambda'^2 + \gamma(\lambda)\lambda'',$$

where λ is the stretch ratio. A simple comparison of the above equation with $(4.2)_2$ shows that our equation is pretty general since it admits arbitrary dependence on λ and λ', and explicitly on z. Equation (4.3), however, shows a particular dependence on λ' and moreover on λ''.

5. Conclusions

The concept of non-uniform extensional motions (NUEM) of materially non-uniform simple locally isotropic solids leads, in the case of steady motions, to the constitutive equations in a form of isotropic function of the deformation gradient and the velocity gradient, depending explicitly on the position of a particle.

For drawing processes of solid polymer fibres, a simplified form of the constitutive equations depending on the velocity, its axial gradient and the place along the fibre axis may be very useful.

References

1. S. ZAHORSKI, *Non-uniform stagnant motions of materially non-uniform simple fluids*, Arch. Mech., **48**, 3, 577–582, 1996.
2. C. TRUESDELL, *A first course in rational continuum mechanics*, The Johns Hopkins University, Baltimore 1982.
3. A. ZIABICKI, *Fundamentals of fibre formation. The science of fibre spinning and drawing*, Wiley, London 1976.
4. S. ZAHORSKI, *Mechanics of viscoelastic fluids*, Martinus Nijhoff, The Hague 1982.
5. B.D. COLEMAN, *Necking and drawing in polymeric fibres under tension*, Arch. Rat. Mech. Anal., **83**, 115–137, 1983.

POLISH ACADEMY OF SCIENCES
INSTITUTE OF FUNDAMENTAL TECHNOLOGICAL RESEARCH

Outlooks in Saint Venant theory
Part II. Torsional rigidity, shear-stress "and all that" in the torsion of cylinders with section of variable thickness

F. DELL'ISOLA and L. ROSA (ROMA)

WE EXTEND the perturbative procedure developed in [7] to the case of Saint Venant Cylinders with sections of variable thickness. In this way we are able to generalize the Kelvin and Bredt formulas for torsional rigidity of open and closed sections, respectively. We recover all the results available in technical literature. In particular we deduce an explicit analytical expression for warping function in the cases of open sections of triangular shape [17] and of the closed section studied using numerical methods by WANG [18].

1. Introduction

IN A RECENT PAPER [7] the authors tried to use a "perturbative development" [5] to generalize the well known Bredt formulas in the theory of thin hollow elastic beams. This development is possible for sections of the Saint Venant Cylinders (SVC) constructed from a given curve (the mean curve) as the union of its homotopic curves. The perturbation parameter ε is related to the thickness of the sections. However in [7] the particular homotopic transformation used allows only for the consideration of sections of constant thickness.

Here we want to overcome this limitation by generalizing the results found in [3] and use a similar procedure, but allowing the homotopic transformation to shift along the normal and the tangent directions both depending on the curvilinear coordinate along the inner curve of the sections.

We recover all the classical formulas found by BREDT [1] (see also VLASOV [2]) considering terms of first order in ε in the development. The new procedure we propose in the present paper is general enough to be applied, for instance, to SVC whose doubly connected cross-sections are bounded by ellipses, the case being out of the scope of applicability of the previous ones. In this way we can check our perturbation method on the exact solutions (available in the literature, see [4]) of Saint Venant torsion problem for the homothetic elliptic cross-sections. Moreover, we can give an approximate expression for the warping field in the case of the tubolar section of WANG (cf. [18]) and for the thin isosceles triangle [17].

For the reasons expounded in DELL'ISOLA and RUTA [7] we choose to state the Saint Venant torsion problem in terms of the Prandtl stress function ϕ.

Let $\mathcal{D}$ be the cross-section of the SVC, and let us distinguish two cases: closed sections and open sections. In both cases D can be represented as fol-

lows: $\mathcal{D} = \mathcal{D}_1 \backslash \mathcal{D}_0$, where $\mathcal{D}_i$, $i = 0, 1$, are simply connected domains, $\mathcal{D}_0 \subset \mathcal{D}_1$ and $\partial \mathcal{D}_0 \cap \partial \mathcal{D}_1 = \emptyset$ but, in the case of open sections we have $D_0 = \emptyset$.

Prandtl function ϕ is the solution of the following elliptic boundary value problem:

$$\Delta \phi + 2 = 0 \quad \text{in} \ \mathcal{D} \subset \Pi,$$

$$\phi = 0 \quad \text{on} \ \partial \mathcal{D}_1,$$

(1.1)

$$\phi = \overline{\phi} \quad \text{on} \ \partial \mathcal{D}_0,$$

$$\oint_{\partial \mathcal{D}_0} \nabla \phi \cdot n = -2 A_{\partial \mathcal{D}_0}.$$

Here Π is a plane, Δ is the Laplace operator, ∇ is the gradient operator, n is the outer normal of the domain $\mathcal{D}_0$, and $A_{\partial \mathcal{D}_0}$ is its area. The value of ϕ on $\partial \mathcal{D}_0$, $\overline{\phi}$, is an arbitrary constant to be determined from the integral condition $(1.1)_4$.

We will assume that the Prandtl function ϕ [6] can be expanded in terms of ε:

$$\phi = \sum_{k=0}^{\infty} \phi_k \varepsilon^k$$

(1.2)

in this way we get a hierarchy of ordinary differential equations for the coefficient ϕ_k, which allow us to generalize the well-known Bredt formulas.

Once we have found the expansion for the Prandtl function, we can calculate the corresponding one for the torsional rigidity R, the warping w and the tangent stress t using the following formulas [8, 9, 10]:

$$R = 2G \int_{\mathcal{D}_1} \phi + A_{\partial \mathcal{D}_0} \overline{\phi},$$

(1.3)

$$\nabla w(y) = -\tau \left(*\nabla \phi(y) + *(y - o) \right), \qquad t = -G\tau *\nabla \phi,$$

where $o \in \Pi$, $*$ is the $\pi/2$-rotation operator in Π, $y \in \mathcal{D}$, G is the modulus of elasticity in shear and τ is the angle of twist.

To this end, we will try the formal expansions also of all the other quantities appearing in the Saint Venant torsion theory in terms of the small parameter ε (for an accurate analysis of these slightly heuristic procedure see NAYFEH [5]):

$$(1.4) \qquad R = \sum_{n=0}^{\infty} R_n \varepsilon^n, \qquad w(s, z) = \sum_{n=0}^{\infty} w_n(s, z) \varepsilon^n, \qquad t(s, z) = \sum_{n=0}^{\infty} t_n(s, z) \varepsilon^n,$$

thus obtaining, in a very straightforward manner, all the known formulas of the technical theories as terms of the first order in ε. We can find all the terms of higher order in ε and here we quote the next non-zero corrections to these.

2. Families of cross-sections

Let $\Gamma_0 : [0, l] \to \Pi$ be the curve of equation

(2.1) $$r_0 : s \mapsto r_0(s).$$

We will consider two cases: closed sections and open sections. In the first case we will identify the two extrema $0 \sim l$ (we will identify s with the arc-length of the curve Γ_0, thus l will be the length of Γ_0).

Starting from Γ_0, we will consider a family of domains, parameterized by ε. The domain D_ε is obtained as the union of the curves Γ_z: $s \in [0, l] \to \Pi$, with $z \in [0, 1]$, z-lifted from Γ_0 by the scalar fields (δ_1, δ_2): $\left(f_{,x} = \dfrac{df(x)}{dx} \right)$

(2.2) $$r(s, z) = r_0(s) + z\varepsilon \left(\delta_1(s) r_{0,s} - \delta_2(s) * r_{0,s}(s) \right), \qquad D_\varepsilon = \bigcup_{z \in [0,1]} (\Gamma_z).$$

In this way $\partial \mathcal{D} := \Gamma_0 \bigcup \Gamma_1$ for closed sections while, of course, in the case of open sections we cannot obtain, by means of this procedure, the whole boundary of the domain D because we loose the edges z-lifted from the two distinct points $0, l$.

For these reasons we must assume that for open section the expansion is valid only far away from the ending edges. The expansion we obtain in this paper is an "outer" expansion to be matched with an "inner" one (see NAYFEH [5]) accounting for some edge effect.

We can think of $\delta(s) = \sqrt{\delta_1^2 + \delta_2^2}$ as of a thickness of the section in the point of coordinate s measured along Γ_0, and we will call $(\Gamma_0, \delta_1(s), \delta_2(s))$ the "shape" of the section.

In the following we will consider the cylinder of section $\mathcal{D} = \mathcal{D}_1 \backslash \mathcal{D}_0$ whose boundary is $\partial \mathcal{D} = \Gamma_0 \bigcup \Gamma_1$. Γ_0 is a closed curve for closed SVC sections and an open curve for open SVC sections. In the latter case we have $\mathcal{D}_0 = \emptyset$.

Considering the couple (s, z) as a coordinate system on D_ε, we get the following holonomic basis (when not necessary we omit the explicit s-dependence of the various functions)

(2.3)
$$e_1(s, z) = \frac{\partial r}{\partial s} = r_{0,s} \left(1 + z\varepsilon(\delta_{1,s} + \delta_{2,s}K) \right) + z\varepsilon * r_{0,s}(K\delta_1 - \delta_{2,s}),$$

$$e_2(s, z) = \frac{\partial r}{\partial z} = \varepsilon(r_{0,s}\delta_1 - *r_{0,s}\delta_2)$$

($K(s)$ is the curvature of Γ_0, $i = 1, 2$) and the following metric-tensor:

(2.4) $$g^{ij} = \frac{1}{g} \left(\begin{array}{c} \varepsilon^2(\delta_1^2 + \delta_2^2) \\ -(\varepsilon\delta_1 + z\varepsilon^2(\delta_1\delta_{1,s} + \delta_2\delta_{2,s})) \\ \qquad\qquad -(\varepsilon\delta_1 + z\varepsilon^2(\delta_1\delta_{1,s} + \delta_2\delta_{2,s})) \\ \qquad (1 + z\varepsilon(\delta_{1,s} + K\delta_2))^2 + z^2\varepsilon^2(\delta_{2,s} - K\delta_{1,s})^2 \end{array} \right),$$

where $g = \varepsilon^2 \left[\varepsilon z \left(\delta_1\delta_{2,s} - \delta_{1,s}\delta_2 - K(\delta_1^2 + \delta_2^2)\right) - \delta_2\right]^2$ is the determinant of the metric tensor.

For the sake of completeness we quote here the expression of the gradient and Laplacian that will be used in the following [11, 12]:

(2.5)
$$\nabla\phi = g^{ij}\phi_{,i}e_j\,,$$

$$\Delta\phi = g^{ij}\left(\frac{\partial^2\phi}{\partial x^i\partial x^j} - \frac{\partial\phi}{\partial x^h}\begin{Bmatrix} h \\ i\,j \end{Bmatrix}\right) = \frac{1}{\sqrt{g}}\left(\frac{\partial}{\partial x_i}\sqrt{g}g^{ij}\phi_{,i}\right),$$

$\begin{Bmatrix} h \\ i\,j \end{Bmatrix}$ are the Christoffel symbols, $i, j, h = 1, 2$; $x_1 = s$, $x_2 = z$.

3. Formal expansion of the Prandtl function

Using (1.2) and (2.5)$_2$ Eq. (1.1) becomes:

(3.1)
$$\sum_{n=0}^{\infty}\Big\{\ \varepsilon^n A\phi_{n,zz}$$
$$+ \varepsilon^{n+1}\left(B_1\phi_{n,z} + B_2\phi_{n,zz} + B_3\phi_{n,sz}\right)$$
$$+ \varepsilon^{n+2}\left[C_1\phi_{n,z} + C_2\phi_{n,zz} + C_3\phi_{n,s} + C_4\phi_{n,sz} + C_5\phi_{n,ss}\right]$$
$$+ \varepsilon^{n+3}\left[D_1\phi_{n,z} + D_2\phi_{n,zz} + D_3\phi_{n,s} + D_4\phi_{n,sz} + D_5\phi_{n,ss}\right]\Big\}$$
$$= -2\varepsilon^2\left[\varepsilon z\left(\delta_1\delta_{2,s} - \delta_{1,s}\delta_2 - K(\delta_1^2 + \delta_2^2)\right) - \delta_2\right]^3.$$

Here

$A = -\delta_2\,,$

$B_1 = K(\delta_1^2 - \delta_2^2) - 2\delta_1\delta_{2,s}\,,$

$B_2 = z\delta_1\delta_{2,s} - 3z\delta_2\delta_{1,s} - 3zK\delta_2^2 - zK\delta_1^2\,,$

$B_3 = 2\delta_1\delta_2\,,$

$C_1 = z\Big(-2K^2(\delta_1^2\delta_2 + \delta_2^3) - K(\delta_1^2\delta_{1,s} + 3\delta_2^2\delta_{1,s} + 2\delta_1\delta_2\delta_{2,s}) - 2\delta_1\delta_{1,s}\delta_{2,s} - 2\delta_2\delta_{2,s}^2$
$$\qquad - K_{,s}\left(\delta_1^3 + \delta_1\delta_2^2 + \delta_1^2\delta_{2,ss} + \delta_2^2\delta_{2,ss}\right)\Big),$$

$C_2 = z^2\Big(-3K^2\delta_2(\delta_1^2 + \delta_2^2) - \delta_{1,s}K(2\delta_1^2 - 6\delta_2^2) + \delta_{1,s}(-3\delta_{1,s}\delta_2 + 2\delta_1\delta_{2,s})$
$$\qquad + \delta_2\delta_{2,s}(4\delta_1 K - \delta_{2,s})\Big),$$

$C_3 = \delta_1\left(2\delta_1\delta_{2,s} - \delta_1^2 K - \delta_2^2 K - 2\delta_2\delta_{1,s}\right),$

$C_4 = 2z\left(\delta_1^3 K + \delta_1\delta_2^2 K + 2\delta_1\delta_2\delta_{1,s} - \delta_1^2\delta_{2,s} + \delta_2^2\delta_{2,s}\right),$

$$C_5 = -\delta_1^2 \delta_2 - \delta_2^3,$$

$$D_1 = -z^2 \left(\delta_1^2 + \delta_2^2\right) \delta_1^2 k^3 - \delta_2^2 K^3 - 3\delta_2 \delta_{1,s} K^2 - 2\delta_{1,s}^2 K + 3\delta_1 \delta_{2,s} K^2 - 2\delta_{2,s}^2 K$$
$$- \left(\delta_1 \delta_{1,s} + \delta_2 \delta_{2,s}\right) K_{,s} + \delta_1 \delta_{1,ss} K - \delta_{1,ss} \delta_{2,s} + \delta_2 \delta_{2,ss} K + \delta_{1,s} \delta_{2,ss},$$

$$D_2 = z^3 \left(-\delta_1^4 K^3 - 2\delta_1^2 \delta_2^2 K^3 - \delta_2^4 K^3 - 3\delta_1^2 \delta_{1,s} \delta_2, K^2 - 3\delta_2^3 \delta_{1,s} K^2 - \delta_1^2 \delta_{1,s}^2 K\right.$$
$$-3\delta_{1,s}^2 \delta_2^2 K - \delta_{1,s}^3 \delta_2 + 3\delta_1^3 \delta_{2,s} K^2 + 3\delta_1 \delta_2^2 \delta_{2,s} K^2 + 4\delta_1 \delta_2 \delta_{1,s} \delta_{2,s} K$$
$$\left. + \delta_1 \delta_{1,s}^2 \delta_{2,s} - 3\delta_1^2 \delta_{2,s}^2 K - \delta_2^2 \delta_{1,s} \delta_{2,s}^2 + \delta_2^2 \delta_{2,s}^2 K + \delta_1 \delta_{2,s}^3\right),$$

$$D_3 = z \left(-2\delta_1 \delta_{1,s}^2 \delta_2 + 2\delta_1^2 \delta_{1,s} \delta_{2,s} - 2\delta_{1,s} \delta_{2,s} \delta_2^2 + 2\delta_1 \delta_2 \delta_{2,s}^2 + \delta_1^4 K_{,s} + 2\delta_1^2 \delta_2^2 K_{,s}\right.$$
$$\left. + \delta_2^4 K_{,s} + \delta_1^2 \delta_2 \delta_{1,ss} + \delta_{1,ss} \delta_2^3 - \delta_1^3 \delta_{2,ss} - \delta_1 \delta_2^2 \delta_{2,ss}\right),$$

$$D_4 = 2z^2 \left(\delta_1^2 K + \delta_2^2 K + \delta_{1,s} \delta_2 - \delta_1 \delta_{2,s}\right) \left(\delta_1 \delta_{1,s} + \delta_2 \delta_{2,s}\right),$$

$$D_5 = z \left(\delta_1^2 + \delta_2\right) \left(-\delta_1^2 K - \delta_2^2 K + \delta_1 \delta_{2,s} - \delta_{1,s} \delta_2\right).$$

3.1. Closed section

Noticing that $(2.5)_1 \ \nabla\phi \cdot n|_{z=0} = -\dfrac{\delta_1}{\delta_2}\phi_{,s} + \dfrac{1}{\delta_2}\phi_{,z}$ and using (1.2), we get for condition $(1.1)_4$

$$\text{(3.2)} \qquad \sum_{n=0}^{\infty} \varepsilon^n \oint_{\Gamma_0} \left\{-\varepsilon\frac{\delta_1}{\delta_2}\phi_{,s} + \frac{1}{\delta_2}\phi_{,z}\right\} = -2\varepsilon A_0.$$

In this way we get for the first three terms of the ε-expansion of the Prandtl function:

$$\phi_{0,zz}(z,s) = 0, \qquad \phi_0(0,s) = \overline{\phi}_0,$$
$$\phi_0(1,s) = 0, \qquad \oint_{\Gamma_0} \frac{1}{\delta_2}\overline{\phi}_0 = 0,$$

$$\phi_{1,zz}(z,s) = 0, \qquad \phi_1(0,s) = \overline{\phi}_1,$$
$$\text{(3.3)} \qquad \phi_1(1,s) = 0, \qquad \oint_{\Gamma_0} \frac{1}{\delta_2}\overline{\phi}_1 = 2A_0,$$

$$A\phi_{2,zz} + B_1\phi_{1,z} = 2\delta_2^3, \qquad \phi_2(0,s) = \overline{\phi}_2,$$
$$\phi_2(1,s) = 0, \qquad \oint_{\Gamma_0} \frac{1}{\delta_2}\overline{\phi}_2 = -\oint_{\Gamma_0} \frac{A_0}{I_0}J - \delta_2,$$

with $I_0 = \displaystyle\oint_{\Gamma_0} \delta_2^{-1}$, $I(s) = \displaystyle\int_0^s \delta_2^{-1}$, $J = \dfrac{2\delta_1 \delta_{2,s} + \left(\delta_2^2 - \delta_1^2\right)K}{\delta_2^2}.$

Solving Eqs. (3.3) we get

$$\phi_0(s, z) = 0, \qquad \phi_1(s, z) = \frac{2A_0}{I_0}(1 - z),$$

(3.4)

$$\phi_2(s, z) = \frac{(1 - z)}{I_0}\left\{\oint_{\Gamma_0} \delta_2 - \frac{A_0}{I_0}\oint_{\Gamma_0} J\right\} + (z^2 - z)\frac{2A_0}{I_0}\left\{J - 2\delta_2^2\right\}.$$

3.2. Open sections

In this case we have (up to ε^4)

$$\phi_{0,zz}(z, s) = 0, \qquad \phi_0(0, s) = 0, \qquad \phi_0(1, s) = 0,$$

$$\phi_{1,zz}(z, s) = 0, \qquad \phi_1(0, s) = 0, \qquad \phi_1(1, s) = 0,$$

(3.5)
$$A\phi_{2,zz} = 2\delta_2^3, \qquad \phi_2(0, s) = 0, \qquad \phi_2(1, s) = 0,$$

$$A\phi_{3,zz} - B_1\phi_{2,z} + B_2\phi_{2,zz} + B_3\phi_{2,sz} = 6z\delta_2^2\left[\delta_2\delta_{1,s} - \delta_1\delta_{2,s} + K(\delta_2^2 + \delta_1^2)\right],$$

$$\phi_3(0, s) = 0, \qquad \phi_3(1, s) = 0,$$

from which

(3.6)
$$\phi_0 = 0, \qquad \phi_1 = 0, \qquad \phi_2 = \delta_2^2(z - z^2),$$

$$\phi_3 = \frac{1}{6}g(s)(z^3 - z) + \frac{1}{2}f(s)(z^2 - z),$$

with the following notations:

$$g(s) = -\delta_2\left[6\delta_{2,s}\delta_1 + 2K(\delta_1^2 + \delta_2^2)\right], \qquad f(s) = \delta_2\left[6\delta_{2,s}\delta_1 + K(\delta_2^2 - \delta_1^2)\right].$$

4. Torsional rigidity, warping and shear stress

Using formulas (1.3) and the expansions (1.4), we obtain the following results.

4.1. Closed sections

$$R_0 = 0, \qquad R_1 = \frac{4GA_0^2}{I_0},$$

(4.1)

$$R_2 = \frac{4GA_0}{I_0^2}\left\{I_0\oint_{\Gamma_0} \delta_2 - \frac{A_0}{2}\oint J\right\}.$$

For the warping

$$\frac{w_0(s,z)}{\tau} = 2A_0 \frac{I(s)}{I_0} - \int_0^s r_0 \times r_{0,s},$$

(4.2)
$$\frac{w_1(s,z)}{\tau} = \frac{A_0}{I_0} \int_0^s J\delta_2^2 + \frac{I(s)}{I_0} \left\{ \oint_{\Gamma_0} \delta_2 - \frac{A_0}{I_0} \oint_{\Gamma_0} J \right\} - \int_0^s \delta_2$$

$$+ z \left\{ 2\frac{A_0}{I_0}\frac{\delta_1}{\delta_2} - \delta_1 * r_0 \cdot r_{0,s} + \delta_2 r_0 \cdot r_{0,s} \right\},$$

and finally for the tangential stress

$$\frac{t_0(s,z)}{G\tau} = \left(\frac{t_{0s}}{G\tau}, \frac{t_{0z}}{G\tau} \right) = \left(2A_0 \frac{I_0}{\delta_2}, 0 \right),$$

(4.3)
$$\left(\frac{t_{1s}}{G\tau}, \frac{t_{1z}}{G\tau} \right) = \left(2\frac{A_0}{I_0} [J/2 + z(\delta_2\delta_{1,s} - \delta_1\delta_{2,s})] + \delta_2(2z-1) \right.$$

$$\left. + \frac{1}{\delta_2 I_0} \left\{ \oint_{\Gamma_0} \delta_2 - \frac{A_0}{I_0} \oint_{\Gamma_0} J \right\}, \ 2\delta_1 A_0 \frac{I_0}{\delta_2} \right).$$

The values R_1, w_0 and t_0 are the usual ones quoted in the literature [14, 15, 16]; they are due to BREDT [1]. We emphasize that for the rather general cross-sections considered here, the first non-zero contribution to the z–component of the shearing stress is of the first order in ε. This means that the procedure proposed by Bredt in deducing his formulas (in which this z-component is assumed as vanishing), cannot be applied for the sections considered in the present paper, being valid only for the class of sections dealt with in [7].

4.2. Open sections

We find for the torsional rigidity:

$$R_0 = 0, \qquad R_1 = 0,$$

$$R_2 = 0, \qquad R_3 = \frac{G}{3} \oint_{\Gamma_0} \delta_2^3,$$

(4.4)
$$R_4 = \frac{1}{12} \oint_{\Gamma_0} \left\{ \delta_2^2 \left[\delta_{1,s}\delta_2 - \delta_{2,s}\delta_1 + K(\delta_1^2 + \delta_2^2) \right] \right\}$$

$$- \frac{1}{12} \oint_{\Gamma_0} \delta_2 \left(f(s) + \frac{g(s)}{2} \right).$$

For the warping

(4.5)
$$\frac{w_0(s, z)}{\tau} = -\int_0^s r_0 \times r_{0,s},$$

$$\frac{w_1(s, z)}{\tau} = z \left(r_0 \cdot r_{0,s} \delta_2 - r_0 \times r_{0,s} \delta_1 \right) - \int_0^s \delta_2,$$

and finally for the tangential stress

(4.6)
$$\frac{t_0(s, z)}{G\tau} = \left(\frac{t_{0s}}{G\tau}, \frac{t_{0z}}{G\tau} \right) = (0, 0),$$

$$\left(\frac{t_{1s}}{G\tau}, \frac{t_{1z}}{G\tau} \right) = \left(-\delta_2(1 - 2z), 0 \right).$$

As in this case we do not consider the effect due to the "short ends" of the section, it seems reasonable that there is no influence of the edge affect up to the fourth order, at least in connection with torsional rigidity, but this needs more investigation.

5. Conclusions and perspectives

In this final section we consider some applications of the results found in the previous ones. The first application concerns the torsion of a section bounded by two ellipses: in particular we find the expression for torsional rigidity available in the literature for sections bounded by homothetic ellipses. As a second application we find the warping field for a section studied by WANG [18] (who used a rather sophisticated numerical method): we are able to supply a simple explicit polynomial perfectly matching his numerical results.

Finally as a third application, we recover the results found in [17] concerning torsion of the cylinder whose cross-section is an isosceles triangle, under the assumption that its base is much shorther than its altitude.

5.1. Section bounded by two non-homothetic ellipses

Let $\mathcal{D}$ be the section enclosed between two non-homothetic ellipses Γ_0 and Γ_1 whose parametric representations are, respectively:

(5.1)
$$r_0 : \quad [0, 2\pi] \to \Pi, \quad r_0 = (a \cos \varphi, b \sin \varphi),$$

$$r : \quad [0, 2\pi] \to \Pi, \quad r = (ka \cos \varphi, (k + q)b \sin \varphi);$$

we get for the torsional rigidity

$$R_1 = 2G\pi a^3 b^3 \frac{q}{p},$$

(5.2)

$$R_2 = G\pi a^3 b^3 \frac{q^2}{p^2} \left\{ \frac{2(b^2 - a^2)(1 - k)}{q}(1 + c) + 2a^2 + c \left[\frac{b^2}{2} - \frac{a^2(1 - k)}{2(k + q - 1)} \right] \right\}$$

with $c = \sqrt{\dfrac{q + k - 1}{k - 1}}$ and $p = a^2 - b^2 + c \left[\dfrac{(b^2 - a^2)(k - 1) + b^2 q}{k + q - 1} \right]$.

When $q \to 0$ we find

(5.3) $$R_1 = 4\pi G \frac{a^3 b^3 (k - 1)}{a^2 + b^2}, \qquad R_2 = 6\pi G \frac{a^3 b^3 (k - 1)^2}{a^2 + b^2}$$

in agreement with the well-known (exact) formula.

We observe that for fixed a, b and k, the ratio R_2/R_1 is a function of q. Choosing $a = 4$, $b = 2$ and $k = 1.3$ we get

(5.4) $$\frac{R_2(k - 1)^2}{R_1(k - 1)} \simeq 0.135 + 0.292q - 0.091q^2 + 0.122q^3 + O(q^4);$$

so, for example, with $q = 0.2$ we find $\dfrac{R_2(k - 1)^2}{R_1(k - 1)} \simeq 20\%$.

5.2. The warping field for a flattened tube

The efficiency of our asympthotic expansion is here tested on a section which is not thin and which was studied by WANG [18] using numerical methods. For a discussion of the limits of the present form of our expansion we refer to [19]. We consider the linear (in z coordinate) terms appearing in the first four terms of the asymptotic expansion for warping, calculated in the particular case examined, thus finding:

$$\frac{w}{\tau} = \left(9 - \frac{8}{3(8 + 3\pi)} \right) \frac{s}{(8 + 3\pi)} - \frac{1}{2}(1 - z)\sin(2s), \qquad \text{if } s \in (0, \pi/4),$$

(5.5) $$\frac{w}{\tau} = \frac{\left[(4s - 4 - \pi)(384 + 80\pi - 27\pi^2 + 384z + 288\pi z + 54\pi^2 z) \right]}{48(8 + 3\pi)^2},$$

$$\text{if } s \in (\pi/4, 1 + \pi/4).$$

It is very easy to check that the contour plots we produce exactly coincide with those given by Wang. Because the (s, z) coordinate-system is meaningful also outside the section and because the Prandtl and warping functions are determined as elementary functions of these coordinates, they can be extended outside of the section. Thus we have a hint about the form of warping for larger sections. The scale is immaterial for the elliptic problem determining warping (see [4]).
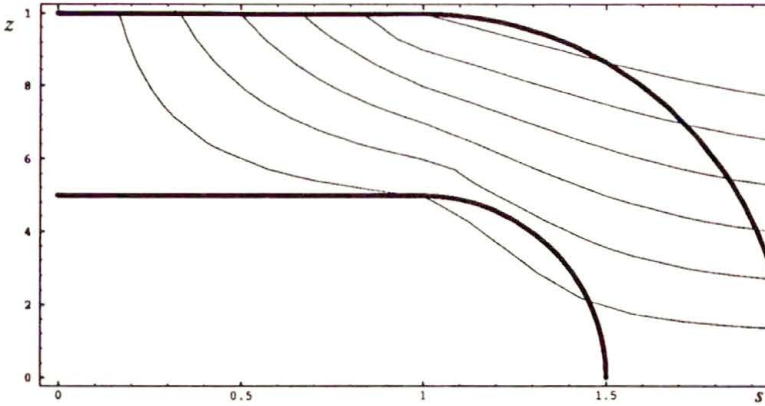
FIG. 1. The figure shows the iso-warping contour lines for the flattened tube studied in [18].

5.3. Warping field of thin triangular cross-sections

It is easy to generate the triangular cross-section considered on page 74 of [17] using the following values of δ_1 and δ_2 expressed as functions of the altitude C and basis h of the triangle:

$$(5.6) \qquad \delta_1 = s\frac{2(h/C)^2}{4 + (h/C)^2}, \qquad \delta_2 = s\frac{4(h/C)}{16 + (h/C)^2}.$$

Using formulas (4.5) we prove the validity of assumption (1.3) p.6 [17] at the first order of the ratio h/C. The warping field we find at the same order is given by:

$$(5.7) \qquad \frac{w(s,z)}{\tau} = s^2\left(\frac{1}{2} - z\right)\frac{4h/C}{16 + (h/C)^2}.$$

It is easy to see that Eq. (5.7) coincides with formula (2.19) on p. 75 of [17] modulo a rigid motion.

5.4. Conclusions

Finally we want make a few comments on the results obtained. Despite the fact that our procedure is rather general, it is not capable of reproducing the most general cross-section. Maybe this task can be solved by means of the Conformal Mapping Theory [20].

In [19] are studied some cases in which the proposed expansion does not converge. Therefore – assuming that before diverging the expansion seems to approach reasonably the solution – a regularizing method seems to be necessary to increase its scope of applicability.

On the other hand – from the mathematical point of view – our results seem to open some interesting estimation problems which most likely can be solved using the methods of the papers [21, 22].

References

1. R. Bredt, *Kritische Bemerkungen zur Drehungselastizität*, Zeits. Ver. deutsch. Ing., **40**, 815, 1896.
2. V.Z. Vlasov, *Thin-walled elastic rods* [in Russian], Fitzmagiz, Moskva 1959 [English translation in Israel Program for Scientific Translations, Jerusalem 1961].
3. F. dell'Isola and L. Rosa, *Perturbation methods in torsion of thin hollow Saint–Venant cylinders* [accepted for publication in Mechanics Research Communications, 1996].
4. S. Timoshenko and J.N. Goodier, *Theory of elasticity*, Mc Graw-Hill, New York 1951.
5. A. Nayfeh, *Perturbation methods*, John Wiley and Sons, New York 1973.
6. L. Prandtl, *Zur Torsion von prismatischen Stäben*, Phys. Zeits., **4**, 758, 1903.
7. F. dell'Isola and G. Ruta, *Outlook in Saint Venant Theory. I. Formal expansions for torsion of Bredt-like section*, Arch. Mech., **46**, 6, 1005, 1994.
8. A. Clebsh, *Théorie de l'élasticité des corps solides (Traduite par MM. Barré de Saint-Venant et Flamant, avec des Notes étendues de M. Barré de Saint-Venant)*, Dunod, Paris 1983 [Reprinted by Johnson Reprint Corporation, New York 1996].
9. I.S. Sokolnikoff, *Mathematical theory of elasticity*, McGraw-Hill, New York 1946.
10. A.E.H. Love, *A treatise on the mathematical theory of elasticity*, Dover, New York 1949.
11. C.E. Weatherburn, *An introduction to Riemnnian geometry and the tensor calculus*, Cambridge University Press, 1963.
12. P. Germain, *Cours de mecanique des milieux continus*, Tome 1, 2, Masson 1973.
13. S. Kobayashi and K. Nomizu, *Foundations of differential geometry*, Vol. 1,2, New York Interscience, 1969.
14. V. Feodosyev, *Strength of materials* [in Russian], MIR, Moskva 1968 [Italian translation: *Resistenza dei materiali*, Editori Riuniti, Roma 1977].
15. J. Chase and A.H. Chilver, *Strength of materials and structures*, Edward Arnold, London 1971.
16. R. Baldacci, *Scienza delle costruzioni*, UTET, Torino 1970.
17. Atle Gjelsvik, *The theory of thin-walled bars*, John Willey and Sons, New York 1981.
18. C.Y. Wang, *Torsion of flattened tube*, Meccanica, **30**, 221, 1995.
19. K. Frischmuth, M. Hötanler and F. dell'Isola, *Numerical methods versus asymptotic expansion for torsion of hollow elastic beams*, preprint 95/20 Universität Rostock Fachbereich Mathematik, 1995.
20. C. Caratheodory, *Theory of functions of a complex variable*, Vol. 1, 2, Chelsea Publishing Company, New York 1954.
21. C.O. Horgan and L.T. Wheeler, *Maximum principles and pointwise error estimates for torsion of shells of revolution*, J. Elasticity, 7, 4, 387, 1987.
22. C.O. Horgan and L.T. Wheeler, *Saint-Venant's principle and torsion of thin shells of revolution*, J. Appl. Mech., **98**, 4, 663, 1976.

DIPARTIMENTO DI INGEGNERIA STRUTTURALE E GEOTECNICA
UNIVERSITÀ DI ROMA "LA SAPIENZA", ROMA, ITALIA.

The stationary Stokes flow through a spherical region with large variations of density and viscosity coefficient

Z. PŁOCHOCKI, B. KAŹMIERCZAK

and Z. PERADZYŃSKI (WARSZAWA)

WE ARE INTERESTED in flows of a fluid whose density changes abruptly after entering a certain region in R^3. Flows of this kind may be useful in modelling such phenomena as propagating flames. Assuming that the region is a ball we find a closed-form solution for the flow homogeneous at infinity in the Stokes approximation. It is compared with the analytical solution in the Euler approximation. Such solutions can also be used as a test for numerical algorithms solving the flow equations.

1. Introduction

FOR GAS SYSTEMS with strong local heat sources (e.g. flames, laser-generated or sustained plasma) there arise at least two important problems concerning the influence of a gas flow on heat exchange processes, and velocity of propagation of the hot region front. In general, such problems are complicated. However, simple hydraulic models of a gas flow through a region with large density variations based on analysis of particular solutions, offer some possibilities of simplification of such problems.

The first such a solution was proposed by GUS'KOV *et al.* [1] as an attempt to study the propagation of plasma front in case of laser-generated plasma. The authors considered a stationary, homogeneous at infinity, inviscid (the Euler approximation, i.e. Re → ∞) gas flow through a spherical region. The density of the gas is assumed to be constant outside, and also constant but much smaller inside the sphere. The gas is therefore assumed to be incompressible outside and inside the sphere. Such assumptions allow to find an analytical solution of the problem (by dividing the whole flow region into two subregions, finding solutions to the continuity and Euler equations separately in each of them, and then by matching these solutions by means of continuity conditions for densities of mass and momentum fluxes at the surface of the sphere).

Next, Z. PERADZYŃSKI and E. ZAWISTOWSKA [2] treated numerically the same problem for a different Reynolds number, assuming however constant viscosity coefficient in the whole flow region.

The aim of the present paper is to find an analytical solution of this problem in the Stokes approximation (Re → 0) and to compare it with the analytical solution of the problem in the Euler approximation, and also with the numerical solution mentioned.

2. Statement of the problem

Consider a stationary gas flow through the spherical region of radius R. The density of the gas is assumed in the form:

(2.1)
$$\varrho = \varrho^{int} + (\varrho^{ext} - \varrho^{int})H(\bar{r} - 1),$$

$$\varepsilon_\varrho := \frac{\varrho^{int}}{\varrho^{ext}} \ll 1,$$

where ϱ^{int} and ϱ^{ext} are constants representing the gas density inside and outside the sphere, respectively; $H(x - x_0)$ is the Heaviside function; and $\bar{r}$ stands for the dimensionless r-coordinate in the spherical coordinate system (as referred to the radius R). The density variation may be thought as generated by a constant high temperature field inside the sphere and (relatively) low (and also constant) temperature field outside. In such a case, also the viscosity coefficient should be assumed in the form:

(2.2)
$$\eta = \eta^{int} + (\eta^{ext} - \eta^{int})H(\bar{r} - 1),$$

$$\varepsilon_\eta = \frac{\eta^{ext}}{\eta^{int}} \ll 1,$$

where η^{int} and η^{ext} are constants representing the shear viscosity coefficient of the gas inside and outside the sphere, respectively. Since for an ideal gas $\varrho \propto 1/T$ and $\eta \propto \sqrt{T}$, therefore for a gas, which can be approximately treated as an ideal one, we have

(2.3)
$$\varepsilon_\eta \cong \sqrt{\varepsilon_\varrho}.$$

The flow at infinity is assumed to be homogeneous. At the sphere surface there are no mass and momentum sources.

In order to find the solution to this problem, the method of dividing the whole region into two subregions is applied. Then, the governing equations for the interior of both subregions, i.e. for $r < R$ and $r > R$, are:

$$\nabla \cdot \mathbf{v} = 0, \qquad \nabla p = \eta \nabla^2 \mathbf{v},$$

where $\mathbf{v}$ and p stand for the velocity vector and pressure, respectively. By introducing the spherical coordinate system r, φ, θ (with z-axis directed along the flow velocity at infinity and centered in the center of the sphere), these equations can be rewritten in the following detailed form:

(2.4) $$\frac{1}{r^2}\frac{\partial}{\partial r}(r^2 v_r) + \frac{1}{r \sin\theta}\frac{\partial}{\partial\theta}(v_\theta \sin\theta) = 0,$$

(2.4)
[cont.]
$$\frac{1}{\eta}\frac{\partial}{\partial r}p = \frac{1}{r^2}\frac{\partial}{\partial r}\left(r^2\frac{\partial}{\partial r}v_r\right) + \frac{1}{r^2\sin\theta}\frac{\partial}{\partial\theta}\left(\sin\theta\frac{\partial}{\partial\theta}v_r\right)$$
$$-\frac{2v_r}{r^2} - \frac{2\cos\theta}{r^2\sin\theta}v_\theta - \frac{2}{r^2}\frac{\partial v_\theta}{\partial\theta},$$

$$\frac{1}{\eta}\frac{\partial}{\partial\theta}p = \frac{1}{r}\frac{\partial}{\partial r}\left(r^2\frac{\partial}{\partial r}v_\theta\right) + \frac{1}{r\sin\theta}\frac{\partial}{\partial\theta}\left(\sin\theta\frac{\partial}{\partial\theta}v_\theta\right) - \frac{v_\theta}{r\sin^2\theta} + \frac{2}{r}\frac{\partial v_r}{\partial\theta},$$

where v_r and v_θ stand for the r- and θ-coordinate of the velocity vector, respectively, and the axial symmetry of the flow has been assumed (i.e. $v_\varphi \equiv 0$).

The boundary conditions are assumed in the form:

(2.5)
$$r = \infty: \quad \begin{cases} v_r = v_\infty\cos\theta, \\ v_\theta = -v_\infty\sin\theta, \\ p = p_\infty, \end{cases}$$

$$r = 0: \quad |v_r|, \ |v_\theta|, \ p < \infty,$$

where v_∞ and p_∞ stand for the velocity modulus and pressure at infinity, repectively. In order to match the solutions outside and inside the sphere, the local conservation principles of mass and momentum are used. The equations, which express these conservation principles, are assumed to be valid in the whole space (i.e. – also at the sphere surface). Then the continuity conditions for the r-th coordinates of the flux density of mass and that of momentum at the sphere surface read:

$$r = R: \qquad [\![\varrho v_r]\!] = 0,$$

(2.6)
$$\left[\!\left[p - 2\eta\frac{\partial v_r}{\partial r}\right]\!\right] = 0,$$

$$\left[\!\left[\eta\left(\frac{\partial v_\theta}{\partial r} - \frac{v_\theta}{r} + \frac{1}{r}\frac{\partial v_r}{\partial\theta}\right)\right]\!\right] = 0,$$

where

(2.7)
$$[\![\psi]\!] := \psi^{\text{ext}}(r = R) - \psi^{\text{int}}(r = R),$$

where, in turn, the superscripts ext and int refer to the outside and to the inside of the sphere, respectively.

3. Solution

The solution of the problem expressed by Eqs. (2.4)–(2.6) is sought in the form:

(3.1)
$$v_r = v_\infty f(r)\cos\theta,$$
$$v_\theta = -v_\infty g(r)\sin\theta.$$

Substituting Eqs. (3.1) into Eq. (2.4)$_1$ one obtains:

$$(3.2) \qquad g = \frac{1}{2}rf' + f,$$

where prime denotes the derivative with respect to r. Substituting Eqs. (3.1) into Eqs. (2.4)$_{2,3}$ and using Eq. (3.2) one obtains:

$$\frac{1}{\eta v_\infty}\frac{\partial p}{\partial r} = \left(f'' + \frac{4}{r}f'\right)\cos\theta,$$

$$\frac{1}{\eta v_\infty}\frac{\partial p}{\partial \theta} = -\left(\frac{1}{2}r^2 f''' + 3r f'' + 2f'\right)\sin\theta.$$

Integrating the latter equation and substituting the result into the former equation we obtain:

$$(3.3) \qquad \frac{1}{\eta v_\infty}p = C_1 + \left(\frac{1}{2}r^2 f''' + 3r f'' + 2f'\right)\cos\theta,$$

$$(3.4) \qquad r^3 f^{\mathrm{IV}} + 8r^2 f''' + 8r f'' - 8f' = 0,$$

where C_1 is a constant. The general solution of the latter equation is:

$$f = C_2 + C_3 r^2 + \frac{C_4}{r} + \frac{C_5}{r^3},$$

where C stand for constants. Thus, according to Eqs. (3.1)–(3.3) the solutions of Eqs. (2.4) outside and inside the sphere, which satisfy the boundary conditions as expressed by Eqs. (2.5), may be written in the form (all the constants occuring in the formulae describing the flow in the Stokes approximation will be denoted by tilde, to distinguishing them from the analogous constants in the case of the Euler approximation, which will be discussed later):

$$(3.5)$$

$$\bar{r} := \frac{r}{R} > 1: \qquad v_r^{\mathrm{ext}} = v_\infty\left(1 + \frac{\tilde{D}}{\bar{r}} - 2\frac{\tilde{A}}{\bar{r}^3}\right)\cos\theta,$$

$$v_\theta^{\mathrm{ext}} = -v_\infty\left(1 + \frac{\tilde{D}}{2\bar{r}} + \frac{\tilde{A}}{\bar{r}^3}\right)\sin\theta,$$

$$p^{\mathrm{ext}} = p_\infty + \frac{\eta^{\mathrm{ext}}v_\infty}{R}\frac{\tilde{D}}{\bar{r}^2}\cos\theta,$$

$$\bar{r} := \frac{r}{R} < 1: \qquad v_r^{\mathrm{int}} = v_\infty(\tilde{B} + \tilde{C}\bar{r}^2)\cos\theta,$$

$$v_\theta^{\mathrm{int}} = -v_\infty(\tilde{B} + 2\tilde{C}\bar{r}^2)\sin\theta,$$

$$p^{\mathrm{int}} = \tilde{E} + \frac{\eta^{\mathrm{ext}}v_\infty}{R}\frac{10\tilde{C}}{\varepsilon_\eta}\bar{r}\cos\theta.$$

The constants $\tilde{A}$, $\tilde{B}$, $\tilde{C}$, $\tilde{D}$, $\tilde{E}$ have to be determined from the continuity conditions as expressed by Eqs. (2.6). In fact, substituting Eqs. (3.5) into Eqs. (2.6) we obtain the following set of equations for the constants considered:

$$1 + \tilde{D} - 2\tilde{A} = \varepsilon_\varrho(\tilde{B} + \tilde{C}),$$

$$\tilde{E} = p_\infty,$$

$$\tilde{D} - 4\tilde{A} = \frac{2\tilde{C}}{\varepsilon_\eta},$$

$$2\tilde{A} = -\frac{\tilde{C}}{\varepsilon_\eta}.$$

It follows immediately from the latter two equations that

(3.6) $$\tilde{D} = 0,$$

and therefore:

(3.7)
$$1 - 2\tilde{A} = \varepsilon_\varrho(\tilde{B} + \tilde{C}),$$

$$\tilde{A} = -\frac{\tilde{C}}{2\varepsilon_\eta},$$

and

(3.8) $$\tilde{E} = p_\infty.$$

It is seen that we have two equations for three constants: $\tilde{A}$, $\tilde{B}$ and $\tilde{C}$.

Thus, in order to obtain a unique solution we should adopt an additional condition, and the continuity condition of the tangent component of velocity at the surface of the sphere ($r = R$) is assumed:

(3.9) $$\llbracket v_\theta \rrbracket = 0 \qquad (r = R),$$

which leads to the following additional equation:

(3.10) $$1 + \tilde{A} = \tilde{B} + 2\tilde{C}.$$

From a formal point of view the problem of an additional constant of integration, for which there is no suitable condition, follows naturally from the applied method of dividing the whole flow region into two subregions. From the physical point of view the assumption expressed by Eq. (3.9) may be argued as follows. The expression in $\llbracket \ \rrbracket$ in Eq. (2.6)$_3$ represents the $r\theta$–coordinate of the momentum flux density, which should be a continuous function in the whole flow region (in particular – at $r = R$). The quantities: η, v_r, v_θ are assumed to be limited. If the

function v_θ was discontinuous (as a function of r) at $r = R$, then this coordinate of the momentum flux density would be singular at $r = R$, and this singularity can not be compensated by discontinuities of the other terms. It would denote, that at the boundary between subregions there are some momentum sources (surface tangent forces), which are absent by the assumption. Short discussion of the assumption considered, which is based on the properties of a weak solution of the flow equations in the Stokes approximation, is presented in the Appendix. It may be treated as a formal support for the continuity condition expressed by Eq. (3.9).

Now, solving Eqs. (3.7) and (3.10) we obtain:

$$
(3.11) \qquad
\begin{aligned}
\tilde{A} &= \frac{1 - \varepsilon_\varrho}{2 + \varepsilon_\varrho(1 + 2\varepsilon_\eta)}, \\[2mm]
\tilde{B} &= \frac{3 + 4\varepsilon_\eta - 2\varepsilon_\eta\varepsilon_\varrho}{2 + \varepsilon_\varrho(1 + 2\varepsilon_\eta)}, \\[2mm]
\tilde{C} &= -\frac{2\varepsilon_\eta(1 - \varepsilon_\varrho)}{2 + \varepsilon_\varrho(1 + 2\varepsilon_\eta)}.
\end{aligned}
$$

Inserting the approximate relation $\varepsilon_\eta \cong \sqrt{\varepsilon_\varrho}$ into the above formulae we may obtain the asymptotic expressions as $\varepsilon_\varrho \to 0$, namely:

$$
(3.12) \qquad
\begin{aligned}
\tilde{A} &\cong \frac{1}{2}\left(1 - \frac{3}{2}\varepsilon_\varrho\right), \qquad \tilde{B} \cong \frac{3}{2}\left(1 + \frac{4}{3}\sqrt{\varepsilon_\varrho}\right), \\[2mm]
\tilde{C} &\cong -\sqrt{\varepsilon_\varrho}\left(1 - \frac{3}{2}\varepsilon_\varrho\right) \cong -\sqrt{\varepsilon_\varrho}.
\end{aligned}
$$

On the other hand, by putting $\varepsilon_\eta = 1$ we obtain respectively:

$$
(3.13) \qquad
\begin{aligned}
\tilde{A} &= \frac{1 - \varepsilon_\varrho}{2 + 3\varepsilon_\varrho} \cong \frac{1}{2}\left(1 - \frac{5}{2}\varepsilon_\varrho\right), \\[2mm]
\tilde{B} &= \frac{7 - 2\varepsilon_\varrho}{2 + 3\varepsilon_\varrho} \cong \frac{7}{2}\left(1 - \frac{25}{14}\varepsilon_\varrho\right), \\[2mm]
\tilde{C} &= -2\frac{1 - \varepsilon_\varrho}{2 + 3\varepsilon_\varrho} \cong -\left(1 - \frac{5}{2}\varepsilon_\varrho\right).
\end{aligned}
$$

Thus, Eqs. (3.5) with Eqs. (3.6), (3.8) and (3.11) represent the solution of the problem expressed by Eqs. (2.4)–(2.6), which is unique in the class of functions specified by Eqs. (3.1).

4. Results

From the formulae given in the previous section one may obtain all the information about the flow examined. Examples of two types of such an information will be presented.
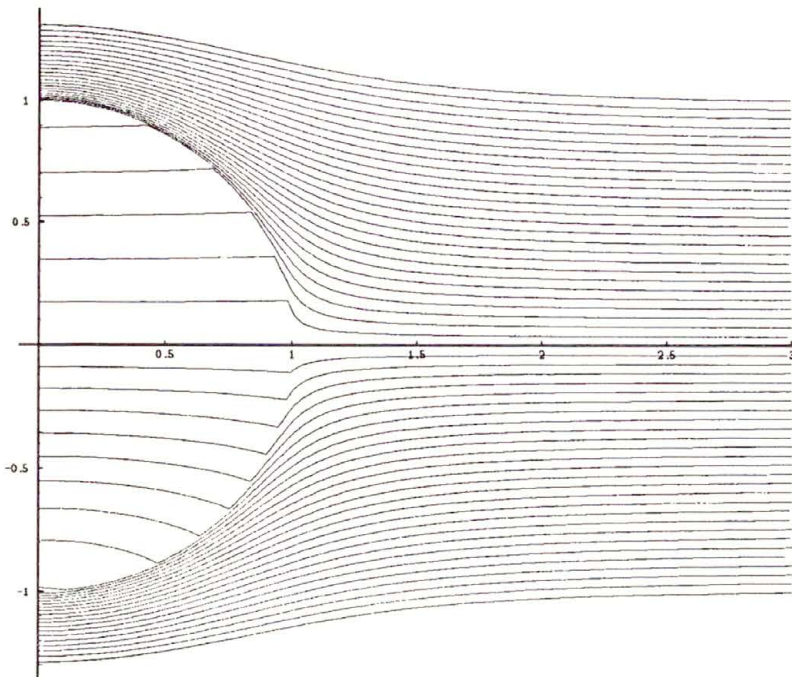
FIG. 1. Streamlines pictures for the flow through the sphere in the Euler (the lower half) and Stokes (the upper half) approximations under the assumptions: $\varepsilon_\eta = \sqrt{\varepsilon_\varrho}$, $\varepsilon_\varrho = 2.5 \times 10^{-2}$.
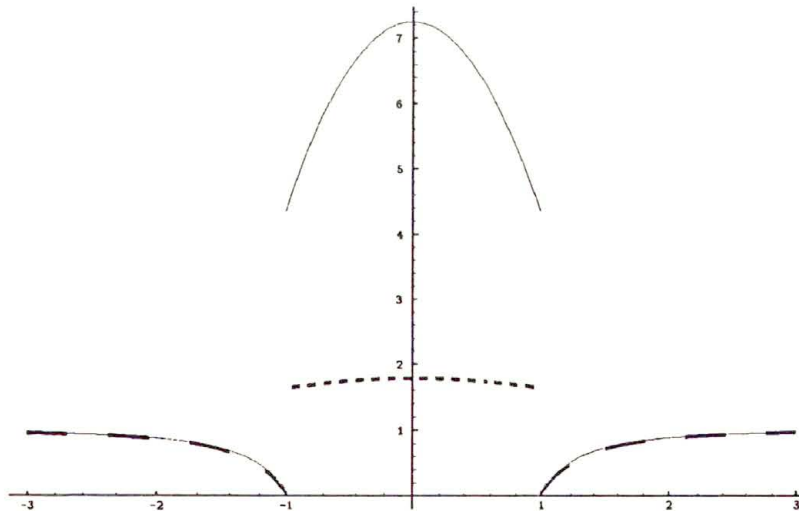

FIG. 2. Dimensionless velocity (as referred to v_∞) at the flow symmetry axis as a function of the dimensionless z-coordinate (as referred to R) under the same assumptions about ε_η and ε_ϱ as in the case of Fig. 1 in the Euler (solid line) and Stokes (dashed line) approximations.

[771]

The information of the first type concerns the flow fields at a given ε_ϱ. As an example, value $\varepsilon_\varrho = 2.5 \times 10^{-2}$ is assumed as a typical one for the laser-sustained plasma. Thus, the upper half of Fig. 1 presents the streamlines pictures. Figure 2 b (dashed line) presents the dimensionless z-coordinate of velocity:

$$\bar{v}_z = \frac{v_r}{v_\infty} \cos\theta - \frac{v_\theta}{v_\infty} \sin\theta$$

at the flow symmetry axis ($\theta = \pi$, 0, respectively) as a function of dimensionless z-coordinate ($\bar{z} = (z/R)\cos\theta$), under the same assumptions about ε_η and ε_ϱ as above. Figure 3 presents the dependence of the dimensionless pressure difference:

$$\overline{\Delta p} = 2\frac{p - p_\infty}{\varrho_\infty v_\infty^2}$$

on the dimensionless z-coordinate at the flow symmetry axis under the same assumptions about ε_η and ε_ϱ as in the case of Fig. 1, where the Reynolds number

$$\mathrm{Re} = \frac{\varrho_\infty v_\infty R}{\eta_\infty}$$

plays the role of the scale factor only.

The information of the second type concerns the characteristics of the flow considered as functions of ε_ϱ, as for example: velocity and pressure on the flow symmetry axis at the center and at the boundary of the sphere (Fig. 4 b, Fig. 5b)[1]:

		$\varepsilon_\eta = \sqrt{\varepsilon_\varrho}$	$\varepsilon_\eta = 1$
	$\bar{v}_z^{\mathrm{ext}}(1) = 1 - 2\tilde{A}$	$\cong \dfrac{3}{2}\varepsilon_\varrho,$	$\cong \dfrac{5}{2}\varepsilon_\varrho,$
	$\bar{v}_z^{\mathrm{int}}(1) = \tilde{B} + \tilde{C}$	$\cong \dfrac{3}{2} + \sqrt{\varepsilon_\varrho},$	$\cong \dfrac{5}{2} - \dfrac{15}{4}\varepsilon_\varrho,$
	$\bar{v}_z^{\mathrm{int}}(0) = \tilde{B}$	$\cong \dfrac{3}{2} + 2\sqrt{\varepsilon_\varrho},$	$\cong \dfrac{7}{2} - \dfrac{25}{4}\varepsilon_\varrho,$
(4.1)	$[\![\bar{v}_z]\!] = 1 - 2\tilde{A} - \tilde{B} - \tilde{C}$	$\cong -\dfrac{3}{2} - \sqrt{\varepsilon_\varrho},$	$\cong -\dfrac{5}{2} + \dfrac{25}{4}\varepsilon_\varrho,$
	$\overline{\Delta p}^{\mathrm{ext}}(1) = 0$		
	$\dfrac{Re}{20}\overline{\Delta p}^{\mathrm{int}}(1) = -\dfrac{\tilde{C}}{\varepsilon_\eta}$	$\cong 1 - \dfrac{3}{2}\varepsilon_\varrho,$	$\cong 1 - \dfrac{5}{2}\varepsilon_\varrho,$
	$\overline{\Delta p}^{\mathrm{int}}(0) = 0$		
	$[\![\overline{\Delta p}]\!] = -\overline{\Delta p}^{\mathrm{int}}(1),$		

[1] Note that the part of the gas flux flowing through the sphere as referred to the flux incoming from infinity is given by $\bar{v}_z^{\mathrm{ext}}(1)$.
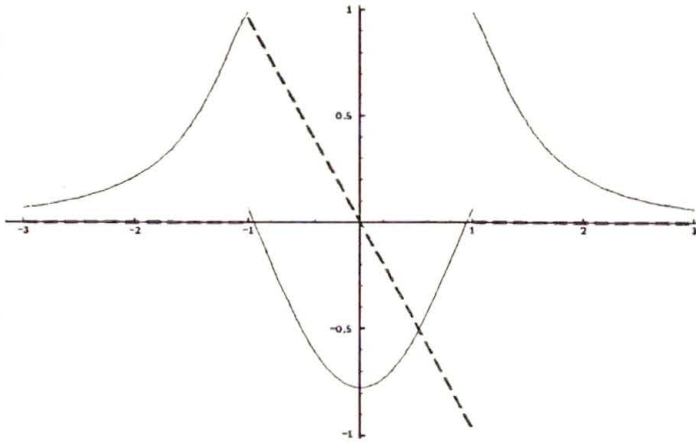
FIG. 3. Scaled relative pressure at the flow symmetry axis for $\varepsilon_\eta = \sqrt{\varepsilon_\varrho}$, $\varepsilon_\varrho = 2.5 \times 10^{-2}$.
solid line – the Euler approximation: $2(p - p_\infty)/(\varrho_\infty v_\infty^2)$,
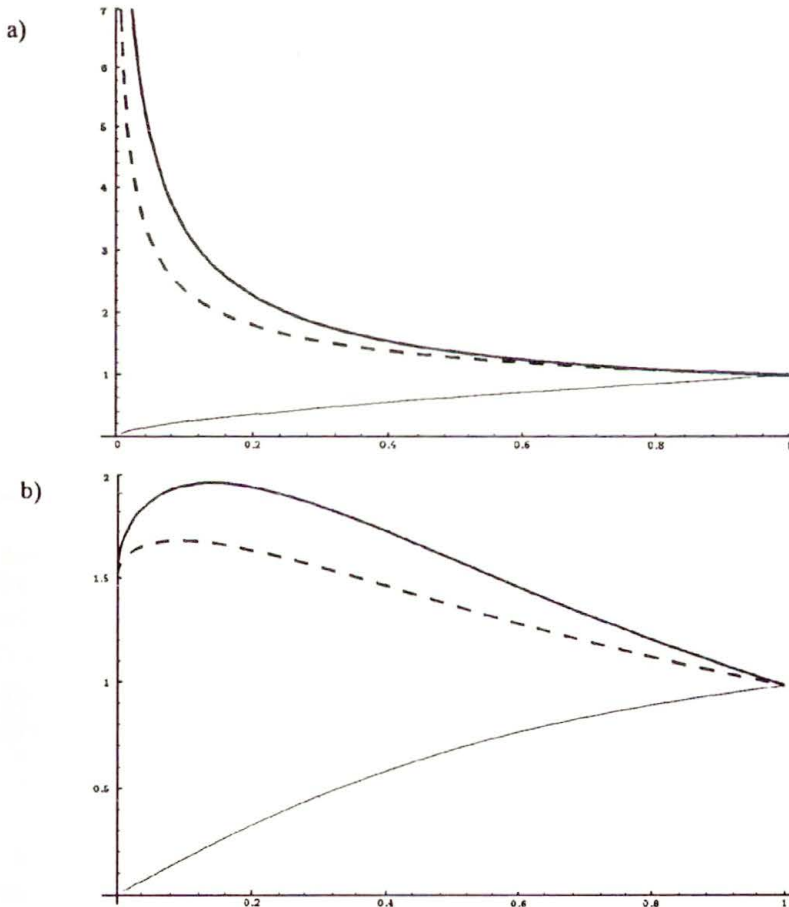dashed line – the Stokes approximation: $2(p - p_\infty)/(\varrho_\infty v_\infty^2)(\mathrm{Re})/(20)$.

a)

b)

FIG. 4. Dependence of $\bar{v}_z^{\mathrm{ext}}(1)$ (solid line), $\bar{v}_z^{\mathrm{int}}(1)$ (dashed line) and $\bar{v}_z^{\mathrm{int}}(0)$ (bold line) on ε_ϱ
for the flow through the sphere in the Euler (a) and Stokes (b) approximation
under the assumption: $\varepsilon_\eta = \sqrt{\varepsilon_\varrho}$.

[773]
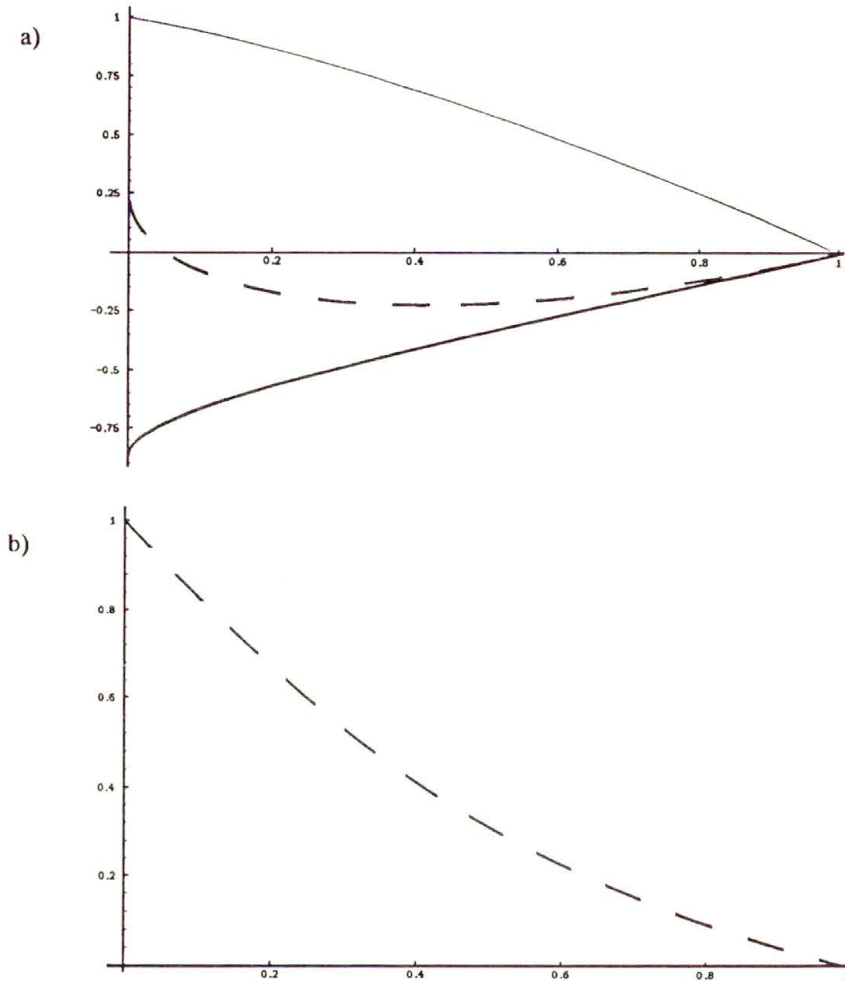
FIG. 5. Dependence of $\overline{\Delta p}^{\text{ext}}(1)$ (solid line), $\overline{\Delta p}^{\text{int}}(1)$ (dashed line) and $\overline{\Delta p}^{\text{int}}(0)$ (bold line) on ε_ϱ for the flow through the sphere in the Euler (a) and Stokes (b) approximations under the same assumptions about ε_η as in the case of Fig. 3.

where the first column represents the exact formulae, the second one – the asymptotic formulae for small ε_ϱ under the assumption $\varepsilon_\eta = \sqrt{\varepsilon_\varrho}$, the third one – the asymptotic formulae for small ε_ϱ under the assumption $\varepsilon_\eta = 1$;

$$\psi(1) := \psi(\theta = \pi, \, r = R),$$
$$\psi(0) := \psi(\theta = \pi, \, r = 0);$$

and $\left[\!\left[\psi \right]\!\right]$ is defined by Eq. (2.7).

5. Discussion

The velocity field in the Stokes approximation is, from the qualitative point of view, similar to that in the Euler approximation (Fig. 1). It follows from the fact that the dependence of the velocity coordinates on r and θ has the same structure in both approximations (Eqs. $(3.5)_{1,2,4,5}$ with Eq. (3.6)). However, quantitative pictures in both cases are different (Fig. 2), because the integration constants A, B and C in the Euler approximation (they have no tilde, for distinguishing) are given by different functions of ε_ϱ. Namely, in the case of the Euler approximation they are the solutions of the set (the typing error in the sign is corrected):

$$A = \frac{2 - \varepsilon_\varrho - \varepsilon_\varrho B}{4 + \varepsilon_\varrho}, \qquad C = \frac{3 - (2 + \varepsilon_\varrho)B}{4 + \varepsilon_\varrho},$$

$$3A(2 - A) + 2(1 - 2A)^2 = -\varepsilon_\varrho C(3B + 2C) + 2\varepsilon_\varrho(B + C)^2.$$

Solving this equation set with respect to A, B, C one may obtain the velocity characteristics in the Euler approximation analogous to those given by Eqs. $(4.1)_{1-4}$ in the case of the Stokes approximation (number errors are corrected) (Fig. 4 a):

$$\overline{v}_z^{\,\text{ext}}(1)_{\text{Eu}} = 1 - 2A \qquad \cong \frac{1}{2}\sqrt{\frac{3}{2}}\sqrt{\varepsilon_\varrho},$$

$$\overline{v}_z^{\,\text{int}}(1)_{\text{Eu}} = B + C \qquad \cong \frac{1}{2} + \frac{1}{2}\sqrt{\frac{3}{2}}\frac{1}{\sqrt{\varepsilon_\varrho}},$$

$$\overline{v}_z^{\,\text{int}}(0)_{\text{Eu}} = B \qquad \cong -\frac{1}{2} + \sqrt{\frac{3}{2}}\frac{1}{\sqrt{\varepsilon_\varrho}},$$

$$\left[\!\left[\overline{v}_z\right]\!\right]_{\text{Eu}} = 1 - 2A - B - C \cong -\overline{v}_z^{\,\text{int}}(1)_{Eu},$$

where the same convention was used as in the case of Eqs. (4.1).

Therefore, from the quantitative point of view the velocity field in the Stokes approximation is remarkably different (especially inside the sphere) as compared to that in the Euler approximation. Generally, one may say, that viscosity forces (when they are dominating over the inertia forces) accommodate the flow, although (inside the sphere) not as much as it follows from the numerical results presented in [2]. For example, the (nondimensional) internal velocity (as referred to v_∞) on the z-axis for $\varepsilon_\varrho = 2.5 \times 10^{-2}$ increases parabollically from about 4.35 at $\overline{r} = 1$ to about 7.25 at $\overline{r} = 0$ in the Euler approximation, whereas in the Stokes approximation (under the assumption: $\varepsilon_\eta = \sqrt{\varepsilon_\varrho}$) it increases (also parabolically) from about 1.63 to about 1.78, respectively.

Comparison of the analytical results presented here (under the assumption: $\varepsilon_\eta = 1$) and numerical results presented in [2] for Re $\to 0$ shows some differences

inside the sphere. The numerical results are lower and more weakly depending on z-coordinate. For example, the analytical formulae for the internal (dimensionless) velocity (as referred to v_∞) on z-axis for $\varepsilon_\varrho = 2.5 \times 10^{-2}$ give the value about 2.46 at $\bar{r} = 1$ and about 3.40 at $\bar{r} = 0$, whereas the values in [2] are about 1.85 and 1.96, respectively.

The pressure field obtained in the Stokes approximation has different structure as compared to that in the Euler approximation, although variations of pressure are relatively small in both of them (Fig. 3). General difference in pressure behaviour is seen by comparing Eqs. $(3.5)_{3,6}$ (with $\tilde{D} = 0$) and the following formulae for pressure given in [1]:

$$p_{Eu}^{ext} = p_\infty + \frac{\varrho v_\infty^2}{2}\frac{A}{\bar{r}^3}\left\{-\left(2 + \frac{A}{\bar{r}^3}\right) + 3\left(2 - \frac{A}{\bar{r}^3}\right)\cos^2\theta\right\},$$

$$p_{Eu}^{int} = p_0 + \varepsilon_\varrho \frac{\varrho v_\infty^2}{2}C\bar{r}^2\left\{B + C\bar{r}^2 - (3B + 2C\bar{r}^2)\cos^2\theta\right\},$$

where

$$p_0 = p_\infty - \frac{1}{2}\varrho_\infty v_\infty^2\left\{A(2 + A) + \varepsilon_\varrho C(B + C)\right\}.$$

Using these formulae one may obtain the pressure characteristics in the Euler approximation analogous to those given by Eqs. $(4.1)_{5-8}$ in the case of the Stokes approximation (Fig. 5 a):

$$\overline{\Delta p}^{ext}(1)_{Eu} = 4A(1 - A) \cong 1 - \frac{3}{8}\varepsilon_\varrho,$$

$$\overline{\Delta p}^{int}(1)_{Eu} = -\{A(2 + A) + \varepsilon_\varrho C(3B + 2C)\} \cong \frac{1}{4} - \sqrt{\frac{3}{2}}\sqrt{\varepsilon_\varrho},$$

$$\overline{\Delta p}^{int}(0)_{Eu} = -\{A(2 + A) + \varepsilon_\varrho C(B + C)\} \cong -\frac{7}{8} + \frac{1}{2}\sqrt{\frac{3}{2}}\sqrt{\varepsilon_\varrho},$$

$$[\![\overline{\Delta p}]\!]_{Eu} = 3A(2 - A) + \varepsilon_\varrho C(3B + 2C) \cong \frac{3}{4} + \sqrt{\frac{3}{2}}\sqrt{\varepsilon_\varrho},$$

where the same convention was used as in the case of Eqs. (4.1).

Appendix

Below we will show that, if a weak solution to the conservation laws exists, then the tangent component of the velocity must be continuous. In a Cartesian system of coordinates the conservation laws for mass and momentum can be written as:

(A.1)
$$\nabla \cdot (\varrho \mathbf{v}) = 0,$$
$$\nabla \cdot \sigma_i = 0,$$

where σ_i is the i-th row of the matrix

$$\sigma_{ij} = -\delta_{ij}p + \lambda\delta_{ij}\nabla\cdot\mathbf{v} + \eta\left(\frac{\partial}{\partial x_j}v_i + \frac{\partial}{\partial x_i}v_j\right),$$

η is a shear viscosity coefficient, $\lambda = \zeta - \dfrac{2\eta}{3}$ and ζ is a bulk viscosity coefficient.

Weak formulation can be obtained by multiplying the Eq. (A.1) by smooth test functions and formal integration by parts. Thus, for given ϱ, η and ζ we say that $v_i \in L^2_{\text{loc}}$, $i \in \{1,2,3\}$, and a distribution $p \in \mathcal{D}'$ satisfy the system (A.1) in the weak sense, if for all $C_0^\infty(R^3)$ functions ϕ and ψ_i, $i \in \{1,2,3\}$, we have:

(A.2)
$$\sum_i \int \varrho v_i \phi_{,i}\, dx = 0,$$
$$\sum_j \int \sigma_{ij}\psi_{,j}\, dx = 0, \qquad i \in 1,2,3,$$

where the integrals are taken over R^3. Still, the integration in (A.2)$_1$ must be understood as action of a distribution on ψ_j, because σ_{ij} is a combination of derivatives of the components of $\mathbf{v}$ and they are, in general, discontinuous. At the beginning let us assume that η and ζ are smooth functions. For the sake of brevity, let us assume that the boundary dividing the regions of different ϱ is a flat surface, e.g. the plane $x_3 = 0$. (In the case of smooth though not flat boundary, the complication would be only technical: curvilinear coordinates and covariant derivatives.) Let us examine the equations for the components of σ_1 and σ_2. If we suppose, for example, that v_1 is discontinuous while crossing the plane $x_3 = 0$ in the vicinity of the point $x = (0,0,0)$, then there exist bounded continuous functions $A_{11}(x)$, $A_{1p}(x)$ and $A_{13}(x)$ with $A_{13}(0) \neq 0$ such that:

$$\sigma_{13}(x) = \eta(x)A_{13}(x)\delta(x_3) + \{\text{bounded terms}\},$$
$$\sigma_{11}(x) = \lambda(x)A_{11}(x)\delta(x_3) + A_{1p}(x)p + \{\text{bounded terms}\},$$

whereas σ_{12} is bounded. But then Eq. (A.2)$_1$ cannot be satisfied for functions ψ_1. To see this, let us take for example

$$\psi_1 = x_3\,\omega\left(\frac{1}{\varepsilon}x_3\right)\omega\left(\frac{1}{\varepsilon}\sqrt{x_1^2 + x_2^2}\right),$$

where $\omega(y)$ is a $C_0^\infty(R^3)$ function such that $\omega(y) \equiv 1$ for $|y| \leq 1$, $0 \leq \omega(y) \leq 1$ and $\omega(y) \equiv 0$ for $|y| \geq 2$, and choose ε sufficiently small. So, v_1 must be continuous. In the same way we may prove that v_2 must be continuous. When the tangent component of $\mathbf{v}$ is continuous, then the distributional sense of derivatives of the components of $\mathbf{v}$ retains its validity even for discontinuous coefficients η and λ

(while crossing the plane $x_3 = 0$). Then, however, the pressure p ceases to be well determined even in the distributional sense, since according to the equation (A.2)$_3$:

$$\int \{(-p + (\lambda + 2\eta)v_{3,3} + S_3)\psi_{3,3} + S_2\psi_{3,2} + S_1\psi_{3,1}\}\, dx = 0,$$

where S_j are bounded, its singular part should be equal to the singular part of the expression $(\lambda + 2\eta)v_{3,3}$. Thus it must be proportional to $(\lambda + 2\eta)\delta(x_3)$ and the last expression is not a well determined distribution (at the boundary surface $x_3 = 0$).

Acknowledgments

References

1. K.G. Gus'kov, Yu.P. Rayzer and S.T. Surzhikov, *On an observed speed of the optical discharge slow propagation* [in Russian], Kvantovaya Elektronika, **17**, 7, 937–942, 1990.
2. Z. Peradzyński and E. Zawistowska, *Flow in a region with large density variations*, Arch. Mech., **46**, 6, 881–891, 1994.

Changes of temperature during the simple shear test of stainless steel

S.P. GADAJ, W.K. NOWACKI and E.A. PIECZYSKA (WARSZAWA)

INVESTIGATION of the simple plane shear of stainless steel was carried out. The stress-strain curves and the distributions of infrared radiation for various shear rates have been registered. Temperature changes of the shearing paths were obtained on this ground. It was observed, that this temperature increases both with the increase of the deformation and the rate of shear. The capabilities of the used thermovision system allow us to notice the asymmetry of the thermal distribution of the shear paths caused by the macroscopic shear bands. Finally the results were compared with the results of numerical simulation, obtained for this kind of material deformed in adiabatic conditions.

1. Introduction

EXPERIMENTAL INVESTIGATIONS of the static simple shear are in general limited to the analysis of mechanical curves [1, 2, 3] and examination of the texture and microscopic pictures obtained for the material subjected to such deformation [3, 4, 5]. Theoretical approaches concern the analysis of the shear testing under the isothermic or adiabatic conditions [3, 6, 8]. In reality, the process of shear is accompanied by the heat emission and its almost immediate transmission to the surroundings, that significantly influences this process. This means, that the thermomechanical coupling occurs in nonadiabatic conditions. There are no papers on that problem published up to now, where the results of the investigations of the thermomechanical coupling during nonadiabatic static shear would be presented, though such investigations were undertaken during dynamic tests [7].

In this paper, the investigations of the static simple plane shear in nonadiabatic conditions have been carried out. Their goal was to obtain the mechanical curves as well as the temperature distributions in the shear areas. The results obtained enable us to present the temperature changes of the specimens subjected to the shear test with different rates of deformation, as well as to describe the macroscopic shear band, developing at higher deformations. Finally, experimental results were compared with the results of numerical simulations, calculated for the model of elasto-plastic material deformed in adiabatic conditions [8].

2. Description of experiment

The investigations were performed on the specimens of stainless steel 1H18N9T of composition: 0.076wt% C, 0.89wt% Mn, 0.45wt% Si, 0.02wt% P, 17.78wt% Cr, 9.24wt% Ni, 0.48wt% Ti. The samples of dimensions $30 \times 42.3 \times 0.5$ mm, cut out from the same sheet, were placed in a specially designed grip (Fig. 1), allowing

for replacing the compression by the simple shear. This grip was fitted in the Instron machine. Construction of this arrangement practically eliminates sliding of the specimen in the grip and ensures that the process of shear takes place on two parallel shear bands (paths) of the specimen, of 30 mm length and 3 mm width (Figs. 1 and 2). A change of temperature of the surface of these paths has been observed.
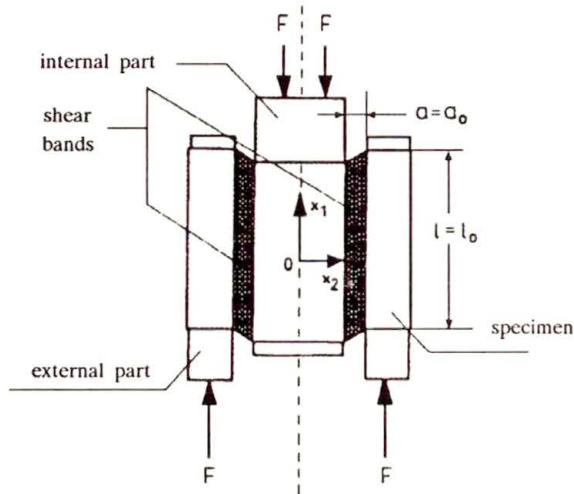

FIG. 1. Project of the device for fixing the specimens.

During the deformation, the load vs Instron's crosshead displacement, the load and this displacement vs time and the distribution of infrared radiation emitted by shear paths, were continuously registered. The infrared radiation was measured using the thermovision camera AGA 680 coupled with a system of data acquisition and conversion PTR WIN.

In order to secure higher and more homogeneous emissivity, the surface of the samples was blackened with carbon powder.

The shear tests were carried out with various, properly chosen rates of deformation: $2.77 \cdot 10^{-3}$, $5.55 \cdot 10^{-3}$, $11.1 \cdot 10^{-3}$ s^{-1}. These rates should be high enough in order to provide the sufficiently high temperature increments, measurable by the used thermovision set. The mean-square error of temperature evaluation was $0.3°$ C.

The system PTR WIN allows us to obtain the thermovision pictures with various precision. A thermovision camera scans the examined object collecting the infrared radiation from its surface. During 0.06 s the camera creates an image called frame. A thermal picture of the frame contains few details but, in spite of that, it can be very valuable. Short time of creation of these frames enables us to register more accurately the beginning of temperature changes of chosen areas of the object. An analysis of these temperature changes can be helpful for exact determination of the beginning of the process of shear or elongation. Four such

frames superimposed over each other create a thermal picture, obtained during 0.24 s. This thermal picture is a basis for analysing temperature distributions of the examined surface. Such distributions can be presented in different units depending on the chosen curve of calibration.

The PTR WIN software enables the user to obtain the following data:

• the temperature distribution on the surface of the examined body, with the chosen grade of discrimination: both black and white and coloured, stored on hard disc of a computer;

• the average temperature of the selected part of the picture, its mean-square error and the area of it;

• the real time temperature evaluation at several chosen points (up to 10);

• the temperature distribution along the line, arbitrarily chosen on the picture;

• the digital form of the obtained temperature distribution, which enables its further processing by other software.

3. Experimental results

The time, force and the crosshead displacement, registered during investigations, allow us to determine the stress and strain fields and to control the rate of shear. The stress tensor, defined in the coordinates shown in Fig. 1, has only 3 non-vanishing components: σ_{11}, σ_{22}, σ_{12} during simple shear. The single component of the tensor of deformation is $\gamma = \varepsilon_{12}$.

It was assumed that, in the case of simple plain shear in static conditions, there is no change in the cross-section: $S_E = $ const ($S_E = a_0 d$, where a_0 – width of the shear band, d – thickness of the specimen). Then the stress $\sigma_{12} = F/S_E$ and deformation $\gamma = \Delta l/a_0$, where Δl – displacement of the grips of the device holding the specimen (Fig. 1).

The distributions of intensity of the infrared radiation, recorded during investigation in digital form, allow us to reconstruct thermal pictures (thermograms) of the specimens. The maximal sensitivity of the system, conditioned by the 12 bit registration, is 0.01° C. In Fig. 2 an example of thermogram of the shear zones of specimen, deformed at the rate of $11.1 \cdot 10^{-3} \mathrm{s}^{-1}$, and registered at the deformation $\gamma = 1.59$, is shown. A photograph of the undeformed specimen fixed in the grips of the holding device is given as well. The thermovision camera was focused on the shear zones since the grips are rather thick (15 mm). The coloured temperature scale is concerned with these shear zones only.

Because of the large mass of grips relative to the mass of specimen and because of the high heat conductivity of steel, there is a large temperature gradient in the direction perpendicular to the shear direction. The areas of maximum temperature are hence situated in the central part of the shear paths (along the direction of shear).

The occurence of the stress components σ_{11} and σ_{22} is caused by the condition $a = a_0 = \text{const}$ (the internal and external jaw of the grip move parallely, as shown in Fig. 1). The existence of free edges of specimen $x_1 = \pm l_0/2$, where the normal stress component must vanish, induces the heterogeneity of the strain field. However, it is assumed that this boundary region is small as compared to the length of the specimen. Theoretical considerations indicate that for $a_0/l_0 = 1/10$ ($l_0 = 30$ mm) this region covers almost 5% of specimen's length. An example of the strain field obtained numerically by the ABAQUS code for the steel 1H18N9T, under the assumption of elasto-plastic adiabatically deformed material at the strain level $\gamma = 0.322$, is shown in Fig. 3 A. Results of these calculations will be published in [9].

The disturbances of the stress and strain fields existing on free ends of the specimen during shear test are visible in the temperature distribution. The temperature of these areas is higher than in remaining part of the specimen. This is easily seen in the initial stage of the process. At higher deformations this effect is difficult to observe because of large temperature increments of the shear zones and due to high heat conductivity of this steel.

3.1. Temperature changes of the specimens subjected to various shear rates

The temperature changes of the shear paths for three deformation rates were investigated. Taking advantage of PTR WIN, 5 points were marked in the central part of the thermogram of one of these paths, where the temperature seemed to be homogeneous (Fig. 4, left picture). The coordinates of these points and their temperatures at the end of the process are given below. The graph of temperature evolution for these points during the shear time is shown on the right-hand side of Fig. 4.

The same approach was used for other rates of shear. The averaged values of temperature obtained this way are presented in Fig. 6 A as a function of deformation γ. The process of shear is accompanied by the increase in temperature. However, the temperature behaviour of the shearing specimen is a result of the heat emission and of its instantaneous flow to the grips; more particularly, that the used grips are solid, in comparison with the specimen. The temperature increments during shear test are not proportional to the stress of specimen. Looking at curves $\Delta T(\gamma)$ (Fig. 6 A) it can be noticed that for the deformation $\gamma \simeq 0.3$, an disorder in the monotonic temperature increase is observable, and an inflection point can be noticed. It can be related to the changes of the mechanisms of deformation at this stage of shear, however a full explanation of this phenomenon requires further investigations.

Figure 6 B presents the relations between the stress σ_{12} and the deformation γ, obtained for three shear rates. There are very small differences between these curves; the rate of deformation has no considerable influence on the mechanical characteristics of the material. Moreover, it is easy to notice that $\sigma_{12}(\gamma)$ curves are
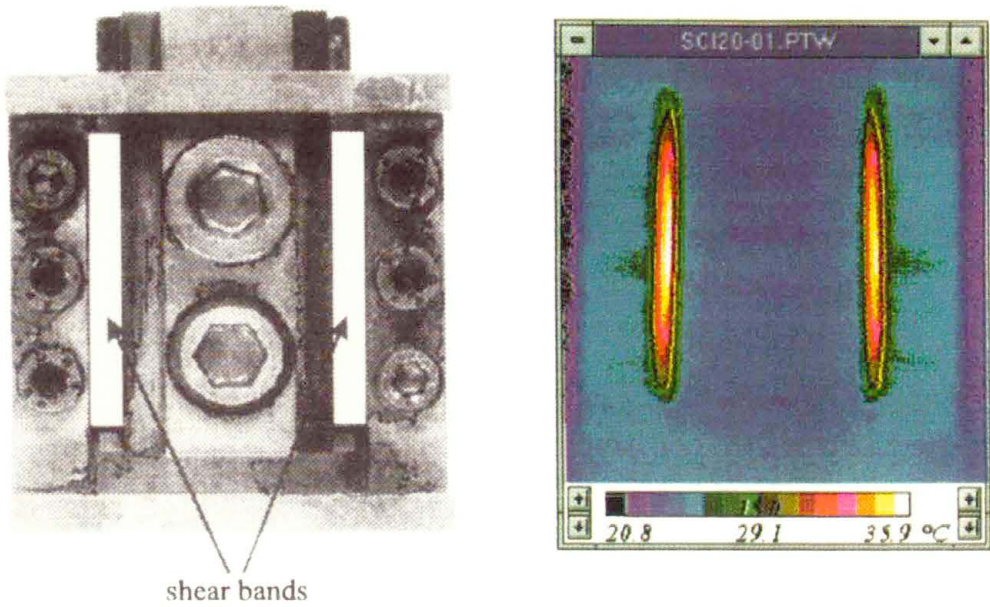
shear bands

FIG. 2. Photograph of the specimen inserted in the holding device and a thermogram showing the temperature distribution in the sheared areas.
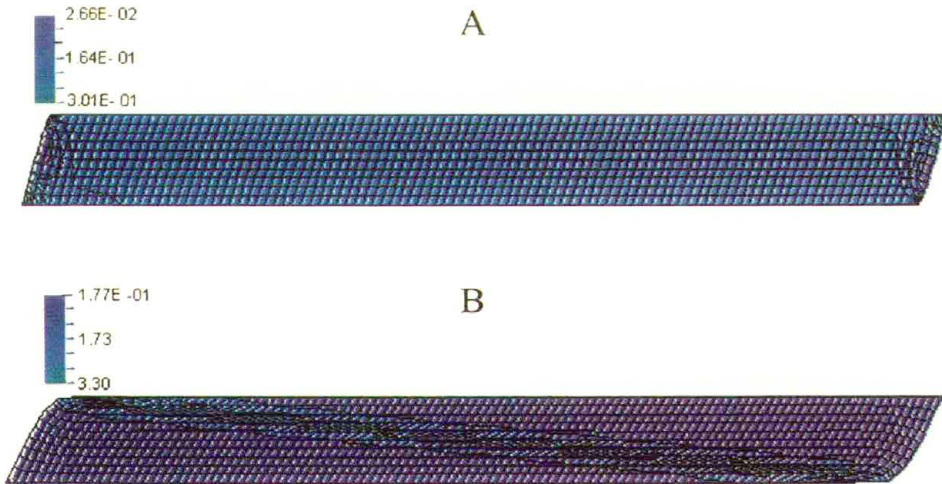

FIG. 3. (A) – heterogeneity of the field of deformation on the free edges of the sheared areas at $\gamma = 0.322$ and (B) – stress distribution in the shear areas at $\gamma = 1.11$; theoretical evaluation [9].
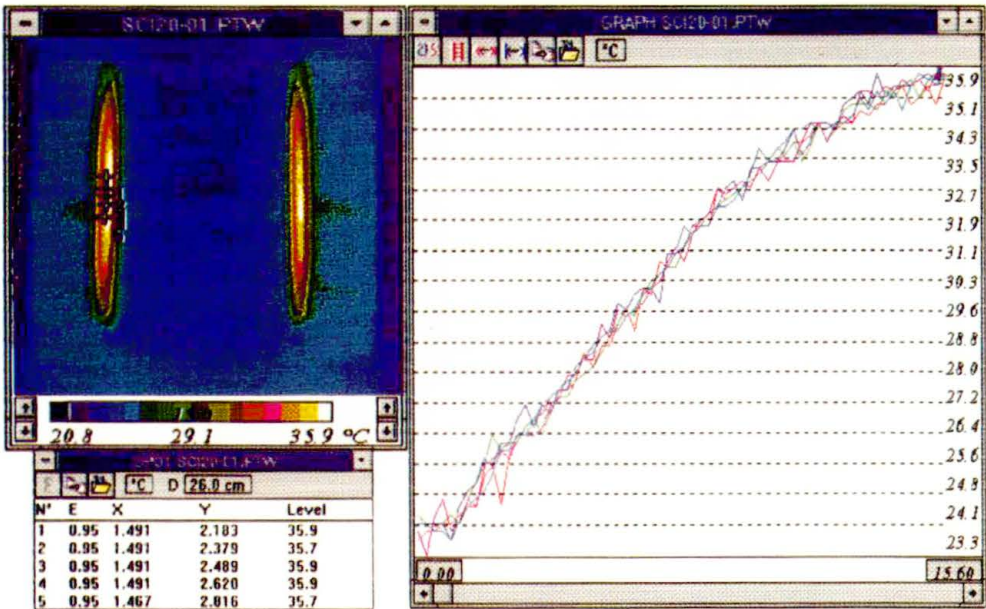
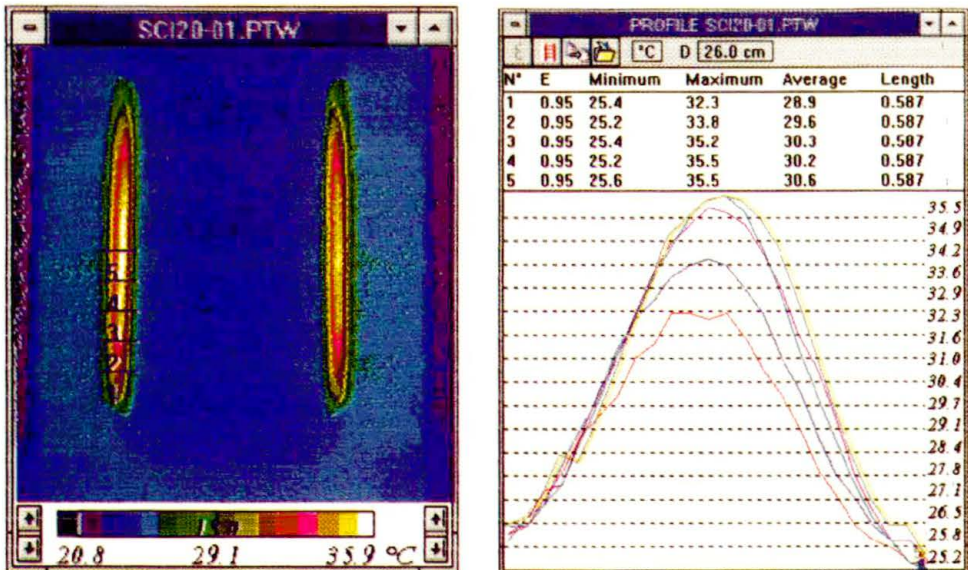FIG. 4. A thermogram obtained during the shear test of 1H18N9T steel ($\gamma = 1.60$) and the temperature vs time for the chosen 5 points.

FIG. 5. A thermogram of the zones of shear with the 5 segments denoted. At right – the temperature distributions along these segments.

smooth up to $\gamma \simeq 70\%$. It gives evidence about the homogeneity of the process of shear in this stage of deformation. Then, the oscillating values of the stresses occurred, indicating the change of the character of deformation.
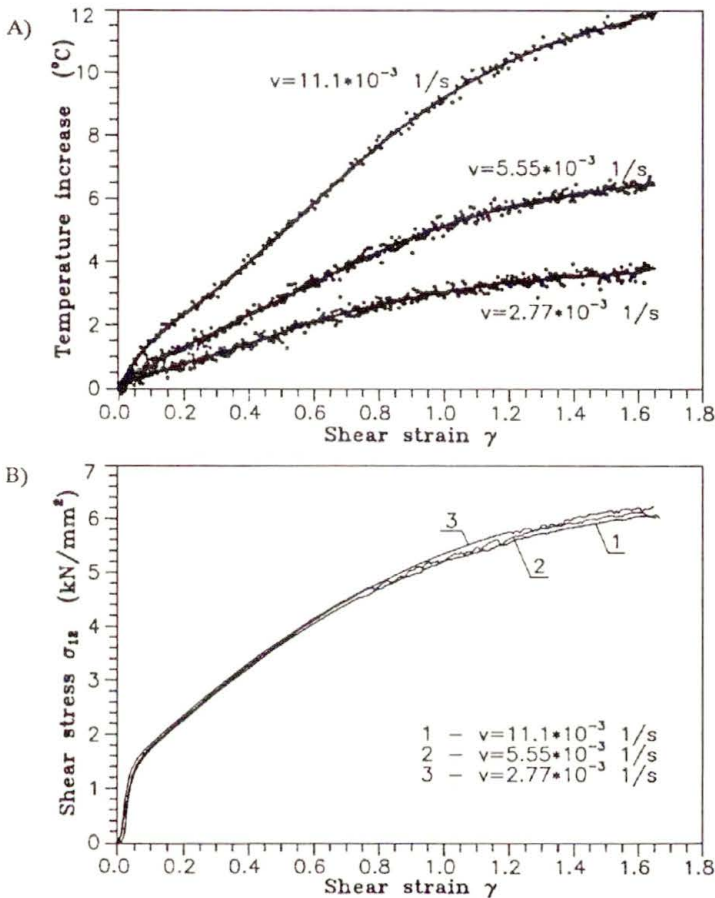

FIG. 6. Changes in temperature in the central part of the sheared path of the specimen made from 1H18N9T – (A), and the mechanical characteristics of this steel – (B); obtained at various rates of shear.

Summarizing the presented results (Fig. 6 A, B), it can be stated that there is a strong dependence of the temperature of shear paths on the shear rate, while the differences between the mechanical curves are insignificant.

3.2. Development of the macroscopic shear band

It follows from theoretical considerations that, during the simple shear test at deformations higher than $70 \div 80\%$, a localization of the deformation, named the macroscopic shear band, appears. The macroscopic shear band develops at a certain angle to the shear path. Figure 3 B presents a picture of this band for

$\gamma = 1.11$ shear deformation. The calculations were made for the elasto-plastic model of the body, under the assumption of combined isotropic-kinematic hardening and adiabatic process of deformation [9].

Suitable processing of thermal pictures recorded during the shear test indicates, that the phenomenon of localized deformation is noticeable also in nonadiabatic conditions, in which the experiment has been conducted. For that purpose the following approach was adopted.

On the thermograms obtained in non-homogeneous range of deformation ($\gamma \simeq 1.50$), 9 segments were chosen, intersecting the shear path perpendicular to the shear direction (Fig. 5). A coordinate x_2 of the beginning of each sector was the same (Figs. 1 and 5). Along these segments the distributions of temperature were determined. The determination of the temperature distributions was carried out in two approaches for each path, because the system PTR WIN enables us to obtain such distributions simultaneously for 5 segments only.

An example of the obtained thermograms with 5 marked segments and with the temperature distribution determined along them, is shown in Fig. 5. Ends of specimens are characterised by the inhomogeneous stress and strain state and, moreover, the temperature distribution is there influenced by other factors than in the remaining area. That is why these ends were omitted in the analysis of temperature distribution.

The procedure described above of obtaining the temperature distribution was applied to both shear paths. Subsequently, these distributions were approximated by the product of the exponential function and the Gauss function (Fig. 7). Since the exact scaling of the distances was very difficult, the coordinates of the points on the picture and the distances between them were given in relative units.

In agreement with the results obtained theoretically, the macroscopic shear bands of both paths obtained for the same specimen were directed towards each other (Figs. 1 and 3 B). Thus, the symmetrical superposition of the points indicating the temperature maxima in both paths and calculation of the mean value of the coordinate x_1 for these points (deviation of the temperature maximum from the shear direction) should eliminate a possible error caused by rotation of the paths relative to the shear direction.

The positions of points having maximum temperature were found for each specimen sheared at the rates $5.55 \cdot 10^{-3} \, \text{s}^{-1}$ and $11.1 \cdot 10^{-3} \, \text{s}^{-1}$. These positions were obtained for the deformations $\gamma = 0.63, 1.04, 1.59$. Small temperature increments accompanying the shear rate $2.77 \cdot 10^{-3} \, \text{s}^{-1}$ made it impossible to find the maximum of temperature.

The results of calculations obtained for extreme values of γ, where the macroscopic shear band occurs, are shown in Figs. 8 and 9. These are the mean values for both paths. The coordinate system was taken according to the Fig. 1; the x_1 axis – along the shear direction, and the x_2 axis – perpendicular to this direction. The position of maximum temperature, found for the segment lying in the middle of the path, was assumed as the origin of the coordinate system.
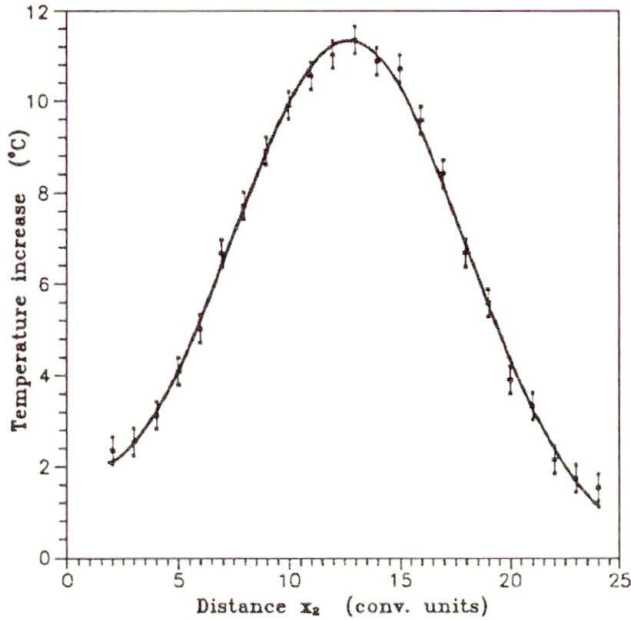
Fig. 7. Approximation of temperature distribution of the chosen sector by the product of the exponential and the Gauss functions. Accuracy of the measurement – 0.3° C.
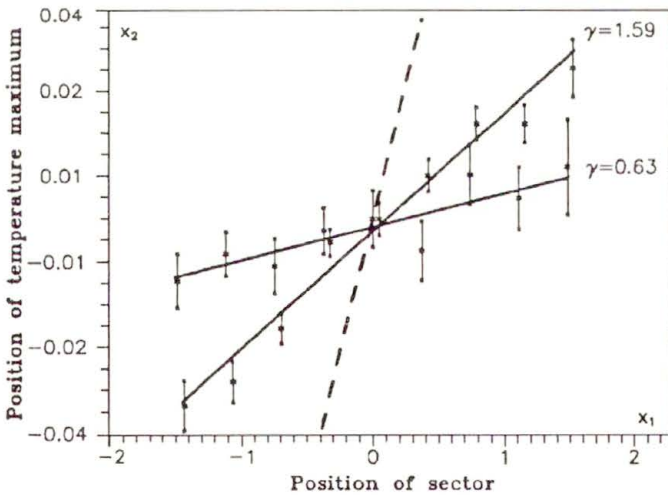

Fig. 8. Positions of maximum temperature in shear zones of the specimens at the strain rate $5.55 \cdot 10^{-3} \, \text{s}^{-1}$. Dashed line indicates the position of macroscopic shear band predicted by the theory (the direction of coordinate axes are given in Fig. 1).

For each point, the statistical error of the determined position of maximum temperature was calculated (Figs. 8, 9). Its value depends on the relative error of the temperature determination and decreases in accordance with a decrease
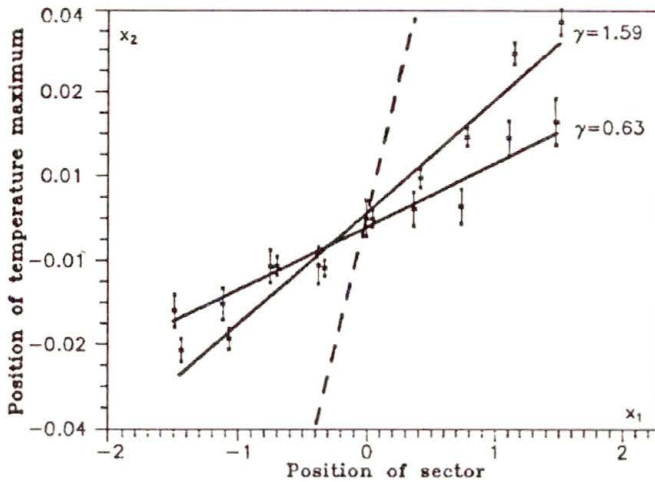
FIG. 9. Positions of maximum temperature in shear zones of the specimens at the strain rate $11.1 \cdot 10^{-3}\,\mathrm{s}^{-1}$. The dashed line indicates the position of macroscopic shear band predicted by the theory (the direction of coordinate axes are given in Fig. 1).

in the temperature error. Other, nonstatistical errors of this determination were not taken into consideration.

The obtained values of the temperature maximum positions were approximated by the straight line $x_2 = mx_1 + n$, where m, n – the calculated coefficients. Results of this approximation were marked by solid lines, while the dashed line shows the position of the macroscopic shear band found from the theoretical calculations [8]. These results indicate that the line describing the position of the maximum temperature is not always situated in the middle of the shear path.

Table 1 shows the slopes, m, of the straight lines, obtained by the procedure described above, and the error, Δm, of its determination. The theoretical value of m is 0.1.

Table 1. The values of the slope m for different shear strain levels γ.

Shear rate	$\gamma = 0.63$		$\gamma = 1.04$		$\gamma = 1.59$	
$[\mathrm{s}^{-1}]$	m	Δm	m	Δm	m	Δm
$5.55 \cdot 10^{-3}$	0.00624	0.00191	0.00979	0.00147	0.0220	0.0014
$11.1 \cdot 10^{-3}$	0.0120	0.0012	0.0136	0.0008	0.0212	0.0007

Results presented in Figs. 8, 9 and in Table 1 indicate that the slopes m increase accordingly to the rate of shear deformation.

The theoretical considerations [8, 9] were related to the shear rate $2.77 \cdot 10^{-3}\mathrm{s}^{-1}$. At such rate, the position of the temperature maximum was impossible to determine in experiment. Besides that, in theoretical approach the macroscopic shear

band started and developed along the shear path. However, our results would rather indicate the change of the slope of the macroscopic shear band with the deformation. Discrepancies between the theoretical and experimental investigations may be caused by the immediate flow of heat to solid grips. At small temperature increments it can cause an effect of apparent change of inclination of the macroscopic shear band. Moreover, larger slope of this band obtained for $\gamma = 0.63$ and 1.04 and observed at higher rate of shear, would indicate this type of effect (Fig. 10).
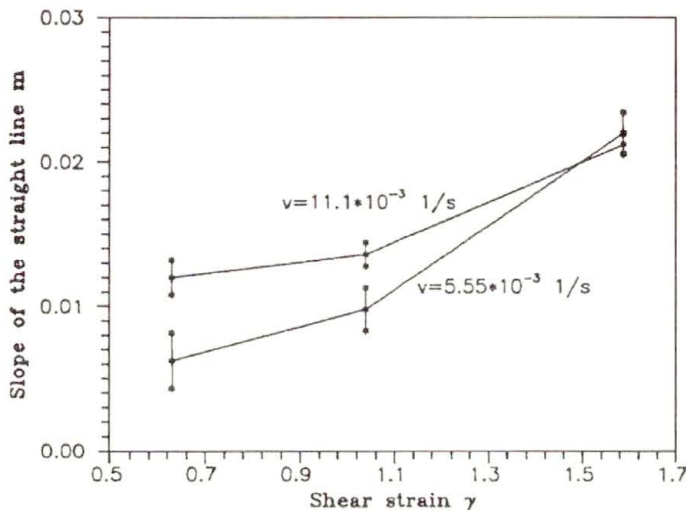

FIG. 10. The dependence of the coefficient m on the strain function γ.

It is also possible that our experimental results are correct and that discrepancies between the theoretical and experimental approaches are caused by deficiency of the theoretical model. This model does not take into account, for instance, the influence of gradients of temperature on the process of shear. In order to clear up these doubts, further studies and correlation of the investigations of temperature evolution with the microscopic observations, carried out at various magnifications, are needed.

4. Conclusions

Investigations of temperature distribution on the surface of the shear paths confirm the existence of the theoretically predicted fields of strain heterogeneity. At the ends of shear zones these heterogeneities are manifested by the increase of temperature, particularly noticeable in the initial stage of shear. As the deformation continues, the line describing the positions of maximum temperature departs from the shear direction. It gives evidence for the development of the macroscopic shear band, running along the specimen at a certain angle to the

direction of shear. Differences between the angles predicted by the theory and those observed in the experiment are probably caused by the flow of heat to solid grips, by the influence of temperature on the process of deformation, and by the assumptions adopted in the theoretical model. Explanation of these divergences requires further investigations.

Measurements of the temperature evolution in central parts of the shear paths indicate, that in the considered range of deformation, the temperature of these shear paths increases rapidly with the increase of the shear rate, in spite of the minor changes in mechanical characteristics. The disturbance of the monotonic increase in temperature observed at $\gamma \simeq 0.3$ can indicate the change of the mechanisms of deformation. However, this should be confirmed by further investigations. Moreover, the shape of $\sigma_{12}(\gamma)$ curves, obtained at higher deformations $\gamma > 0.7$, gives evidence for the changes of the character of the process of deformation during the shear test. Up to the shear deformation $\gamma \simeq 0.7$, these curves are smooth; at higher deformation, jumps of stresses occur, manifesting the heterogeneity of the process.

References

1. E.F. Rauch and C. G'sell, *Flow localization induced by a change in strain path in mild steel*, Mater. Sci. Engng., A 111, 71, 1989.

2. C.A. Bronhorst, S.R. Kalidini and L. Anand, *Polycrystalline plasticity and the evolution of crystallographic texture in FCC metals*, Phil. Trans. R. Soc. Lond., A 341, 443, 1992.

3. S. Harren, T.C. Love, et al., *Analysis of large-strain shear in rate-dependent face-centered cubic polycrystals: Correlation of micro- and macromechanics*, Phil. Trans. R. Soc. Lond., A 328, 443, 1989.

4. L. Ananand and S.R. Kalidindi, *The process of shear band formation in plane strain compression of FCC metals: Effect of crystallographic texture*, Mech. of Materials, 17, 223, 1994.

5. E.S. Dzikowski, *The mechanism of shear fracture in the aspect of the micro- and macrolocalization of strains*, Proc. Inter. Semin. MECHMAT'91, Large Plastic Deformation, Rotterdam 1993.

6. J.E. Paulun and R.B. Pecherski, *On the relation for plastic spin*, Arch. Appl. Mech., 62, 376, 1992.

7. K.A. Hartley, J. Duffy and R.H. Hawley, *Measurement of the temperature profile during shear band formation in steel deforming at high strain rates*, J. Mech. Phys. Solids, 35, 3, 283, 1987.

8. W.K. Nowacki and Nguyen Huu Viem, *Dynamic simple shear test. Experiment and numerical investigation*, Proc. 9th DYMAT Technical Conference, Munich, October 10–11th, 1995.

9. Nguyen Huu Viem and W.K. Nowacki, *Dynamic simple shear of metal sheets*, [to be published in Arch. Mech.].

POLISH ACADEMY OF SCIENCES
INSTITUTE OF FUNDAMENTAL TECHNOLOGICAL RESEARCH.